Hydraulics of Flow
in the Kaskaskia River, Illinois

by NANI G. BHOWMIK

VELOCITY

FLOW →

REPORT OF INVESTIGATION 91

Hydraulics of Flow
in the Kaskaskia River, Illinois

by NANI G. BHOWMIK

Title: Hydraulics of Flow in the Kaskaskia River, Illinois

Abstract: The hydraulics of flow was investigated at two reaches in the Kaskaskia River. The discharge varied from 58 to 4000 cfs and the flow frequency varied from 5 to 88 percent. The head loss varied from 0.96 ft/ mile for high flows to 1.98 ft/mile for low flows. The vertical velocity distribution was found to follow a logarithmic distribution. A theoretical distribution predicted the lateral velocity distribution in the bends reasonably well. In all, 79 isovels were developed for all flow conditions. The average value of the energy coefficient was 1.45 for straight reaches and 1.43 for bends. Similarly, the average value of the momentum coefficient was 1.22 for straight reaches and 1.18 for bends. Manning's roughness coefficient varied from 0.039 to 0.053. During low flows. the river flows through a series of pools and riffles. The median diameter of bed materials varied from 40 mm in the riffle to 0.04 mm in the pool, whereas the Froude number changed from 0.7 to 0.01. During high flows, the effect of the pool and riffle on the flow condition is minimal or non-existent.

CONTENTS

Hydraulics of Flow
in the Kaskaskia River, Illinois

by Nani G. Bhowmik

ABSTRACT

The hydraulics of flow was investigated at two reaches in the Kaskaskia River. Hydraulic data were collected for 58, 1040, 1420, and 4000 cfs from Reach 1 below Lake Shelbyville and for 290, 2160, and 3700 cfs from Reach 2 below Carlyle Lake. The flow frequencies varied from 5 to 88 percent. In all, 79 bed and bank material samples were collected and analyzed to determine the particle size distribution. In all cases, the flow can be approximated by uniform flow equations. Head loss varied from 0.96 ft/mile for high flows to 1.98 ft/mile for low flows. The vertical velocity distribution was found to follow a logarithmic distribution. The average velocity at 0.5 foot above the bed was approximately 95 percent of the average velocity in the cross section. Altogether 79 isovels, or lines of equal velocity, in the cross sections were developed on the basis of the hydraulic data collected in the field.

The ratio of the maximum velocity to the average velocity remained almost unchanged for low, medium, and high flows. The maximum average velocity was about 145 percent more than the average velocity. In a few cross sections, a considerable amount of bed scour took place during high flows.

A theoretical distribution was found to predict the lateral velocity distribution in the bends satisfactorily. The magnitude of the superelevation in the bends was small. At least 3 theoretical equations predicted the superelevation within the same percent of accuracy. Direction, pattern, and the number of secondary circulation cells in the bends and in the straight reaches can be sketched from the isovels developed.

The average value of the energy coefficient was 1.45 for straight reaches and 1.43 for bends. Similarly, the average value of momentum coefficients was 1.22 for straight reaches and 1.18 for bends. Average Manning's roughness coefficients varied from a minimum of 0.039 to a maximum of 0.053. Roughness coefficients showed a decrease in value with an increase in discharge. Analyses showed that unit discharges across the width of the river for various flow conditions are proportional to the respective water depths in the section.

During low flows, the Kaskaskia flows through a series of pools and riffles with larger diameter bed materials in the riffle and fine materials in the pool. The median diameter varied from 40 mm in the riffle to 0.04 mm in the pool. The Froude number varied from 0.7 in the riffle to 0.01 in the pool. Head loss was about 2.48 ft/mile in one pool-riffle sequence and about 4.44 ft/mile in another. During high flows, the pools and riffles are all submerged and their effects on the overall flow condition are minimal or nonexistent.

INTRODUCTION

The hydraulics of flow in a natural channel is a function of numerous variables. Some of these variables can be identified and accounted for easily; however, some of them are not yet fully understood. In a laboratory experiment, many of the variables can be controlled and adjusted to stay within some prescribed limits. However, in nature, it is an exception rather than a rule to have a controlled flow condition where the numerical values of different flow variables remain constant. Flow in a river or stream is never steady nor uniform, and rarely will one find a straight prismatic channel in which to conduct experiments.

An understanding of the hydraulics of flow must have been known to mankind for a long time. Ancient irrigation systems that are now abandoned in various parts of the world are a testimony to this fact. Men learned either from experimentation or from trial and error how to divert water from natural streams to irrigate their land. Basic theories of hydraulics of flow must have started with these initial experiments or observations.

Most of the hydraulic data that have been collected from the field by various researchers are basically for one set of conditions and for a single discharge. Rarely has any investigator collected field data from the same stream or river and from the same location for various flow conditions. The hydraulics of flow in natural stream-segments under varying degrees of flow conditions has not been studied in any detail. The mechanics of flow in the stream may or may not show any significant variation as the discharge changes with changing stages. Thus it is believed that an investigation of the flow hydraulics in a natural river for various discharges will be of great importance to explain, to verify, or to understand the hydraulics of flow in such

1

a stream. On the basis of this premise, two segments of the Kaskaskia River in Illinois were selected, monumented, and surveyed. In all, seven sets of hydraulic data were collected and analyzed, and the results are presented in this report.

The segments of the river selected contained both straight reaches and bends. The river flows through an erodible channel, typical of many streams in Illinois. Greater understanding of the mechanics of flow in natural rivers will enable engineers and planners to better manage the waterways and maintain them against excessive erosion or bank caving.

The work described here required planning and execution over a considerable period of time. The results should have valuable applications in the field and should be of value to design engineers and planners alike.

Plan of Report

This report is divided into four main sections. The first section discusses the background analyses needed for the investigation. The second section describes the procedures followed in the collection of field data. The analyses of the data are presented in the third section and the fourth section summarizes the results of the investigation. Also provided are listings of the references cited and the notations for symbols used throughout the report. The basic hydraulic data collected and analyzed for the report are presented in the Appendix.

Acknowledgments

BACKGROUND ANALYSES

The flow of water in sand bed alluvial channels has been studied by a number of researchers for a long time. Most of the major rivers of the world flow through alluvial materials consisting mostly of sand and silt. The mechanics of flow in a deformable channel is different from that in a fixed boundary channel. In a sand bed channel, the flow velocity, the turbulence associated with the flow velocity, and the patterns of the secondary circulation all have the capability and the opportunity to mold the shape of the channel. The shapes of the natural channels are never geometrically regular. The flow in a natural channel is obviously affected by so many variables that a clear, straightforward analysis is not possible unless one resorts to some acceptable simplification and assumptions. Researchers have been trying

to express the characteristics of flow in an alluvial channel with some theoretical relationships based on the laws of nature. In many instances the attempts were successful, whereas others met with failure.

The end product of all the constraints in an alluvial channel is the development of a velocity distribution in both the lateral and the vertical directions. These velocity distributions vary in time and space. The longitudinal water surface slope, or the hydraulic gradient, also constantly adjusts to reflect the constraints of the channel geometry on the flow in a natural channel. The variability of the water surface profile is more pronounced for flow around a bend than it is for a straight reach of the river.

The theoretical treatment of flow in an alluvial channel can be divided into two broad divisions, namely, flow in straight reaches and flow around bends. Some of the important contributions related to flow in alluvial channels are described in the following subsections.

Flow in Straight Reaches

Velocity Structure

Figure 1 depicts the flow in an open prismatic channel. The prismatic channel is defined as a channel with constant bed slope and unvarying cross-sectional shape. The theoretical relationships for open channel flow that have been developed by various investigators are normally applicable for prismatic channels. The velocity distribution equation at any vertical in a prismatic channel can be developed starting with the Navier-Stokes equation (Lamb, 1945).

With Reynolds method of averaging, the Navier-Stokes equation for turbulent flow of an incompressible fluid becomes

$$\rho_f [(\partial u_i/\partial t) + u_j(\partial u_i/\partial x_i)] = \rho_f F_i - (\partial P/\partial x_i) \qquad (1)$$
$$+ (\partial/\partial x_j)\{[\mu(\partial u_i/\partial x_j) - \rho_f (\overline{u_i' u_j'})] \}$$

where

ρ_f	=	density of the fluid
u_i, u_j	=	mean velocity in the ith, jth directions
t	=	time
x_i, x_j	=	distance in the ith, jth directions
F_i	=	body force in the ith direction
P	=	pressure force
μ	=	dynamic viscosity of water
$\overline{u_i' u_j'}$	=	Reynolds stress

The continuity equation is:

$$\partial u_i/\partial x_i = 0 \qquad (2)$$

Equation 1 can be integrated for steady, uniform two-dimensional open channel flow with constant fluid properties. The x-component of equation 1 (x-axis parallel to the invert slope and positive in the downstream direction, figure

1) is given by the following equation.

$$\gamma D \sin \phi\, (1 - y/D) = \mu(du/dy) - \rho_f \overline{u'v'} \qquad (3)$$

Here ϕ is the inclination of bed slope, γ is the unit weight of water, μ is the dynamic viscosity of water, and du/dy is the rate of change of u with y. If we substitute $\sin \phi$ as equal to the bed slope S_O, and assume that laminar friction is negligible compared with Reynolds stress, i.e., $\mu(du/dy) << \rho_f \overline{u'v'}$, and that this assumption is valid except for very close to the boundary, equation 3 becomes

$$\gamma D S_O(1 - y/D) = -\rho_f \overline{u'v'} \qquad (4)$$

If we use Prandtl's mixing length theory with a constant value for von Karman's universal constant k, equation 4 can be further integrated and simplified. With this simplification, equation 4 becomes

$$v/V_* = A_1 \log(y/k_S) + B_1 \qquad (5)$$

Here v is the point velocity at a depth y from the bottom, k_S is the equivalent roughness length, V_* is the shear velocity, and A_1 and B_1 are constants to be evaluated from field and experimental data.

Many researchers have proposed different numerical values for the coefficients A_1 and B_1. Most of the original work was done for rigid boundary channels. In open channel flow, it is much easier to determine the average velocity $\overline{V}$, the average depth $\overline{D}$, or hydraulic radius R in a cross section than the values of point velocity v and the point depth y. Here hydraulic radius R is defined as the ratio of the cross-sectional area to the wetted perimeter.

Keulegan (1938), using the experimental data of Nikuradse, has proposed the following equation intended to be valid for practical open channel flow problems.

$$\overline{V}/V_* = 6.25 + 5.75 \log (R/k_S) \qquad (6)$$

In this analysis von Karman's universal constant k was assumed to be 0.4 and k_S was taken to be the average roughness height of a bed composed of uniformly compacted sand. Burkham and Dawdy (1976) have indicated that equation 6 should be valid for turbulent flow in alluvial channels.

In order to estimate a numerical value of k_S for various flow conditions in an open channel, researchers have turned their attention to the size distribution of the bed materials. Leopold et al. (1964) have proposed use of the d_{84} size as the value of k_S for flow in channels with beds of coarse grained materials and have obtained the following equation.

$$\overline{V}/V_* = 2.83 + 5.75 \log (D/d_{84}) \qquad (7)$$

Here d_{84} is the size of the bed materials where 84 percent of the bed materials are finer than this size. Richardson (1965) used the d_{85} size of the bed materials as the equivalent roughness height and replaced k_S by d_{85} in an equation similar to equation 5. He found that the relationships re-
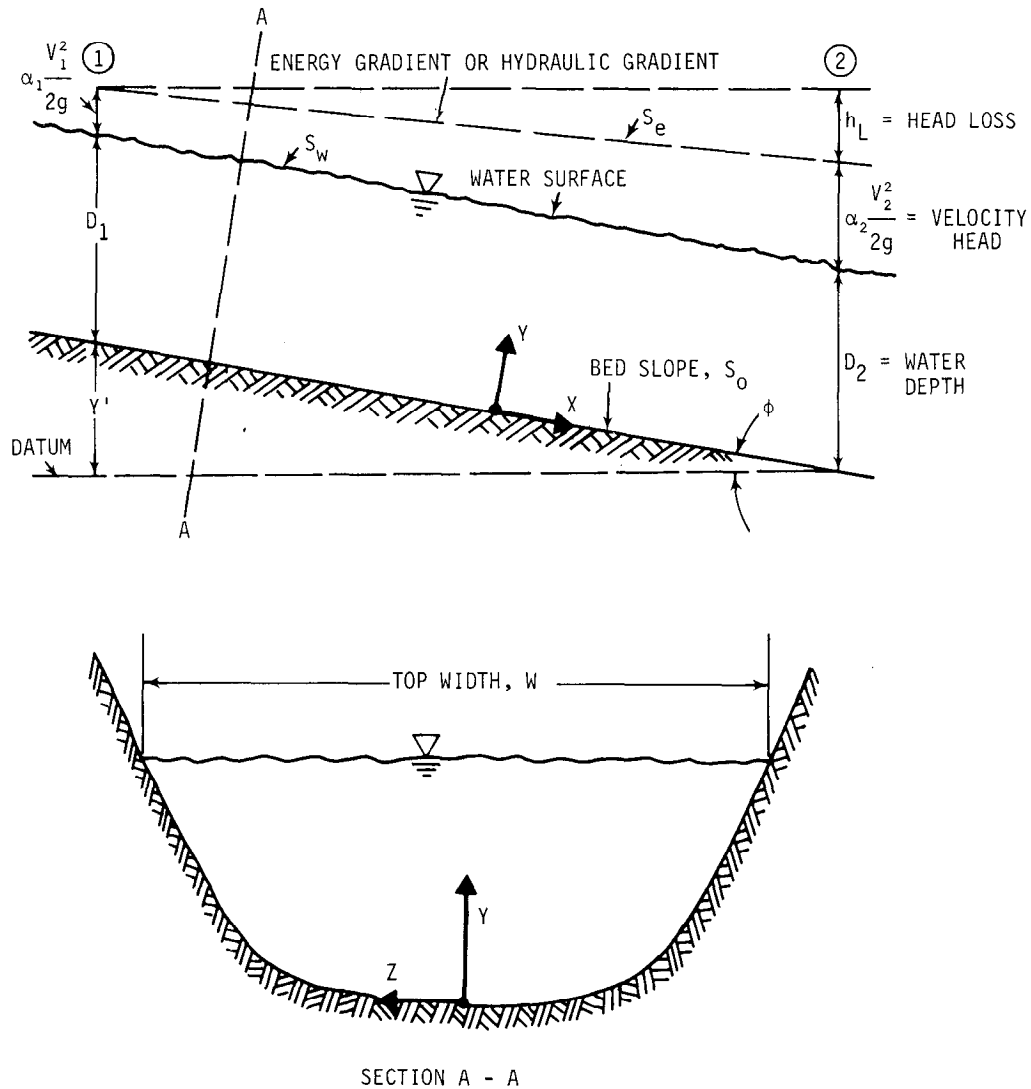
SECTION A - A
Figure 1. Flow characteristics in a prismatic open channel

mained valid for plane bed, ripples, and dune bed channels with and without appreciable sediment load. Bhowmik (1968) has shown that the d_{85} size can replace k_S in equation 5 for alluvial channels stabilized with riprap particles. For a set of data from an irrigation canal, equation 8 predicted the velocity distribution in any vertical quite well (Bhowmik, 1968).

$$v/V_* = 6.96 + 5.11 \log(y/d_{85}) \qquad (8)$$

Sentürk (1978) proposed an equation similar to equation 6 where d_{35} and d_{50} sizes of the bed materials were used as the equivalent roughness length. The equation proposed by Sentürk (1978) was postulated to be valid for lower flow regimes (Simons and Richardson, 1961) in alluvial channels. Burkham and Dawdy (1976) have concluded that an equation similar to equation 6 with the d_{95} size as the equivalent

roughness height replacing k_S should be a better estimator of the resistance to turbulent flow in an open channel.

Resistance to Flow

Equations 6 through 8, or any other equation similar to them, are also designated as the resistance to flow equation in an open channel. Flow resistance in an alluvial channel is a function of many variables (Simons and Richardson, 1971). Some of the important ones are: velocity V, depth D, slope of the energy grade line S_e, density of the water-sediment mixture ρ_f, dynamic viscosity of the water-sediment mixture μ, gravitational constant g, fall diameter of the bed material d_f, standard deviation σ, shape factor of the particles S_p, shape factor of the reach of the river S_R, shape factor of the cross section of the river S_c, and seepage force on the bed of the river f_{ss}.

4

These variables in turn will determine the bed form in an alluvial channel flowing on a sand bed. There are about eight different types of bed forms that may be present in an alluvial river. These bed forms are shown in figure 2 (Simons and Richardson, 1971) for bed materials having a median diameter d_{50} less than 0.6 mm. Whenever the median diameter is more than 0.6 mm, dunes will form rather than ripples after the bed materials begin to move.

The first three bed forms shown on the left side of figure 2 are called "lower flow regime." The last bed form on the left side is called washed-out dunes or the transition zone, and the four bed forms on the right side are called "upper flow regime."

In the lower flow regime, the resistance to flow is large and sediment transport is small. For most of the stable channels formed in alluvial materials, the dominant feature of the bed form is "dunes with ripples superimposed." Total resistance to flow is a function of the bed roughness. On the other hand, in the upper flow regime, the resistance to flow is small but the sediment transport is large and the Froude number F, is usually greater than 1. The Froude number expresses the ratio between the inertia force and the gravitational force and is given by equation 9 shown below.

$$F = V/(gD)^{1/2} \tag{9}$$

The flow passes through a critical stage whenever the numerical value of F is 1.

In a sand bed channel the bed forms that can develop for any flow condition may or may not remain the same across the whole width of the channel. In some instances, the bed form can be a combination of ripples, dunes, or plane and dunes as one passes from one side of the river to the other (Simons and Richardson, 1971). This was observed in a large river during low flow stages. The median diameter d_{50} of the bed material was 0.17 mm.

Turbulent flow in a rigid boundary open channel is independent of the viscous drag, i.e., the viscosity of the water has minimum effect on the flow resistance in the channel. However, this is not really true in the case of flow in alluvial streams with sediment movement. Here the viscosity of the fluid may change because of the change in water temperature or the change in the concentration of fluid-sediment mixture. This change in viscosity may change the bed form, which in turn will change the resistance to flow. Thus, a sand bed channel which has a dune bed during summer or fall may change to a plane bed during the late fall as the temperature decreases. This was found to be true for the Missouri River between Sioux City, Iowa, and Omaha, Nebraska (U.S. Corps of Engineers, 1968) where the average depth decreased by about 1 foot for the same discharge when the temperature dropped by about 31 degrees Fahrenheit in a period of 1 month. The bed form was found to have changed from dune bed to

plane bed indicating a decrease in the magnitude of the resistance to the flow.

This short analysis indicates that the determination of the resistance to flow in an alluvial sand channel is a very complex subject. The true effects of the various variables are not yet fully understood. Attempts have been made by a number of investigators to estimate a resistance coefficient for flow in an open channel. One of the simplest equations is the Darcy-Weisbach (Chow, 1959) formula, This formula was developed for flow in pipes. The Darcy-Weisback friction factor f is given by equation 10.

$$f = 8gRS_e/\overline{V}^2 \tag{10}$$

Equation 10 can be also be written as

$$f = 8V_*^2/\overline{V}^2 \tag{11}$$

where V_* is the shear velocity and is equal to $(gRS_e)^{1/2}$ By manipulating equation 11 one can obtain

$$\overline{V}/V_* = (8/f)^{1/2} \tag{12}$$

Thus, the right hand side of equations 6 or 7 can be taken to be equal to $(8/f)^{1/2}$. This indicates a direct relationship between the vertical velocity distribution in the stream and the friction factor f.

Simons and Richardson (1971) have indicated that the variables S_e, D, d_f ω, g, and ρ_f will determine not only the magnitude of f but also the bed configuration in an alluvial sand bed channel. Here ω is the fall velocity of the bed material and the other variables are as defined previously.

Two of the most widely used equations in open channel flow are Chezy's and Manning's equations. These equations are called uniform-flow formulas and are used to compute the average velocity in a stream when hydraulic and geometric characteristics are either estimated or measured in the field. Chezy's formula is given by equation 13.

$$\overline{V} = C(RS_e)^{1/2} \tag{13}$$

where C is a factor indicating the resistance to flow and is also called Chezy's C. Equation 13 can be modified as follows.

$$\overline{V} = [C/(g)^{1/2}] \, (gRS_e)^{1/2} = [C/(g)^{1/2}] \, V_*$$

Therefore, $\overline{V}/V_* = C/(g)^{1/2}$
and from equation 12 we obtain

$$\overline{V}/V_* = C/(g)^{1/2} = (8/f)^{1/2} \tag{14}$$

Equation 14 indicates that Chezy's C, Darcy-Weisbach friction factor f, and the ratio of the mean velocity to the shear velocity are all interrelated.

Manning's equation given by equation 15 below is one of the most widely used equations in river hydraulics around the world.

$$\overline{V} = (1.49R^{2/3} S_e^{1/2})/n \tag{15}$$

where n is the coefficient of roughness and is also called Manning's n. Comparison of equations 13 and 15 indicates

LOWER FLOW REGIME   UPPER FLOW REGIME

Typical ripple pattern   Plane bed

Dunes with ripples superimposed   Antidune standing wave

Dunes   Antidune breaking wave

Washed-out dunes (transition)   Chutes and pools
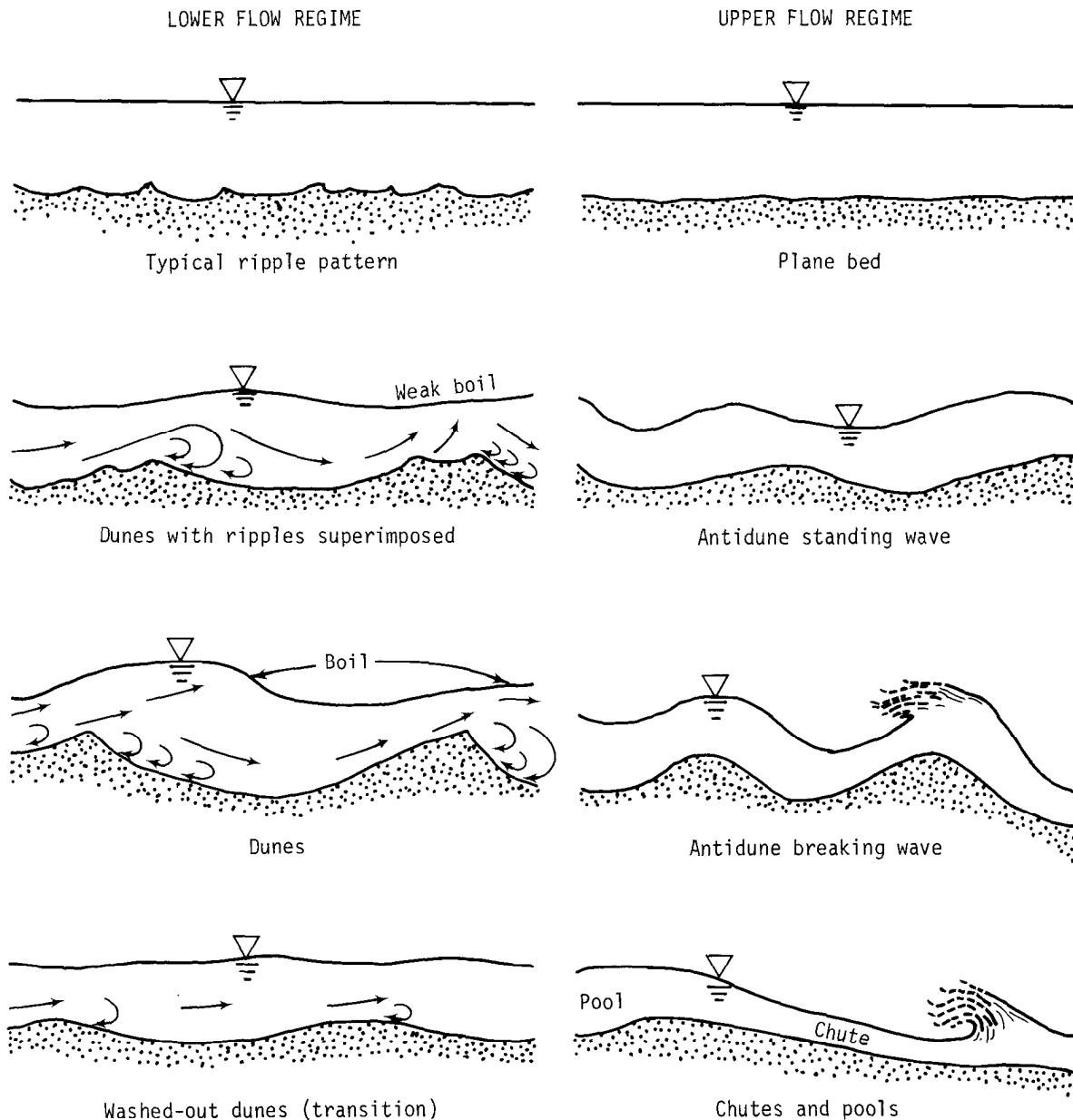
Figure 2. Typical bed forms in an alluvial sand bed channel

that Chezy's C is related to Manning's n by equation 16.

$$C = (1.49R^{1/6})/n \qquad (16)$$

Therefore

$$C/(g)^{1/2} = (1.49 \ R^{1/6})/n \ (g)^{1/2} = \overline{V}/V_* = (8/f)^{1/2} \qquad (17)$$

It must now be clear that all the resistance-to-flow equations described so far are related to one another in some way.

Over the last 50 to 70 years researchers have worked to determine the numerical values of n for anticipated flow conditions in open channels. Chow (1959) has summarized most of the research work that was done up through the mid-1950s. He has shown a number of photographs of flow in open channels with corresponding n values. Barnes (1967) also has compiled a list of n values for flow conditions in channels of varied characteristics which are shown by color photos of the flowing stream.

Head Loss

The head loss between two cross sections in an open channel is normally computed by determining the total energies between the respective sections (figure 1). Accord-

6

ing to Bernoulli's principle, the total energy at section 1 (figure 1) should be equal to the total energy at section 2 plus any head loss that may have occurred between these two sections.

Bernoulli's energy equation is used to obtain equation 18 for determining the head loss between sections 1 and 2 in figure 1.

$$h_L = (Y' + D_1 + \alpha_1 V_1{}^2/2g) - (D_2 + \alpha_2 V_2{}^2/2g) \qquad (18)$$

It is assumed that the bed slope is very small and as such the depth of water in a direction normal to the bed is approximately the same as the depth of water in the vertical direction. In case of uniform flow, $S_e = S_w = S_o$. However, in natural channels, flow is never uniform and gradually varied flow equations must be used to describe the flow variability.

The term $V^2/2g$ in equation 18 is called velocity head. Lateral velocity distribution in an open channel is never uniform and the velocity head computed by $V^2/2g$ is usually smaller than the actual velocity head in the cross section. It is usual practice to compute the velocity head by the relationship $\alpha V^2/2g$, where α is known as the energy coefficient or Coriolis coefficient. The value of α was shown to vary from 1.03 to 1.36 by Chow (1959) and from 1.03 to 4.70 by Hulsing et al. (1966). The technique for computing the value of α based on field data is given by Chow (1959).

The nonuniformity of velocity distribution across a cross section also affects the determination of the momentum flux in an open channel. The momentum M of the fluid passing a cross section per unit time is given by equation 19.

$$M = \beta\gamma Q\overline{V}/g \qquad (19)$$

where β is known as the momentum coefficient or Boussinesq coefficient, γ is the unit weight of water, Q is the discharge, $\overline{V}$ is the mean velocity, and g is the gravitational constant. Chow (1959) has indicated that for a fairly uniform straight prismatic channel the value of β varies approximately from 1.01 to 1.12.

Hydraulic Geometry of Alluvial Channels

The average velocity $\overline{V}$, the average depth $\overline{D}$, width W, and hydraulic gradient S_e are some of the parameters termed the hydraulic geometry parameters at a cross section in an alluvial channel. There are three different methods that can be used to determine the hydraulic geometry parameters in streams and rivers. These are:

1) Tractive force method
2) Permissible velocity method
3) Regime concept method

In the tractive force method, the allowable shear force exerted by the flowing water on the bed and bank of the stream is estimated. With known values of tractive force,

measured bed and bank slopes, and measured bed and bank material sizes, the stability of the bed and the bank is tested and a stable geometry of the stream is determined. One of the foremost methods for determining the hydraulic geometry of open channels based on tractive force is given by Lane (1955). Lane's method is valid for streams and rivers flowing through coarse or fine alluvial materials.

In the permissible velocity method, an allowable or permissible velocity is estimated on the basis of the size distribution of the bed and bank materials. The relationships between the permissible velocity and the bed and bank material sizes are given by Lane (1955), Chow (1959) and others. If the existing average velocity in the stream cross section is larger than the estimated permissible velocity, then it is assumed that the stream geometry will be unstable. Either a change in the stream geometry or a milder slope of the stream will be needed to reduce the average velocity in the stream within the allowable limit. This technique is normally used to test the stability of an existing stream cross section rather than to design a conveyance channel.

The regime concept is one of the most widely used methods in open channel flow to design a stable alluvial channel flowing on a mobile sandy bed. This concept was initially developed in India and was based on the data collected from stable channels in the Punjab region.

The original definition of the regime theory is given by Lindley in 1919 (ASCE, 1963) as follows:

> When an artificial canal is used to convey silty water, both bed and banks scour or fill, changing depth, gradient and width until a state of balance is obtained at which the channel is said to be in regime.

The regime type of equations proposed by various researchers relate average velocity $\overline{V}$ with depth $\overline{D}$ or hydraulic radius R and energy slope S_e. Over the years the regime concept has been modified, better and more useful relationships have been developed, and presently the design engineer will usually use some type of regime equation to design a conveyance channel flowing through alluvial materials.

Kennedy (Lacy, 1958) proposed the following equation in 1895 which was based on his work with the regime type canals in India.

$$\overline{V} = K D^m \qquad (20)$$

where K ranges from 0.39 to 0.84 and m ranges from 0.52 to 0.73. Then in 1919 Lindley (Lacy, 1958) proposed equations relating velocity $\overline{V}$, depth $\overline{D}$, and width W. From 1919 to 1958 a number of researchers, such as Lacy, Bose, Malhotra, Blench, White, Inglis, Leliavsky, and others made significant contributions toward the understanding of the regime type of canals (ASCE, 1963; Simons and Richardson, 1971). Lacy (1958) related wetted perimeter WP, hydraulic radius R, and slope S_e to discharge Q and silt factor f_s.

Blench (1969) in 1941 proposed a division of f_s into bed-factor and side-factor to take into account the roughnesss and material variabilities between the side and the bed of the stream. Blench also replaced wetted perimeter and hydraulic radius by width and depth of the channel.

Leopold and Maddock (1953) found that width, depth, and velocity of flow in rivers varied with mean annual discharge at any specified cross section. These parameters were shown to increase in value in the downstream direction. The relationships proposed by Leopold and Maddock (1953) are given by equations 21, 22, and 23.

$$W = aQ^b \tag{21}$$
$$\overline{D} = cQ^i \tag{22}$$
$$\overline{V} = jQ^l \tag{23}$$

Here a, b, c, i, j, and l are coefficients to be determined from field observations. The mean values of the coefficients b, i, and l for a number of river basins in the United States are given by equation 24.

$$
\begin{aligned}
b &= 0.5 \\
i &= 0.4 \\
l &= 0.1
\end{aligned}
\tag{24}
$$

On the basis of field data collected from noncohesive and partly cohesive channels in India, Pakistan, and the United States, Simons and Albertson (1963) have proposed a set of regime type equations to determine the stable cross-sectional shape of an alluvial stream. The relationships proposed by Simons and Albertson are given below.

$$WP = 2.51Q^{0.512} \tag{25}$$
$$R = 0.43Q^{0.361} \tag{26}$$
$$A = 1.076Q^{0.873} \tag{27}$$
$$\overline{V} = 16R^{2/3} S^{1/3} \tag{28}$$

Here, WP is the wetted perimeter in feet, R is the hydraulic radius in feet, A is the cross-sectional area in square feet, $\overline{V}$ is the average velocity in fps, Q is the discharge in cfs, and S is the slope. The relationships given by equations 25 through 28 are valid for streams and canals with sand beds and cohesive banks. Simons and Albertson also have given relationships valid for streams flowing on a noncohesive bed with noncohesive bank materials.

Stall and Fok (1968) have developed hydraulic geometry relationships for 18 river basins in Illinois. Their approach is basically similar to that of Leopold and Maddock (1953). They have developed hydraulic geometry relationships with the Horton-Strahler stream order (Stall and Fok, 1968) as a parameter. Their relationships should enable the design engineer to determine the hydraulic geometry parameters at any location in the river basin for a specified discharge of known frequency. Later, Stall and Yang (1970) showed that the hydraulic geometry relationships are also valid for 12 river basins located in the humid areas of the United States. A recent investigation by Bhowmik and Stall (1979)

has definitely shown that the hydraulic geometry relationships are also valid for the floodplains of the streams and rivers in the humid areas of the United States.

Maddock (1970) commented that the relationships among W, $\overline{D}$, $\overline{V}$, and S are not determinate unless the constraints on the development of the bed form is known. When the rate of sediment transport in the stream is known, the indeterminate part between the hydraulic variables can to some extent be eliminated. However, the flow in a natural channel is a complex phenomenon and no easy solution exists. Still, with the research work already completed and the work that is now being conducted, the design engineer should be able to arrive at a technically sound design of a conveyance channel flowing through alluvial materials.

Flow around Bends

The mechanics of flow in a curved open channel has some distinct characteristics that are absent in a straight channel. The forces that the flow encounters not only are different in nature, but also are very complex and not easily understood. Some generalized comments and theoretical equations can be developed for flows with Froude numbers equal to or less than 0.5. The regime of flow in natural channels is such that the numerical value of F is normally less than 0.5. Leopold et al. (1960) analyzed the Froude number for 62 stream gaging stations around the United States. The values of F for bankfull discharges were found to be less than 0.45 in 92 percent of the cases. Thus, any theory or equation that is developed for flow in open channels for F equal to or less than 0.5 should be valid for the majority of streams and rivers.

When the flow starts to enter a bend, the streamlines become curved in plan because of the restraint exerted by the stream banks. For potential flow, the shapes of the streamlines can be determined by integrating Laplace's equation. However, flow in natural channels never follows potential flow theory. The governing equations for open channel flow can only be solved in conjunction with some simplified assumptions.

In the following subsections some of the theories pertaining to the flow around a bend are described briefly.

Superelevation

As the flow moves around a bend, the streamlines are curved, centrifugal forces are developed, and the transverse water surface profile becomes inclined with an increase of water depth near the outer bank and a consequent decrease of water depth near the inside bank. The difference between the water levels near the outside bank and the inside bank is called superelevation. The magnitude of superelevation is

normally high in case of rigid boundary channels where the geometry of the channel remains the same in both the straight and the curved reaches of the stream.

Investigators, such as Woodward (1920), Shukry (1950), Rozovskii (1957), Ippen and Drinker (1962), and many others, have worked on the development of theory and the analysis of flow around bends. A number of analytical relationships have already been developed to estimate the magnitude of the superelevation for a set of flow conditions. The basic equation for estimating the numerical value of the superelevation is equation 29.

$$\Delta Z = \int_{r_i}^{r_o} (V_v^2/r)\, dr \tag{29}$$

Here ΔZ is the superelevation, V_v is the average velocity in any vertical inside the bend, r_i and r_o are the inside and outside radius of curvature of the bend, respectively, and r is the variable. In order to integrate equation 29, the distribution of flow velocity across the width of the channel along any radius in the bend must be known. Woodward (1920) assumed a constant transverse velocity distribution and obtained equation 30 to determine the superelevation.

$$\Delta Z = \overline{V}^2 W/gr_c \tag{30}$$

In this case, $\overline{V}$ is the average velocity in the cross section, W is the top width, g is the acceleration due to gravity, and r_c is the radius of curvature of the centerline of the bend.

When the transverse velocity distribution is approximated by a free vortex pattern, the equation for superelevation becomes (Shukry, 1950) as follows.

$$\Delta Z = [(\overline{V} r_o r_i)/(2g)]\, [1/r_i^2 - 1/r_o^2] \tag{31}$$

Ippen and Drinker (1962) assumed that the average specific head remains constant and that the high velocities occur near the outer bank of the channel. For situations similar to this, a forced vortex pattern of velocity distribution can approximate the transverse velocity distribution in the bend. With these assumptions, equation 32 is obtained for estimating the superelevation.

$$\Delta Z = [(\overline{V}^2 W)/(gr_c)]\, [1/(1 + W^2/12r_c)] \tag{32}$$

When the transverse velocity distribution is approximated by a combination of forced vortex for the inner half of the width and free vortex for the outer half of the width, with the maximum average velocity in the vertical staying close to the centerline of the bend, equation 33 is obtained for computing the superelevation.

$$\Delta Z = [(V_{max}^2/2g)]\, [2 - (r_i/r_c)^2 - (r_c/r_o)^2] \tag{33}$$

Equations 30 through 33 are some of the equations that are used to compute the superelevation in an open channel bend.

Velocity Structure

The presence of the superelevation in the bend develops another phenomenon called secondary circulation. Com-

bined effects of these factors change the velocity structure inside a bend. The core of high velocity flow is normally located near the center of the channel in a straight reach. But as the flow moves around the bend, a transverse inclination of the free water surface will occur decreasing the water depth near the inside bank at the entrance of the bend. This decrease in flow depth is associated with an increase in flow velocity at that location. However, as the flow proceeds downstream, the centrifugal force and the exchange of momentum between horizontal layers due to transverse circulation will change the velocity structure, and move the higher velocity filament near the outside bank. This high velocity flow may stay close to the outside bank for a considerable distance in the downstream direction unless the stream again meanders and initiates another change in the velocity structure.

Most of the researchers assumed the transverse velocity distribution to follow a relation similar to the one given by equation 34.

$$V_v = k_1 r^{m_1} \tag{34}$$

If m_1 equals +1, the velocity distribution is called a forced vortex pattern and if m_1 equals -1, the velocity distribution is called a free vortex pattern.

Rozovskii (1957) presented a detailed study of flow around bends for an open channel with low Froude number (F < 0.15). He has presented a set of plots which can be used to determine transverse velocity distribution around an open channel bend. Rozovskii's (1957) curves and plots needed for estimating the transverse velocity distribution at any cross section inside the bend are shown in figure 3. The cross-sectional shape of the bend was assumed to be parabolic and is given by equation 35 below.

$$D = D_{max}(1 - 2X'/W)^2 \tag{35}$$

Here, D_{max} is the maximum depth, W is the top width, and X' is the distance of the individual vertical from the centerline of the stream. D_{max} was assumed to occur at the centerline of the channel. The value of Δ in figure 3a is to be taken in degrees. This is the numerical value of the included angle at the center of the curve made by a line extending from the cross section under consideration and a line extending from the cross section at the beginning of the bend. In figure 3a, V_{vm} is the maximum average velocity at a vertical in the straight portion of the stream. It was assumed that V_{vm} occurs at the centerline of the channel. The distribution of V_v is given by equation 36.

$$V_v = V_{vm}(d/D_{max})^{0.4} \tag{36}$$

Here d is the depth of water at any individual vertical.

In order to calculate the transverse velocity distribution at any cross section in a bend, the value of Δ', is calculated by the equation shown in figure 3a. Here D_{max} is the depth of water at the centerline of the stream, $C/(g)^{1/2}$ is obtained from equation 14, and W and Δ

9
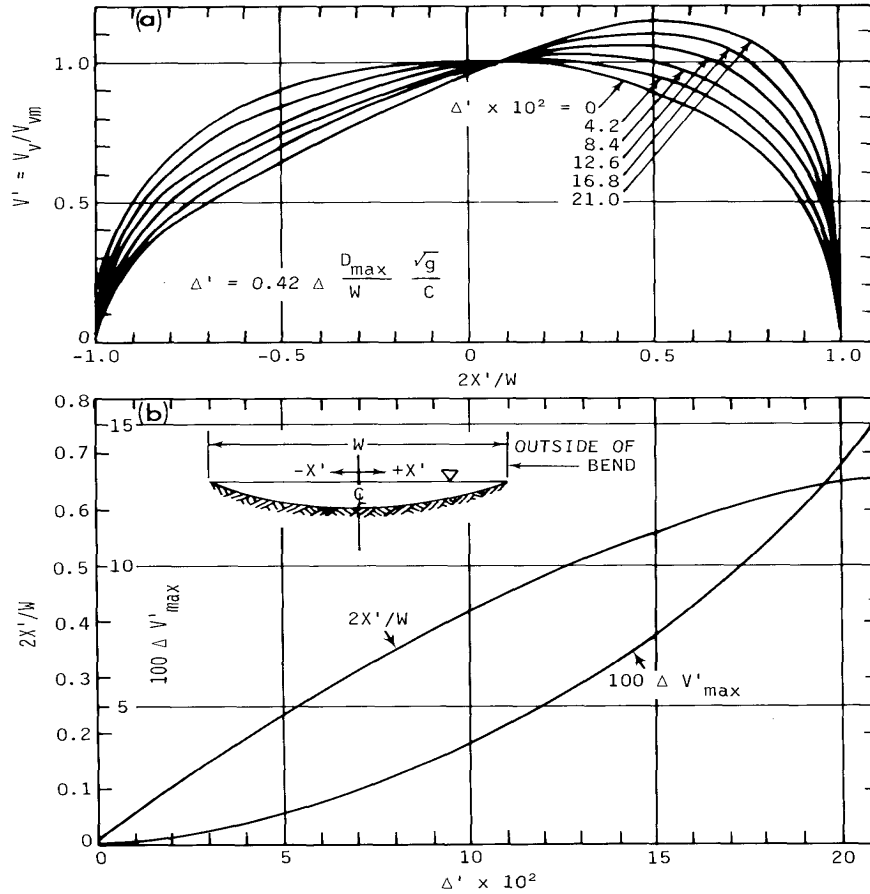
Figure 3. Dimensionless curves to determine transverse velocity distribution in a bend

are taken from the stream geometry data. Depending upon the value of Δ', the transverse velocity distribution is estimated from a curve or curves given in figure 3a. However, figure 3b which is developed from figure 3a can also be used to estimate the transverse velocity distribution in the bend.

Secondary Circulation

Secondary circulation can be defined as a pattern of circulation that will develop in an open channel mainly because of the presence of curves in its alignment. The mechanics of initiation of the secondary circulation can be

explained by considering the transverse inclination of the water surface and the centrifugal force that is exerted on the water particles as the water moves around a bend.

If we divide both sides of equation 30 by W, the transverse inclination of the water surface designated as I_r becomes independent of the width of the stream as follows.

$$I_r = \Delta Z/W = \overline{V}^2/gr_c \qquad (37)$$

This shows that the inclination of the water surface or the transverse slope of the water surface in a bend is a function of the flow velocity, radius of curvature, and the acceleration due to gravity.

10

Because of the presence of frictional resistance at the bed and sides of the channel, the velocities along any vertical in a bend vary from a maximum value at or near the water surface to a minimum value at the bottom. The flow velocity near the water surface will consequently be more than the average velocity in the respective verticals. The centrifugal force C_f is a function of the square of the flow velocity. In order to maintain the balance of the forces, the centrifugal force, which is trying to push the water particles away from the stream in a radial direction, must be counterbalanced by the pressure force ΔP. The pressure force is generated by the differential increase in water depths as a result of the superelevation. Depth-integrated values of C_f and ΔP are equal. However, near the water surface where the flow velocity is greater than the average velocity, C_f is greater than ΔP. Similarly, near the bed of the stream, the flow is less than the average velocity and consequently ΔP is greater than C_f. At the point where the water is flowing with an average velocity, ΔP equals C_f. This differential between the ΔP and C_f will displace the water particles away from the centerline near the water surface. A similar displacement near the bed of the stream toward the inner side of the bend will take place.

As a result of this opposite radial displacement of the water particles, a helicoidal motion will develop in a bend in addition to the normal longitudinal flow. This helicoidal motion is termed the secondary circulation in a bend.

The secondary circulation in the bend will have a vertical velocity component directed downward on the outside bank of the bend. This vertical component of the velocity will help to dislodge the bank materials from the outside bank and will contribute to the instability of the outside bank. The resultant of this vertical velocity component and the normal flow velocity vector at or near the outside bank will be deflected by an angle ψ from the axis of the channel. Rozovskii (1957) reported the following equation for ψ based on field observations.

$$\tan \psi = 11\ D_{max}/r_c \tag{38}$$

Prus-Chacinski (1966) indicated that equation 38 should be applicable for natural and laboratory channels.

Energy Dissipation

Changes in the flow structure in a bend lengthen the path of motion of an individual particle for its journey around the bend. Exchange of momentum between separate layers of flow is increased, which in turn increases the dissipation of mechanical energy. Ippen and Drinker (1962) found that the rate of energy dissipation is maximum at the end of the bend. This rate of energy dissipation was expressed by them as a ratio of energy slope at the end of the bend to that at the beginning or at the entrance section of the bend.

For uniform flow in a prismatic channel, the S_0, S_W, and S_e on figure 1 should be parallel, that is, $S_e/S_W = S_W/S_0 = 1$. But whenever $S_e/S_W > 1$, the energy dissipation is greater than uniform flow and an accelerating flow is implied. When $S_e/S_W < 1$, the energy dissipation is less than uniform flow, the depth of flow increases, and a conversion of kinetic energy to potential energy takes place. Thus, a plot of S_e/S_W or S_e/S_0 can shed some light as to the rate of energy dissipation in an open channel.

Bed Topography

The presence of the secondary circulation and the lateral movement of the high velocity flow toward the outside bank of the bend will erode the bed and the bank of the channel if they lack protection. The magnitude of scour will vary depending upon many physical factors. As the water moves around a bend with erodible bed and bank, the secondary circulation increases, exchange of momentum accelerates, the high velocity flow moves gradually toward the outside bank, and a gradual change in the bed topography takes place. The trapezoidal or symmetrical parabolic cross section that may be present at the beginning of the bend, may for all practical purposes be transformed into a skewed cross section. The maximum depth is usually located near the outside bank and sediment will be deposited near the inside bank forming the so called 'point bars.' A knowledge of the variability of cross-sectional shapes in any open channel bend is needed to investigate the dispersion of materials and the hydraulics of natural streams.

Researchers such as Yen (1970), Engelund (1974), Bridge (1976), Gottlieb (1976), and others have developed empirical relationships to estimate the bed topography in an open channel bend.

Pools and Riffles

Natural streams and rivers flow through a series of pools and riffles during low stages. During high stages, when the river is full from flood flows, the pools and riffles are usually suppressed, the longitudinal water surface profile becomes smooth, and the variability in the flow due to the presence of pools and riffles disappears.

The change in the flow regime of a river from the pool and riffle sequence to a regime with high stages is a normal occurrence in a stream located just downstream of a controlled man-made reservoir. The operation and management of the reservoir may require different quantities of water to be released within a period of a couple of days. Thus a stream which is flowing through a series of pools and riffles during low releases, may carry bankfull discharge within a period of two weeks. Therefore, it is essential that the low flow dynamics of streams and rivers be studied.

Keller (1978) has indicated that the maintenance of pools and riffles is very important in any channelization project. Pools and riffles help not only to maintain an adequate aquatic life in the stream ecosystem by creating alternatively deep and shallow waters, but also to dissipate the excess energy and maintain a stable flow regime. Channelization projects where pools and riffles are artificially created to maintain a better balance of the stream ecosystem are better than a straight and lined canal.

Stall and Yang (1972) have analyzed the hydraulic geometry of pools and riffles for a 53-mile segment of the Kaskaskia River. From their analysis, it was concluded that the length of the pools can be expected to be about 8 times longer than the length of the riffles.

Keller (1978) has noted that the geometric patterns of the pools and riffles remains unaltered during and after the passage of high magnitude floods. However, changes in the land use pattern, upstream construction, and bank failures will change drastically the pattern and the location of the pools and riffles in a natural channel or in an artificial one.

DATA COLLECTION

Data used in this research project were collected from two reaches of the Kaskaskia River. Figure 4 shows the Kaskaskia River drainage basin and the locations of the reaches selected for study. The total drainage area of the river is 5801 square miles. The drainage area at Reach 1 is 1330 square miles and that at Reach 2 is 2720 square miles. Each reach is located downstream of a man-made lake. Reach 1 is located about 12 miles downstream of Lake Shelbyville and Reach 2 is located about 7 miles downstream of Carlyle Lake.

These reaches were selected downstream of the man-made lakes to take advantage of the relatively steady flow that exists below such lakes. The flow in a natural river is never constant, and usually will be unsteady and nonuniform. Short-term prediction of the flow is very difficult. Collecting a precise set of hydraulic data from a segment of a river 2 to 3 miles long requires at least 1 week. In natural streams and rivers, the flow normally changes from day to day. This is especially true during flood stages. But if the flow in a river is controlled by the release rates from a reservoir just upstream of the reach under investigation, then it is possible to keep the rates of flow relatively steady for a short period of time even during flood stages. Keeping the flow steady for such a short period of time should not adversely affect the regime of the river. As a matter of fact, both lakes shown in figure 4 are operated by the U.S. Army Corps of Engineers for flood protection and recreational uses. Thus it is a normal operational procedure to release the water from the lakes at a constant rate extending for a period of a few days, which was an advantage during the data collection phase of this investigation.

Hydraulic Geometry of the Reaches

The preliminary selection of the reaches was made from the plan view of the river as shown on U.S. Geological Survey quadrangle maps. Easy access to the sites, existence of a wide variety of bends and straight segments in the reaches, closeness to the reservoirs, and the availability of support personnel were some of the factors considered in the selection process. A field trip was made to each reach to make sure that these sites satisfied all the initial requirements.

After the final selections were made, the approximate location of the cross sections, the starting points for both reaches, and the total length of the river to be investigated were marked on individual quadrangle maps. Two private surveying firms were contracted to perform the necessary surveying work. The surveyors were asked to determine the cross-sectional elevations of the river at about 15 to 17 well-placed cross sections in each reach. They were also required to develop the plan view of each reach. Permanent concrete surveying monuments were installed on both sides of the river at each of the selected cross sections. The exact position of the monuments related to Illinois State Plane Coordinates and their elevations above mean sea level were also determined. These permanent concrete monuments were used as bench marks in all subsequent data collection trips.

Figure 5 shows the aerial view of Reach 1 below Lake Shelbyville. This photograph was taken on November 13, 1975. The plan view of the reach, the location of the cross sections, and the location of the monuments are given in figure 6. The geometric characteristics of this reach are given in table 1. Here, the exact location of each section, the beginning and end of each bend, the deflection angle and the radius of curvature of the bends, the top widths at each section, and the ratio r_c/W are given. The plan view of Reach 2 is shown in figure 7, and the geometric properties of this reach are given in table 2.

In Reach 1 (figure 6) there are at least four sharp bends. The beginning and the lower part of the reach are basically straight. Whereas for Reach 2 (figure 7), there are three sharp bends and a long straight segment near the lower

12
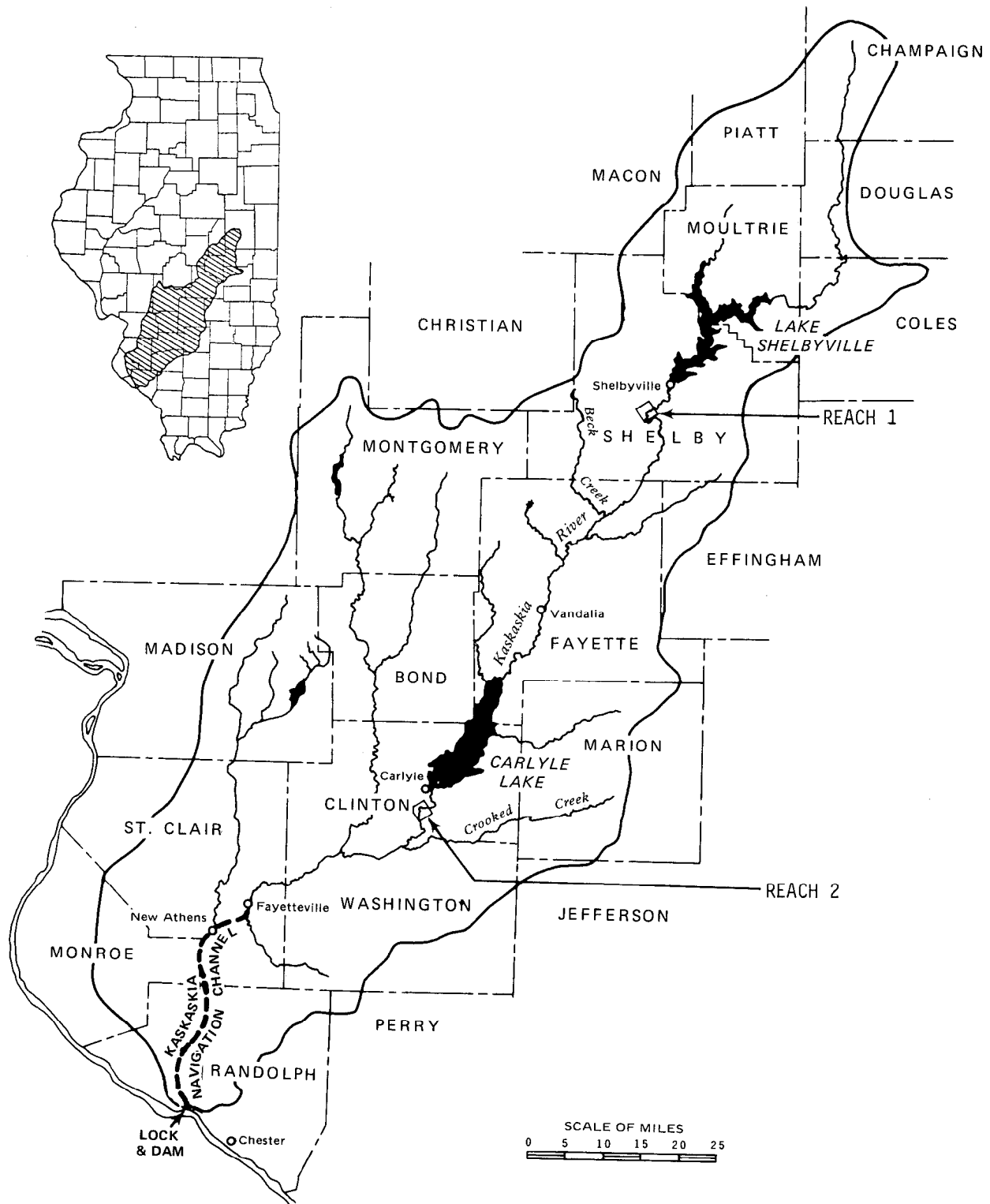
Figure 4. Drainage basin of the Kaskaskia River and locations of the test reaches
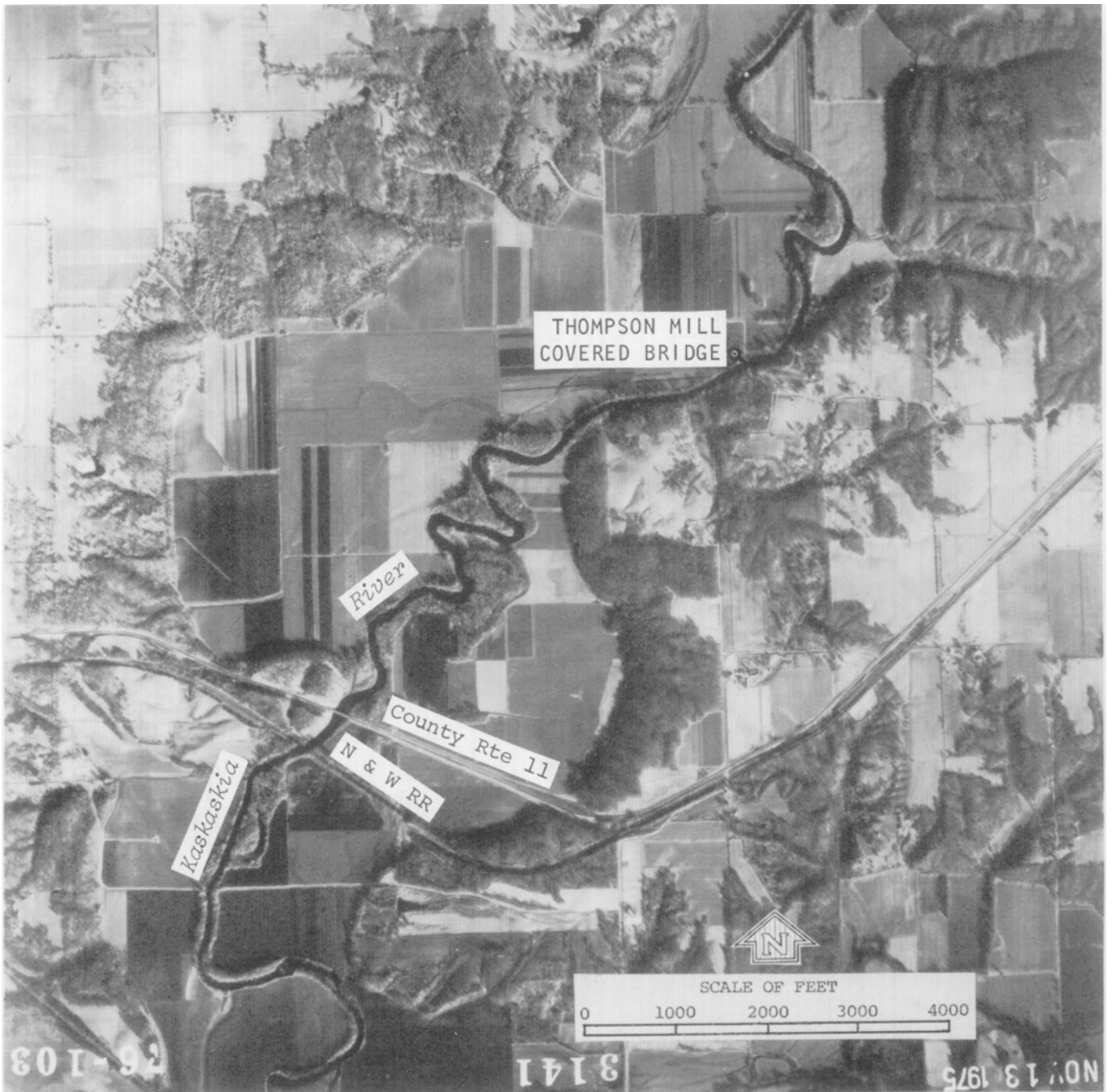
Figure 5. Aerial view of Reach 1

14
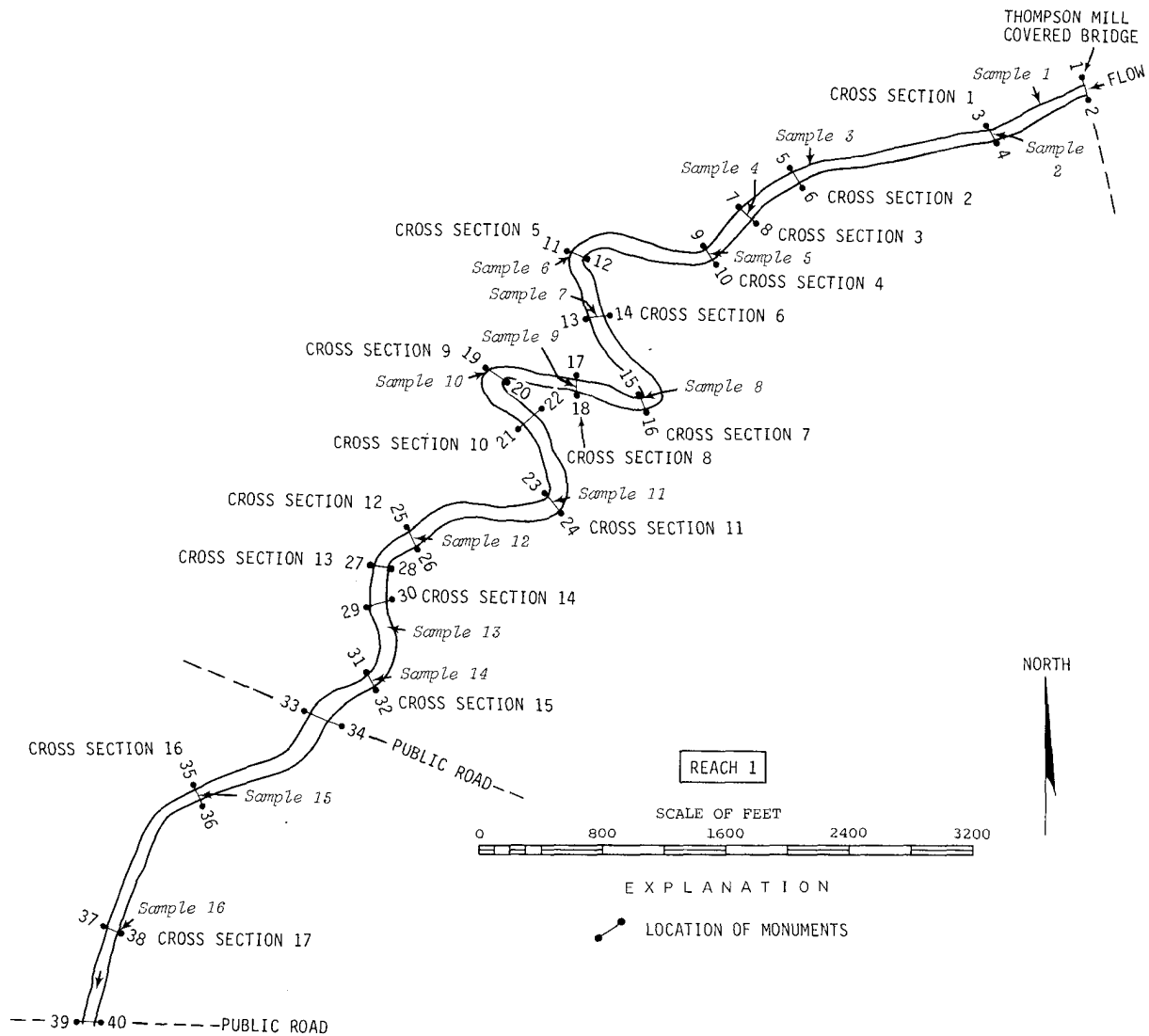
Figure 6. Plan view of Reach 1

part of the reach. Both reaches of the river have a good combination of straight reaches and bends affording a wide variety of conditions in the study of the hydraulics of flow in an open channel.

Velocity Distribution and Water Surface Profiles

Once the initial surveying was completed, a field crew was assembled to collect the basic data. The crew consisted of one or two engineers, two surveyors, and two technicians. One of the technicians was from the U.S. Geological Survey and helped to collect the velocity distribution data with a Price Current Meter following the standard procedure of the U.S. Geological Survey.

Figure 8 shows a photograph of the actual data collection arrangement. A marked steel tag line was stretched across the river to align the boat and also to move it across the river. The procedures followed in data collection were as follows:

1) Organize the field crew so that they are ready to go to the field with short notice.
2) Request the U.S. Army Corps of Engineers to keep the release rates constant for a time period sufficient to collect the data when the runoff condition in the watershed was such that the release rates from the reservoir would be within the specified requirement.
3) Start collecting the data preferably on Monday, beginning at cross section 1 in each reach (figures 6 and 7).

15

Table 1. Geometric Charateristics of Reach 1

Distance along the centerline (ft)	Total deflection angle or central angle of bend, Δ (degrees)	Centerline radius of curvature, r_c (ft)	Top width, W (ft)	r_c /W	Remarks
0					Thompson Mill Covered Bridge
510	38	990			Beginning of Bend 1
680	38	*990*	125	7.92	Cross section 1
1090	38	*990*			End of Bend 1
1550	55	980			Beginning of Bend 2
1980	55	*980*	129	7.60	Cross section 2
2380	55	980	169	5.80	Cross section 3
2490	55	980			End of Bend 2
2490	84	448			Beginning of Bend 3
2743	84	448	133	3.37	Cross section 4
3160	84	448			End of Bend 3
3520	140	134			Beginning of Bend 4
3759	140	134	119	1.13	Cross section 5
3860	140	134			End of Bend 4
4207			136		Cross section 6
4700	148	102			Beginning of Bend 5
4955	148	102	119	0.86	Cross section 7
4980	148	102			End of Bend 5
5407			126		Cross section 8
5830	158	96			Beginning of Bend 6
5959	158	96	143	0.67	Cross section 9
6120	158	96			End of Bend 6
6379			174		Cross section 10
6840	134	114			Beginning of Bend 7
6999	134	114	166	*0.69*	Cross section 11
7130	134	114			End of Bend 7
7971			*155*		Cross section 12
8100	93	160			Beginning of Bend 8
8291	93	160	113	1.42	Cross section 13
8380	93	160			End of Bend 8
8603			148		Cross section 14
9155			108		Cross section 15
10603			141		Cross section 16
11739			120		Cross section 17

4) Collect point velocities at about 5 to 6 points in each vertical and for 20 to 25 verticals in each cross section. Use boat and standard gaging equipment to collect the velocity data.

5) Measure the water surface elevations twice a day on both sides of the river at each cross section with the permanent concrete monuments as bench marks.

6) Repeat the same procedure the following day and continue until velocity distribution data have been collected from all cross sections in each reach.

A crew of three to four persons was needed to collect the velocity data and two other persons were needed to measure the water surface profiles. Measuring the velocity distribution data at each cross section required about 2 hours.

To measure the water surface profiles, the surveyor used a level, a level rod, and the permanent concrete monuments installed on the bank of the river. Figure 9 shows two photographs of the technique used in the field. The surveyor initially took a level reading on the monument (figure 9a) and then another level reading at the water edge (figure 9b). A 24-inch rod with a flat plate welded at one end was hand driven into the soft bank near the water edge making sure that the water surface and the top of the flat plate were at the same level. This flat surface was used as the platform to measure the water surface elevation with the aid of the level rod and the level. With the relative elevation of the water surface with respect to the nearest monument, the water surface profile along the whole length of the reach was easily determined. The data are given in the Appendix.
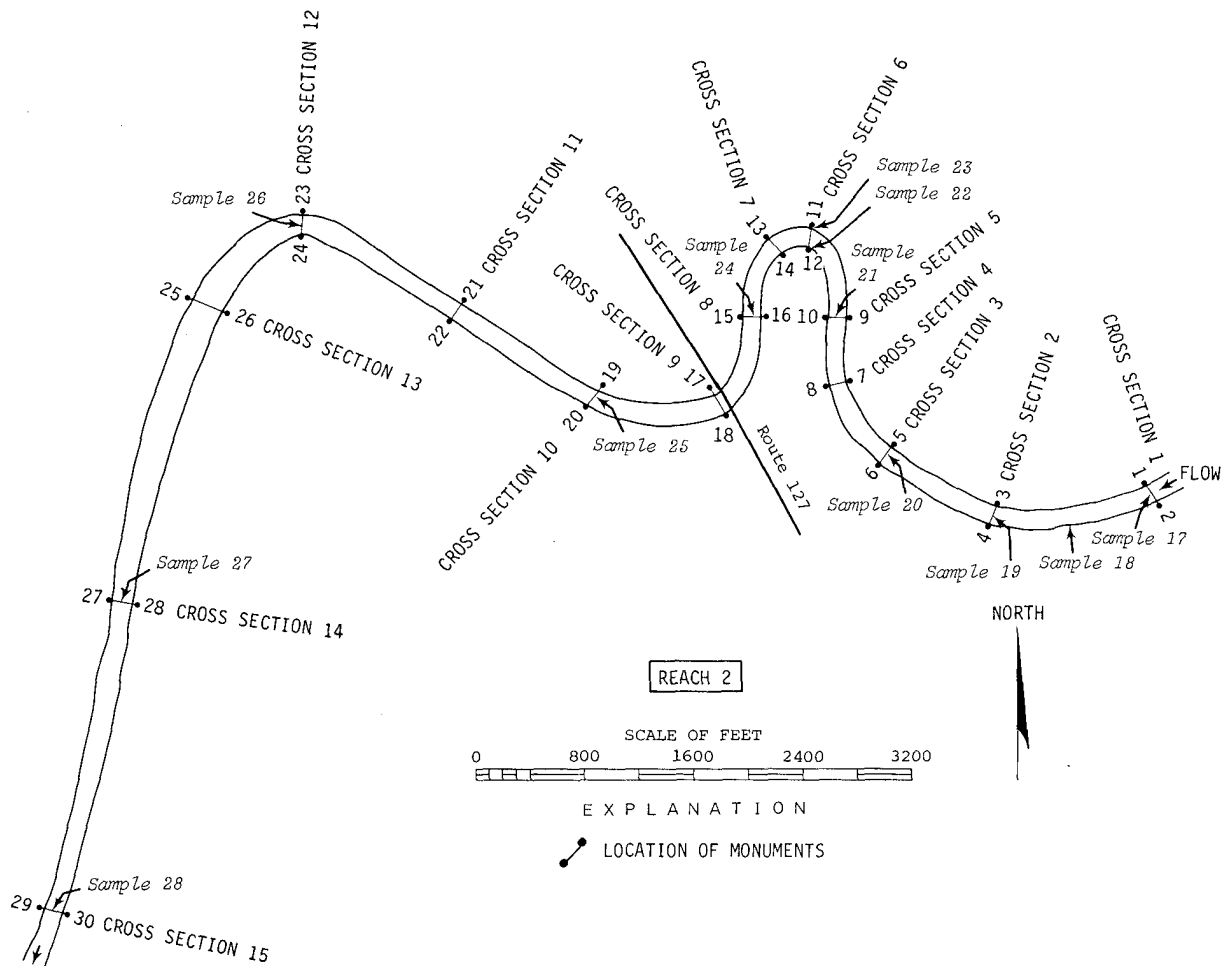
Figure 7. Plan view of Reach 2

Bed and Bank Material Samples

One of the most important physical parameters in an open channel that directly affects the resistance to flow is the nature and distribution of the bed and bank materials. During periods of low flow, three field trips were made to gather the bed and bank material samples from both reaches.

Two different sets of bed and bank material samples were collected. The first set consisted of bed materials collected from the middle of the river at or near each cross section (figures 6 and 7). An Ekman dredge and/or a shovel and a scoop were the only equipment needed to collect the samples. In all 28 bed material samples were collected from the two reaches.

The second set was a special one of bed and bank material samples from two sequences of riffles and pools located in Reach 1. The first sequence of riffle-pool-riffle extended from about 200 feet upstream of the Thompson Mill Bridge to within 300 feet of cross section 2. The second pool-riffle-pool sequence extended from cross sec-

tion 13 to cross section 15. There were other pool and riffle sequences in the two reaches. The two sequences selected for this investigation appeared to have a number of variables which could afford an opportunity to study the low flow hydraulics in a natural river.

Altogether, 51 bed and bank material samples were collected from these two pool and riffle sequences. These samples were collected during low flows when 60 to 70 percent of the bed was dry. Most of the samples were from the bed of the river. Normally three samples were collected from each cross section, one from the center of the river and the other two from each side close to the toe of the banks. Before collecting a sample, the location of the site was selected by visual inspection. The exact position of the site with respect to the ground stations was then determined by using theodolite and stadia measurements. Before collecting the samples, a 2- by 2-foot frame with grid points at 0- to 1-foot intervals was placed on top of the site, and a photograph was taken. Figure 10 shows such a photograph

17

Table 2. Geometric Characteristics of Reach 2

Distance along the centerline (ft)	Total deflection angle or central angle of bend, Δ(degrees)	Centerline radius of curvature, r_C (ft)	Top width, W (ft)	r_C/W	Remarks
0	73	1460	159	9.18	Cross section 1
1200	73	1460	157	9.30	Cross section 2
1660	73	1460			End of Bend 1
1680	75.5	1248			Beginning of Bend 2
2100	75.5	1248	161	7.75	Cross section 3
2760	75.5	1248	171	7.30	Cross section 4
3260	75.5	1248	146	8.55	Cross section 5
3340	75.5	1248			End of Bend 2
3580	183	300			Beginning of Bend 3
3940	183	300	151	1.99	Cross section 6
4222	183	300	158	1.90	Cross section 7
4560	183	300			End of Bend 3
4790			168		Cross section 8
6450			188		Cross section 10
7650			182		Cross section 11
8640	106	700			Beginning of Bend 4
8978	106	700	149	4.70	Cross section 12
9860	106	700			End of Bend 4
12274			188		Cross section 14
14644			199		Cross section 15

Figure 8. Velocity data collection

18

Figure 9. Water surface elevation determination
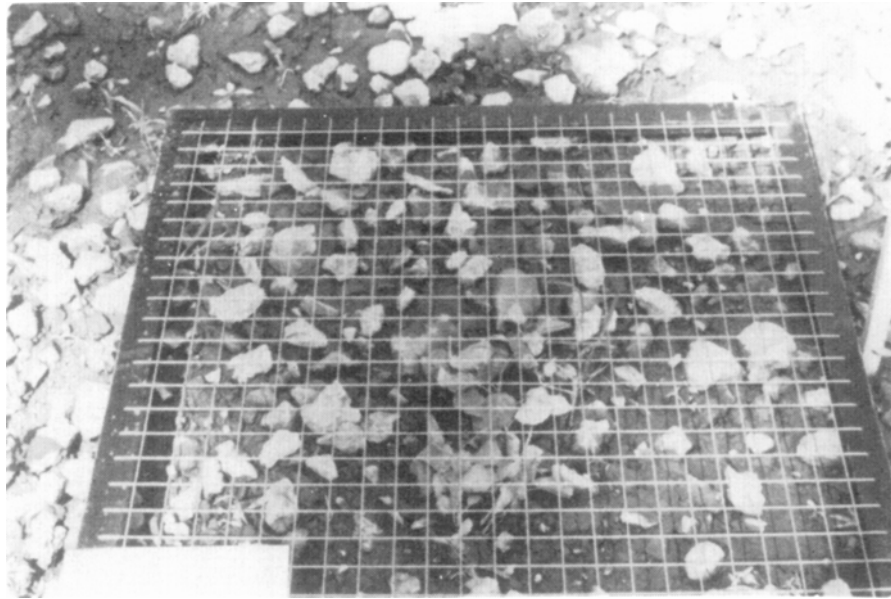
Figure 10. An undisturbed bed material sample

of an undisturbed bed material sampling site. Subsequently, the top layer of the bed material was scraped, bagged, and brought to the laboratory for particle size analysis.

In general, the banks of the river were stable. In some instances, however, the banks were eroding at a steady rate. This was especially true near the outside of the bends. Figure 11a shows the outside bank of the river near cross section 12 (figure 6). The bank erosion at this location is quite vivid. Figure 11b shows the river near cross section 4, Reach 2 (figure 7), looking in the upstream direction.

ANALYSIS AND RESULTS

The results of this research are presented under a number of different headings. This separation of the research results was made in order to be able to discuss the various aspects of flow dynamics in a concise and precise manner. Part of the results of this research has already been presented by Bhowmik and Stall (1978a, 1978b) at two national technical society meetings.

Geomorphology

Physiographically, the Kaskaskia River is located in the glaciated portion of the state of Illinois. The two physiographic divisions through which the river flows are the Bloomington Ridged Plain and the Springfield Plain (Leighton et al., 1948). The drainage pattern in the Bloomington Ridged Plain is in the initial stages of development, whereas the drainage patterns in the Springfield Plain are all well developed.

The reaches selected for the present study are located in the Springfield Plain. Reach 1 is located near the upper end of the plain and Reach 2 is located near its lower end. Geomorphologically, the development of a river basin can be tested by analyzing the partial drainage areas of the river with reference to the respective fall or elevations of the main stem of the river at different locations. Figure 12 shows such a plot for the Kaskaskia River. This type of plot is called either an area-altitude curve or a hypsometric curve. Here, the ratio of the drop of any specified elevation from the highest point in the drainage divide to the total drop of the river is plotted against the ratio of the horizontal area above the respective elevations to the total drainage area of the river. The shape of this curve will vary depending upon the geologic age and the developmental pattern of the river. The shape of the hypsometric curve for the Kaskaskia River indicates that the river has passed through the young stages and is presently in an equilibrium or mature stage of development. The approximate locations of the two reaches are also shown in this figure.

20

Figure 11. Examples of bank erosion: (a) outside bank near cross section 12, Reach 1 and (b) near cross section 4, Reach 2
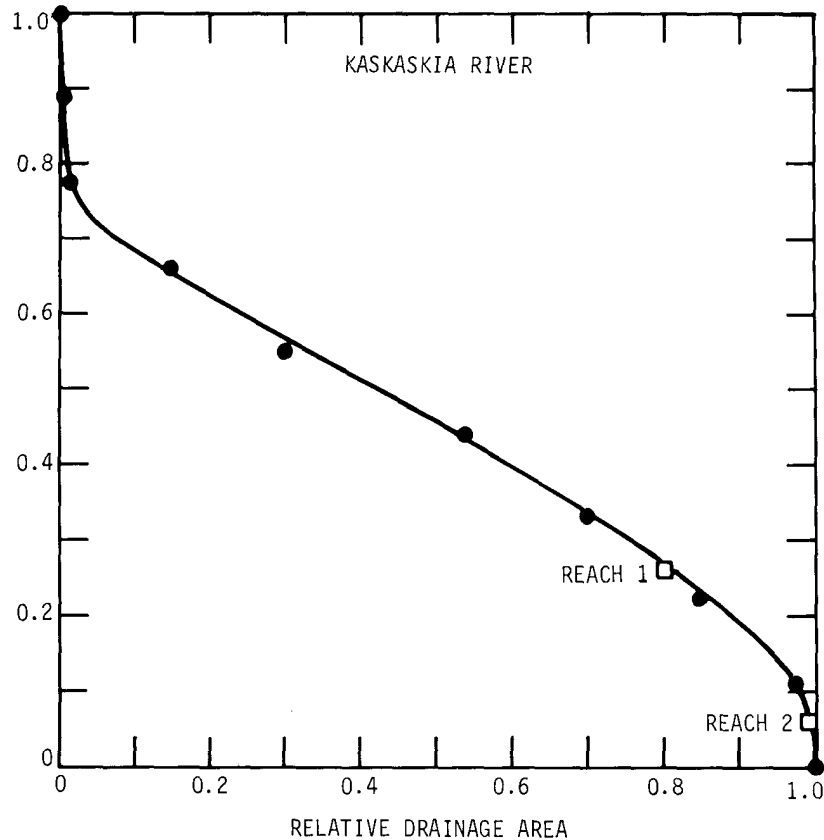
Figure 12. Area-altitude or hypsometric curve for Kaskaskia River

Figure 13 shows the profile of the main stem of the Kaskaskia River. The approximate location of both study reaches is also given here.

Bed Material Sizes

It has already been mentioned that a total of 28 bed material samples was collected from the two reaches. These samples were analyzed to determine the particle size distribution. Figure 14 shows a typical plot of the particle size distribution curve for sample No. 8 from Reach 1 (figure 6). Similar plots were developed for the other 27 samples. Table 3 shows some of the parameters that were determined on the basis of the analysis of particle size of the bed materials. The d_{50} and d_{95} indicate the equivalent particle diameters for which 50 percent and 95 percent, respectively, of the particles are finer in diameter. The standard deviation, σ, is defined by equation 39.

$$\sigma = 1/2 \ [(d_{84.1}/d_{50}) + (d_{50}/d_{15.9})] \tag{39}$$

Here $d_{84.1}$ and $d_{15.9}$ indicate the equivalent particle diameters for which 84.1 percent and 15.9 percent, respectively, of the particles are finer in diameter.

The other parameter shown in table 3 is called the uniformity coefficient U, and is defined by the ratio given in equation 40.

$$U = d_{60}/d_{10} \tag{40}$$

The numerical values of σ and U indicate a measure of the gradation of the particles. Higher values of σ and U will indicate a very well graded material, whereas a lower value of σ and U will demonstrate the uniformity of the particles. The last column in the table shows the general nature of the bed materials. In order to determine if the bed materials for different samples are similar or not, frequency analyses for d_{50} and d_{95} sizes were made, as shown in figures 15 and 16.

Figure 15 shows that 12 out of 16 samples from Reach 1 have d_{50} sizes smaller than 0.42 mm with the lowest value at 0.011 mm (table 3). Basically all these particles are medium to fine sand. For Reach 2 (figure 15) there is some variability in the d_{50} sizes, but they are also sandy. The variability of the median diameters for this reach may have been the result of the sampling of the particles either from pools or riffles. This variability is not the same as the generalized changes that occur in any segment of a river because of its relative position with respect to the total length of the river. The bed materials did not indicate the presence

22
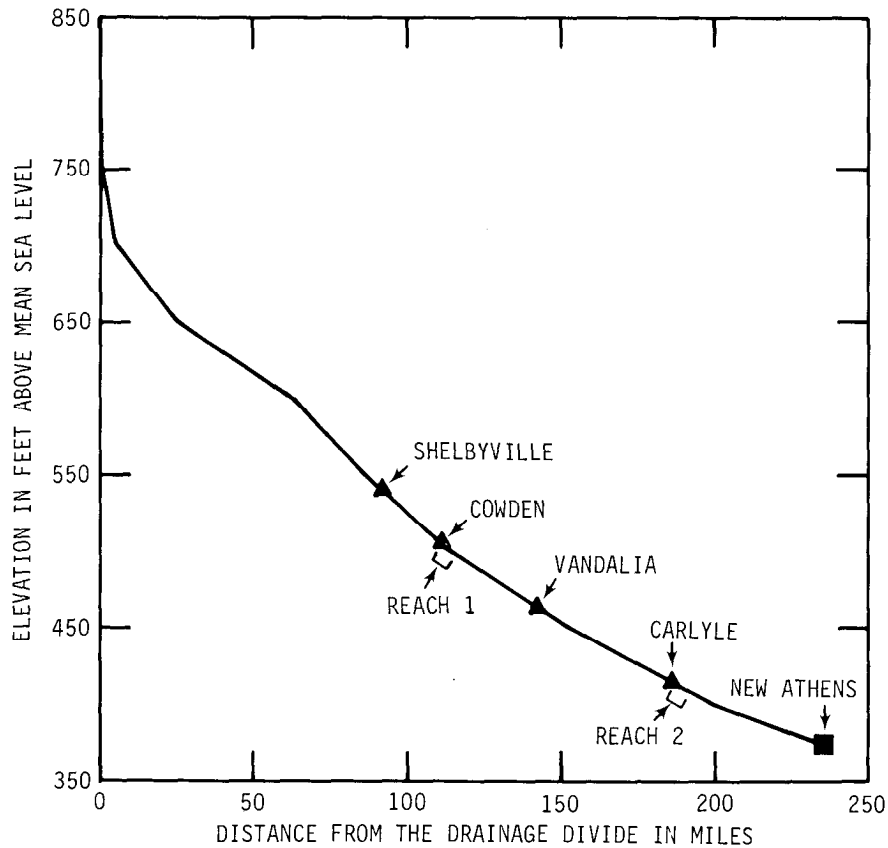
Figure 13. Profile of the Kaskaskia River

of any overall trend for either increasing or decreasing size from upstream to downstream.

The frequency distributions of the d_{95} sizes from both reaches (figure 16) indicate that even the largest sizes from most of the samples are less than about 1.6 to 1.9 mm. This will put most of these particles in the sandy category.

The σ and U values from table 3 indicate that the bed materials from both test reaches are basically well graded materials.

Hydraulic and Geometric Characteristics of the Reaches

Hydraulic and geometric parameters that were either measured or computed from the data collected from the field are shown in tables 4 (Reach 1) and 5 (Reach 2). Data are shown for low, medium, and high flows for both reaches. The date of data collection, computed discharge Q in cubic feet per second based on measured velocity data, cross-sectional area A in square feet, average velocity $\overline{V}$ in feet per second, average depth $\overline{D}$ in feet, and hydraulic radius R in feet are the parameters given.

There was some variability in the measured discharges on the same day at various cross sections because of the changes in the upstream flow rates and the changes in the local inflows. Rather than using an average discharge for all the cross sections based on the measured values of Q at different cross sections for the same day, the measured value of Q at each cross section was used for further analysis.

The cross-sectional shape of the river, a basic hydraulic geometric characteristic, was further analyzed. The cross-sectional shapes in a natural river with erodible bed and banks are neither rectangular, trapezoidal, nor parabolic in shape, Flow hydraulics, bed and bank materials, snags, and human alterations determine the stream's cross-sectional shape. Rozovskii (1957) assumed a parabolic distribution. Other researchers tried to fit either empirical or theoretical shapes based on assumed patterns of secondary circulation or combinations of different dynamic forces, especially in a bend.

Figure 17 shows the nondimensional plots of the cross-sectional shapes for straight reaches and bends from Reach 1. A theoretical curve after Rozovskii (1957) is also shown. It appears that in the straight reaches, if about 55 to 60 per-

23
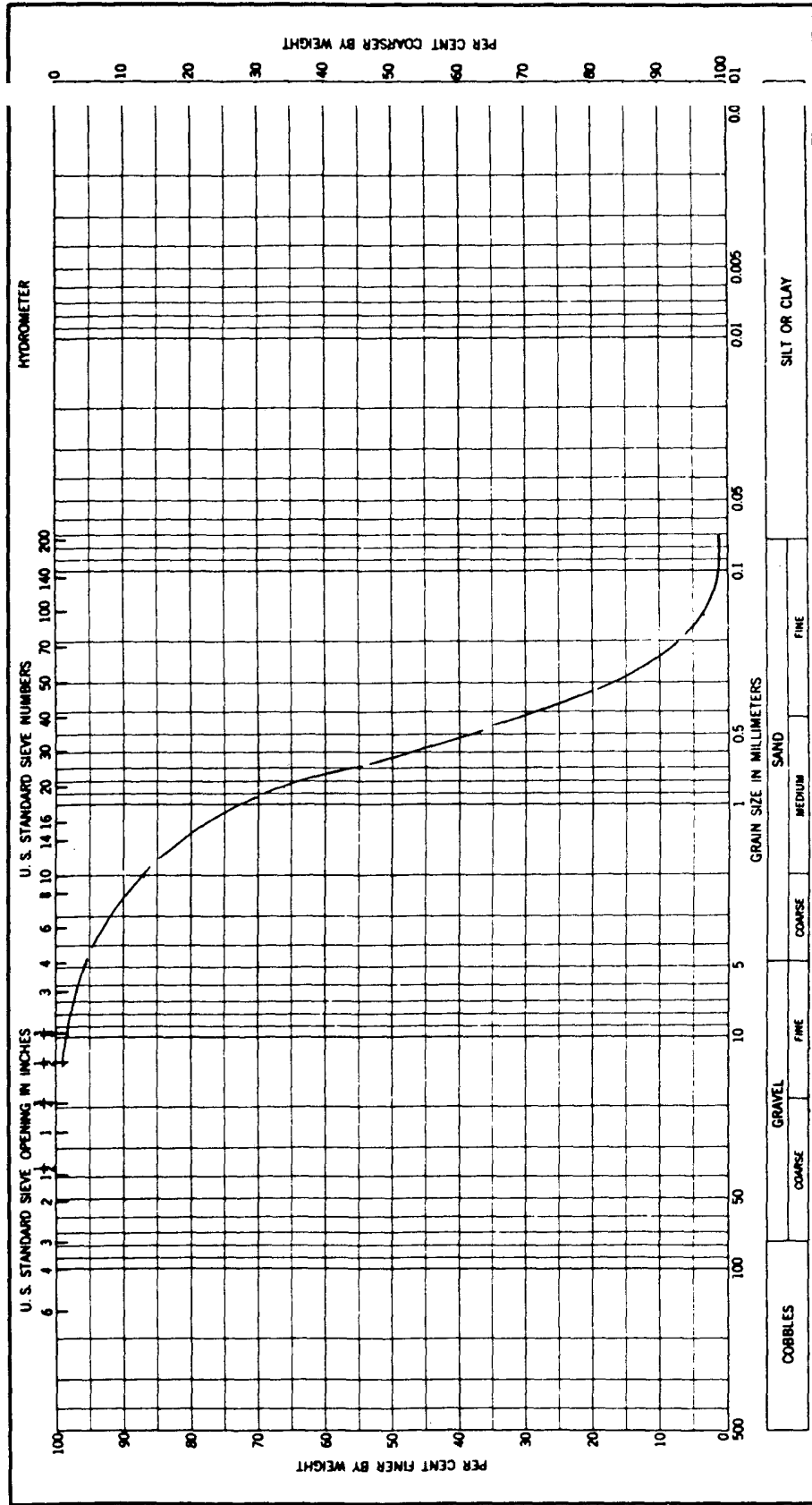
Figure 14. Particle size distribution for bed material sample No. 8

Table 3. Particle Size Characteristics of the Bed Materials, Reaches 1 and 2

Sample number	d_{50} (mm)	d_{95} (mm)	σ	U	Remarks
Reach 1					
1	0.22	0.28	1.41	3.14	Sand
2	0.56	11.0	4.30	3.30	Sand
3	0.37	0.88	1.64	2.35	Sand
4	0.046	0.20	4.50	16.05	Silty loam
5	0.089	0.33	8.42	42.86	Sandy loam
6	0.34	0.70	1.46	2.00	Sand
7	0.84	16.0	6.70	4.48	Sand
8	0.63	4.5	2.44	3.13	Sand
9	0.30	0.94	1.35	1.55	Sand
10	0.023	0.19			Silty loam
11	0.38	0.77	1.40	1.71	Sand
12	0.011	0.047			Silty clay loam
13	2.1	12.0	3.60	7.78	Sand
14	0.37	0.70	1.32	1.58	Sand
15	0.32	1.4	1.76	1.80	Sand
16	0.16	3.3	5.21	6.25	Sand
Reach 2					
17	0.036	0.27			Silty loam
18	0.0048	0.058			Silty clay
19	0.39	1.0	1.60	6.00	Sand
20	0.75	19.0	10.67	15.42	Sand
21	0.28	0.51	1.20	1.47	Sand
22	0.31	0.64	1.25	1.50	Sand
23	0.18	0.29	11.72		Sandy loam
24	0.85	4.1	4.01	24.44	Sand
25	0.32	0.61	1.28	1.62	Sand
26	0.48	4.7	2.80	2.95	Sand
27	0.31	5.0	3.19	2.44	Sand
28	0.22	0.59	2.17	10.45	Sand
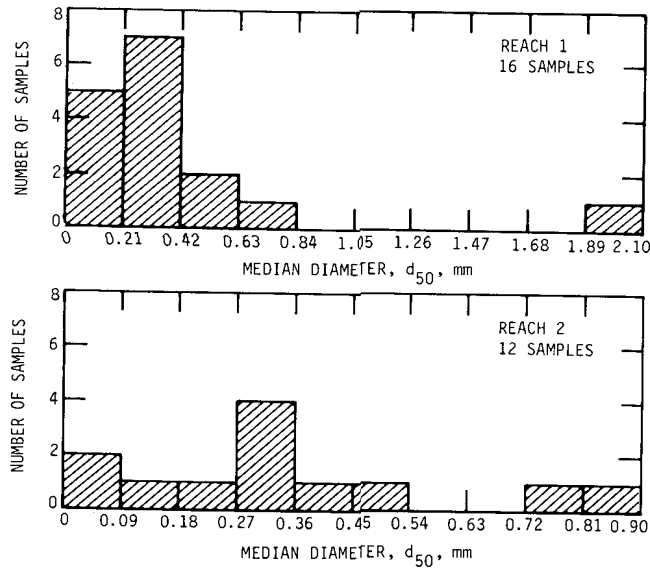
Figure 15. Frequency distribution of d_{50} sizes of the bed materials
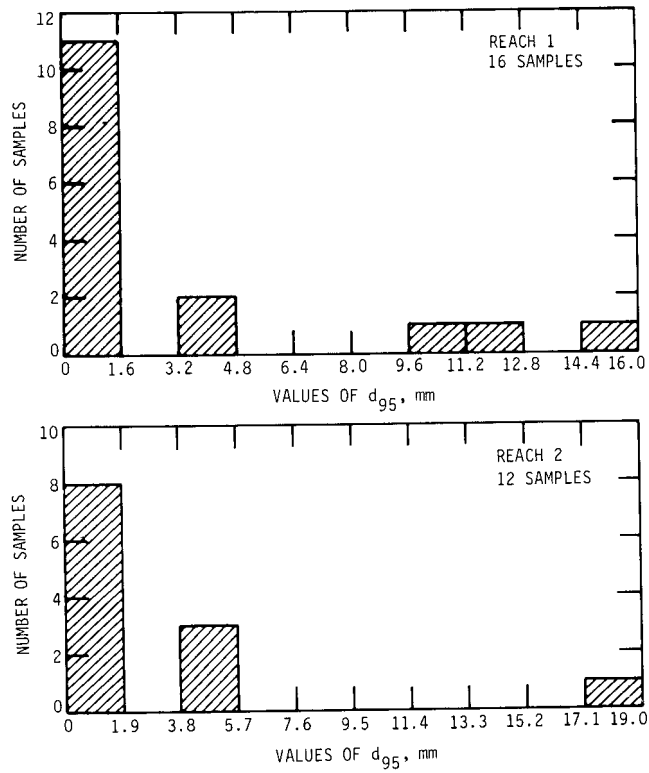
Figure 16. Frequency distribution of d_{95} sizes of the bed materials
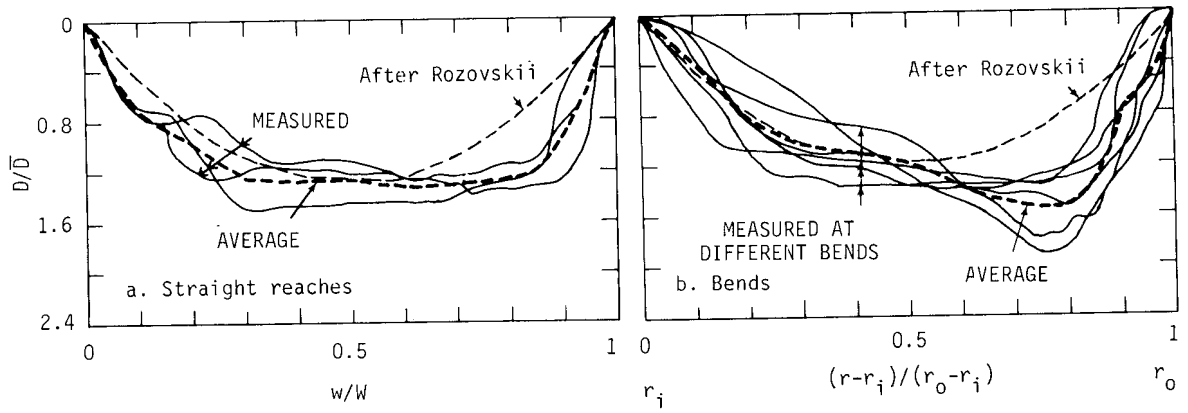
Figure 17. Cross-sectional shapes at Reach 1

26

Table 4. Hydraulic Characteristics of Reach 1

Cross-section number	Date of collection	Discharge Q (cfs),	Area, A (sq ft)	Velocity, $\bar{V}$ (fps)	Depth, $\bar{D}$ (ft)	Hydraulic radius, R (ft)
Low Flow - Collected 1975						
1	10/20	1106	629.0	1.76	6.48	6.17
2	10/20	1058	649.0	1.63	5.69	5.45
3	10/21	1125	623.0	1.81	5.72	*5.56*
4	10/21	1159	622.0	1.86	5.76	5.55
5	10/21	1177	560.0	2.09	6.15	5.71
6	10/21	1170	680.0	1.72	5.67	5.48
7	10/22	1030	605.0	1.70	7.12	6.51
8	10/22	989	563.0	1.76	5.52	5.36
9	10/22	1171	1173.0	1.00	9.24	8.56
10	10/22	900	541.0	1.60	4.96	4.36
11	10/22	953	518.0	1.84	4.39	4.05
12	10/23	984	534.0	1.84	5.18	5.04
13	10/23	933	512.0	1.82	5.82	5.39
14	10/23	945	544.0	1.74	4.57	4.46
15	10/23	954	481.0	1.98	5.12	4.91
16	10/24	950	575.0	1.65	5.13	4.96
17	10/24	939	650.0	1.97	7.30	6.19
Medium Flow - Collected 1977						
1	5/11	1423	817.5	1.74	8.09	7.57
2	5/11	1363	726.3	1.79	6.32	6.10
3	5/11	1378	725.0	1.90	6.47	6.20
4	5/11	1419	773.8	1.83	7.16	6.85
5	5/11	1469	746.3	1.97	7.94	7.31
7	5/12	1495	896.3	1.67	9.34	9.14
8	5/12	1399	712.5	1.96	6.36	6.20
9	5/12	1530	903.8	1.69	8.69	8.07
10	5/13	1391	712.5	1.95	5.24	5.13
11	5/13	1436	775.0	1.85	5.96	5.66
12	5/13	1406	698.8	2.01	6.41	6.19
13	5/13	1454	640.0	2.27	6.53	6.10
14	5/16	1338	687.5	1.95	5.46	5.33
15	5/16	1453	716.3	2.03	7.02	6.57
17	5/16	1401	785.0	1.79	8.01	7.20
High Flow - Collected 1978						
1	3/20	4555	1657.9	2.75	12.37	11.51
2	3/20	4643	1646.7	2.82	11.20	10.56
3	3/20	4674	1830.6	2.55	12.37	11.81
4	3/21	4620	1682.8	2.75	13.15	
5	3/22	3831	1475.9	2.60	12.61	11.46
6	3/21	3366	1668.2	2.02	12.0	10.76
7	3/22	3556	1610.4	2.21	14.25	
8	3/22	3375	1493.9	2.26	10.83	10.16
10	3/23	3532	1694.1	2.09	9.85	9.46
11	3/23	3405	1629.7	2.09	9.88	9.48

Table 5. Hydraulic Characteristics of Reach 2

Cross section number	Date of collection	Discharge, Q (cfs)	Area, A (sq ft)	Velocity, $\overline{V}$ (fps)	Depth, $\overline{D}$ (ft)	Hydraulic radius, R (ft)
Low Flow - Collected 1977						
1	5/17	285	243.8	1.17	1.97	1.94
2	5/17	287	217.5	1.32	2.05	2.02
3	5/17	291	253.8	1.15	2.64	2.59
4	5/17	277	188.8	1.47	2.01	1.97
5	5/17	284	333.8	0.85	3.93	3.80
6	5/18	305	448.8	0.68	4.93	4.78
7	5/17	289	430.0	0.67	5.18	4.94
8	5/18	277	268.75	1.03	2.86	2.80
10	5/18	296	353.8	0.84	3.43	3.34
11	5/19	286	407.5	0.70	4.25	4.12
14	*5/19*	286	387.5	0.74	3.84	3.77
15	5/19	283	400.0	0.71	3.31	3.23
Medium Flow – Collected 1975						
1	12/8	2143	1136.2	1.95	7.95	7.81
2	12/11	2210	971.3	2.26	7.96	7.46
3	12/11	2200	1047.8	2.12	8.45	8.06
4	12/11	2228	1127.3	1.98	8.05	7.81
5	12/9	2169	1141.7	1.76	8.04	8.37
6	12/9	2112	1185.7	1.78	9.34	8.83
7	12/9	2161	1052.3	1.97	8.63	8.22
8	12/9	1583	934.1	1.76	6.77	8.04
11	12/10	2288	1983.2	2.03	8.27	8.02
12	12/10	2025	993.9	2.08	9.04	8.82
14	12/10	2183	1254.9	1.71	9.65	9.53
15	12/10	2165	1409.9	1.53	10.0	9.52
Higb Flow - Collected 1977						
1	12/13	*3999*	1738.9	2.30	11.15	10.48
2	12/13	4013	1491.3	2.69	10.36	9.75
3	12/13	4027	1594.0	2.52	11.81	9.72
4	12/13	3810	1618.3	2.35	10.05	9.30
5	12/14	4013	2001.3	2.01	11.70	11.24
6	12/14	3799	1832.4	2.07	11.90	10.97
7	12/14	3680	1849.5	1.99	12.25	11.21
8	12/14	3573	1783.3	2.00	10.49	9.96
10	12/15	3460	1785.9	1.94	11.20	8.12
11	12/15	3297	1790.1	1.84	12.79	12.01
12	12/15	3461	1731.7	2.00	12.11	11.47
14	12/15	3388	1937.9	1.75	12.46	11.89
15	12/16	3442	2149.6	1.60	13.52	12.80
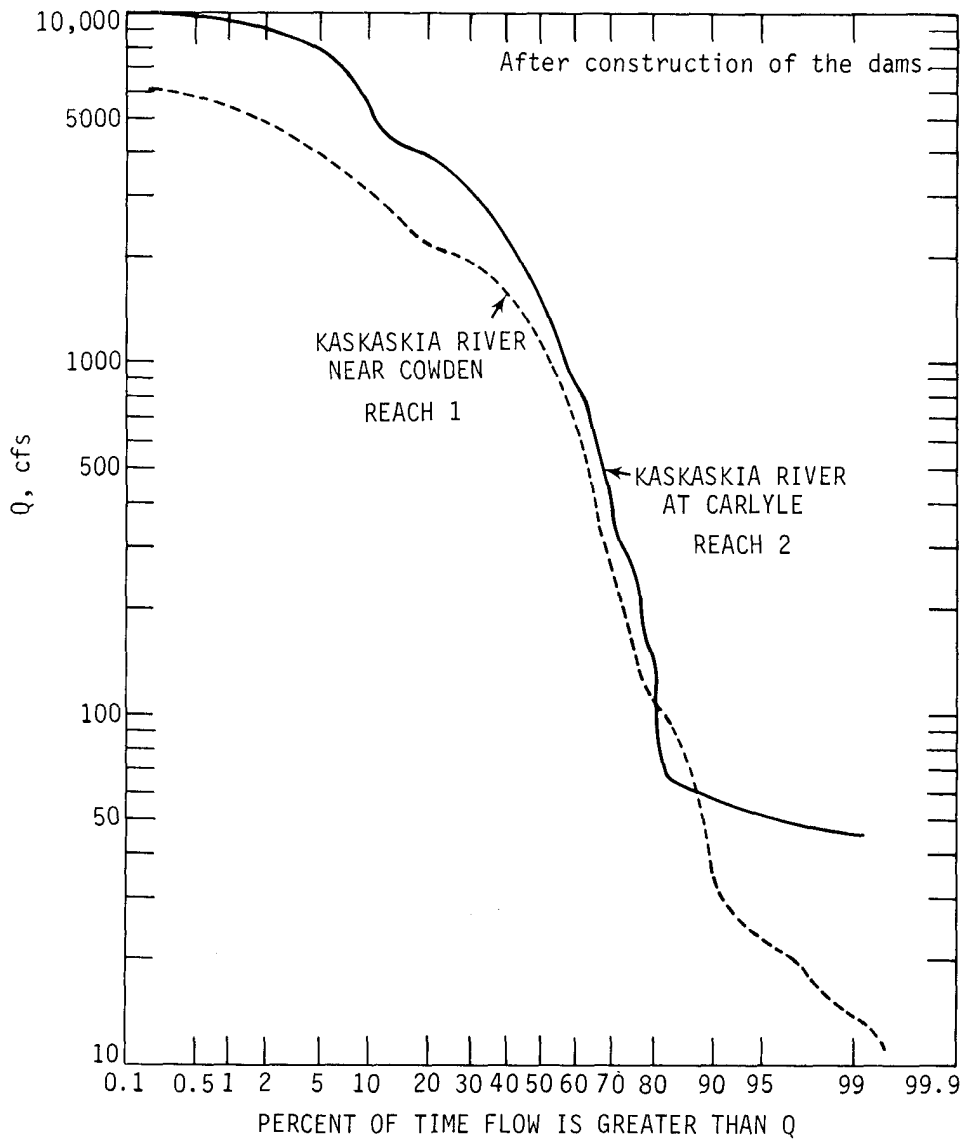
Figure 18. Flow duration curves for Reaches 1 and 2

cent of the bed is assumed to be level, the two natural side slopes can be approximated by Rozovskii's relationship. However, the shape of the section is very close to trapezoidal rather than parabolic. Furthermore, in bends the cross-sectional shape is definitely skewed, with maximum depths occurring near the outside of the bend. The maximum depths varied anywhere from 30 to 90 percent more than the average depths. But the relative magnitudes of the depths near the center of the cross sections for both the straight reaches and bends remained at about 20 percent more than the average depth in the cross section.

This pattern of bed topography may indicate that the lateral shape of the bed in a bend changes about a fulcrum near the centerline. For similar flow and composition of bed materials, the increase in maximum depth near the outside of the bend is associated with a corresponding decrease in depth near the inside of the bend, and this increase and decrease is to some extent proportional to the sharpness of the bend as expressed by the central angle of the bend. Similar types of variability were also observed for Reach 2.

Flow Frequencies

Altogether, seven sets of velocity distribution data were collected from the two reaches. Out of the seven, four sets were collected from Reach 1 and three sets from Reach 2.

Figure 18 shows two flow duration curves for the Kaskaskia River. Both duration curves were developed for

Table 6. Measured Average Discharges and Flow Frequencies for Reaches 1 and 2

Reach number	Date of collection	Measured average discharge (cfs)	Flow frequency in percent of time exceeded
1	7/7/77	58	88
1	10/20/75 - 10/24/75	1040	50
1	5/11/77 - 5/16/77	1420	42
1	3/20/78 - 3/23/78	4000	5
2	5/17/77 - 5/19/77	290	74
2	12/8/75 - 12/11/75	2160	40
2	12/12/77 - 12/16/77	3700	24

discharges occurring after the construction of the dams at Shelbyville and Carlyle (figure 4). One of the curves was developed for discharges below Lake Shelbyville at the U.S. Geological Survey Cowden gaging station just downstream of Reach 1. The other duration curve is for flows just downstream of Carlyle Lake. This duration curve should give a good indication of the variability of the flow at Reach 2. Table 6 shows the flow frequencies and the corresponding average discharges that were measured during the seven data collection trips. As indicated, a wide variety of flow frequencies were covered in the collection of these field data.

For Reach 1, data related to the riffle and pool sequences were collected at the flow of 58 cfs. Detailed water surface profile and velocity data were collected for all other discharges. In this respect, the low, medium, and high flows for Reach 1 will correspond to the discharge of 1040, 1420, and 4000 cfs, respectively. Similarly for Reach 2, the low, medium, and high flows will correspond to the flows of 290, 2160, and 3700 cfs, respectively.

Water Surface Profiles

Water surface profiles were measured daily on both sides of the river at each cross section during each data collection period. Although the release rates from the reservoirs were kept approximately constant, on occasion the discharge changed because of local inflow, with a corresponding change in the water surface elevations. Normally these changes were minimum except during the 1975 trip in Reach 1 (table 4) where a sudden change in the lake level forced a consequent change in the release rates below Lake Shelbyville.

During high release rates from both lakes, water surface elevations fluctuated from day to day. These fluctuations were not only because of the changed release rates, but also because of flooding conditions in the surrounding areas and the influence of the local inflows into the test reaches.

Figures 19 and 20 show the centerline bed profile, thalweg profile, and water surface profiles for low, medium, and

high flow conditions for Reaches 1 and 2, respectively. Cross-sectional data supplied by the surveying crew were used to determine the thalweg and centerline profiles of the beds of the river. In Reach 1 (figure 19) the thalweg and the centerline profiles indicate that the river is flowing through a series of riffles and pools during low flow periods. Similar variability exists to some extent for Reach 2 (figure 20).

The water surface profiles plotted in figures 19 and 20 for three flow conditions show the average water surface elevations at each cross section for a single day during the data collection period. Although there were some minor changes in the water surface elevations from day to day for each data collection trip, the overall patterns for low, medium, and high flows remained identical.

It is interesting to note that the shapes of the water surface profiles for low, medium, and high flows for each reach remained almost the same. During high flows, the river was flowing at or above the bankfull stages at both reaches, whereas for medium and low flows, the discharges were confined within the banks. This may indicate that although the flow conditions in a river may change over the years, some hydraulic parameters such as the shape of the water surface profile may not show any drastic changes.

In Reach 2, there is a rock ledge near cross section 13 (figure 7). This rock ledge appeared to have acted as a control in the river and exerted its effects on the water surface profile even during the bankfull stages (figure 20). Naturally the effect of the rock ledge is more during low flows than during the flooding season. For Reach 1, the drop in water surface profiles remains more or less uniform except near the lower part of the reach where the river is basically straight. Some local changes in the water surface profiles resulted from constraints exerted by local obstructions such as snags and trees.

Velocity Distributions

Vertical Velocity Distribution

The velocity distribution in any vertical changes with the changing characteristics of the turbulence intensity of
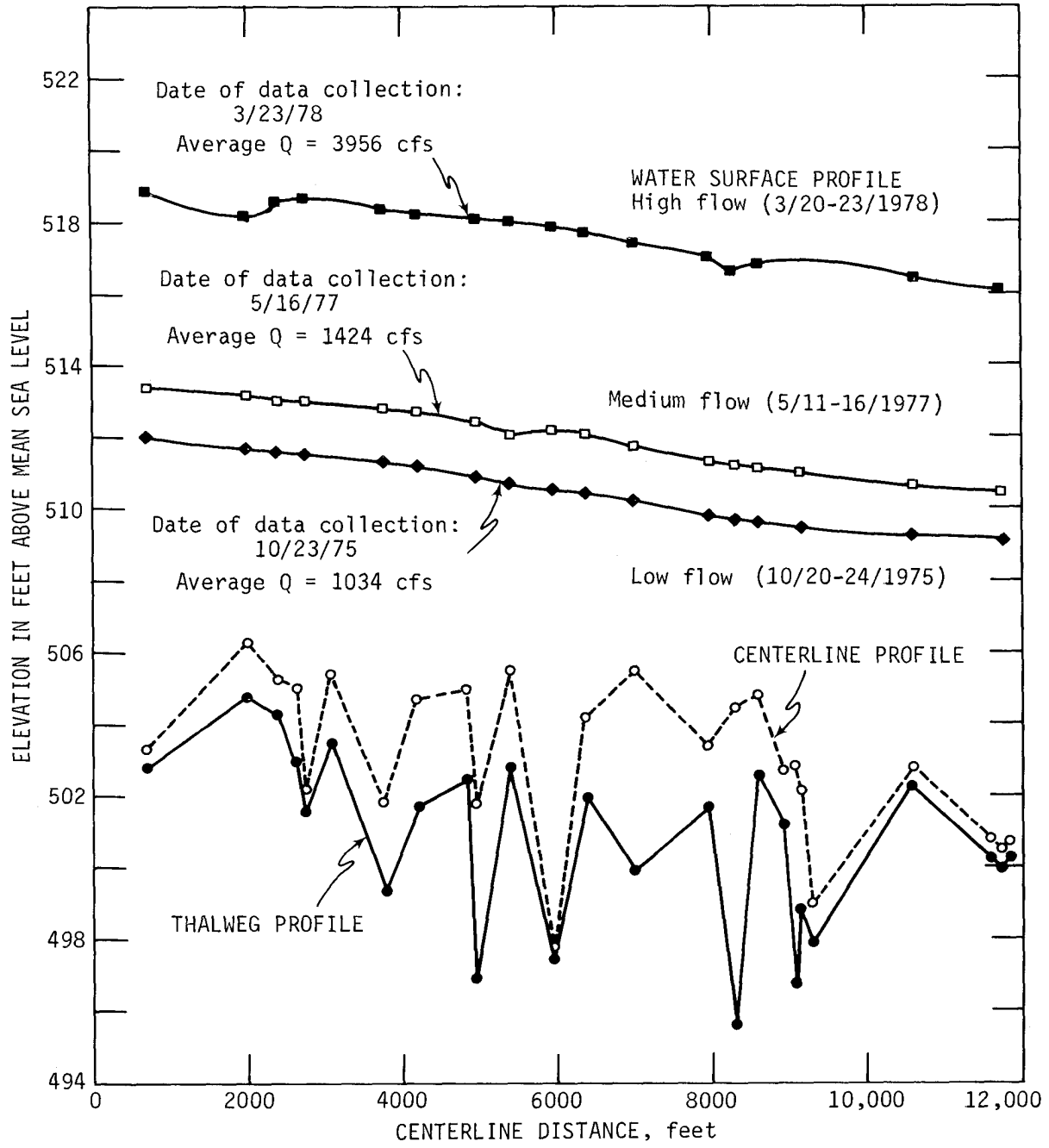
Figure 19. Bed elevation and water surface profiles for Reach 1
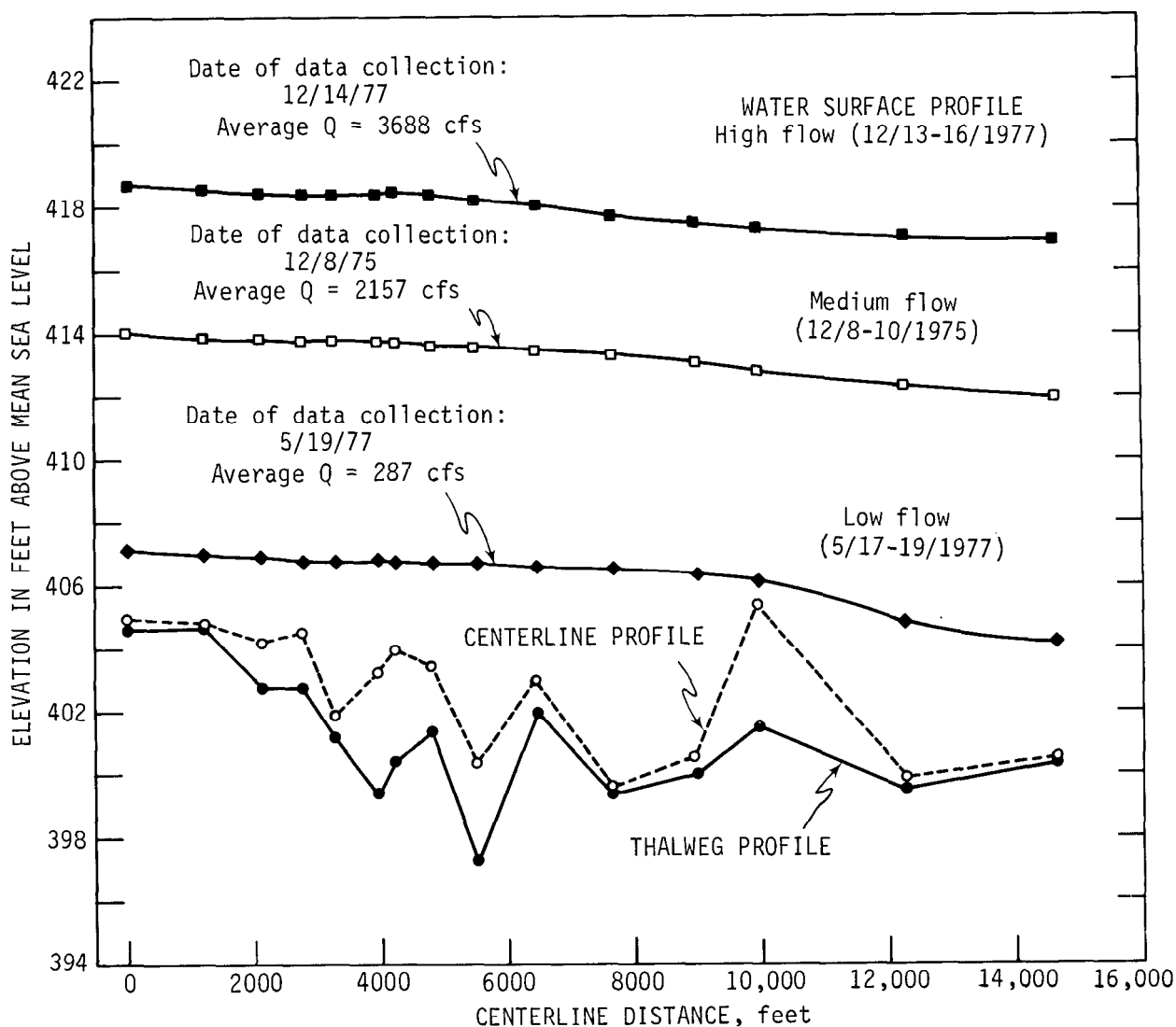
Figure 20. Bed elevation and water surface profiles for Reach 2

the point velocities. However, on the average a general distribution does exist and it can be expressed by an equation similar to the ones given in equations 5 through 8. Figure 21 shows some typical plots of vertical velocity distributions from Reach 2, cross section 15 (figure 7) for high flows. In general, on a semi-logarithmic paper the vertical velocity distribution plots as a straight line indicating the validity of equation 5 for open channel flows at least in the straight portion of the river.

It was previously mentioned that the d_{85} or d_{95} sizes of the bed materials can replace the effective roughness height in equation 5. Table 3 and figures 15 and 16 show that the bed materials of the river at these two reaches consist mainly of sand. Thus the presence of bed forms (figure 2) in the river cannot be ruled out.

Some of the vertical velocity distribution data from the straight reaches were plotted on semi-log paper as $\log(y/d_{95})$

versus v/V_* These points plotted approximately as a straight line (figure 22) and a best fitted equation was developed as follows.

$$v/V_* = 4.65 \log(y/d_{95}) + 3.35 \tag{41}$$

This equation is similar to equation 7 proposed by Leopold et al. (1964) with d_{84} as the roughness element.

Average Velocity in the Individual Verticals

The velocity distribution data used for this research were collected at 5 to 6 points in each vertical. However, it is a standard practice of the U.S. Geological Survey to measure velocities at 0.2 and 0.8 depths in verticals more than 2 feet deep and to take an average of these two values to compute thei average velocity in the vertical. For verticals less than 2 feet deep, normally one measurement is taken at the 0.6
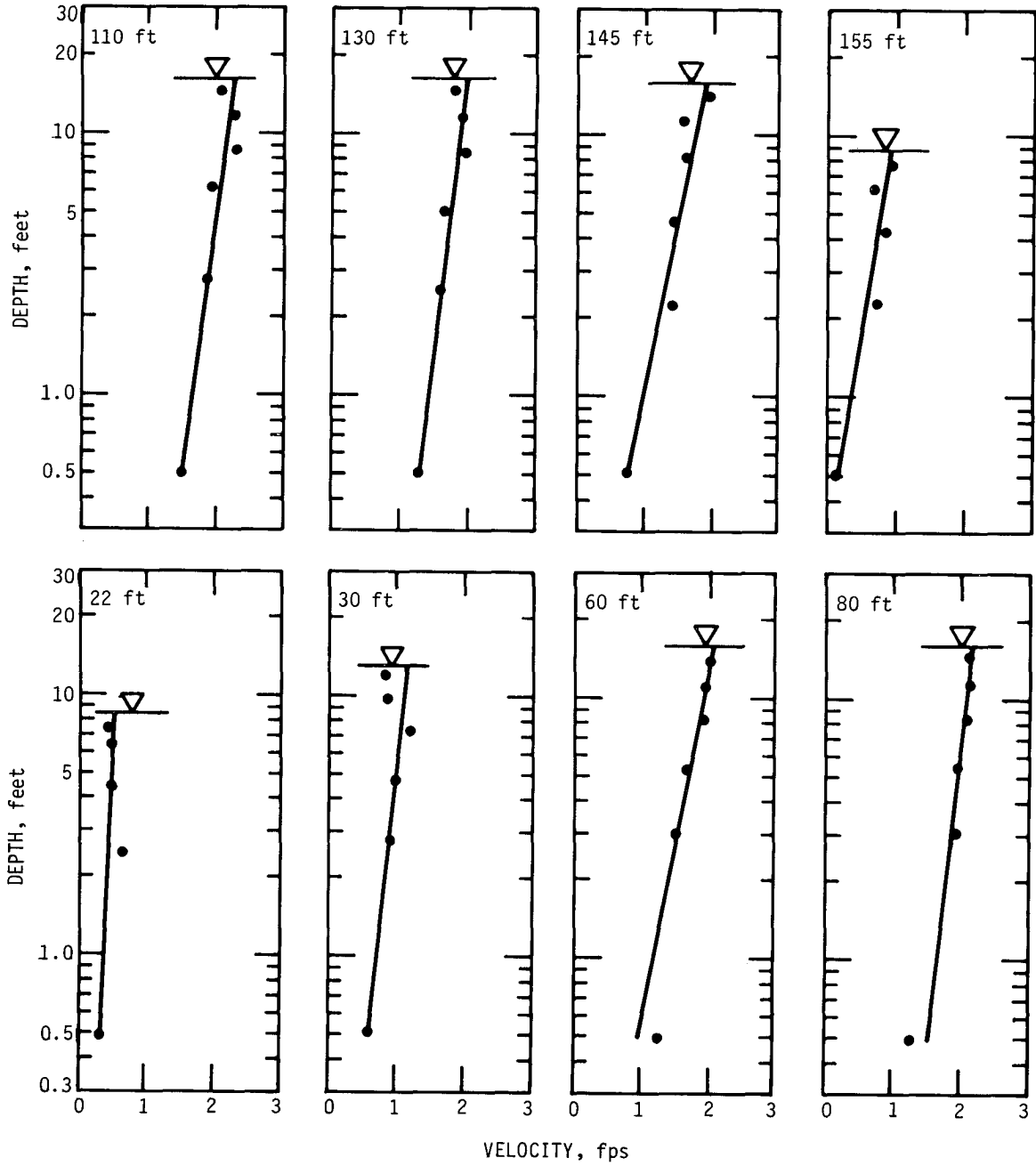
**Figure 21. Typical vertical velocity distributions
(distances shown are from the right side of the river)**
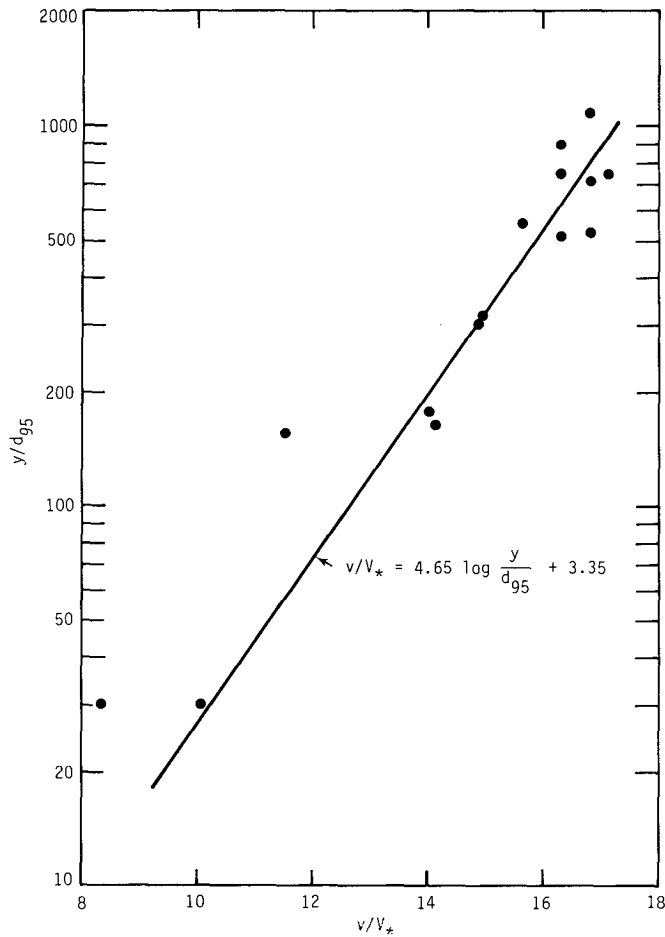
Figure 22. Nondimensional vertical velocity distribution plot

depth and this velocity is assumed to be the average velocity in the vertical.

In order to determine how the average velocities computed from 2 or 1 point measurements relate with the depth-integrated average velocities determined from 5 to 6 point measurements, the average velocities determined by these two methods were compared. Figure 23 shows the comparison between the average velocities for straight reaches. The abcissa shows the average velocities determined by planimetering the area under the velocity distribution plot on coordinate paper and determining the ratio of this area to the corresponding depth in the vertical. For a perfect agreement, all the plotted points should have fallen on a 45 degree line. In general, the average velocities computed from 0.2 and 0.8 depth measurements predicted the velocities by 5 to 7 percent more than the realistic average velocity in each vertical.

A similar plot was also developed for bends and is given in figure 24. Here also, the average velocities determined from 0.2 and 0.8 depth measurements averaged about 5 to 7 percent higher than the average velocities determined

from 5 to 6 point measurements. These two plots show that in some instances, the discharge at a section in a river determined from 0.2 and 0.8 depth measurements may predict the total flow of the river by 5 to 7 percent more than the flow determined from the detailed velocity distribution data.

Average Velocity and Bottom Velocity

In all subsequent analyses, the average velocities used in this report are the velocities that were determined from the depth-integrated velocity distribution plots. The stability analysis of open channel beds and banks requires a knowledge of the bottom velocity or flow velocity close to the bed. In a recent investigation of bank erosion areas along the Illinois River, Bhowmik and Schicht (1979) used the bottom velocity to determine bank stability.

The flow velocities measured at about 0.5 foot above the bed were plotted against the corresponding average velocity in the cross section. This plot indicated that the flow velocity at 0.5 foot above the bed can vary anywhere from 70 to 95 percent of the average velocities in the cross
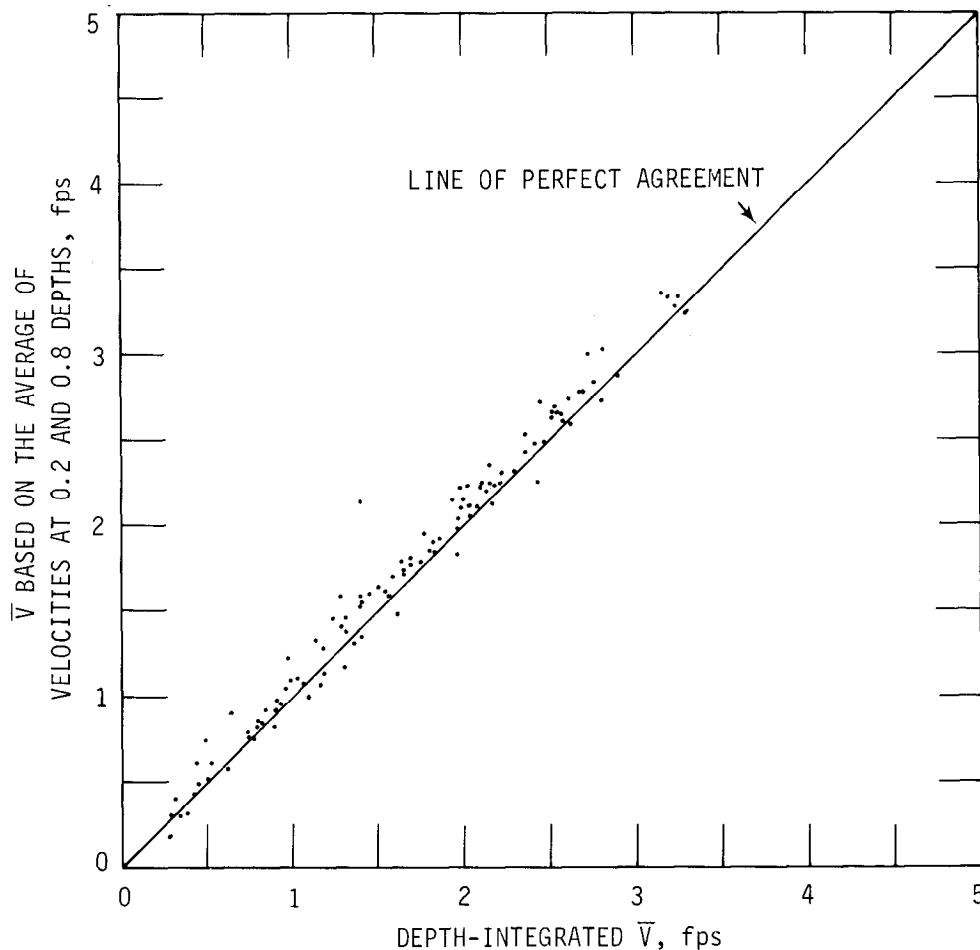
Figure 23. Comparison of average velocities for straight reaches

section. It is suggested that in stability analyses of beds or banks, the critical velocity close to the bed corresponding to any discharge should be taken to be about 95 percent of the average velocity in the cross section. This should give a conservative estimate of the bottom velocity in the stream.

Velocity Structure, Isovels

The point velocity data that were collected from both the reaches for different discharges were made nondimensional by dividing these values with the corresponding average velocity in each cross section. The nondimensional velocities thus obtained were used to draw the isovels or lines of equal velocities at each cross section for all the discharges.

The isovels were plotted on coordinate paper following a systematic procedure. The cross-sectional elevations were plotted always keeping the right hand side of the river on the right side of the graph. The right side of the graph paper

is based on the sense that an observer is assumed to be looking directly on the graph paper. The right side and the left hand side of the river is based on the assumption that one is looking downstream from a vantage point in the middle of the river. Thus all the isovels illustrated will show the left hand side of the river at or near the zero distance on the horizontal scale. This type of uniformity is necessary if any comparative study and/or analyses are to be done from the results obtained at different locations for varying degrees of discharge.

The discussion related to isovels is divided into two subsections, one for Reach 1 and the other for Reach 2.

Reach 1. Figures 25 through 29 show the isovels for Reach 1 for an average discharge of 1040 cfs. This is the lowest discharge for which detailed velocity distribution data were collected. The locations of all the cross sections are shown in figure 6. Note the gradual movement of the core of the highest velocity from the center of the channel in the straight reach toward the outside bank in the bend. A single core of high velocity flow is present at all the

35
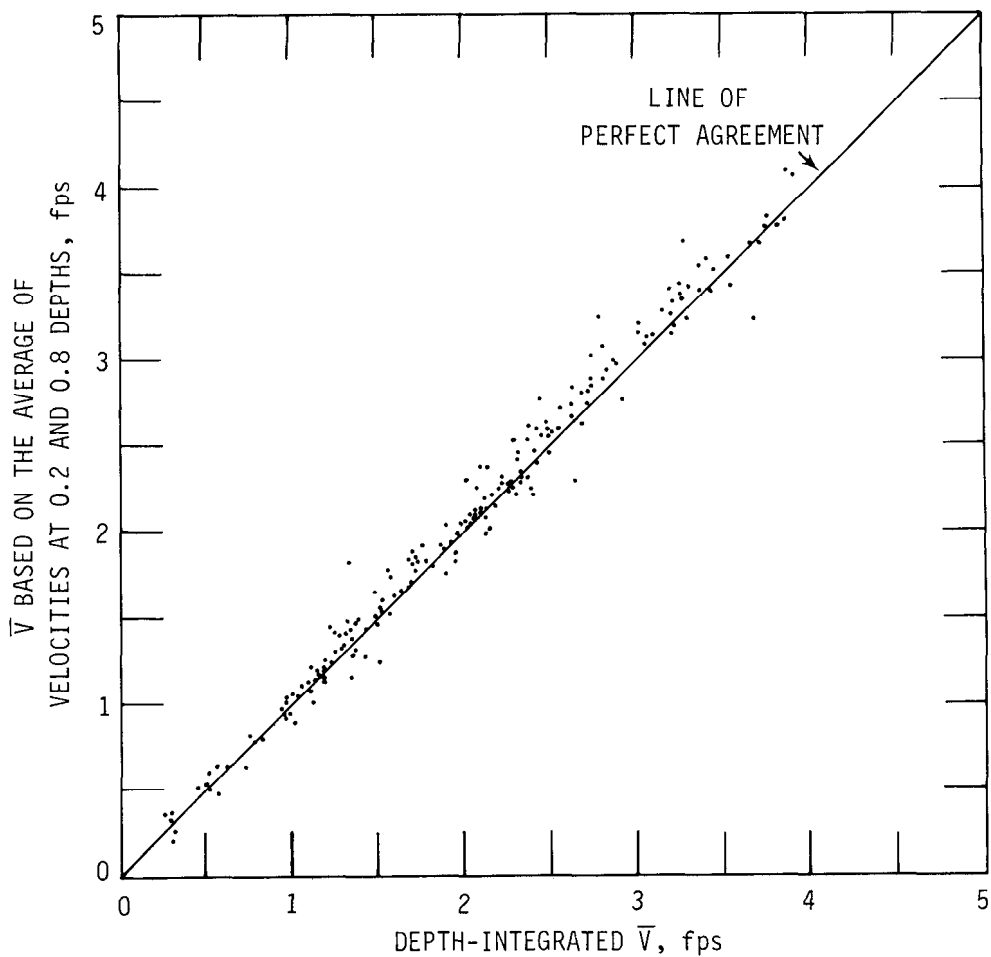
Figure 24. Comparison of average velocities for bends

cross sections except 6 and 7 (figure 26) and possibly 13 (figure 28). Note the approximate symmetrical distribution of the isovels in the straight reaches of the river at cross sections 16 and 17 (figure 29).

The distribution of the isovels and the shapes of the channel are complex in cross sections 5 through 13 (figures 26, 27, and 28). This is because of the presence of a number of sharp bends of opposite direction at this location in the river (figure 6). When the flow enters a bend, the high velocity core moves toward the outside bank and stays close to this bank for a considerable distance. However, if a bend of opposite direction exists just downstream of the first bend, then the core of the high velocity flow located near the outside bank of the first bend will cross over the centerline and move toward the outside bank of the downstream bend near the end of the curved section of the river. This is demonstrated in figure 26 for cross sections 5, 6, and 7 which are located in two consecutive bends of opposite curvature (figure 6).

Because of the piling up of water near the outside bank of the bends due to centrifugal force, sometimes a reversal of flow may occur near the inside bank of the bend. Cross

section 9 (figure 27) shows such a reversal of flow in the bend. Because of the presnece of a portion of eroded bank in the water just upstream of this cross section near the outside bank, a reversal of flow also occurs near the outside bank at this cross section.

The sectional elevation and the isovels at cross sections 10, 11, and 12 (figures 27 and 28) clearly indicate the presence of sand bars in the channel. The sand bar at cross section 11 (figure 28) is in the middle of the stream and the flow is divided into two distinct zones on either side of the sand bar. Isovels at cross sections 12 and 13 (figure 28) and 14 and 15 (figure 29) show the characteristic distribution of velocities in bends with higher velocities, steeper side slopes, and deeper channel staying close to the outside banks. On the other hand, the symmetrical velocity structure about the centerline, typical of the straight reaches, is quite evident at cross sections 16 and 17 (figures 29 and 6).

Figures 30 through 35 show the isovels for Reach 1 corresponding to an average medium flow of 1420 cfs. Velocity distribution data were collected at only 15 cross sections during this data collection trip.

36
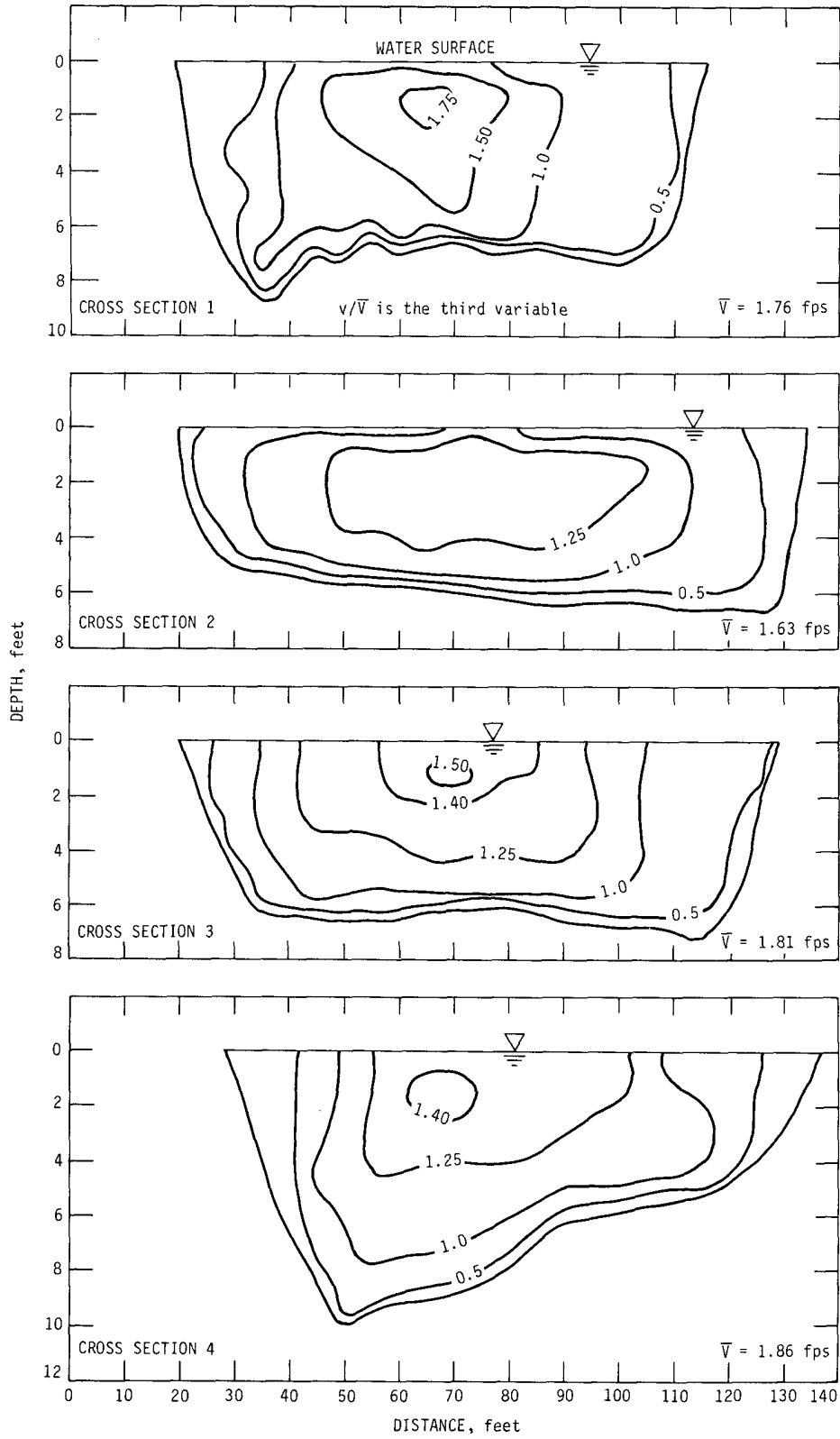
Figure 25. Isovels for cross sections 1, 2, 3, and 4 in Reach 1 at low flow (average Q = 1040 cfs)

Figure 26. Isovels for cross sections 5, 6, and 7 in Reach 1 at low flow (average Q = 1040 cfs)

Figure 27. Isovels for cross sections 8, 9, and 10 in Reach 1 at low flow (average Q = 1040 cfs)

Figure 28, Isovels for cross sections 11, 12, and 13 in Reach 1 at low flow (average Q = 1040 cfs)

Figure 29. Isovels for cross sections 14, 15, 16, and 17 in Reach 1 at low flow (average Q = 1040 cfs)

41

Figure 30. Isovels for cross sections 1, 2, and 3 in Reach 1 at medium flow (average Q = 1420 cfs)

Figure 31. Isovels for cross sections 4 and 5 in Reach 1 at medium flow (average Q = 1420 cfs)

Figure 32. Isovels for cross sections 7 and 8 in Reach 1 at medium flow (average Q = 1420 cfs)

Figure 33. Isovels for cross sections 9 and 10 in Reach 1 at medium flow (average Q = 1420 cfs)

Figure 34. Isovels for cross sections 11, 12, and 13 in Reach 1 at medium flow (average Q = 1420 cfs)

Figure 35. Isovels for cross sections 14, 15, and 17 in Reach 1 at medium flow (average Q = 1420 cfs)

The characteristics of the isovels were almost identical to those present during the low flow conditions. A single core of high velocity flow was present in almost all cross sections except at sections 7 (figure 32), 10 (figure 33), and 11 (figure 34). The locations of the cores of high velocity at section 7 were identical for both the low flow and medium flow conditions (figures 26 and 32). At section 11 (figure 34) it appears that the sand bar present near the middle of the channel has started to divide the flow on two sides of the river in two distinct flow tubes. There was a large fallen tree in the middle of the channel just a few hundred feet upstream of section 11. This tree acted as an obstacle to the flow, reduced the flow velocity in its leeward direction, and accelerated the aggradation of the channel at this location especially during low flows. During low flows, the bulk of the water was flowing through the outside portion of the stream. However, during high flows, the whole width of the river was more or less effective in conveying the discharge. The isovels are symmetrical about the centerline in the straight portion of the river, section 17 (figure 35).

Figures 36 through 39 show the isovels that were developed for Reach 1 corresponding to a high average discharge of 4000 cfs. This discharge is about 4 times larger than the low discharge of 1040 cfs, and more than 2.75 times larger than the medium discharge of 1420 cfs. In many places, the low banks were flooded during this flow. In some instances, short circuiting of the flow on the floodplain was observed, but the total amount of flow short circuiting was estimated to be very small. The floodplains appeared to be acting as a storage reservoir rather than as a conveyance channel. Wherever the flooding of the low lying floodplains was severe, the collection of velocity distribution data was extremely difficult.

The isovels remained similar for low, medium, and high flows at cross sections 1, 2, and 3 (figures 25, 30, and 36). The cores of high velocity flows also stayed more or less at the same relative position in the cross section. These observations were also true for cross section 4 (figures 25, 31, and 37). In all these sections, with an increase in flow depth corresponding to a higher discharge, the core of the high velocity flows moved toward the water surface.

At cross section 5, the core of the high velocity flow was very close to the outside bank during the low and medium flows (figures 26 and 31), but during the bankfull discharge, the core moved down and toward the inside bottom of the section (figure 37). A general shift of the isovels toward the inside bank of the section during this high flow is also noticeable. The effect of the bend near section 4 is to move the high velocity flow toward the outside bank which happens to be the inside bank of the downstream bend close to section 5. At bankfull discharges, the higher momentum of the flow carried the high velocity core emerging from the bend near section 4 farther downstream keeping

it close to the inside bank near section 5 (figure 6) before the effect of the bend at section 5 could shift the core toward the outside bank. This appears to be the main reason why a shift in the core of the high velocity flows was observed between low, medium, and high flows. This also indicates that one cannot always expect to find the high velocity flow near the outside bank of the bend for all possible flow conditions. The flow frequency, the hydraulic characteristics of the channel, and the antecedent conditions in the upstream channel determine the severity of the effects of any bend.

At cross section 6 (figure 37) only one core of high velocity flow is present instead of the two cores that were present during low flow (figure 26). This core of high velocity flow is now closer to the bed and near the right hand side of the bank. This is obviously the after-effects of the upstream bend near section 5 which has effectively moved the high velocity flow toward the outside bank. The core of high velocity flow remains close to the right bank downstream.

Isovels at cross section 7 (figure 38) show the presence of two cores of high velocity flows similar to those present during low and medium flows (figures 26 and 32). The core with the higher velocity is now located close to the bed and near the inside bank of the river. The position of this core is a definite indication of the existence of a higher momentum of flow which has carried the high velocity core in a rather short and straight route to section 7 from section 6. A considerable area of this cross section near the inside bank shows the presence of a large amount of reversed flow. The bend near section 7 is extremely sharp, resulting in a greater centrifugal force. High momentum associated with higher discharge and the sharpness of the bend have helped to concentrate the flow near the outer two-thirds of the channel. The combined effects of these factors is to force a reversal of flow near the inside bank of the river (figure 6).

Isovels at cross section 8 (figure 38) show a single core of high velocity flow near the left hand side of the river. Obviously it is an indication of the effect of the bend near section 7 which has moved the high velocity flow toward the outside bank of the river. This relative movement of the high velocity flow is similar to that observed at section 6 (figure 37). With an increase in discharge, a significant amount of lateral movement of the high velocity flow toward the left side of the river is also quite noticeable (figures 27, 32, and 38).

Isovels for cross section 10 are shown in figure 38. Note the gradual movement of the core of the high velocity flow from near the centerline for low flow (figure 27), to the right side of the river for medium flow (figure 33), and finally very close to the right side of the river for high flow (figure 38). This progressive lateral movement of the high

Figure 36. Isovels for cross sections 1, 2, and 3 in Reach 1 at high flow (average Q = 4000 cfs)

Figure 37. Isovels for cross sections 4, 5, and 6 in Reach 1 at high flow (average Q = 4000 cfs)

50

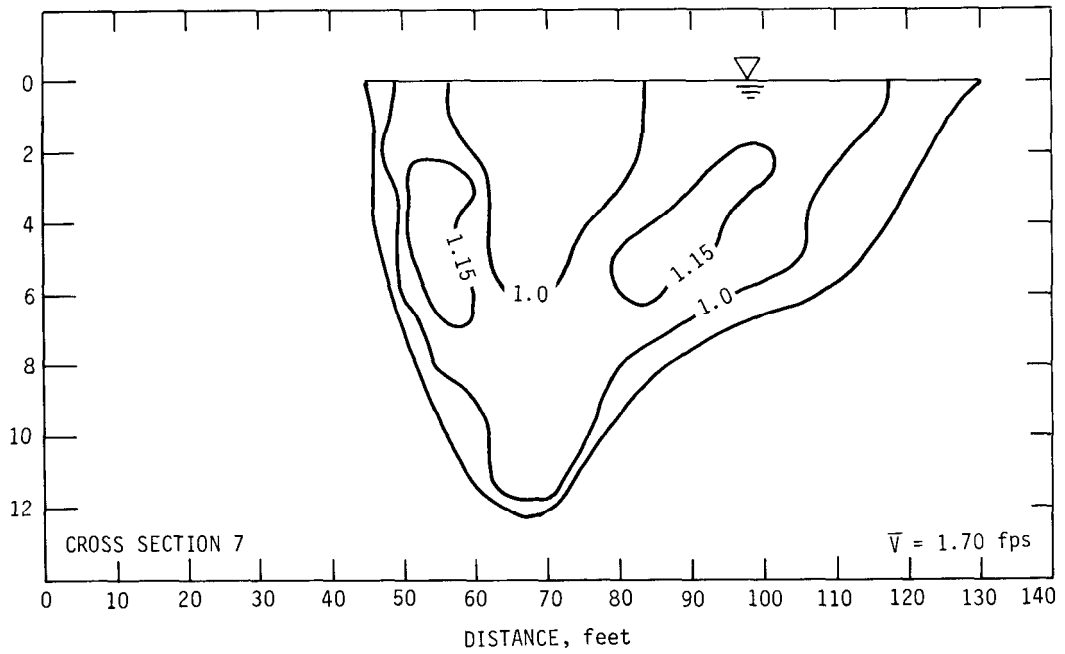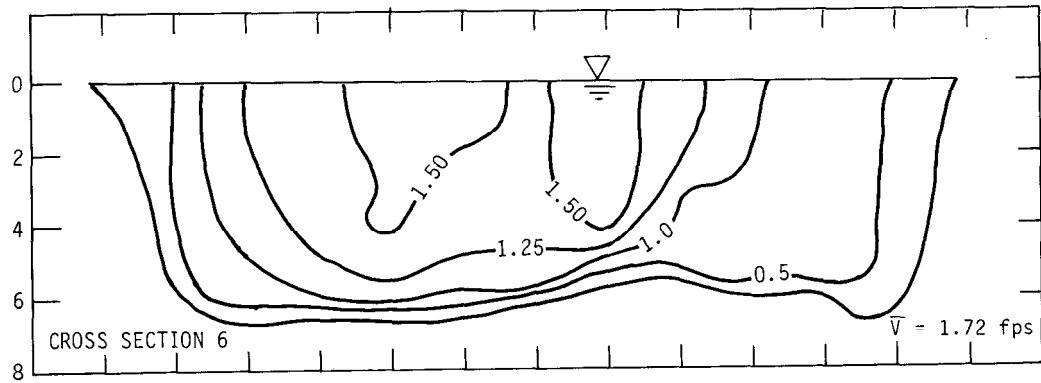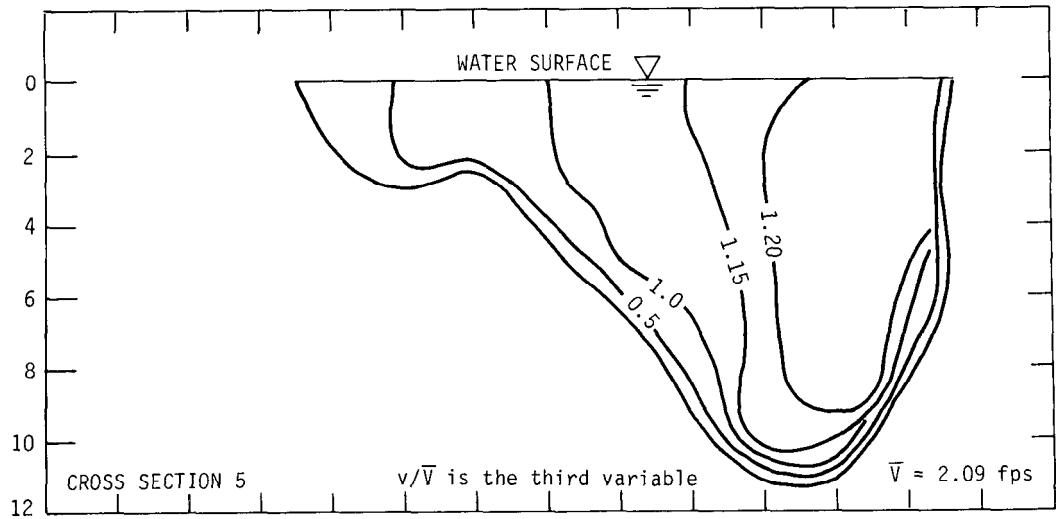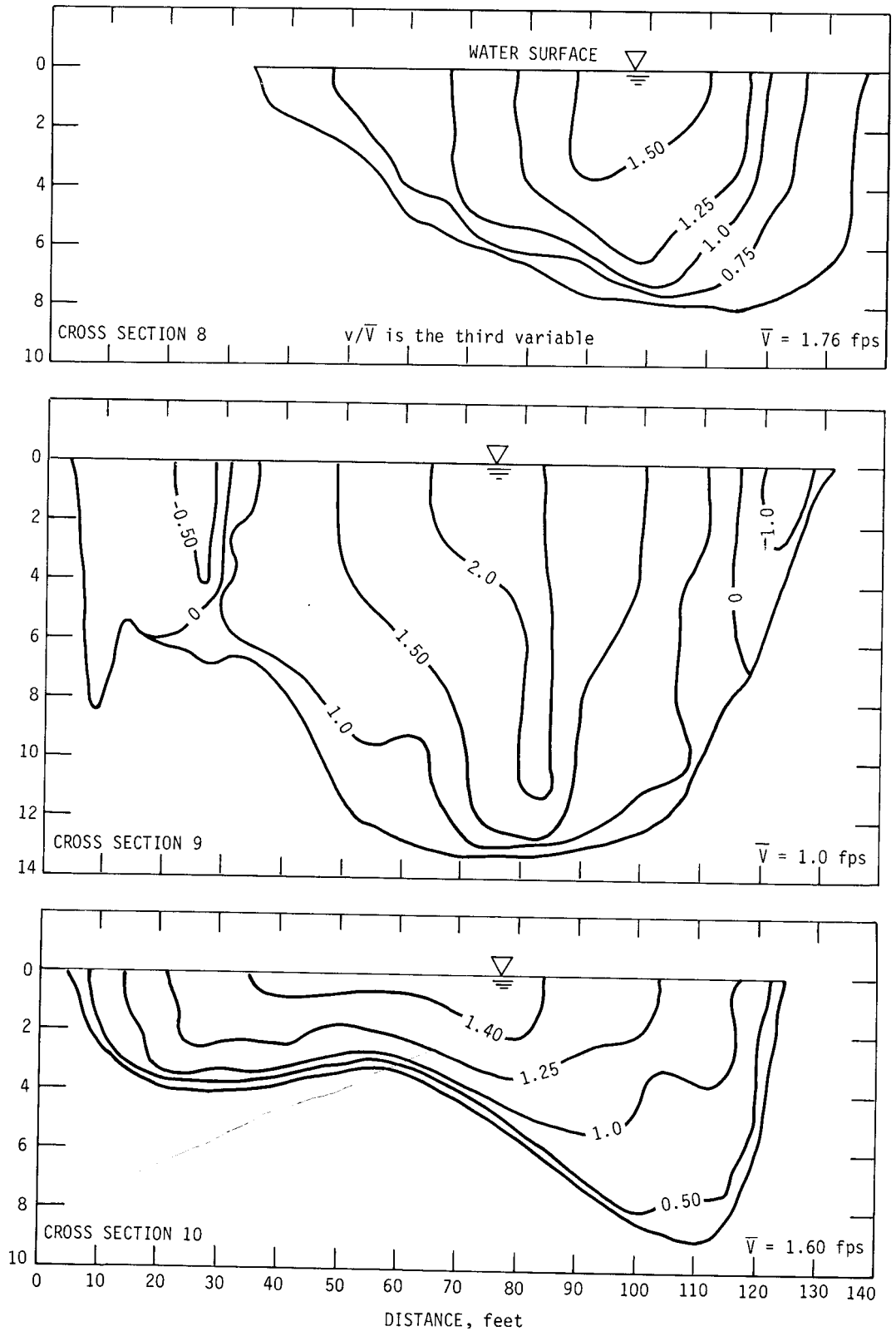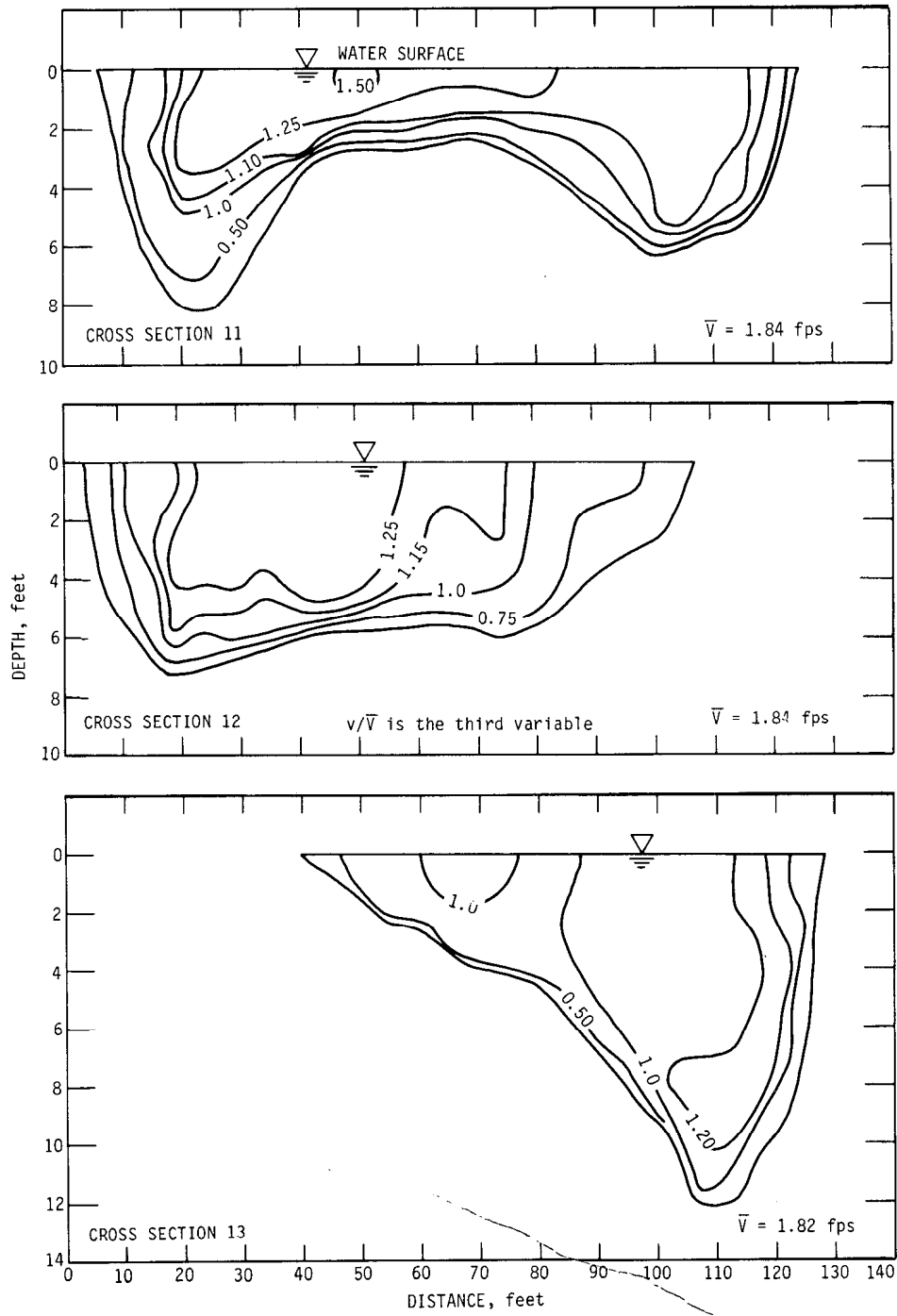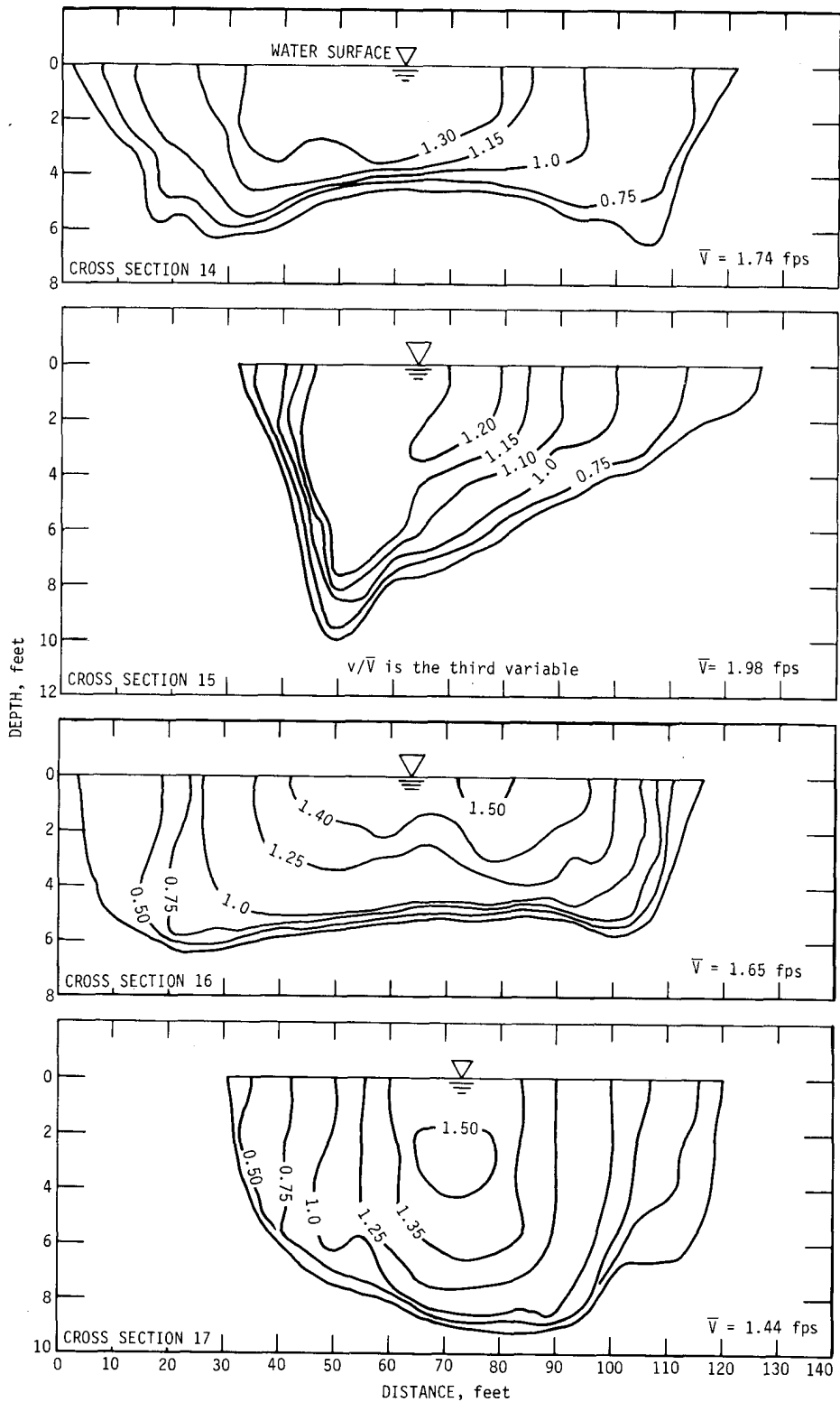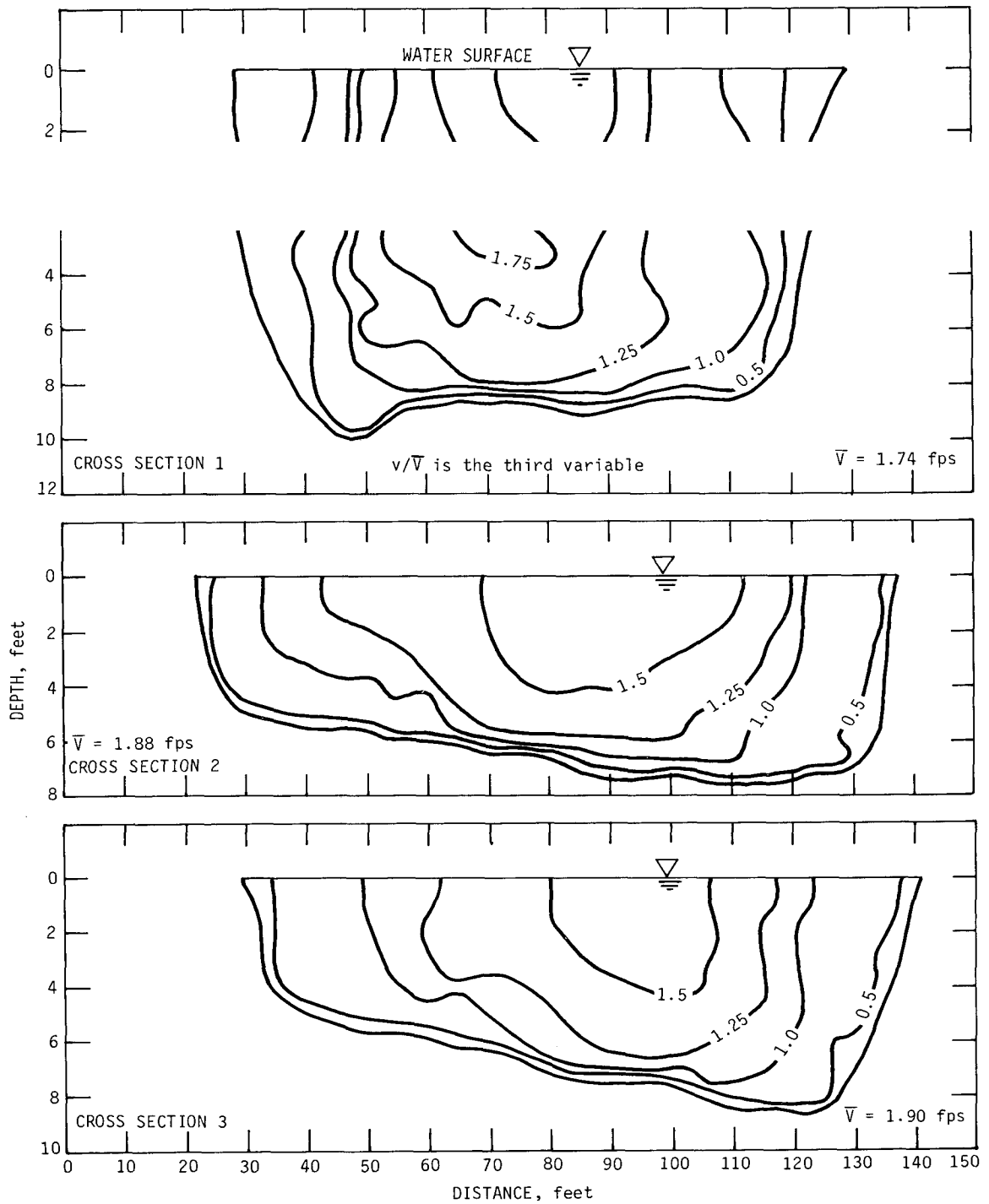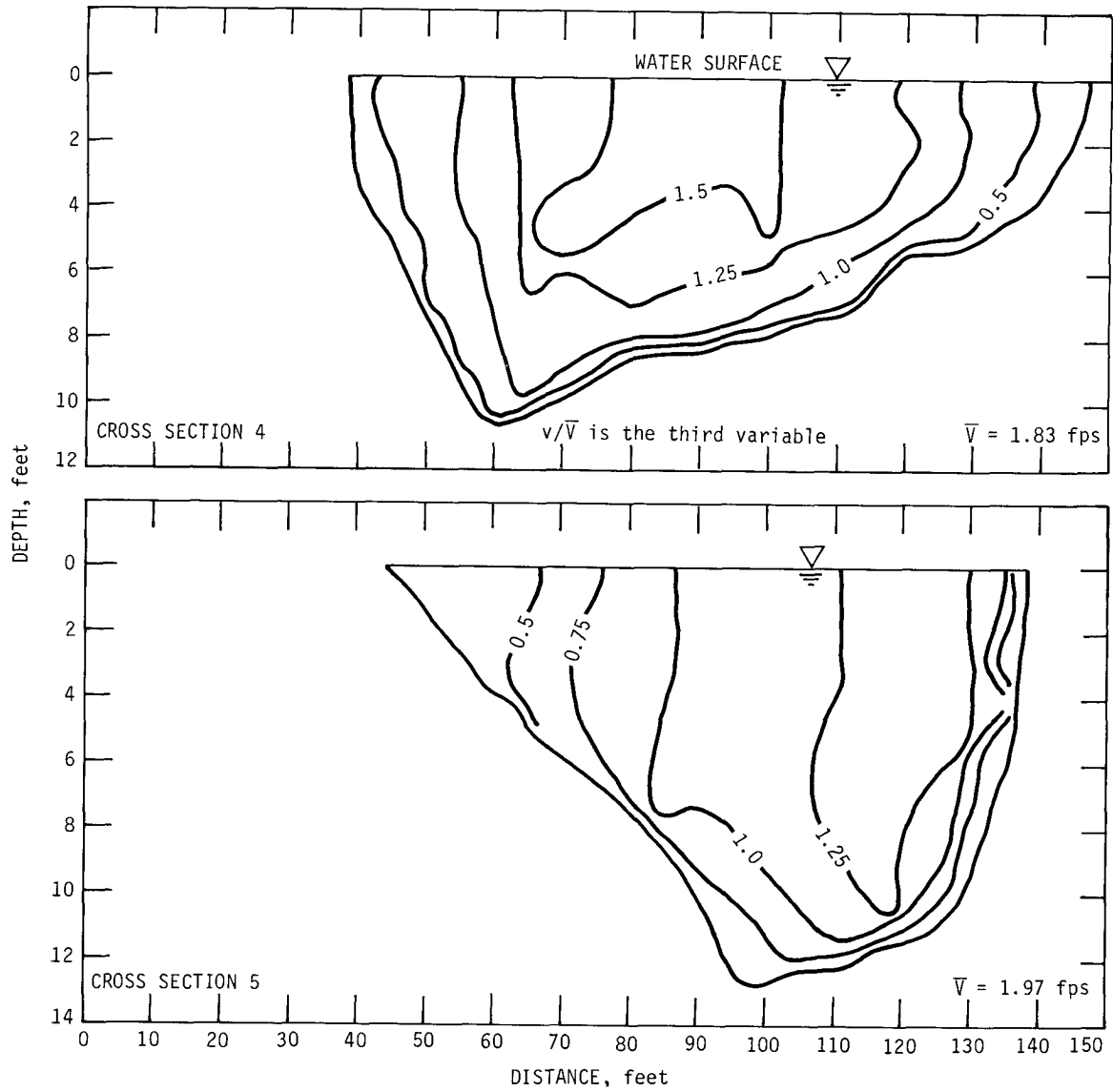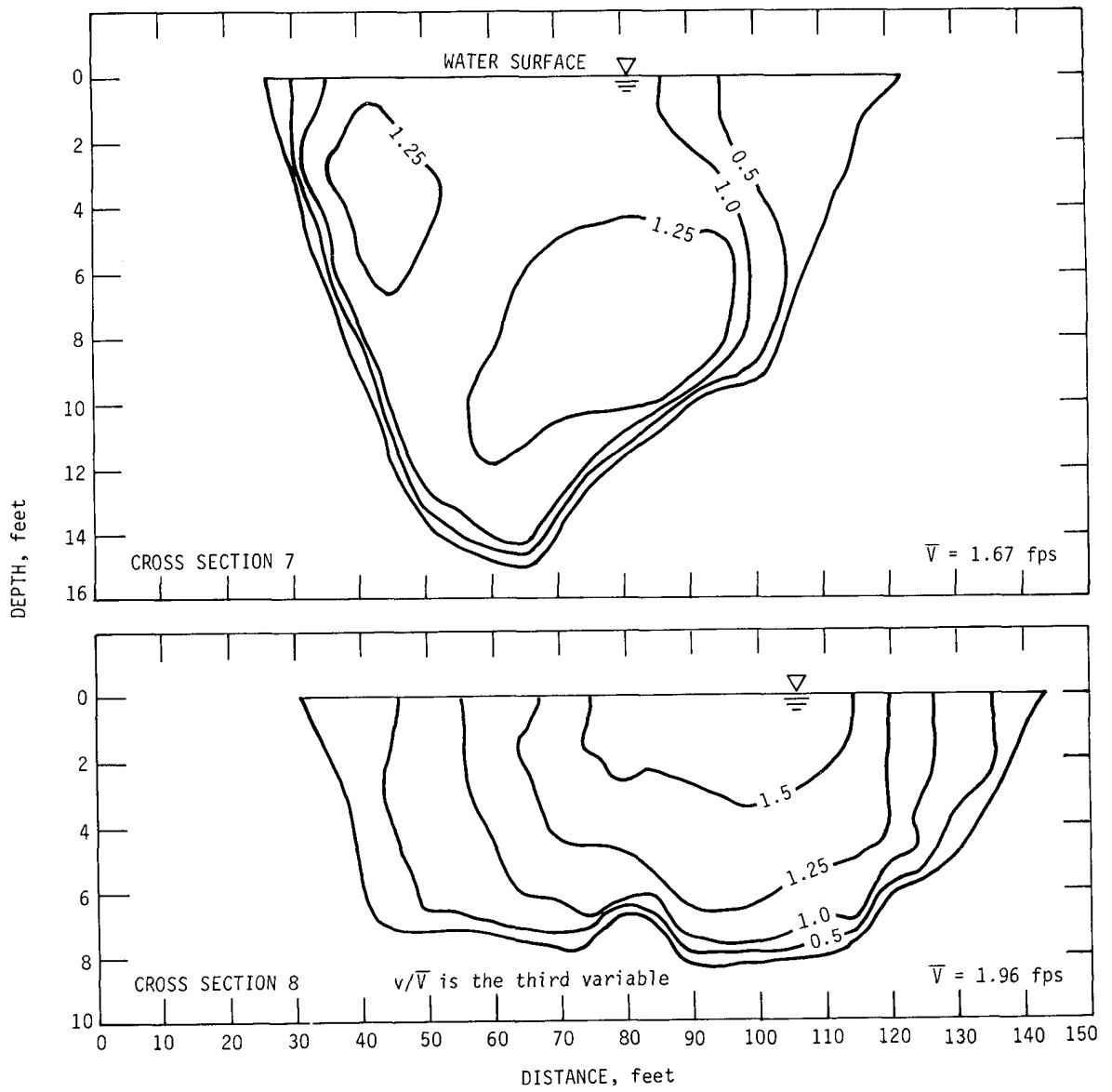Figure 38. Isovels for cross sections 7, 8, and 10 in Reach 1 at high flow (average Q = 4000 cfs)
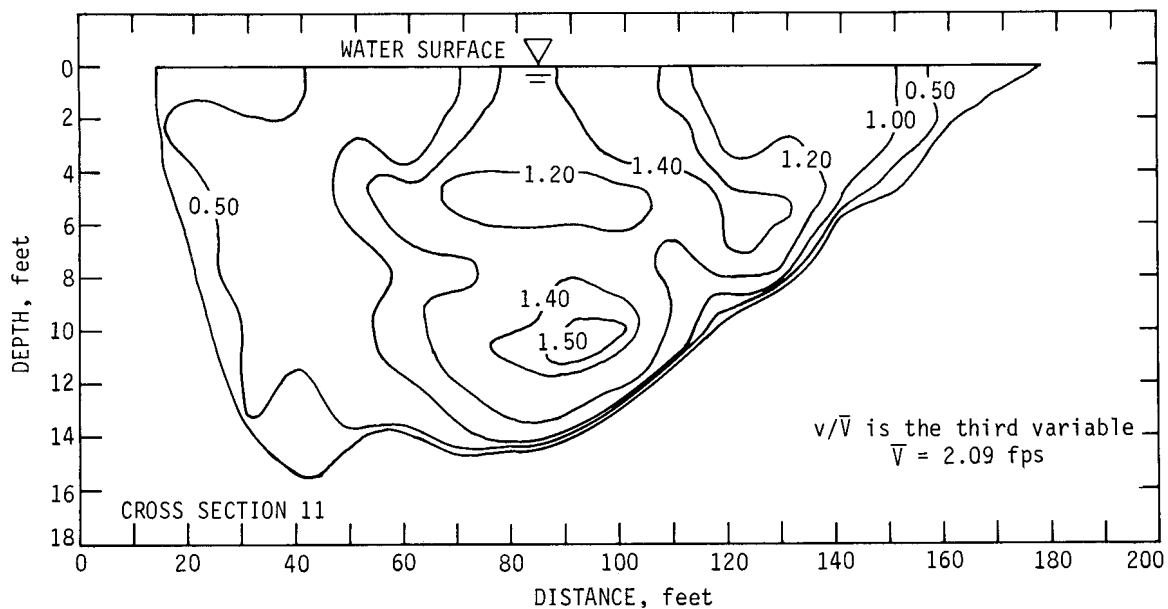
Figure 39. Isovels for cross section 11 in Reach 1 at high flow (average Q = 4000 cfs)

velocity flow at this cross section has resulted from a proportionate increase of the bend-effect near section 9 with an increase in discharge.

These and the other previous observations should make it clear that the flow characteristics in a river will change in both time and place as the discharge increases from low to higher values. An increase in discharge not only increases the depth of water in a river, but it may also shift the potential for bed and bank erosion. Velocity distributions at cross sections 8 and 10 for various flow conditions show that the bank which is stable and is not attacked by high velocity flow during low and medium flows, may be subject to the scouring action of high velocity flows during bankfull discharges as a result of its relative position in the river.

The bed of any river with a movable bed will shift under changing flow conditions. Examination of the isovels at cross section 11 shows this quite clearly. Isovels at section 11 are shown in figure 39. A comparison of the cross-sectional shapes at this location for low, medium, and high flows (figures 28, 34, and 39) indicate that the geometrical shape of the cross section has changed dramatically during the high flow. The hump or the sand bar that was present near the center of the channel during low and medium flows is now completely absent. The bed material at this location is composed of sand (table 3). It appears that during high flows, the river has worked over its bed, completely scoured the sand bar and has developed a new shape at this location that is similar to a shape that can be expected in a bend for a river with a movable bed. The differences in elevations between the highest point of the hump near the centerline of the river and the lowest point on the bed near

the left bank are 5.8 feet for low flow (figure 28), 5.4 feet for medium flow (figure 34), and only 1.8 feet for the high flow (figure 39). Section 10 which is just upstream of section 11 (figure 6) also showed a similar variation. The differences in elevation at section 10 between the hump and the lowest point on the bed varied from 6.4 to 6.0 to 3 feet corresponding to the low, medium, and high flows in the river.

This observation related to the variability and changing shapes of the cross sections of natural rivers has considerable practical implications. When a flood discharge is routed through a stream to determine the flood elevations, the cross-sectional shapes of the river are assumed to be the same as those measured during low flows. In many cases, the river will scour its bed and banks, will change the shape of the river, and may increase or decrease the cross-sectional areas during flood flows. These changes will undoubtedly have an effect on the water surface elevations of the river. Thus, the flood elevations, say for 100-year discharges, that are presently determined by various agencies for floodplain management may not always yield an accurate elevation corresponding to the discharge in the river. Hydraulics of flow, transport of sediment, and the characteristics of the changing bed forms in a sand bed channel must be considered in any actual determination of flood elevations.

A comparison of the isovels developed for the three different discharges has brought out some interesting phenomena. Generally, the average velocity in each cross section increased with an increase in discharge. But the numerical values of the ratio of the highest velocity to the average velocity, taken from the plots of the isovels corresponding to

52

Table 7. Relative Magnitudes of the Maximum Nondimensional Velocities, Reach 1 (Figures 25 through 39)

Cross section	Average Q=1040 cfs		Average Q=1420 cfs		Average Q=4000 cfs,	
	$\bar{V}$ (fps)	Maximum $v/\bar{V}$	$\bar{V}$ (fps)	Maximum $v/\bar{V}$	$\bar{V}$ (fps)	Maximum $v/\bar{V}$
1	1.76	1.75	1.74	1.75	2.75	1.60
2	1.63	1.25	1.78	1.50	2.82	1.55
3	1.81	1.50	1.90	1.50	2.55	1.50
4	1.86	1.40	1.83	1.50	2.75	1.50
5	2.09	1.20	1.96	1.25	2.60	1.40
6	1.72	1.50			2.02	1.50
7	1.70	1.15	1.66	1.25	2.21	1.50
8	1.76	1.50	1.96	1.50	2.26	1.50
9	1.0	2.0	1.69	1.25		
10	1.60	1.40	1.95	1.40	2.09	2.00
11	1.84	1.50	1.85	1.25	2.09	1.50
12	1.84	1.25	2.01	1.50		
13	1.82	1.20	2.27	1.25		
14	1.74	1.30	1.94	1.50		
15	1.98	1.20	2.02	1.20		
16	1.65	1.50				
17	1.44	1.50	1.78	1.50		

each cross section for various discharges, did not show any significant variation as the discharge increased from low to medium to high flows.

Table 7 shows the average velocity $\bar{V}$ and the ratio of $v/\bar{V}$ for each cross section for the three discharges for which data have been collected. Except for cross section 10, the ratio $v/\bar{V}$ at each section for three discharges remained practically unchanged. This is quite remarkable considering that the discharge has increased four times from low to high flows. This constancy of the ratio $v/\bar{V}$ for different discharges at each section remained true for both the straight reaches and bends. Thus, it appears that the maximum velocity in a cross section can be estimated with relative ease and confidence once the average velocity is either known or computed from discharge and cross-sectional areas. The average value of $v/\bar{V}$ for all the data shown in table 7 is 1.45. This means the average of the maximum velocities can be expected to be 145 percent of the average velocity in any cross section. The averages of all the average velocities at all cross sections for low, medium, and high flows were found to be 1.75, 1.89, and 2.41 fps, respectively.

Reach 2. Isovels similar to the ones shown in figures 25 through 39 for Reach 1 have also been developed for Reach 2. The procedure used was the same as that described for Reach 1.

Figures 40 through 44 show the isovels at various cross sections for Reach 2 corresponding to the low flow of 290 cfs. This was one of the lowest flows for which velocity dis-

tribution data were collected. The frequency of occurrence of this flow is 74 percent (table 6).

A single core of high velocity flow existed at all cross sections during this low flow condition. Quite evident even during such low flow conditions are the shifting of the high velocity core from near the center at sections 1 and 2 toward the outside bank at sections 3 (figures 40 and 7) and 4 (figure 41), the shifting back to the middle of the channel at section 5 (figure 41) where it starts to cross over toward the other bank at section 6, and finally the crossing over and clinging to the outside bank of the bend at section 7 (figure 42). Section 8 is more or less located at a crossing between two bends (figure 7) and the isovels at section 8 (figure 42) show some symmetry in their distribution.

The cross-sectional shape at section 10 (figure 43) shows the effect of the bend near section 9 (figure 7). The isovels are not quite symmetrical at this location. Sections 11, 14, and 15 are located in the straight portion of the river, and section 12 is located at the end of a long straight reach and near the entrance of a bend. The isovels at sections 11, 14, and 15 (figures 43 and 44) show the symmetrical velocity distribution typical of any straight reach of the river.

Figures 45 through 48 show the isovels for this reach for the medium discharge of 2160 cfs. The frequency of occurrence of this flow is about 40 percent (table 6). This medium discharge is about 7½ times the low flow of 290 cfs for which velocity data were collected at this reach.

The isovels at sections 1 and 2 (figure 45) are identical to those present during low flow (figure 40). Isovels at sec-
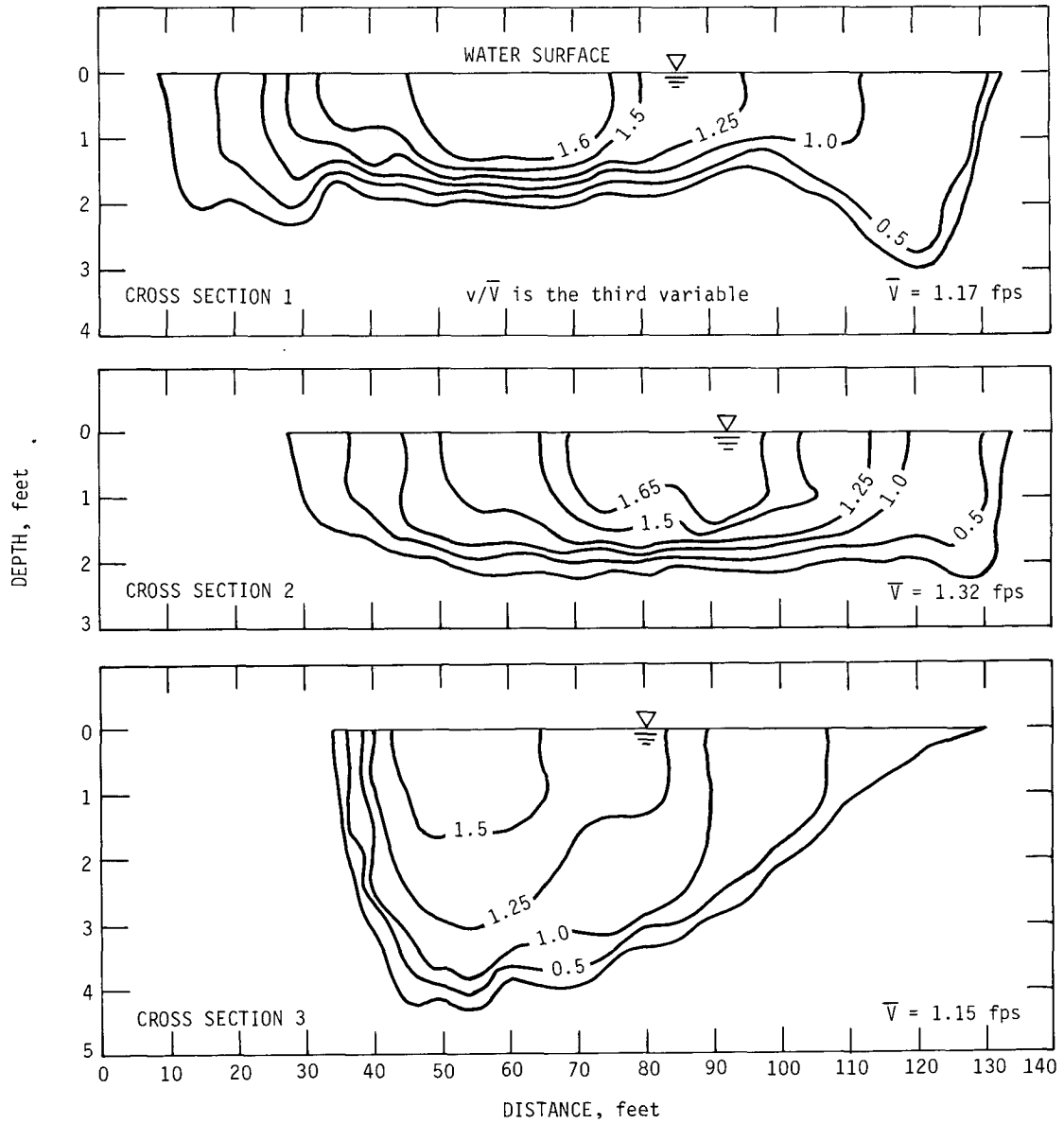
Figure 40. Isovels for cross sections 1, 2, and 3 in Reach 2 at low flow (average Q = 290 cfs)

54
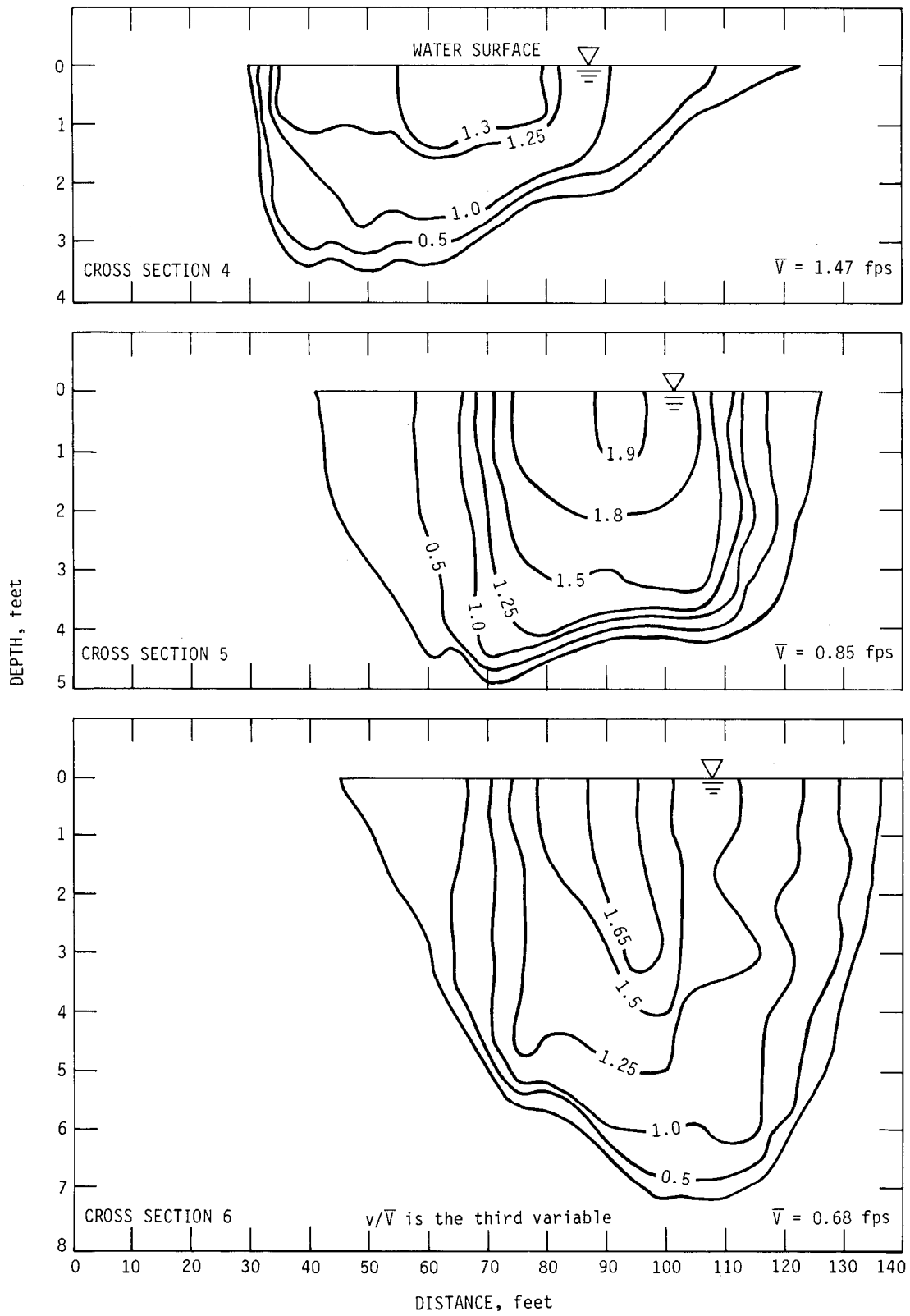
Figure 41. Isovels for cross sections 4, 5, and 6 in Reach 2 at low flow (average Q = 290 cfs)
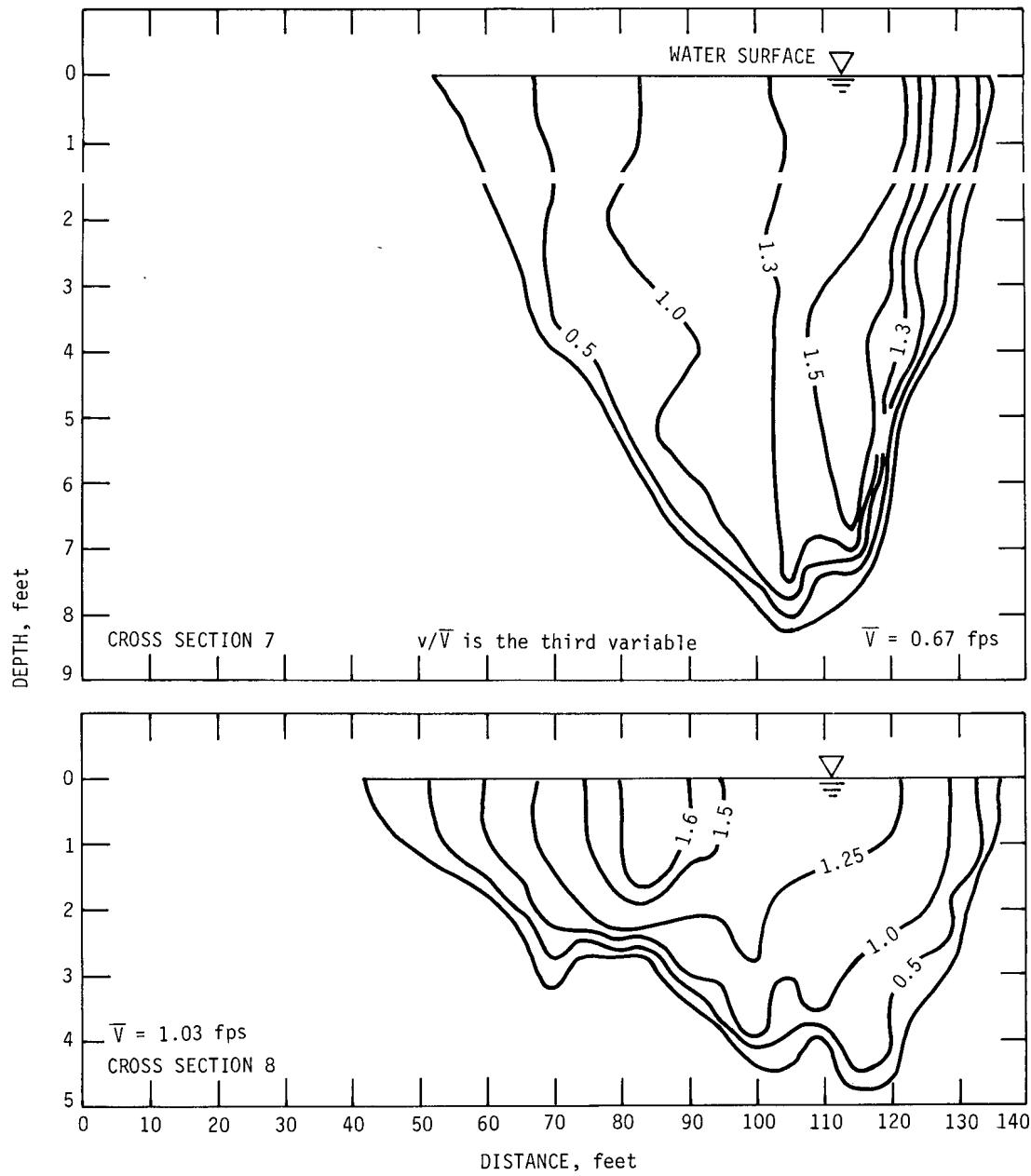
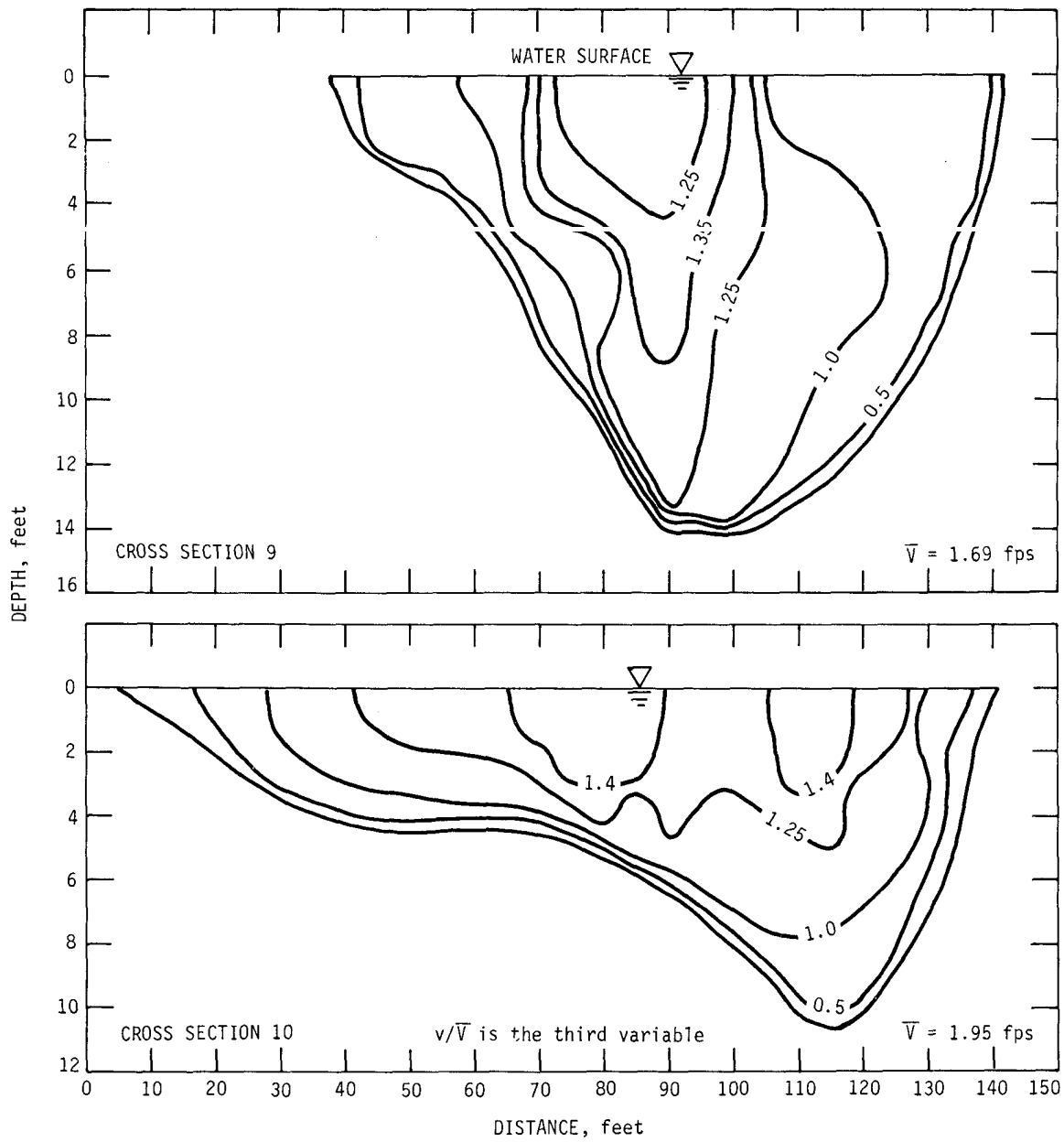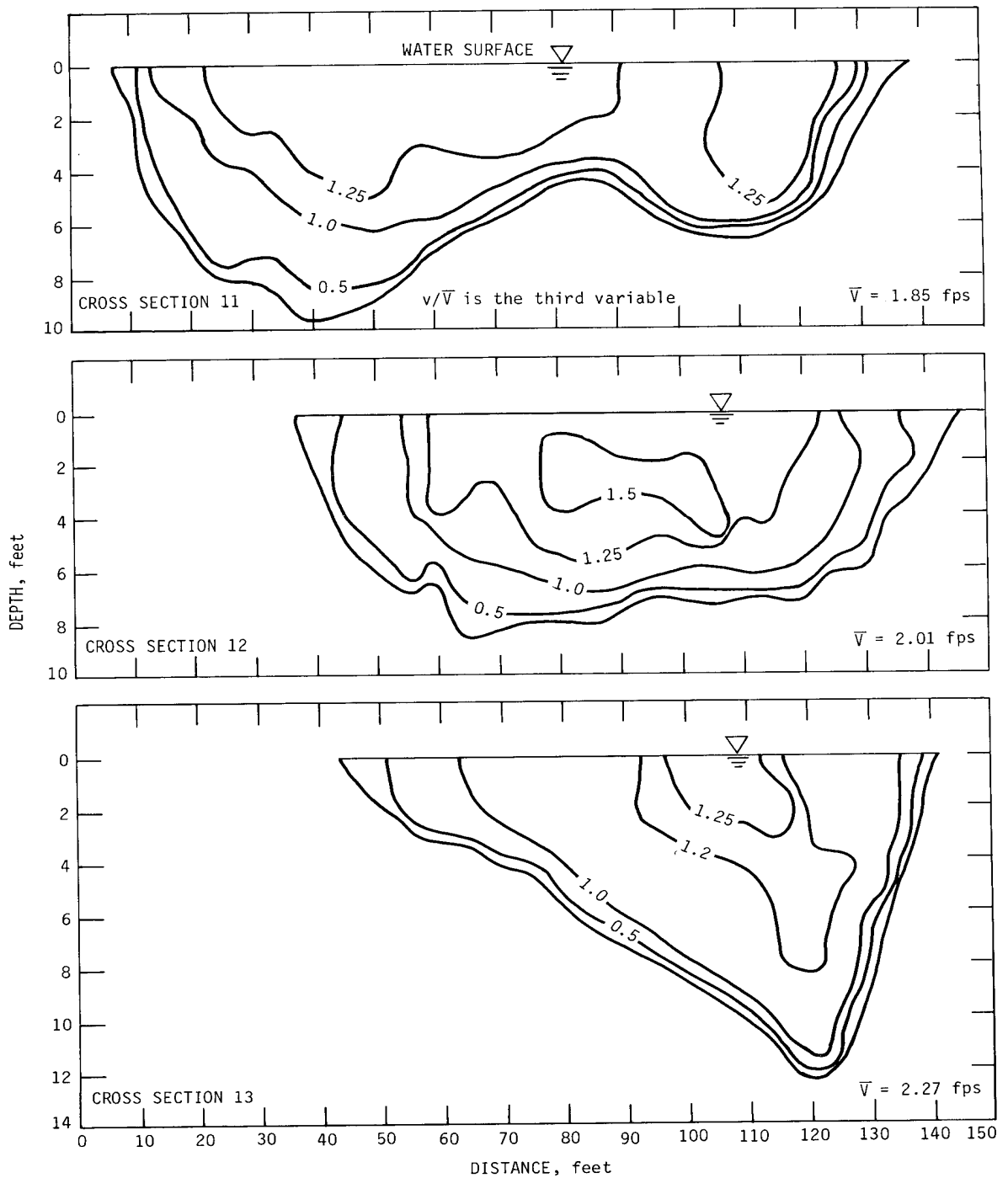Figure 42. Isovels for cross sections 7 and 8 in Reach 2 at low flow (average Q = 290 cfs)

56
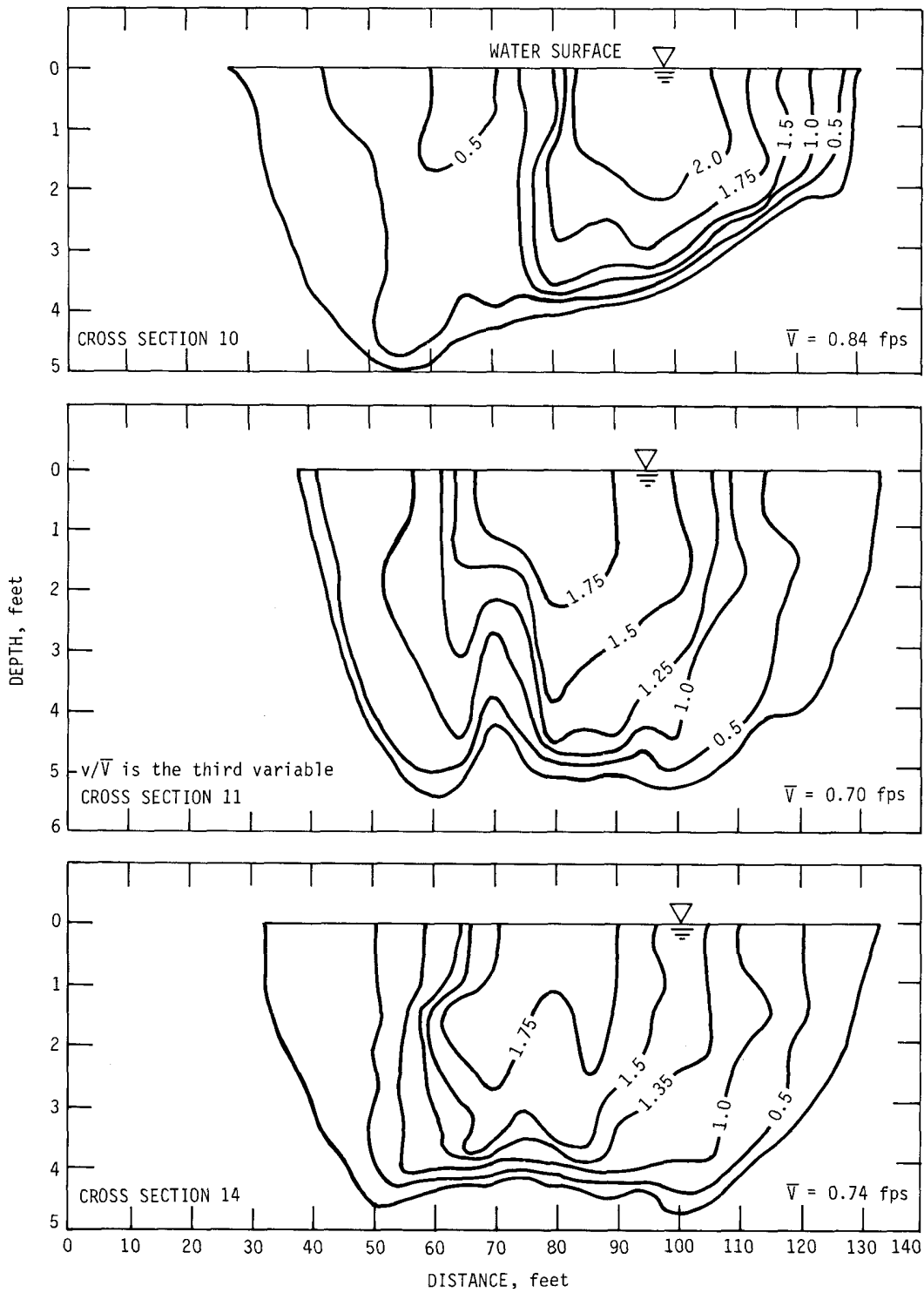
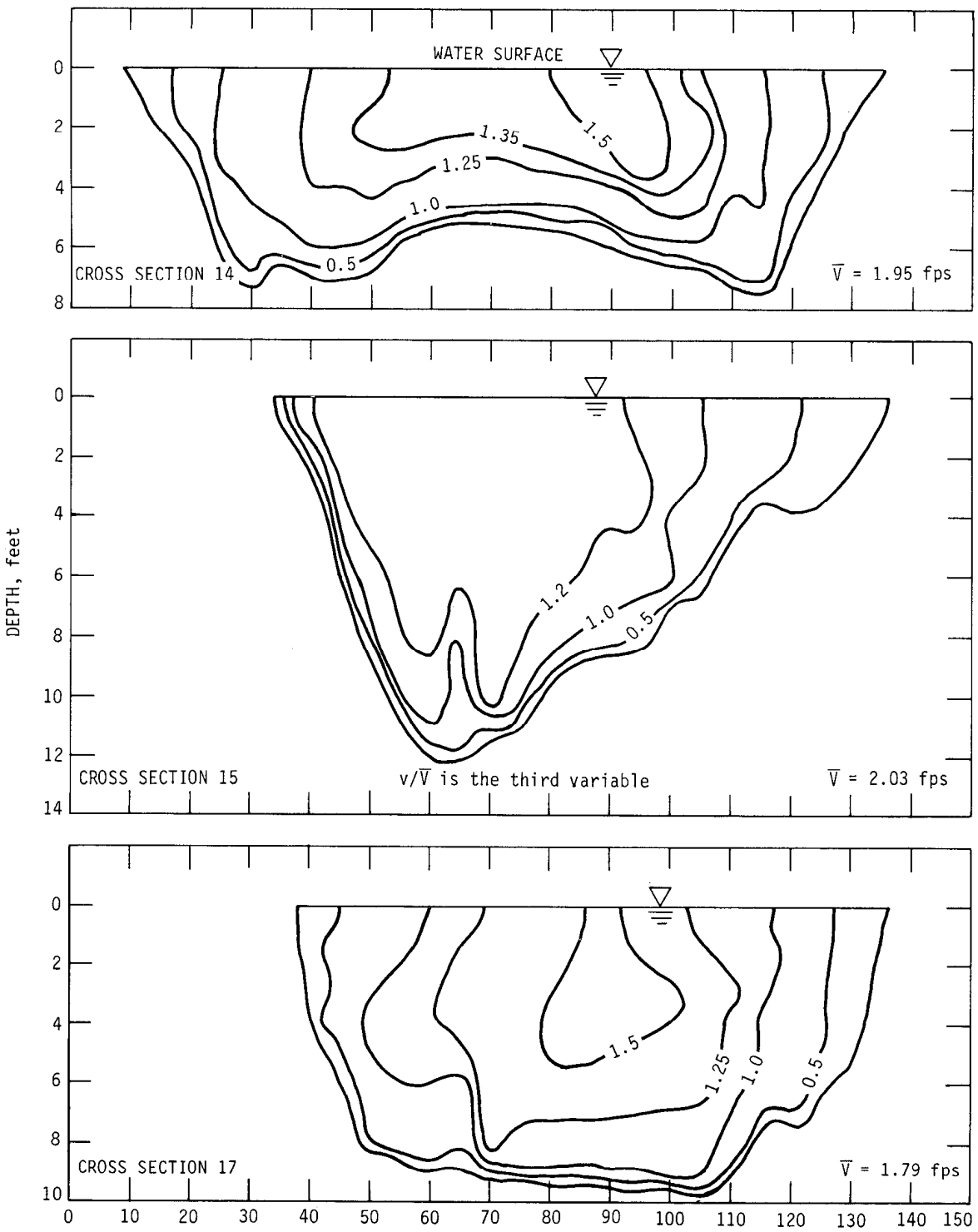**Figure 43. Isovels for cross sections 10, 11, and 14 in Reach 2 at low flow (average Q = 290 cfs)**

57
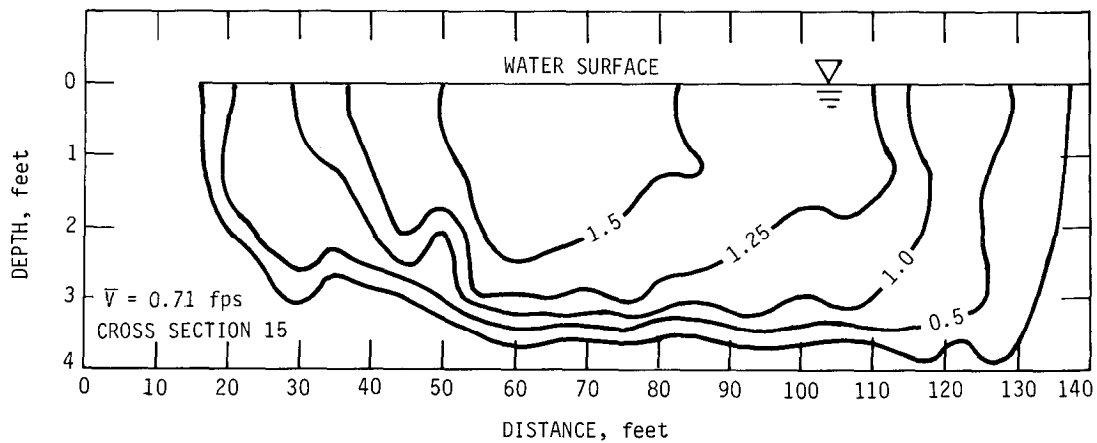
Figure 44. Isovels for cross section 15 in Reach 2 at low flow (average Q = 290 cfs)

tions 3 and 4 (figures 45 and 46) show the characteristic lateral movement of the higher velocity as the flow passes around the bend (figure 7). Isovels at section 5, which is located at the crossing between two bends of opposite direction, show the existence of a somewhat symmetrical velocity distribution about the centerline. The core of the high velocity flow is quite close to the water surface, as it was with low flow conditions (figure 41). At section 6 (figure 46) the core of the high velocity flow is now close to the inside bank of the bend (figure 7). This shifting of the high velocity flow has resulted from the higher momentum of the flow associated with this relatively high discharge which is apparently trying to move the flow in the shortest distance possible, with a minimum amount of momentum transfer between various layers of flow. This pattern of flow is the same as those observed at sections 6 and 8 (figures 37 and 38) in Reach 1.

The isovels at section 7 (figure 47) show the presence of two cores of high velocity with one of the cores staying close to the bed of the river. Section 8 is located at the crossing between two bends of opposite direction in a segment of the river with relatively straight alignment. The structure of the isovels is approximately symmetrical about the centerline (figure 47). Section 11 is located quite a bit downstream from the bend at section 9, but it still shows the effect of this bend in its velocity structure. The high velocity core is biased toward the left hand side of the river which in this case happens to be the continuation of the outside bank of the bend at section 9.

Isovels at section 12 (figure 48) show that the core of the high velocity is close to the outside bank of the bend. The isovels at sections 14 and 15 (figure 48) are quite symmetrical about the centerline. This indicates the establishment of a normal velocity distribution in the straight portion of the river at or near these sections.

Figures 49 through 53 show the isovels at Reach 2 for high flows with an average discharge of 3700 cfs. This flow

is 13 times the low flows and about 1.75 times the medium flow for which velocity distribution data were collected for this reach.

Isovels at section 1 (figure 49) indicate that the high flow velocity is now shifted toward the right side of the river. This is the effect of the bend at this location (figure 7) where the higher flow momentum is forcing the water to traverse a shorter path. Isovels at sections 2 and 3 (figure 49) are similar to those present during the low and medium flows (figures 40 and 45).

The isovels shown in figure 50 for section 4 show that the core of the high velocity flow has now definitely moved toward the left side of the river which happens to be the outside bank of the upstream bend (figure 7). This again demonstrates the effect of the higher momentum associated with higher discharges. Similar shifting of the high velocity flow toward the outside bank is noticeable at section 5. Isovels at section 6 (figure 50) indicate that the core of the high velocity flow is now in the deeper part of the river and has moved close to the bend and near the outside bank of the river. During low and medium flows, the high velocity cores stayed close to the water surface.

At sections 7 and 8, the isovels have shifted toward the outside bank (figures 51 and 7) and away from the water surface moving downward near the bed. These rearrangements of the velocity structure resulted from the presence of the upstream bend. Section 10, which is located downstream of the bend near section 9, shows the eccentricity of the velocity structure with the higher flows staying relatively close to the left side of the river (figure 51).

Isovels at section 11 (figure 52) show the typical pattern of velocity distribution in a straight segment of the river. At section 12, the isovels have shifted toward the inside bank of the river (figure 52). The velocity structures at sections 14 and 15 (figures 53) are symmetrical about rhe centerline of the river. These typical velocity distributions in the straight portion of the river did not show much variability
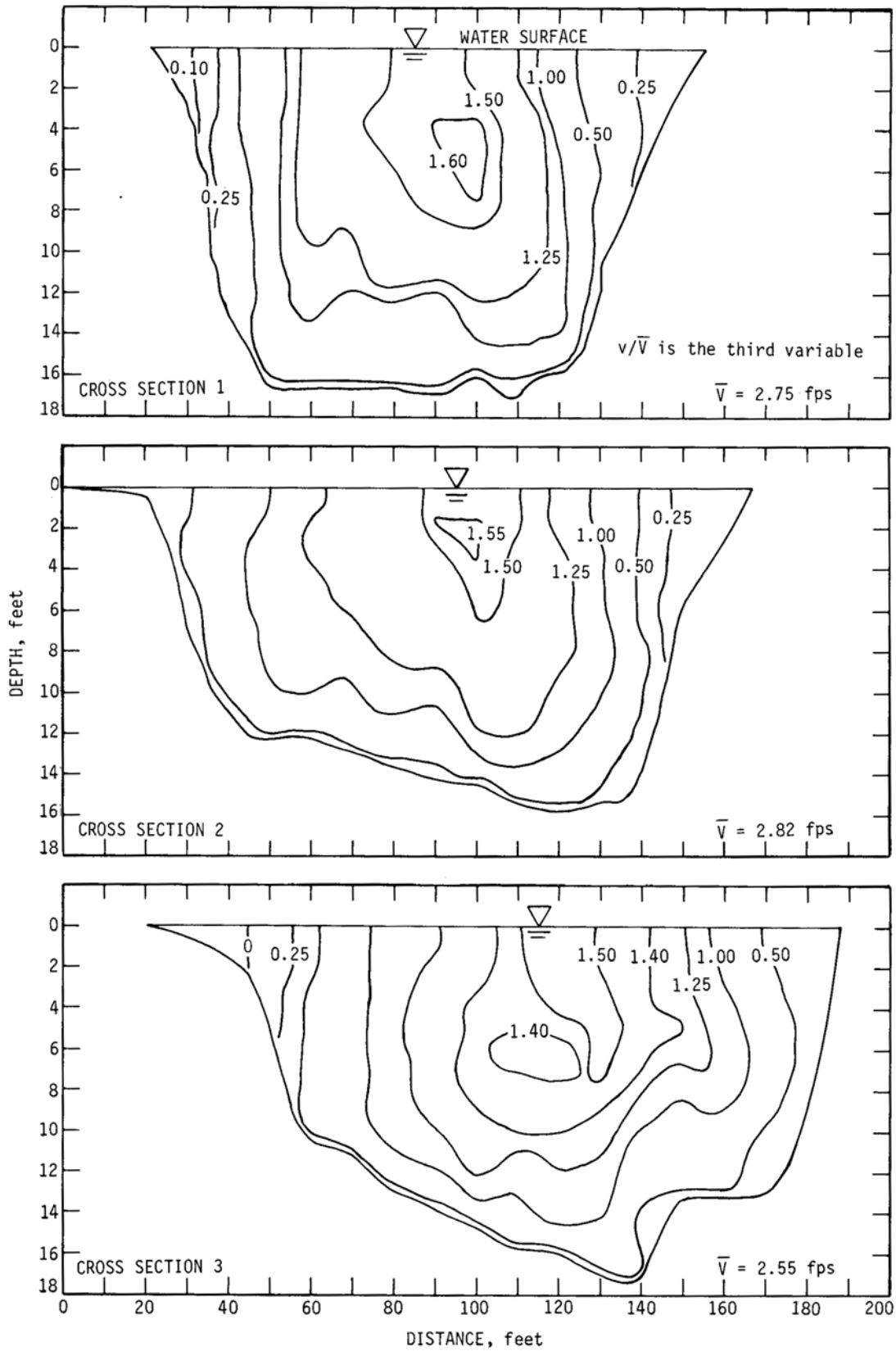
58
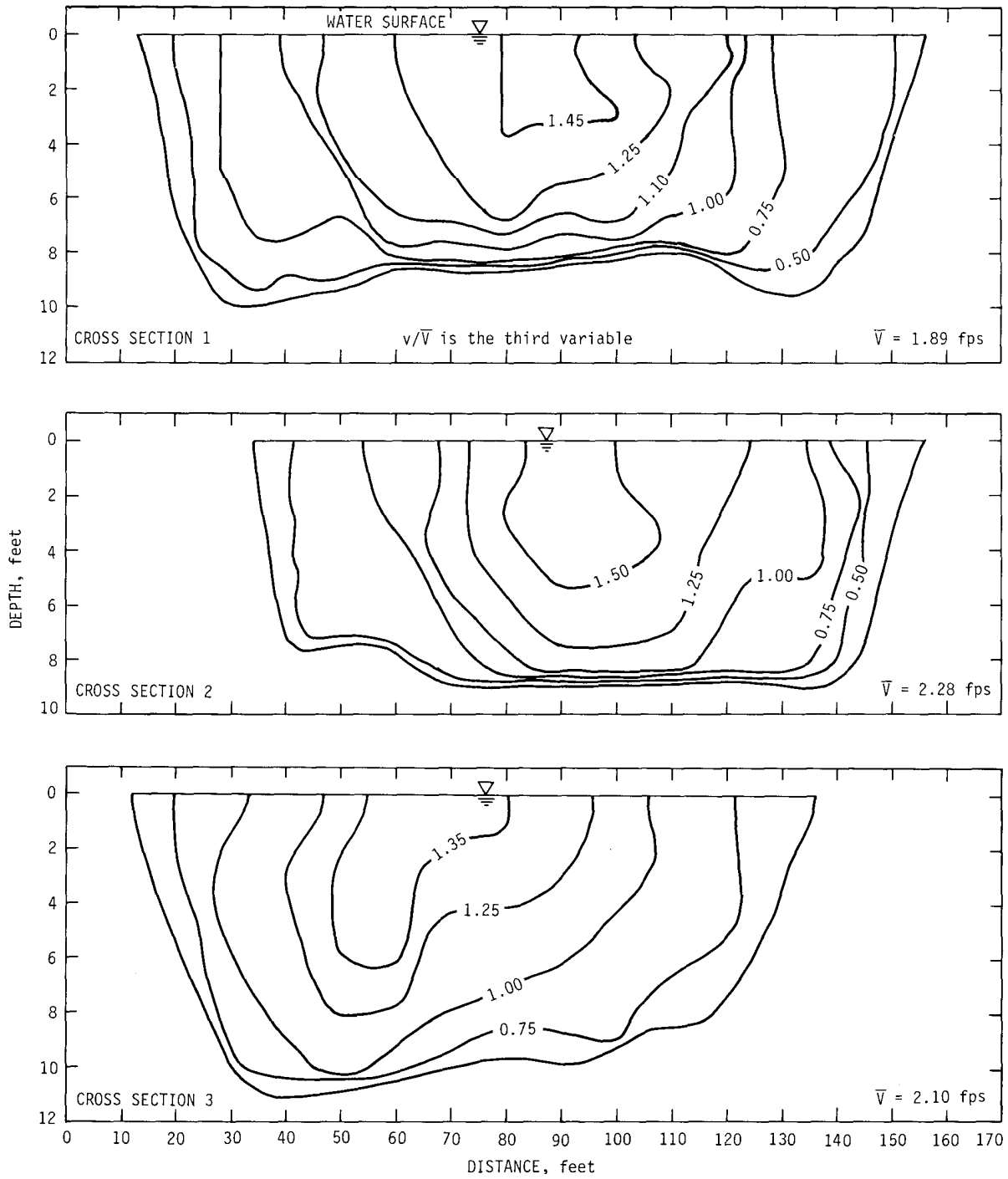
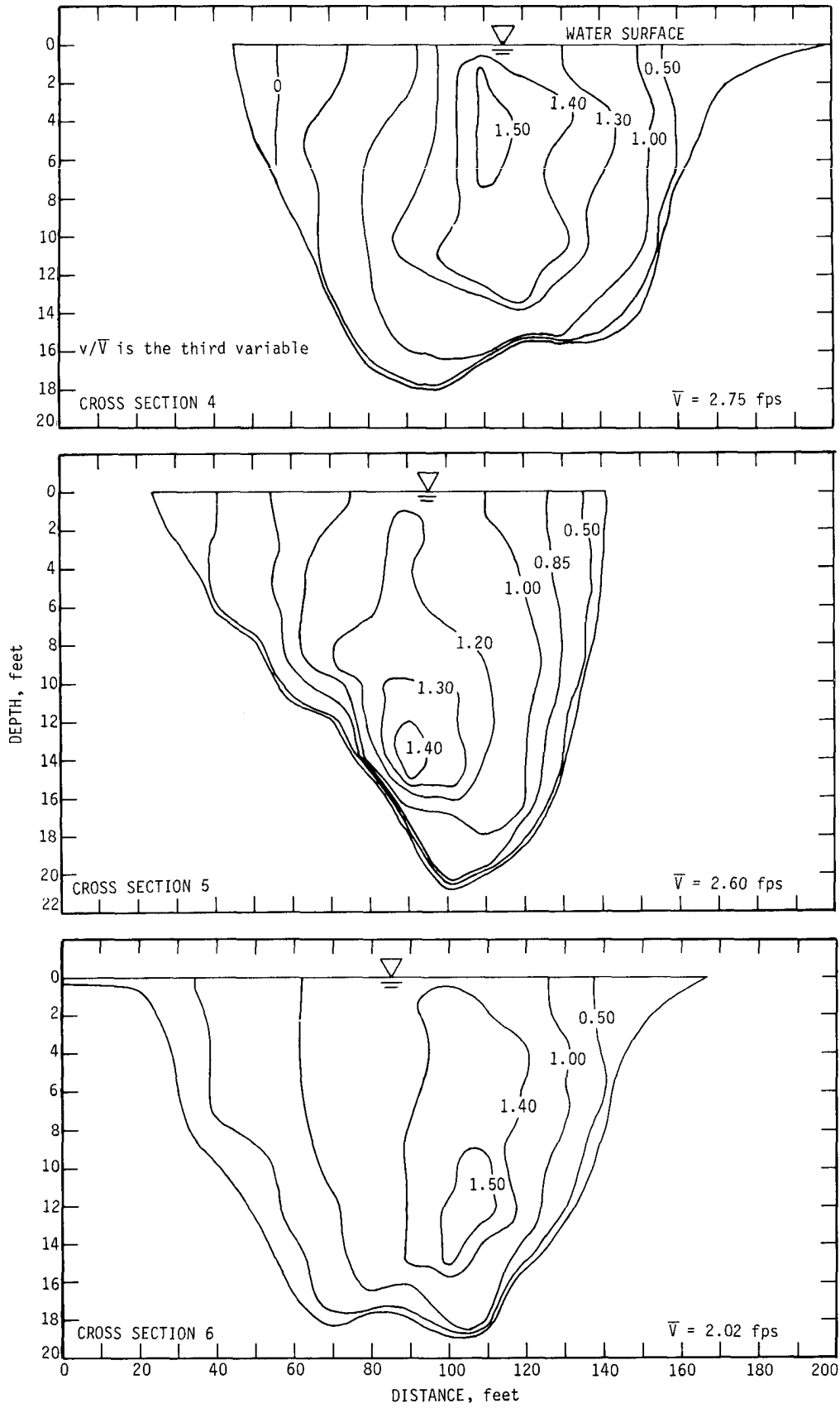**Figure 45. Isovels for cross sections 1, 2, and 3 in Reach 2 at medium flow (average Q = 2160 cfs)**

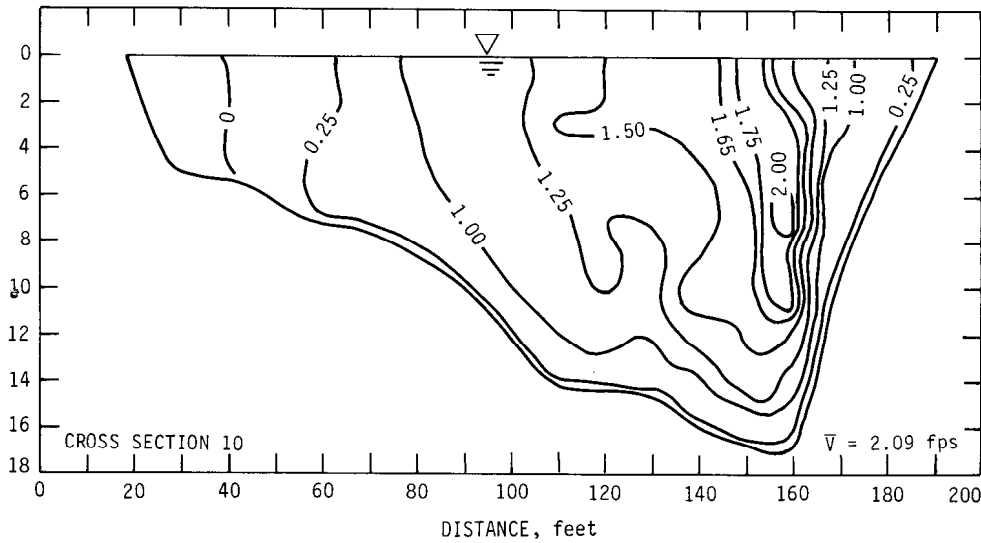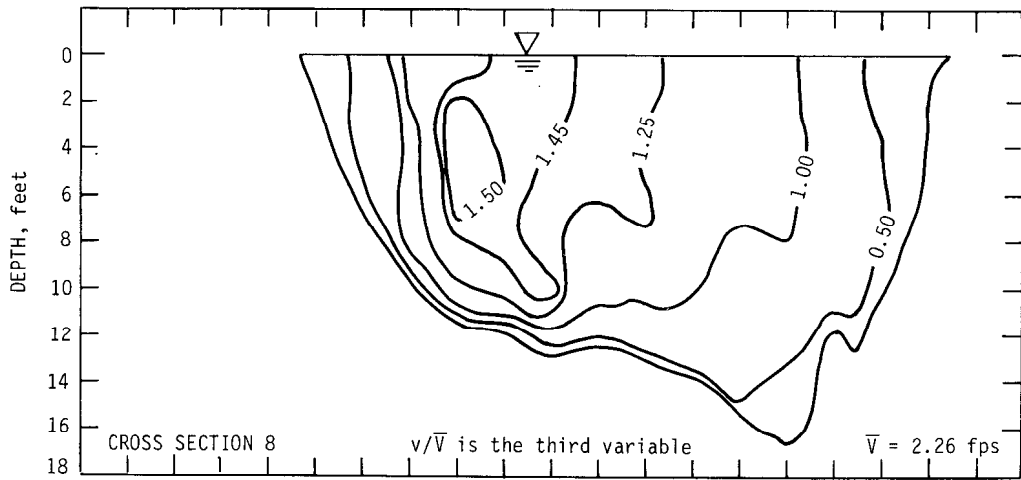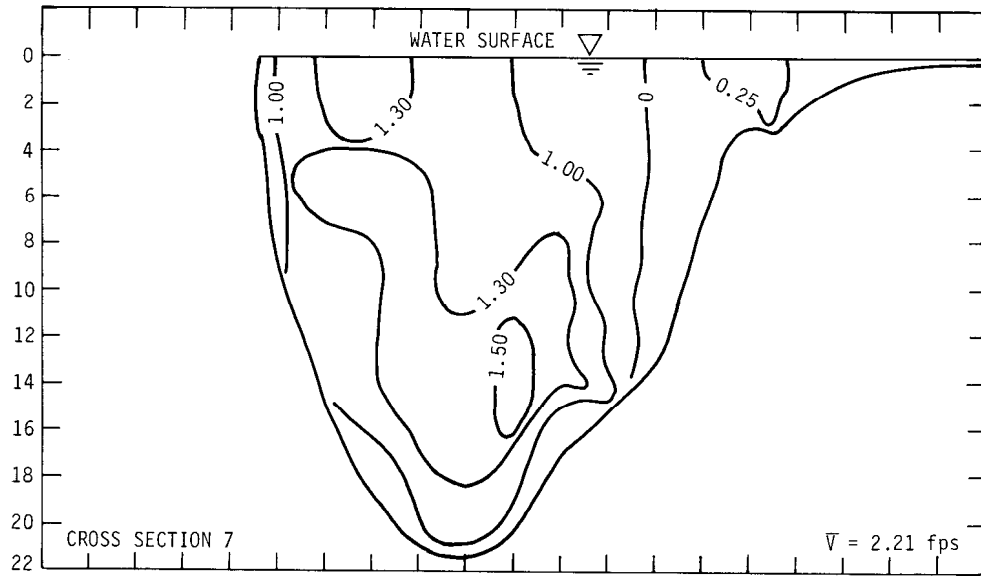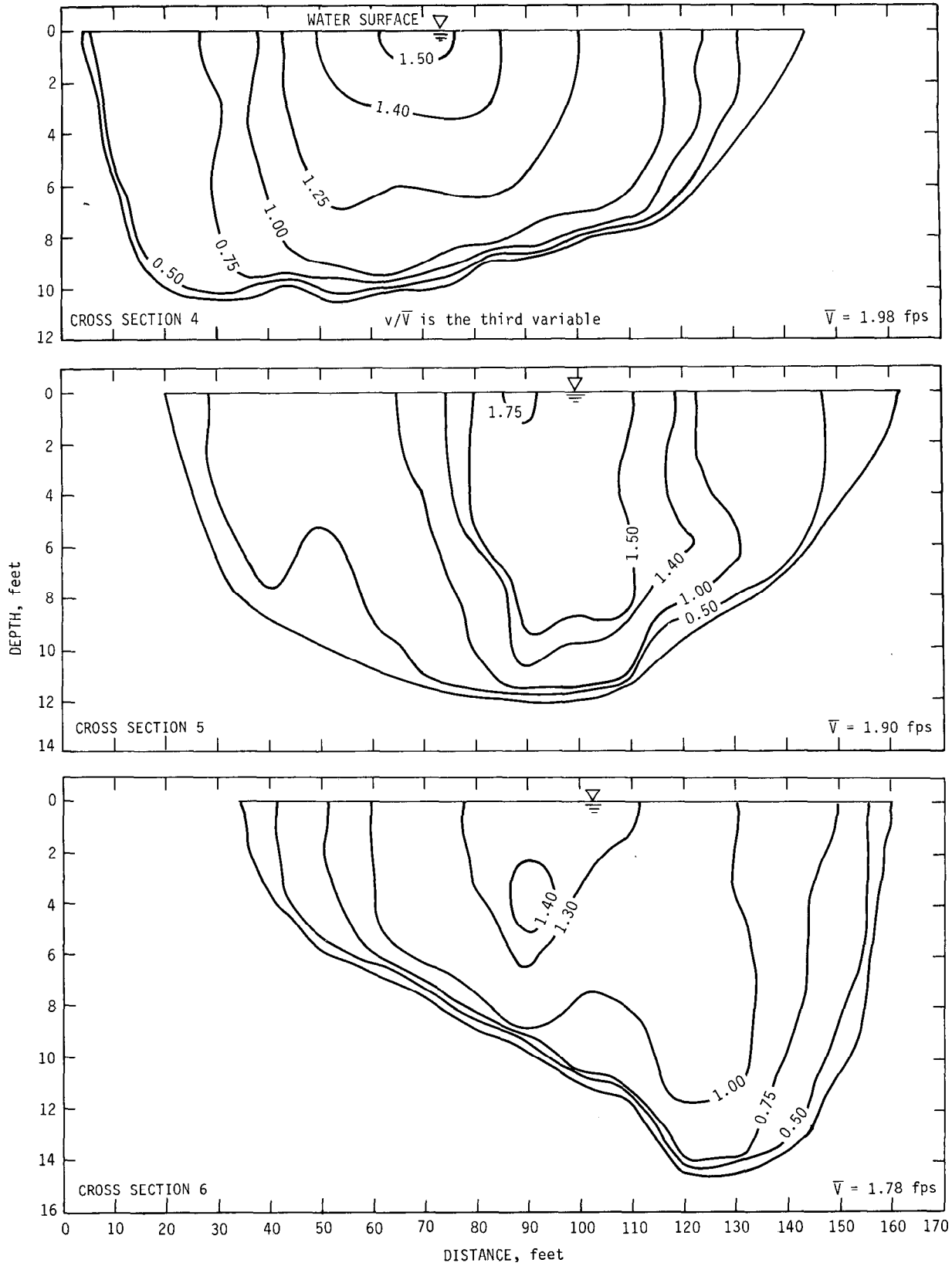**Figure 46. Isovels for cross sections 4, 5, and 6 in Reach 2 at medium flow (average Q = 2160 cfs)**
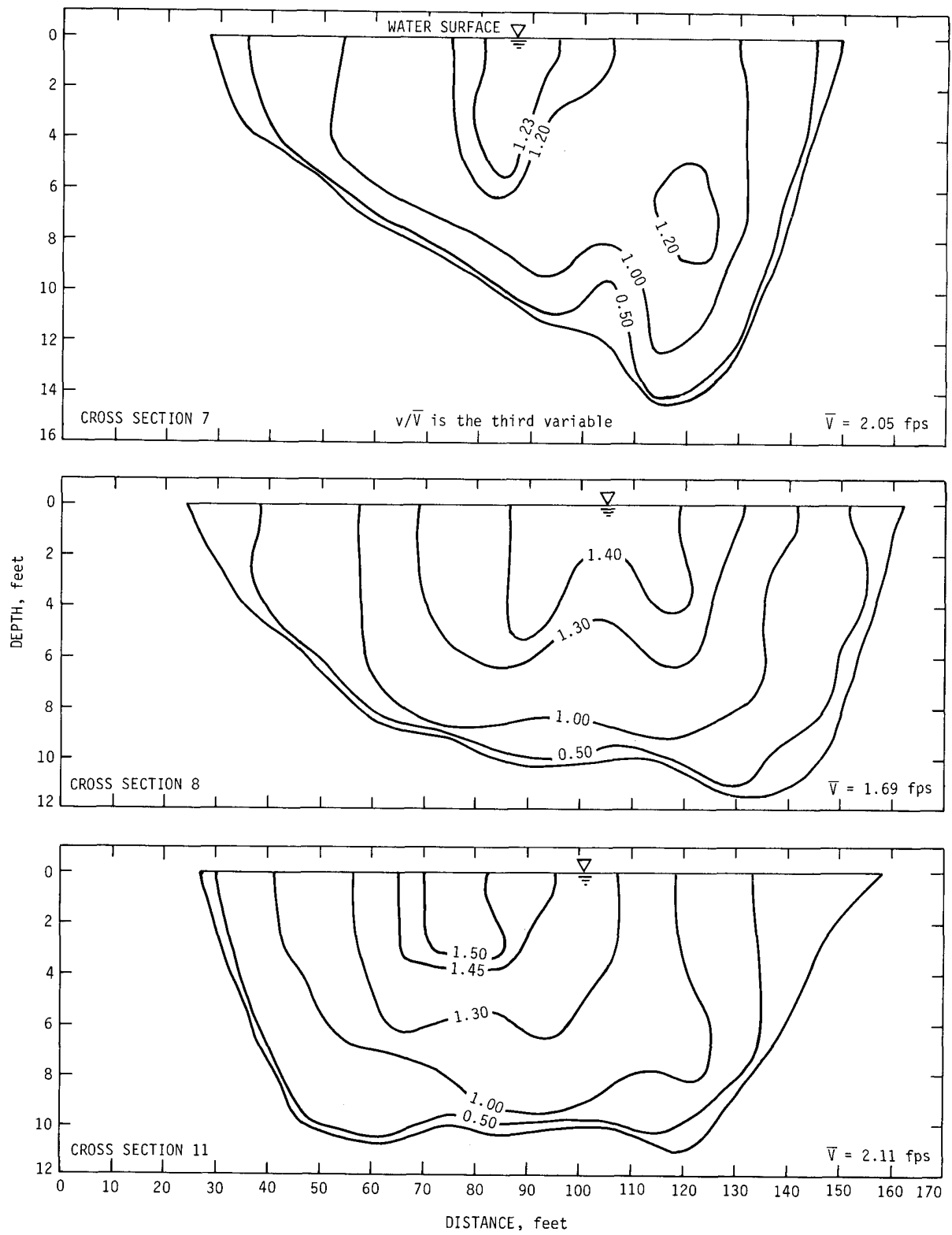
Figure 47. Isovels for cross sections 7, 8, and 11 in Reach 2 at medium flow (average Q = 2160 cfs)
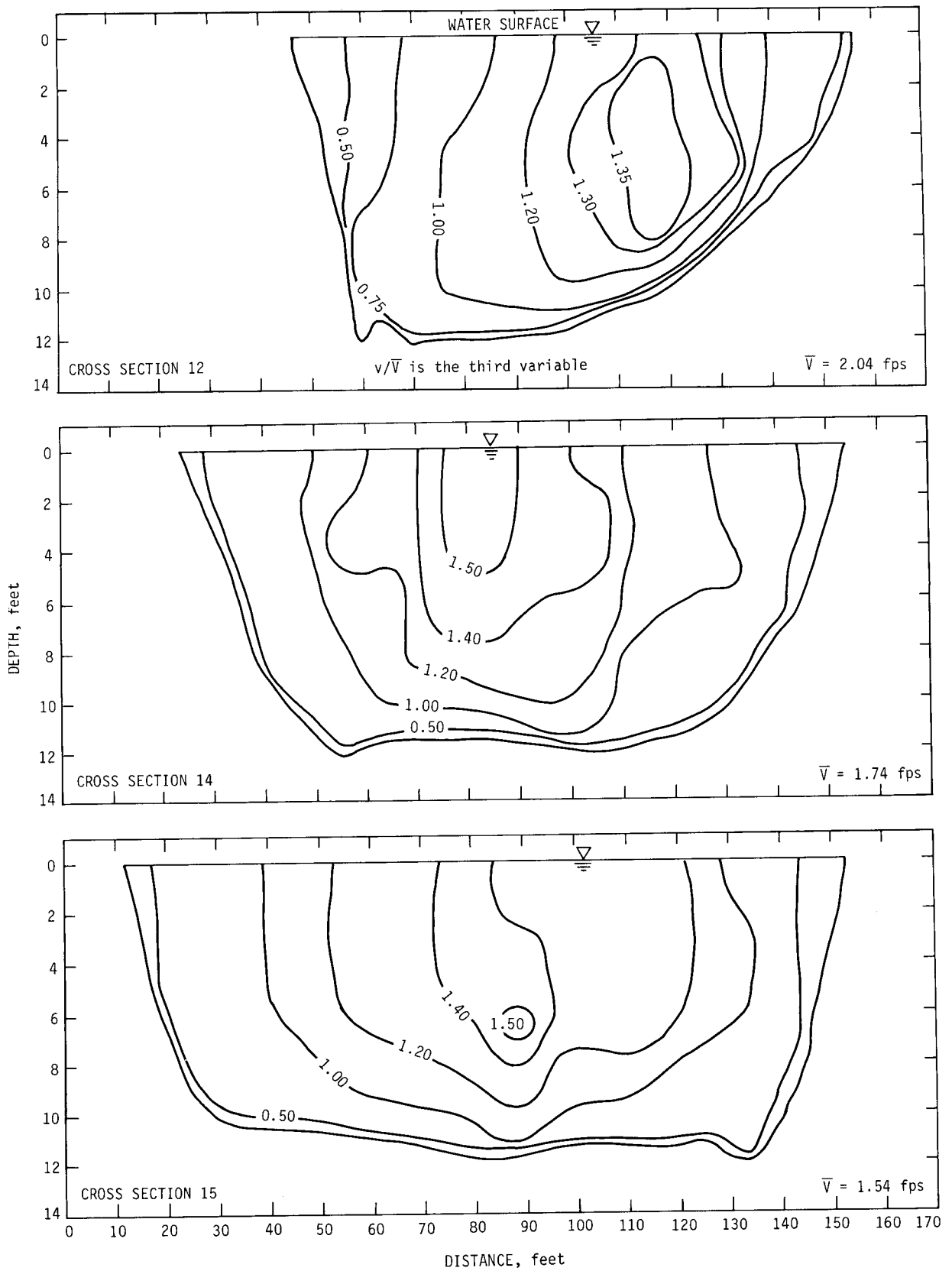
Figure 48. Isovels for cross sections 12, 14, and 15 in Reach 2 at medium flow (average Q = 2160 cfs)
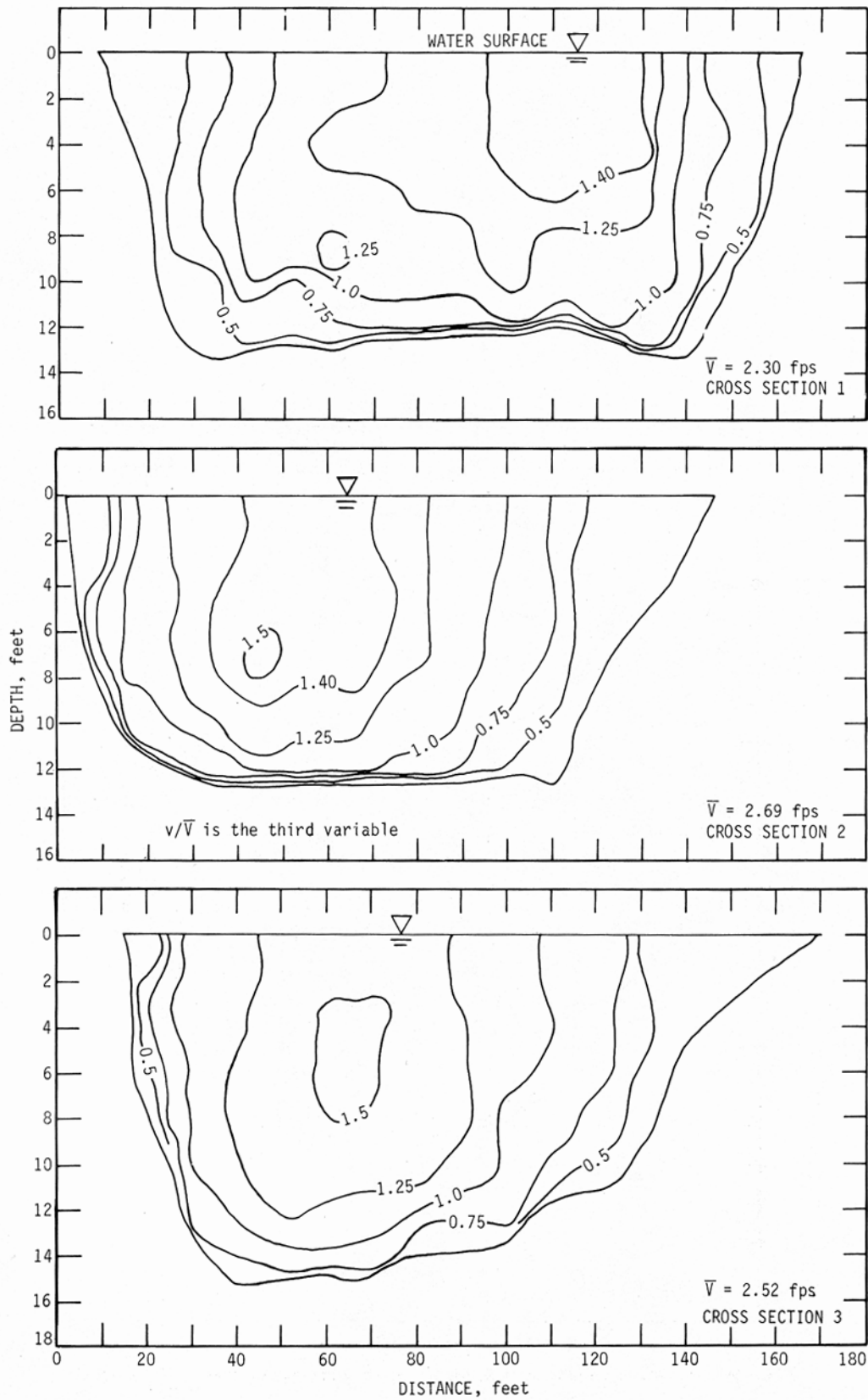
Figure 49. Isovels for cross sections 1, 2, and 3 in Reach 2 at high flow (average Q = 3700 cfs)
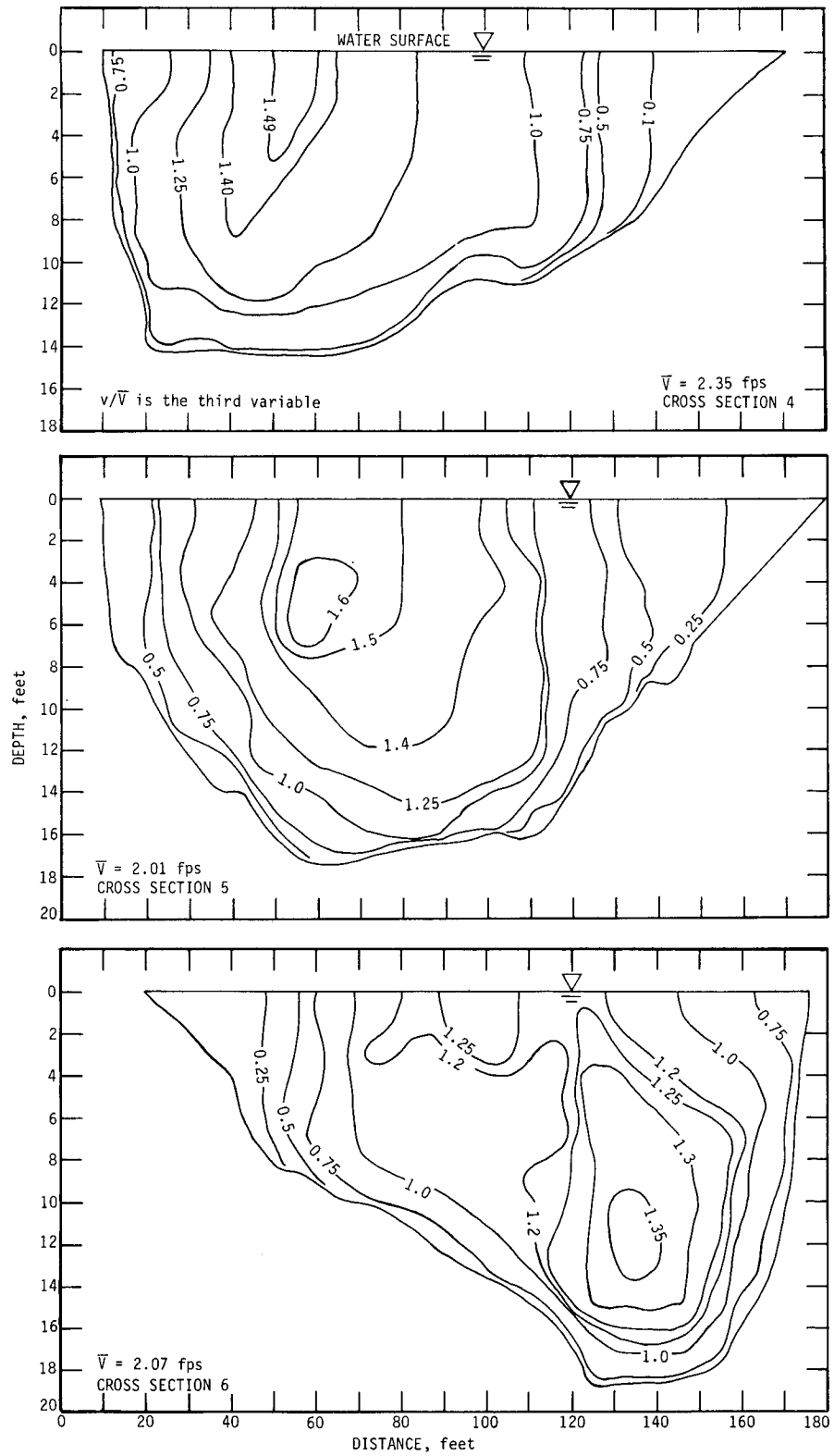
Figure 50. Isovels for cross sections 4, 5, and 6 in Reach 2 at high flow (average Q = 3700 cfs)
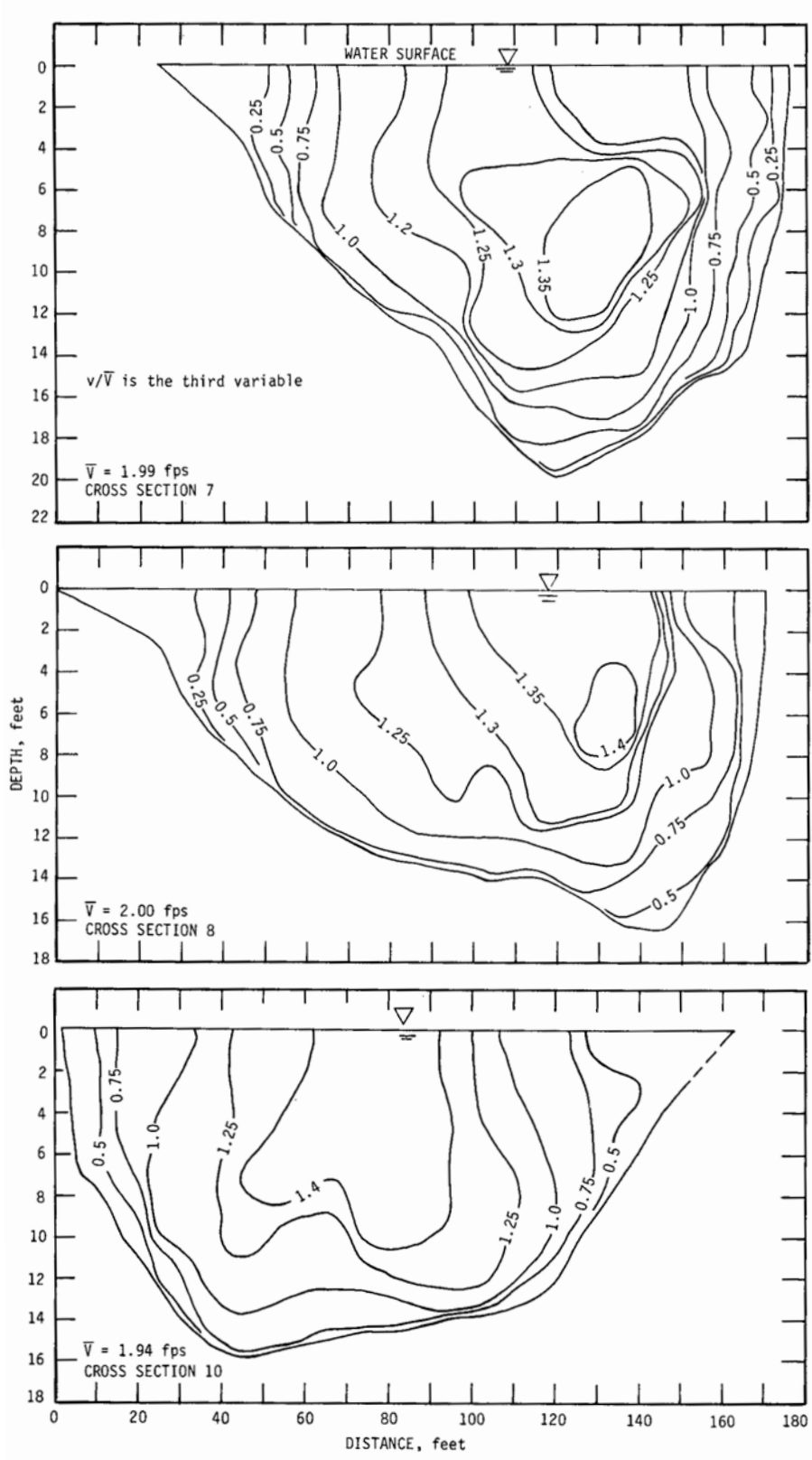
Figure 51. Isovels for cross sections 7, 8, and 10 in Reach 2 at high flow (average Q = 3700 cfs)
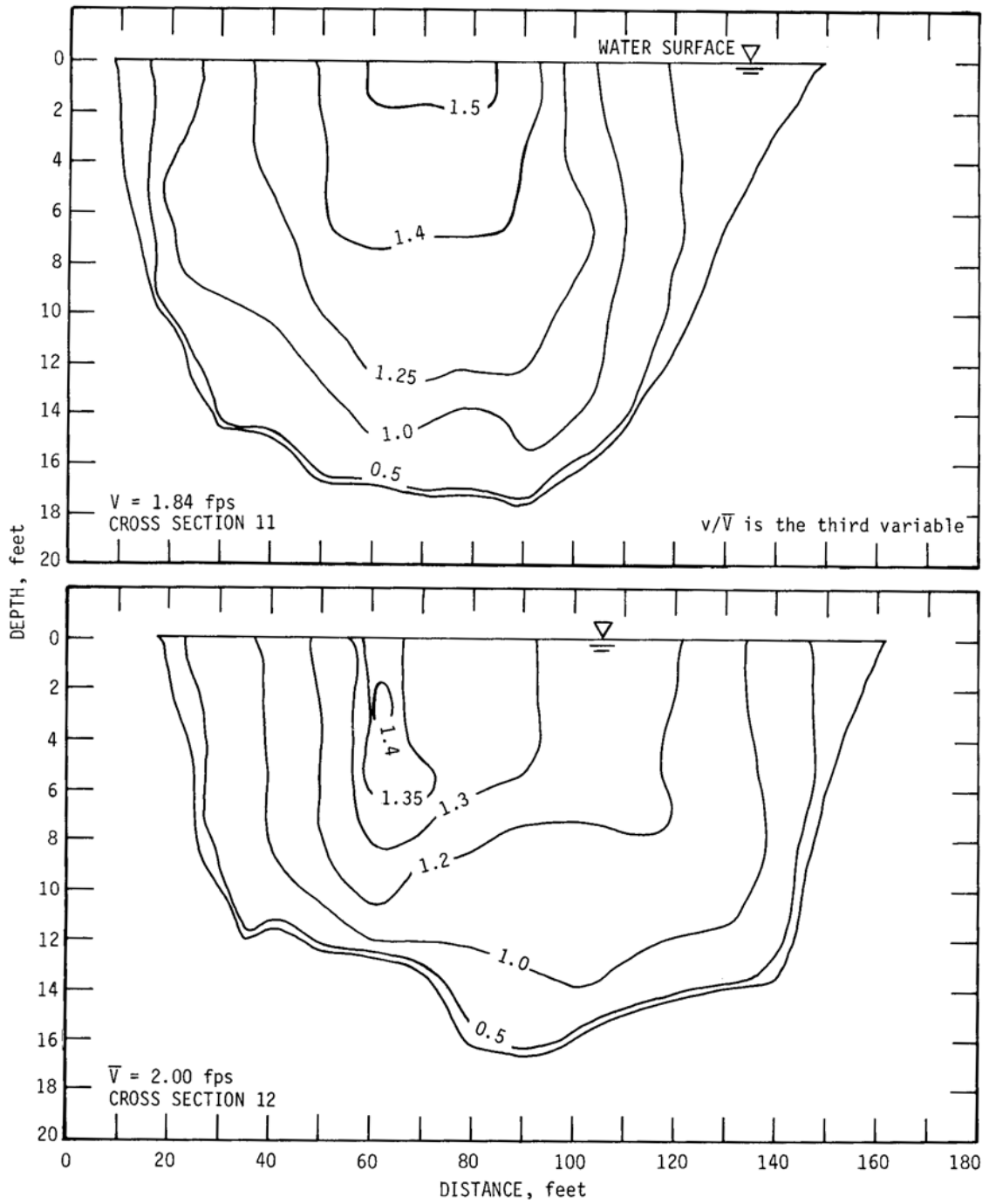
Figure 52. Isovels for cross sections 11 and 12 in Reach 2 at high flow (average Q = 3700 cfs)
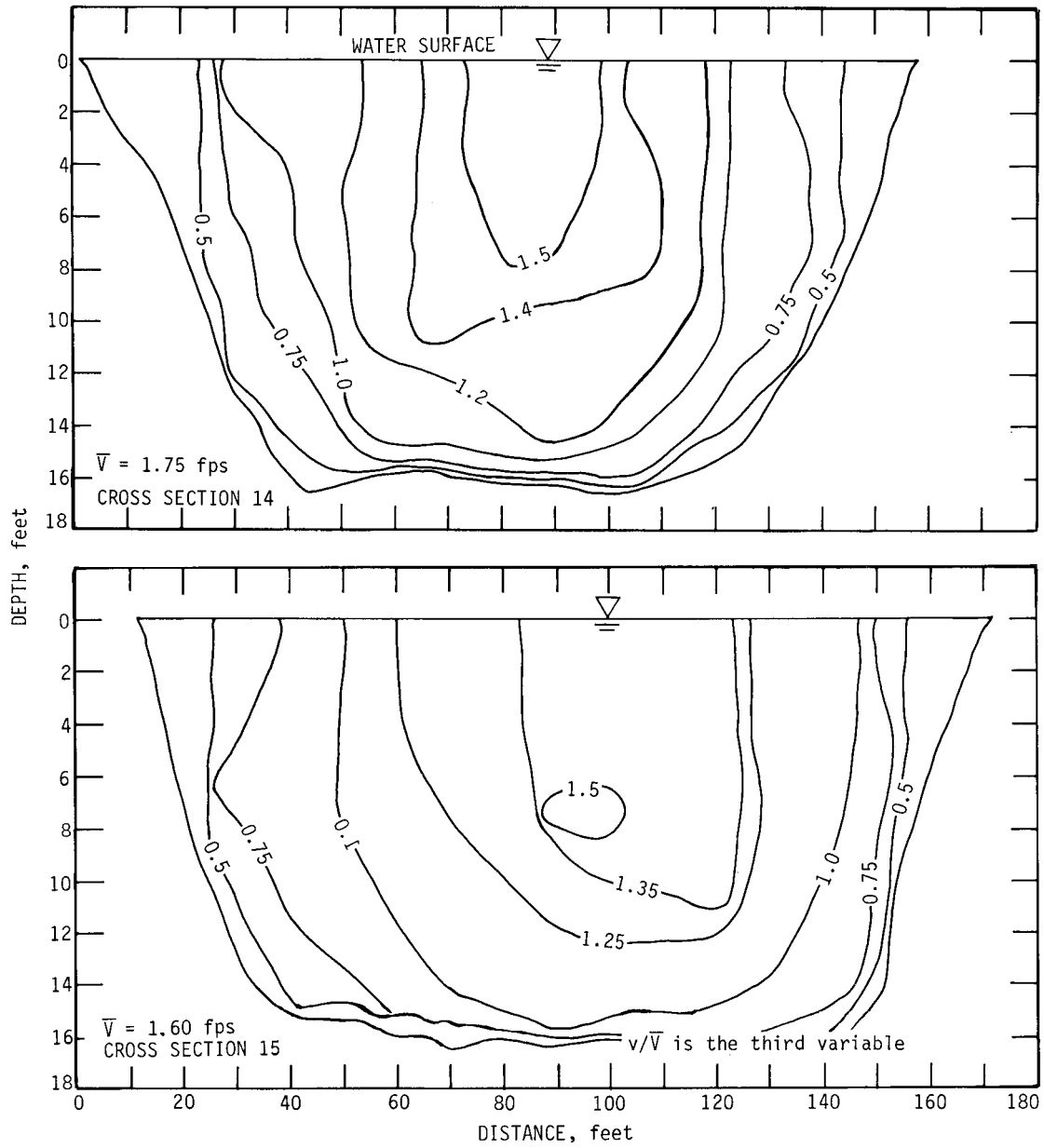
Figure 53. Isovels for cross sections 14 and 15 in Reach 2 at high flow (average Q = 3700 cfs)

Table 8. Relative Magnitudes of the Maximum Nondimensional Velocities,
Reach 2 (Figures 40 through 53)

Cross section	Average Q=1040 cfs		Average Q=1420 cfs		Average Q=4000 cfs,	
	$\overline{V}$ (fps)	Maximum $v/\overline{V}$	$\overline{V}$ (fps)	Maximum $v/\overline{V}$	$\overline{V}$ (fps)	Maximum $v/\overline{V}$
1	1.16	1.60	1.95	1.45	2.30	1.40
2	1.31	1.65	2.26	1.50	2.69	1.50
3	1.14	1.50	2.12	1.35	2.46	1.50
4	1.46	1.30	1.98	1.50	2.35	1.49
5	0.84	1.90	1.76	1.75	2.01	1.60
6	0.68	1.65	1.78	1.40	2.07	1.35
7	0.67	1.50	1.97	1.23	1.99	1.35
8	1.03	1.60	1.76	1.40	2.00	1.40
10	0.83	2.0			1.40	1.40
11	0.70	1.75	2.03	1.50	1.84	1.50
12			2.08	1.35	2.00	1.40
14	0.73	1.75	1.71	1.50	1.75	1.50
15	0.70	1.50	1.53	1.50	1.60	1.50

or change compared with the isovels that were developed for the low and medium flows (figures 43, 44, and 48).

The velocity distribution data for Reach 2 for low, medium, and high flows showed quite a bit of similarity to those analyzed for Reach 1. However, some dissimilarities were also observed for the two sets of data. Table 8 shows the discharges, average velocities, and the ratio of the maximum point velocity to the average velocity $v/\overline{V}$ in each cross section corresponding to low, medium, and high flows. The ratio $v/\overline{V}$ is taken from the isovels shown in figures 40 through 53. At all cross sections, the average velocity showed a general increasing trend with an increasing discharge. The average of all the average velocities at all cross sections for various discharges is 0.94 fps for low flows, 1.91 fps for medium flows, and 2.04 fps for high flows. This change is similar to that observed for Reach 1 (table 7). However, the maximum nondimensional point velocities $v/\overline{V}$ decreased somewhat as the discharge increased from low to medium to high flows. This is in contrast to the observations made in connection with Reach 1 where the maximum average numerical values of $v/\overline{N}$ did not show much change from low to high flows. The reasons for these variations may be explained as follows.

Reach 2 is located about 75 miles downstream of Reach 1. The river is wider at this location and the cross-sectional areas of the river at bankfull discharges are much larger than the cross-sectional areas at Reach 1 during bankfull discharges. The ratios of the top widths to the average depths for bankfull discharges varied from about 9 to 16 for Reach 1 and 11 to 16 for Reach 2. The average of these values for Reach 1 is 12 and for Reach 2 is 13. The river in Reach 2 is capable of carrying a higher volume of discharge corresponding to any flow frequency compared with Reach 1 (figure 18). The average invert slope for Reach 2 is about

1.46 ft/mile compared to 0.95 ft/mile for Reach 1. All these factors have the combined effect of an even momentum transfer between various layers of flows at Reach 2 as the discharge increases from low to higher values. This increased momentum transfer helps to redistribute the velocity structure in both the horizontal and the vertical directions. This is probably the reason why the differences between the average velocity and the maximum velocity at Reach 2 showed a progressive decrease as the discharge increased from low to medium to high flows.

Flow around Bends

Characteristics of the flow around bends have already been discussed under the heading "Velocity Distributions." Some additional analyses of flow characteristics around bends are presented here.

Figures 54 and 55 show the distribution of the depth-averaged velocities in the verticals along the width of the river at various cross sections for Reach 2. These data are shown for medium and high average discharges of 2160 and 3700 cfs, respectively. The changes in the structure of the average velocities at different verticals are quite evident in these two figures. Also shown is the shift of the high velocity flow toward the outside bank in the bends.

The lateral depth-integrated velocity distribution data were also compared with the theoretical distribution suggested by Rozovskii (1957). The relationships used in the computation of the lateral velocity distribution are given in figure 3. Typical plots for three cross sections are shown in figure 56. Here V_v is the depth-integrated velocity at any vertical inside the bend and V_{vm} is the depth-integrated maximum velocity at a vertical in the straight portion of the river. These data were collected during high flows in
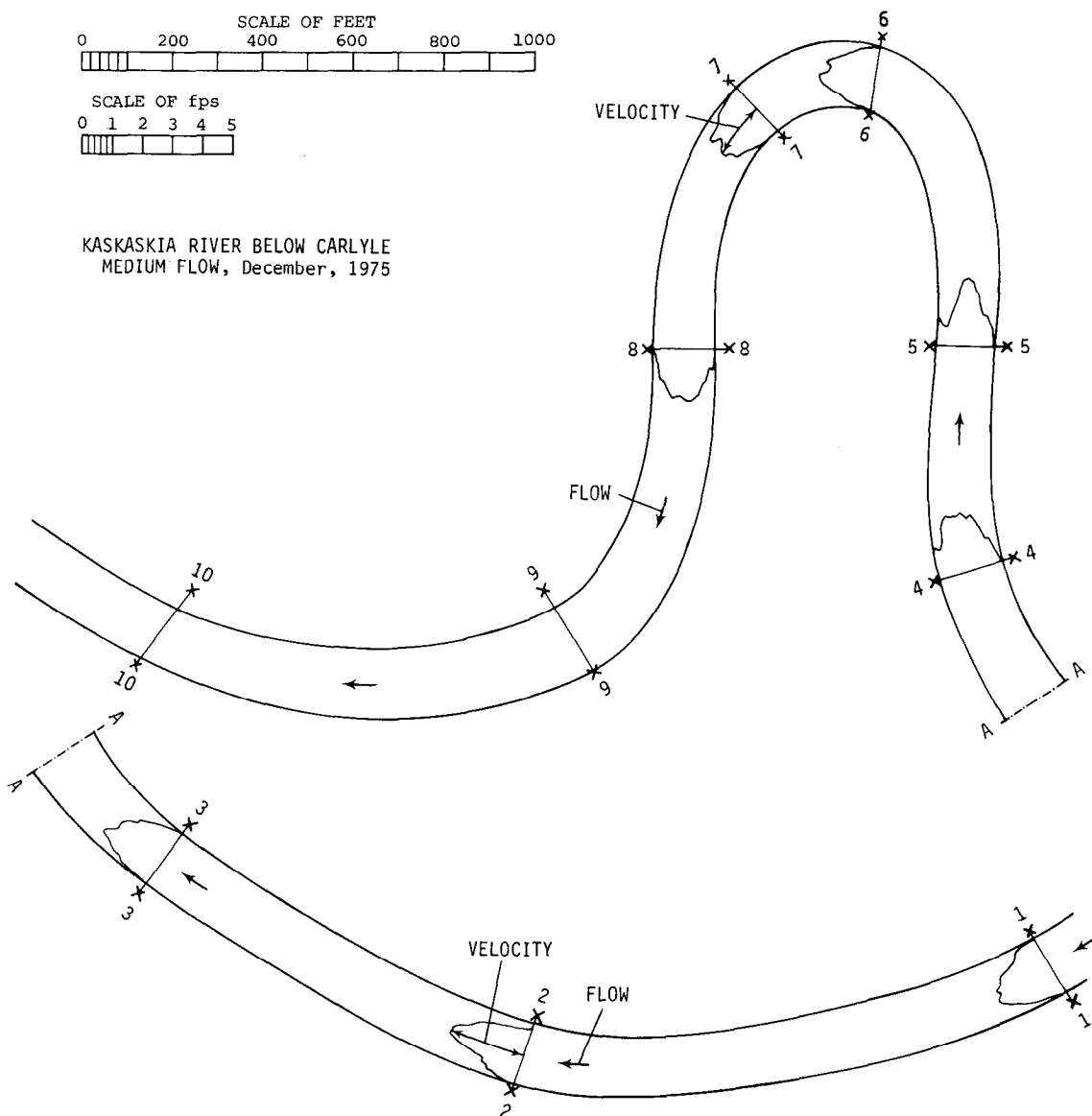
Figure 54. Average velocity distribution in Reach 2 for medium flow

both reaches. Among the three cases shown, the correlation is good for two cross sections; however, for the third cross section, the correlation is good except for the outside bank of the bend where predicted velocities are much lower than those measured.

Superelevations

The superelevations at bends in both reaches for different discharges were determined as the difference in water surface elevations between the inside and the outside bank of the bends. Because of the extreme flatness of the river profile and low average velocities, the numerical values of the superelevations were rather small. In most instances, the

difference between the water surface elevations near the outside and the inside banks of the bend was only a few hundreths of a foot. However, there was an unmistakable inclination of the water surface at all bends especially for medium and high flows.

In both reaches (figures 6 and 7) data related to velocity distributions and water surface elevations were collected from a minimum of one to a maximum of two to three cross sections in each bend. The superelevation measured at the downstream section of the bend was assumed to be the representative superelevation in the bend.

Theoretical values of the superelevations were computed by use of equations 30, 31, 32, and 33. These equations gave the theoretical values of the superelevations based on

69
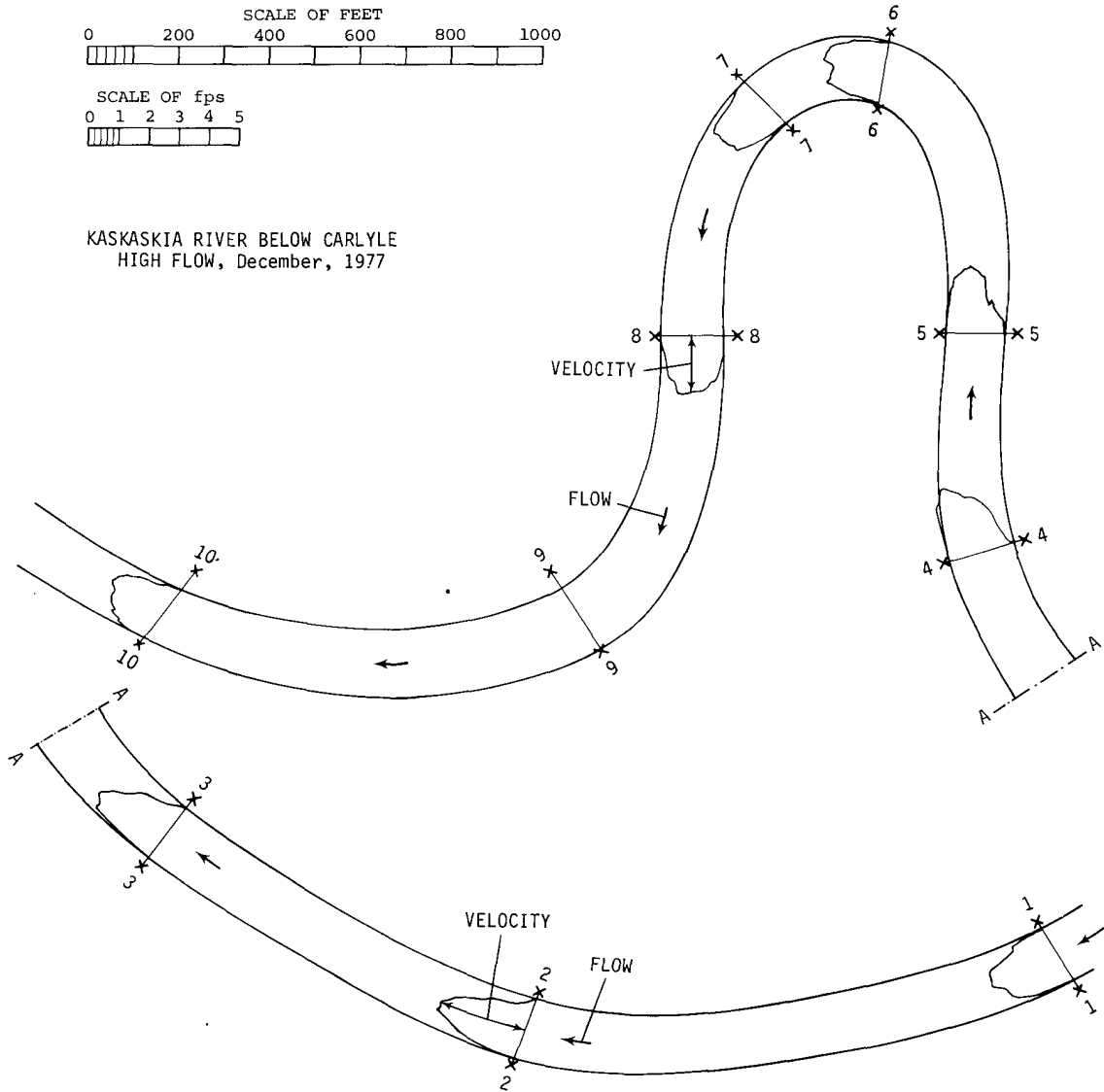
Figure 55. Average velocity distribution in Reach 2 for high flow

an assumed transverse velocity distribution in the bend for a constant velocity, free vortex pattern, forced vortex pattern, and a combination of forced vortex and free vortex patterns, respectively. Superelevations were computed for the medium and high flows in both reaches.

Figures 57a and b show the comparison between the computed and measured superelevations for Reach 1 and Reach 2, respectively, for medium discharges only. In both reaches, the superelevations computed by equation 32 (forced vortex pattern) yielded consistently lower values than those measured in the field. Superelevations computed by the other three equations showed quite a bit of variability compared with the measured values. It appears that for practical purposes, either equation 30, 31, or 33 can be utilized to estimate the superelevation in a natural river, because none of the three equations was found to be superior to the others.

The measured superelevations shown in figure 57 are clustered around some values which are multiples of a hundredth of a foot. This is because the water surface elevations could not be measured closer than a hundredth of a foot.

The variability in the computed and measured values of superelevations for the high discharges was similar to that shown in figure 57. However, during high flows, the low lying banks of the river were flooded and an accurate determination of the superelevation in the field was not always possible.

70
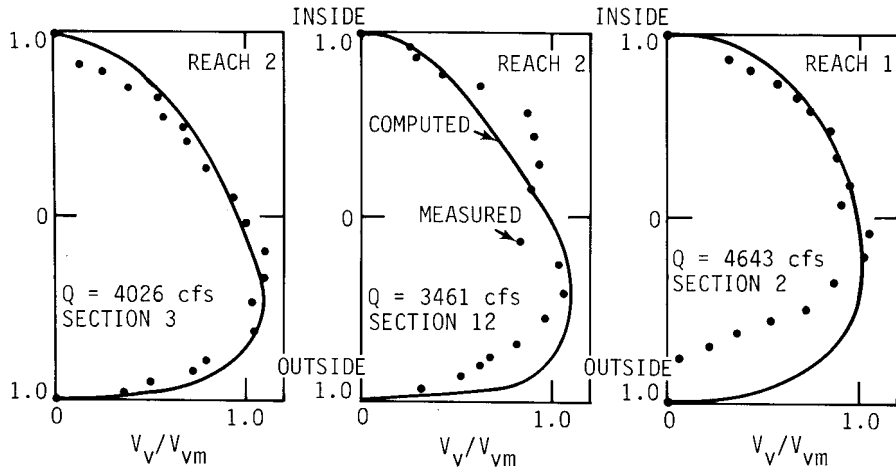
Figure 56. Computed and measured lateral velocity distribution
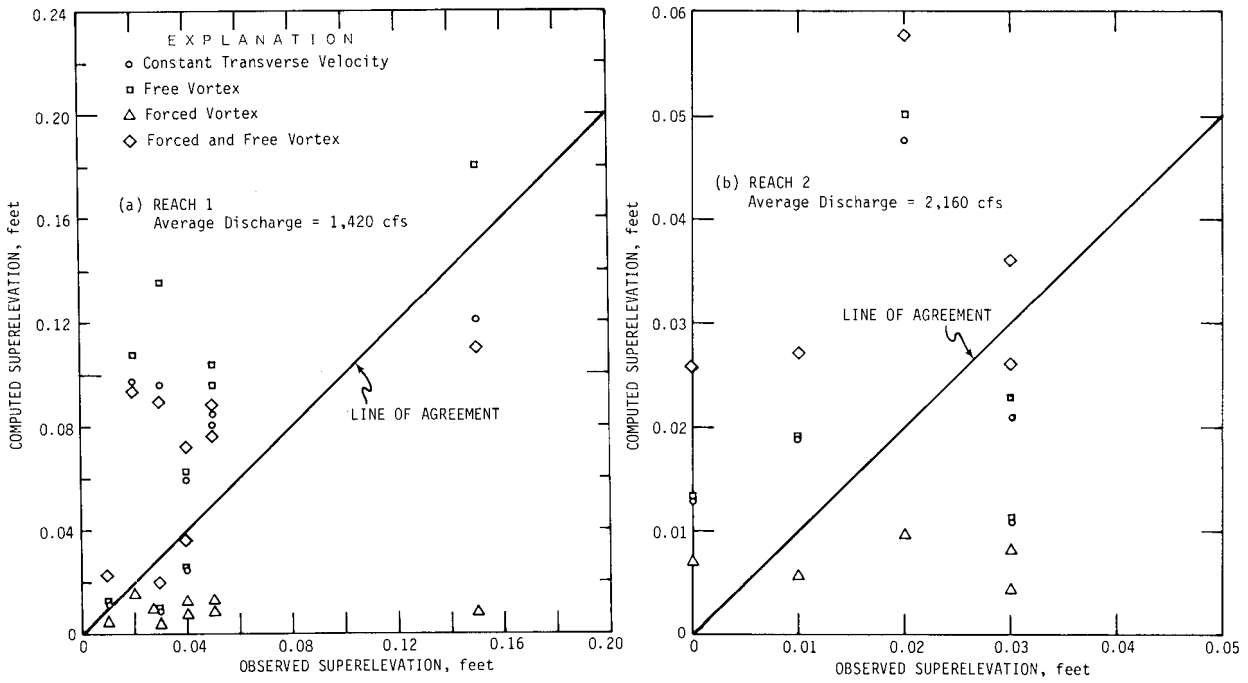
Figure 57. Computed and measured superelevations
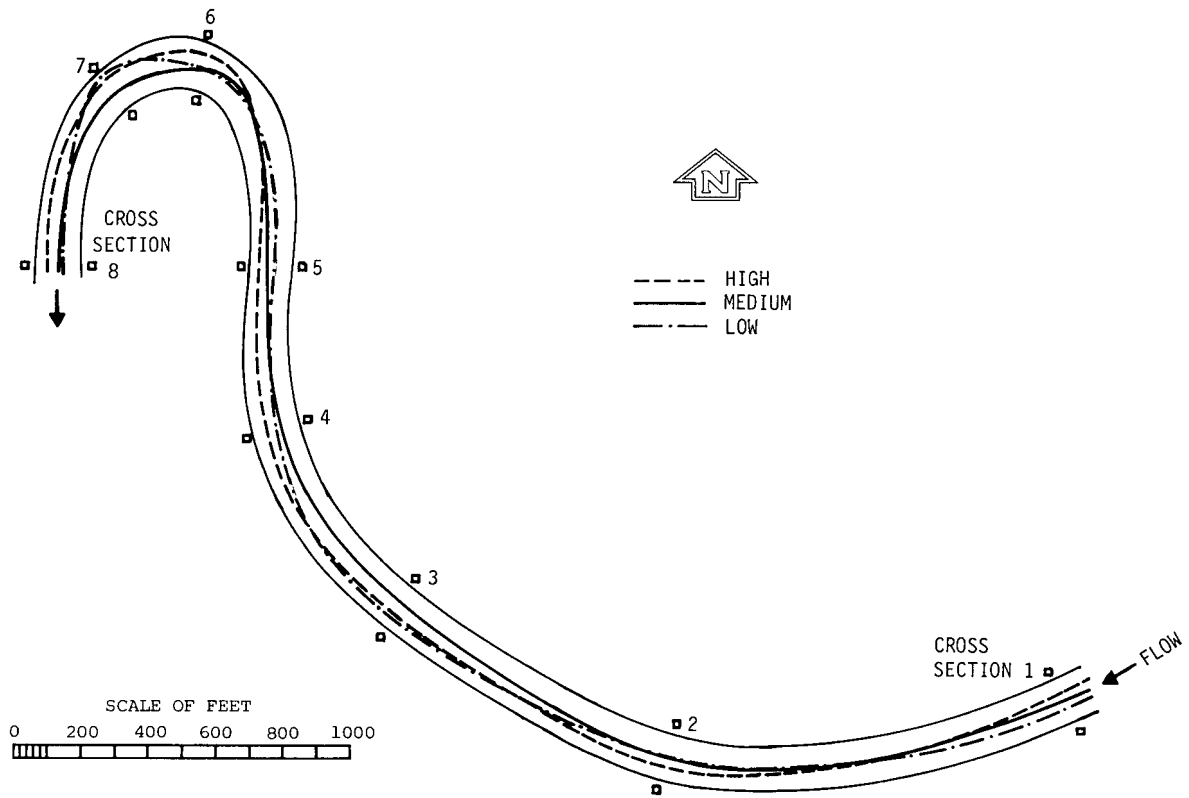
Figure 58. Core of the high velocity flow for low, medium, and high flows in Reach 2

CROSS
SECTION
8

CROSS
SECTION 1

FLOW

SCALE OF FEET

0   200   400   600   800   1000

HIGH
MEDIUM
LOW

Secondary Circulation

Instrumentation and the necessary support were not available to collect data related to secondary currents in the river during the present investigation. However, some generalized comments can be made on the basis of the hydraulic and geometric data that were collected and analyzed for both reaches.

The locations of the thalwegs for both reaches were plotted on plan views to study the pattern of the shifting thalwegs across the width of the channel. It was observed that generally the thalwegs shifted toward the outside bank of the bend and continued to stay close to the outside bank for some distance downstream until the downstream bend initiated a shift in their positions. This shifting of the thalwegs results from the presence of the lateral component of the velocity in and near the bends.

The isovels that were analyzed and presented previously also showed some striking characteristics which demonstrated that the secondary currents not only exist in open channels but also modify the velocity structure. Figure 58 shows the positions of the cores of the high velocity flows for low, medium, and high flows in Reach 2. During low flows, the high velocity flow followed the thalweg closely in the upstream part, shifted toward the outside bank near

section 7, and returned toward the centerline of the river at section 8. Section 8 is located near the crossing between the two bends.

For medium flow, the high velocity core remained close to the centerline of the channel. However, for high flows, the core took a more direct route from section 1 to section 2; stayed close to the left bank (outside bank) near sections 3, 4, and 5; moved straight near the outside bank close to section 6; and stayed at about the same location for the rest of the way to section 8. The variation of the shape of the high velocity core between low, medium, and high flows is associated with the changing characteristics and magnitudes of the secondary currents in the same reach of the river.

The shapes of the isovels also tell us something about the direction and presence of the secondary cells in an open channel. Bathurst et al. (1977) measured currents in open channel bends and found that the shapes of the isovels are a good indicator of the direction and location of secondary cells in the channel. If it is assumed that the isovels are nothing but a set of flexible membranes held in place by fluids between them, then the bulging or the deformity in their shape will indicate the presence of some force acting normal to the face of the membrane. Thus, if the membranes bulge inward, it will indicate the presence of a force
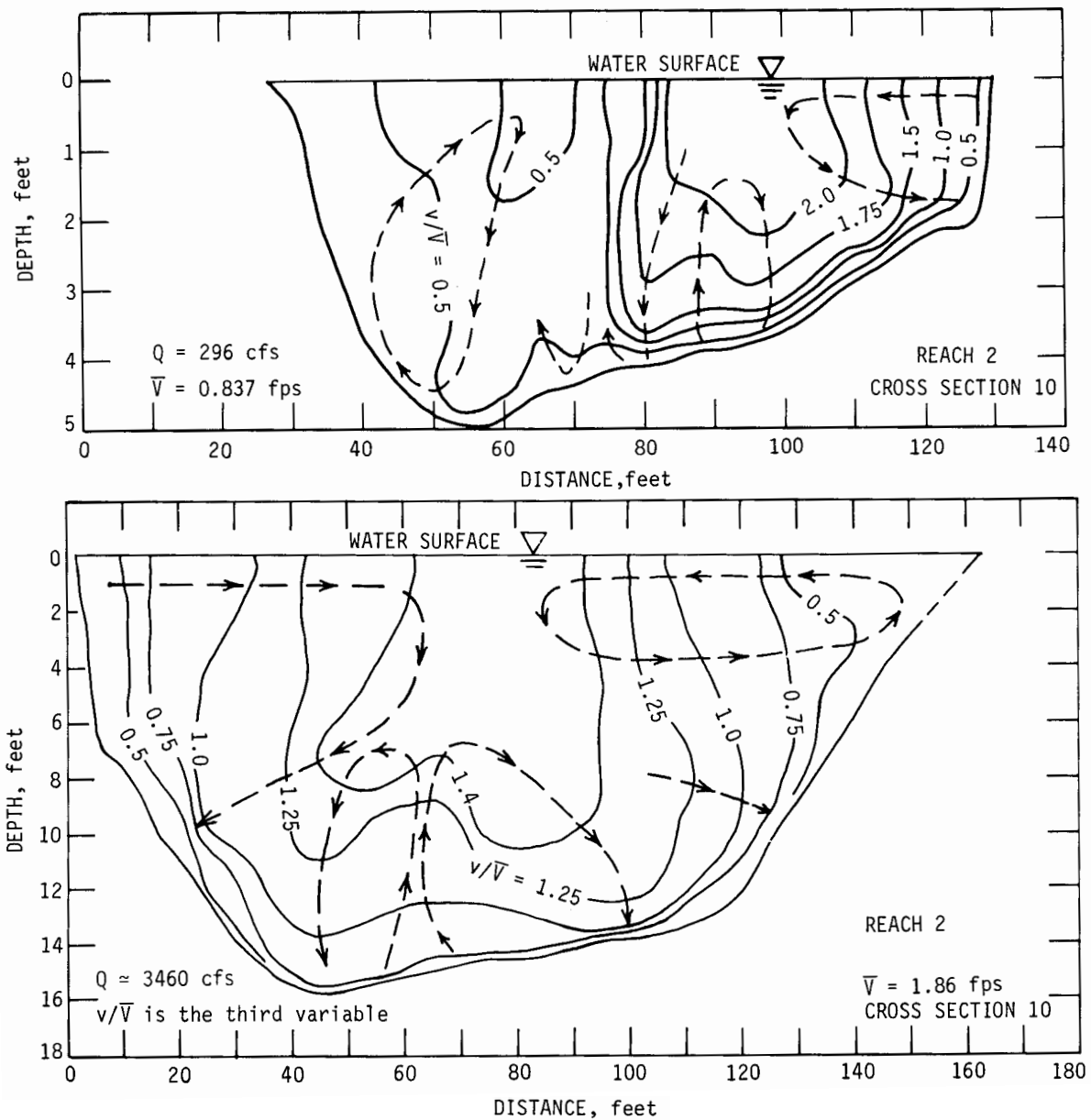
Figure 59. Secondary current cells at low and high flows in Reach 2

from the outside to the inside and vice versa. If this technique is followed through, the approximate locations of the secondary cells can easily be identified and drawn in conjunction with the isovels. Such a plot is shown in figure 59 for Reach 2. The data shown are for the low and high flows at section 10. The shapes of the isovels indirectly give an excellent clue as to the direction and the nature of the secondary cells. As a matter of fact, any one of the isovels shown in figures 25 through 53 could have been utilized to develop plots such as those in figure 59.

An examination of figure 59 will show that the number, location, and nature of the secondary cells remained unchanged between low and high flows. Such similarity was also noted for other reaches of the river.

Equation 38 showed an empirical relationship for computing the magnitude of the angle of the secondary current with the longitudinal direction of flow on the outside bank of the river. The presence of this secondary current and the deflection of the velocity vector was also substantiated by Brooks (1963). Brooks has mentioned that the maximum

73

Table 9. Energy and Momentum Coefficients

Cross section	Low flow		Medium flow		High Flow	
	α	β	α	β	α	β
Reach 1						
1	1.62	1.22	1.95	1.38	1.47	1.14
2	1.39	1.14	1.83	1.38	1.39	1.13
3	1.33	1.12	1.60	1.25	1.43	1.14
4	1.25	1.09	1.57	1.24	1.44	1.15
5	1.22	1.09	1.13	1.01	1.13	1.02
6	1.62	1.22			1.45	1.17
7	1.13	1.05	1.48	1.21	1.33	1.08
8	1.45	1.16	1.67	1.26	1.34	1.10
9	2.54	1.66	1.38	1.16		
10	1.31	1.11	1.49	1.22	1.74	1.26
11	1.32	1.12	1.38	1.16	1.33	1.11
12	1.32	1.12	1.54	1.21		
13	1.20	1.08	1.18	1.06		
14	1.26	1.10	1.56	1.24		
15	1.17	1.07	1.28	1.11		
16	1.45	1.17				
17	1.39	1.14	1.55	1.22		
Reach 2						
1	1.64	1.19	1.14	1.03	1.36	1.13
2	1.75	1.23	1.33	1.12	1.45	1.16
3	1.54	1.20	1.10	1.03	1.43	1.16
4	1.26	1.09	1.20	1.07	1.39	1.15
5	2.38	1.50	1.52	1.18	1.58	1.21
6	1.62	1.23	1.18	1.07	1.27	1.10
7	1.50	1.19	1.12	1.05	1.33	1.12
8	1.62	1.26	1.18	1.07	1.34	1.12
10	2.66	1.54			1.54	1.23
11	1.87	1.30	1.20	1.07	1.44	1.16
12			1.19	1.07	1.26	1.10
14	2.06	1.38	1.23	1.09	1.51	1.20
15	1.69	1.27	1.22	1.07	1.40	1.16

angularity of the secondary currents (ψ) observed by him in laboratory channels was 20 degrees. Equation 38 was used to compute the angle ψ for high flow conditions at different bends. It was observed that ψ varied from about 9 to 66 degrees.

The higher values of ψ were associated with bends having shorter radius of curvature r_c and larger central angles Δ. With an increase in the value of Δ and a decrease in the value of rc, the flow must turn around a sharper bend with an associated greater change in the momentum flux of the flow. This change in the direction of the momentum flux and the larger centrifugal force will significantly increase the magnitude of the secondary currents.

Energy and Momentum Coefficients

The energy coefficient α (equation 18) and the momentum coefficient β (equation 19) were computed for each section for every discharge for which velocity data were collected. The technique used was similar to that given by Chow (1959).

Table 9 shows the numerical values of α and β for Reach 1 corresponding to three different discharges. The average values of α based on data from all the sections for low flows is 1.41 and the corresponding average values of β is 1.16. Similarly, for medium flows, the average values of α and β are 1.51 and 1.21, respectively. The average values of α and β during high discharges became 1.23 and 1.02, respectively.

The arithmetic means of all the α and β values for low, medium, and high flows are 1.41 and 1.14, respectively.

Table 9 also shows the α and β values for Reach 2 for three discharges. The average values of α and β for low flows are 1.80 and 1.28, for medium flows 1.22 and 1.08, and for high flows 1.41 and 1.26. The arithmetic means of all the values of α and β for Reach 2 are 1.47 and 1.21, respectively.

The arithmetic means of all the values of α and β from both reaches are 1.44 and 1.17, respectively, The minimum and maximum values of α based on data from both reaches are 1.1 and 2.66, respectively. Similarly, the minimum and maximum values of β based on data from both reaches are 1.01 and 1.66, respectively.

The values of α and β shown in table 9 are from both straight reaches and bends. If these values for the straight reaches and bends are separated, the average values of α and β are 1.45 and 1.22 for straight reaches and 1.43 and 1.18 for bends. There is a slight decrease in these values in the bends compared with the straight reaches.

These average values appear to be within the limits that were reported by Hulsing et al. (1966) and Chow (1959).

Roughness Coefficient, Head Loss, and Energy Dissipation

Two of the most widely used roughness coefficients in open channel flow analysis are Manning's n and Chezy's C, which can be computed by equations 15 and 13, respectively. Another form of roughness coefficient is expressed by $C/(g)^{1/2}$ and is derived from Chezy's equation. The interrelationships between C, n, and $C/(g)^{1/2}$ are given by equations 16 and 17.

In the computation of n, C, and $C/(g)^{1/2}$ by equations 15, 16, and 17, respectively, the values of average velocity $\overline{V}$, average energy slope S_e, and hydraulic radius R must be known from field measurements. The values of $\overline{V}$ and R have been determined for various discharges from the data measured in the field. However, while computing the average water surface slope and the average energy slope from both reaches for various discharges, it was observed that a considerable amount of additional head loss occurred in Reach 2 for low, medium, and high flows at or near section 13 (figures 7 and 20). This was caused by the presence of bedrock at this location. The rock ledge acted as a low overflow type dam in the course of the river especially during low flows and has consequently modified the water surface profiles both upstream and downstream. The water surface profile resembles an M_1 type backwater curve downstream of the rock ledge and an M_2 type backwater curve upstream of the rock ledge (Chow, 1959). An M_1 curve is produced when the lower end of a long flume having a mild slope is submerged in a reservoir to a greater depth than the normal

depth of flow in the flume. Whereas, an M_2 type backwater curve will result when the bottom of the flume at its lower end is submerged in a reservoir to a depth less than the normal depth.

This phenomenon is amply demonstrated in figure 60 for three typical flow conditions. For the low flow condition, the water surface profile starts to drop near section 12 and continues to drop until near section 15. The approximate drop of the water surface elevation at this location for this flow is 1.2 feet. The average water surface slope upstream of section 12 is 0.43 ft/mile and downstream of section 14 it is 1.25 ft/mile.

For medium flow, the control point has moved upstream and is now located close to section 11 (figure 60). The average drop of water surface at this location is 0.8 foot. Two distinct water surface slopes exist for this flow condition. The average value of S_w upstream of section 11 is 0.51 ft/mile and downstream of section 14 it is 0.78 ft/mile.

In the case of high discharge, which was at or above bankfull stages, the control point has moved upstream near section 9, a distance of about 4500 feet upstream from section 13. The average water surface drop at this location is now close to 0.55 foot.

This change in the location of control points with an increase in discharge is the same as for flow over a low head sill in an open channel. The rock ledge, being immovable and nonerodible, acts as an obstacle in the path of the river and consequently has changed the characteristics of flow.

The above discussion demonstrates that a single roughness coefficient for the entire length of Reach 2 should not be computed. Either the additional head loss due to the presence of the rock ledge must be subtracted from the total head drop before an average energy slope is computed or two separate slopes must be determined, one before the control point and another after the control point. These two energy slopes can then be used in connection with equation 15 to compute Manning's roughness coefficient n. This was done to compute the roughness coefficients for Reach 2. However, for Reach 1, no such control point existed (figure 19) and a single line was fitted by the least square technique to determine an average value of S_w for all discharges.

Another necessary assumption in the computation of n was that the average velocity $\overline{V}$ at any section during a single data collection trip did not vary significantly from day to day. There was some change in the measured discharges from one day to the next in the same reach of the river from section to section, but it is quite reasonable to assume that the average velocity at any section remained approximately unchanged during those consecutive days of data collection when the discharge did not vary significantly. The water surface slope S_w and subsequently the value of S_e needed to compute the values of n, C, and
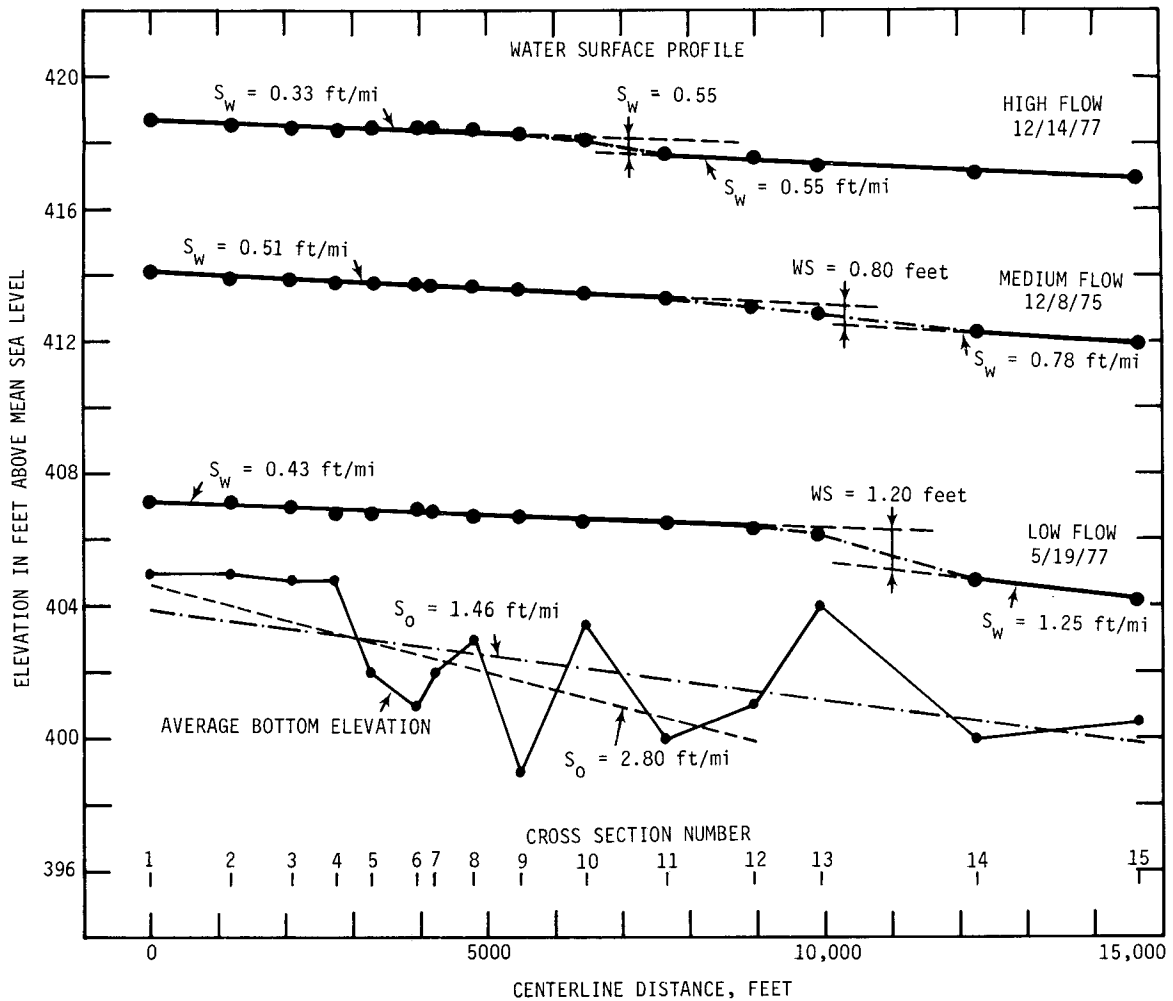
Figure 60. Water surface profile and head loss in Reach 2

$C/(g)^{1/2}$ was the value based on water surface elevations measured during a single day.

Once the values of average velocity $\overline{V}$, energy coefficient α, and water surface elevation WS were known, the energy slope S_e was computed by equation 42:

$$S_e = [(WS_1 + \alpha_1 \overline{V}_1{}^2/2g) - (WS_2 + \alpha_2 \overline{V}_2{}^2/2g)]/L \quad (42)$$

where WS_1 and WS_2 are the water surface elevations at any two sections and L is the distance between these two sections. The other terms have already been explained. This procedure was used to compute S_e either between any two sections or over the entire length of the study reach.

The assumptions outlined above were necessary to compute a reasonable and representative value of the roughness coefficient on the basis of field data. At this point, it must be remembered that a natural channel does not behave like a laboratory channel where the discharge, water surface profile, and other parameters can be kept constant over a

period of time. Therefore, in order to obtain any meaningful information from the data collected from a natural channel, simplification and a few generalized assumptions must be made before any computation can be done. It is the contention of the author that the results obtained by the above procedure should yield a representative value of the roughness coefficient in any natural channel.

Equations normally used in computing roughness coefficients in open channels are based on the assumption that uniform flow exists in the river and that a unified roughness parameter can be estimated. For the present case, uniform flow equations were used to estimate a composite roughness coefficient which should reflect the cumulative effects of all resistance to flow in the river. This procedure does not show the effect of the gain of potential energy for flow around a bend, but it does show the effect of the normal resistance to flow in the channel. Following through with these assumptions, the values of n, C, and $C/(g)^{1/2}$ were computed for all flow conditions for both reaches.

76

Table 10 shows the average values of S_w and S_e, Manning's n, Chezy's C, and the values of $C/(g)^{1/2}$ for Reach 1 corresponding to low, medium, and high flows. Computations were made for each day for each set of data. The average water surface slopes for low, medium, and high flows were 1.57, 1.54, and 1.07 ft/mile, respectively. The average values of S_e varied from 1.58 ft/mile for low flow to 1.54 ft/mile for medium flow to 1.15 ft/mile for high flow. The average values of S_w and S_e for corresponding discharges were almost identical, indicating an even energy dissipation over the whole length of this reach of the river.

The overall head loss h_L in the river, computed by equation 18 and expressed as a function of the unit length of the river, becomes equal to the numerical value of S_e. Thus S_e and h_L are identical. Therefore, the values of S_e shown in tables 10 and 11 also indicate the head loss in the river for different flow conditions.

The average values of Manning's n for low, medium, and high flows are 0.051, 0.053, and 0.044, respectively. A decrease in the value of n is associated with an increase in the discharge. Chezy's C varies from a minimum of 33 to a maximum of 55 for all flow conditions. The average values of C for low, medium, and high flows are 40, 40, and 51, respectively. Similarly, the average values of $C/(g)^{1/2}$ for these flows are 7.1, 7.0, and 8.9, respectively.

Table 11 shows the values of S_w, S_e, n, C, and $C/(g)^{1/2}$ for the three flow conditions in Reach 2. For low and medium flow conditions, computations were made by dividing the reach into two parts above and below the discontinuity point of the water surface profile shown in figures 20 and 60. Computations were also made considering the entire reach as a single unit with no discontinuity in the water surface profile.

For low and medium flows between sections 1 and 8 or 1 and 11, the values of S_w, S_e, and n are smaller than those between sections 1 through 15 or 14 through 15. Here again, the rock ledge near section 13 has effectively developed a flatter water surface slope upstream of this section which in turn yields a smaller overall value of Manning's n for this reach of the river. For high flow conditions, it was assumed that, on the average, a single water surface slope existed for the entire length of this reach and single values of n, C, and $C/(g)^{1/2}$ were computed for the five days of the data collection (table 11). The average values of n, C, and $C/(g)^{1/2}$ for high flow are 0.043, 52, and 9.2, respectively.

The average overall values of n between sections 1 and 15 for low, medium, and high flows are 0.041, 0.044, and 0.043, respectively. The expected reduction in the values of n with an increase in discharge did not really materialize at this location because of the presence of a relatively flat water surface slope during low flow upstream of section 13 which resulted in smaller values of n during low flows. Data from both reaches indicated that the average overall values

of n can be as high as 0.053 and as low as 0.039.

There was considerable variation in the hydraulic properties of the river between any two consecutive sections. Manning's n was computed between successive sections for three typical flow conditions corresponding to low, medium, and high flows for both reaches, as shown in figure 61. In a few instances, there is discontinuity in the values of n because hydraulic data at these cross sections were not available on the specified date.

In Reach 1, the highest computed value of n is 0.084 between sections 7 and 8 for medium flow and the lowest value of n is 0.028 between sections 14 and 15 for low flow. For Reach 2, the highest computed value of n is 0.073 between sections 14 and 15 for low flow and the lowest value is 0.013 between sections 5 and 8 for low flow. In general, the values of n in Reach 2 are lower upstream of section 11 for all discharges (figure 61). This again demonstrates the significant effect of the rock ledge near section 13 on the overall flow pattern in this segment of the river.

In the "Energy Dissipation" section of the background analysis it was mentioned that a plot of the ratio of S_e/S_w versus distance in an open channel can shed some light as to the nature of energy dissipation in the channel. Figure 62 shows such a plot for Reach 1 for three typical flow conditions. The ratio S_e/S_w varies anywhere from 0.8 to 1.4 indicating that in some part of the river, an accelerating flow is present ($S_e/S_w > 1$) and in another part, the flow is decelerating or a conversion of the kinetic energy into potential energy is taking place ($S_e/S_w < 1$). This type of variability is expected in an open channel where the stream banks, bends, snags, and fallen trees change the patterns of flow. Consequently, the flow will pass through a series of localized acceleration and deceleration. However, in general, the flows in Reach 1 for all three flow conditions appear to have been behaving much like a uniform flow pattern.

Figure 63 shows the variability of S_e/S_w for Reach 2 for three typical flow conditions. It appears that during high flow conditions, the flow was accelerating considerably at or near section 4. Some deceleration of the flow is noted near section 6. Otherwise S_e/S_w varies close to unity.

If the ratio of the average energy slope S_e (table 11) and the bed slope S_o (figure 60) between sections 1 through 11 is computed, the value of S_e/S_o becomes 0.14 for low flow data collected on May 19, 1977. Similarly, for medium flow, the ratio of S_e/S_w for sections 1 through 11 is 0.18. For the high flow data shown in figure 60, the ratio S_e/S_o between sections 1 through 9 becomes 0.26. In all these cases, the values of S_e/S_o are much smaller than 1 indicating a decelerating flow condition in this segment of the river. This again shows that a conversion of the kinetic energy into potential energy takes place in this reach of the river with an associated decrease in energy dissipation compared with uniform flow conditions. Thus, it is quite apparent that the presence of bedrock, snags of permanent nature,

Table 10. Roughness Coefficient and Head Loss, Reach 1

Date	Water surface slope, S_w (ft/mi)	Energy slope, S_e or b_L (ft/mi)	Manning's n	Cbezy's C	$C/(g)^{1/2}$
Low flow					
10/20/75	1.29	1.29	0.043	46	8.2
10/21/75	1.96	1.98	0.061	33	5.8
10/22/75	1 54	1.56	0.054	37	6.6
10/23/65	1.57	1.57	0.043	46	8.1
10/24/75	1.48	1.50	0.053	38	6.7
Medium flow					
5/11/77	1.59	1.60	0.056	37	6.5
5/12/77	1.39	1.40	0.048	43	7.5
5/13/77	1.61	1.61	0.051	40	7.1
5/16/77	1.56	1.56	0.055	38	6.7
High flow					
3/20/78	1.18	1.26	0.046	48	8.5
3/21/78	0.90	0.96	0.040	55	9.7
3/22/78	1.09	1.16	0.044	50	8.8
3/23/78	1.12	1.20	0.045	49	8.6

Note. S_w, S_e and b_L were computed for the whole reach from cross section 1 to 17.

Table 11. Roughness Coefficient and Head Loss, Reach 2

Date	Cross section	Water surface slope, S_w (ft/mi)	Energy slope, S_e or b_L (ft/mi)	Manning's n	Cbezy's C	$C/(g)^{1/2}$
Low flow						
5/17/77	1 to 8	0.43	0.44	0.022	79	13.9
5/18/77	1 to 11	0.36	0.38	0.028	63	11.2
	14 to 15	1.27	1.28	0.074	25	4.4
	1 to 15	0.96	0.96	0.040	43	7.6
5/19/77	1 to 11	0.39	0.40	0.029	62	10.9
	14 to 15	1.25	1.26	0.073	25	4.4
	1 to 15	0.97	0.97	0.041	43	7.6
Medium flow						
12/8/75	1 to 11	0.51	0.49	0.029	74	13.0
	14 to 15	0.78	0.81	0.051	43	7.6
	1 to 15	0.78	0.78	0.045	48	8.4
12/9/75	1 to 11	0.48	0.46	0.028	76	13.3
	14 to 15	0.78	0.81	0.051	43	7.6
	1 to 15	0.76	0.77	0.044	48	8.5
12/10/75	1 to 11	0.50	0.48	0.028	74	13.1
	14 to 15	0.76	0.78	0.050	44	7.7
	1 to 15	0.78	0.78	0.045	48	8.4
12/11/75	1 to 11	0.51	0.50	0.029	73	12.9
	14 to 15	0.78	0.81	0.051	43	7.6
	1 to 15	0.79	0.79	0.045	48	8.4
High flow						
12/05/77	1 to 15	0.68	0.70	0.045	50	8.8
12/13/77	1 to 15	0.68	0.70	0.045	50	8.8
12/14/77	1 to 15	0.71	0.73	0.046	49	8.6
12/15/77	1 to 15	0.53	0.55	0.040	56	9.9
12/16/77	1 to 15	0.49	0.51	0.039	58	10.1
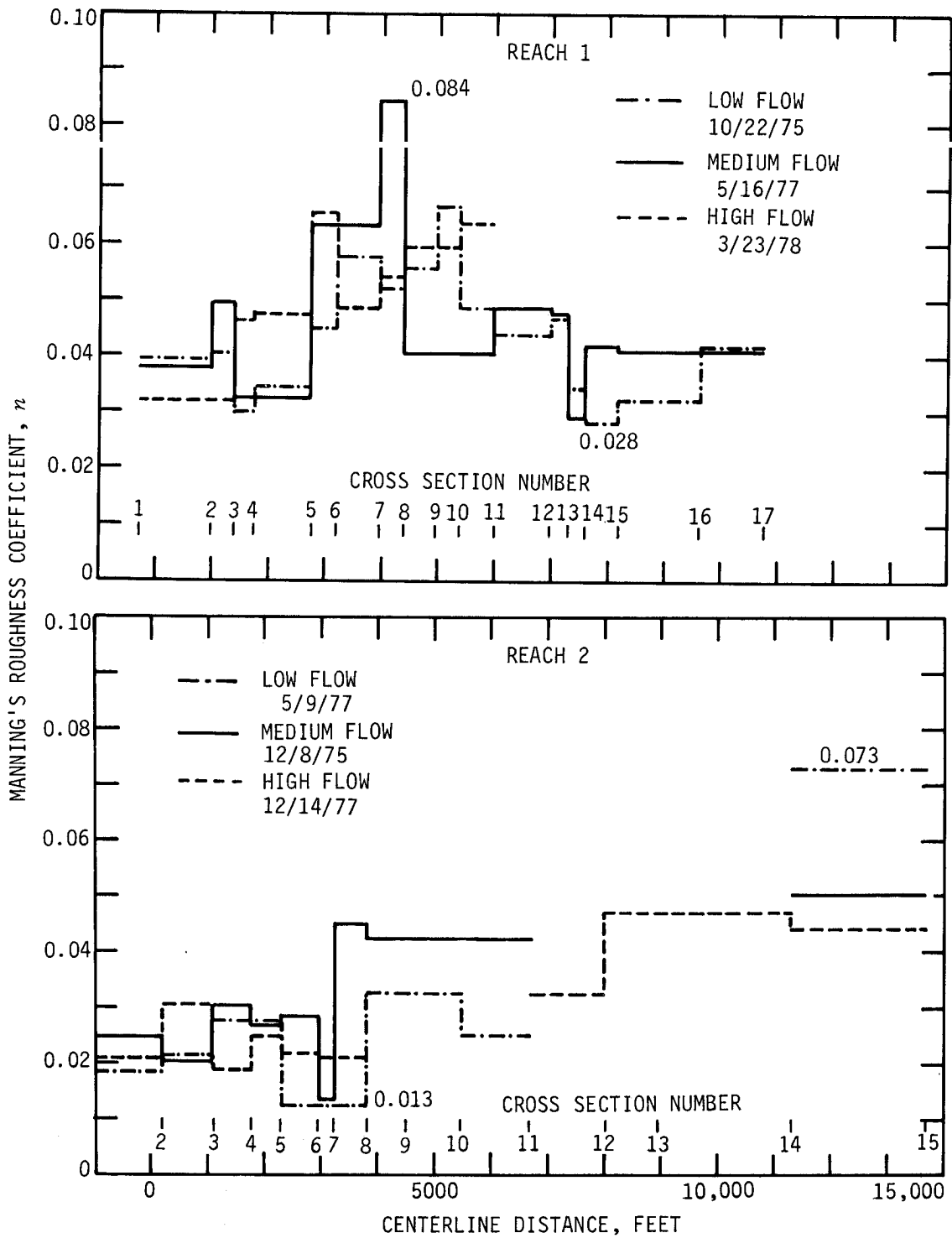
Figure 61. Variation of Manning's roughness coefficient
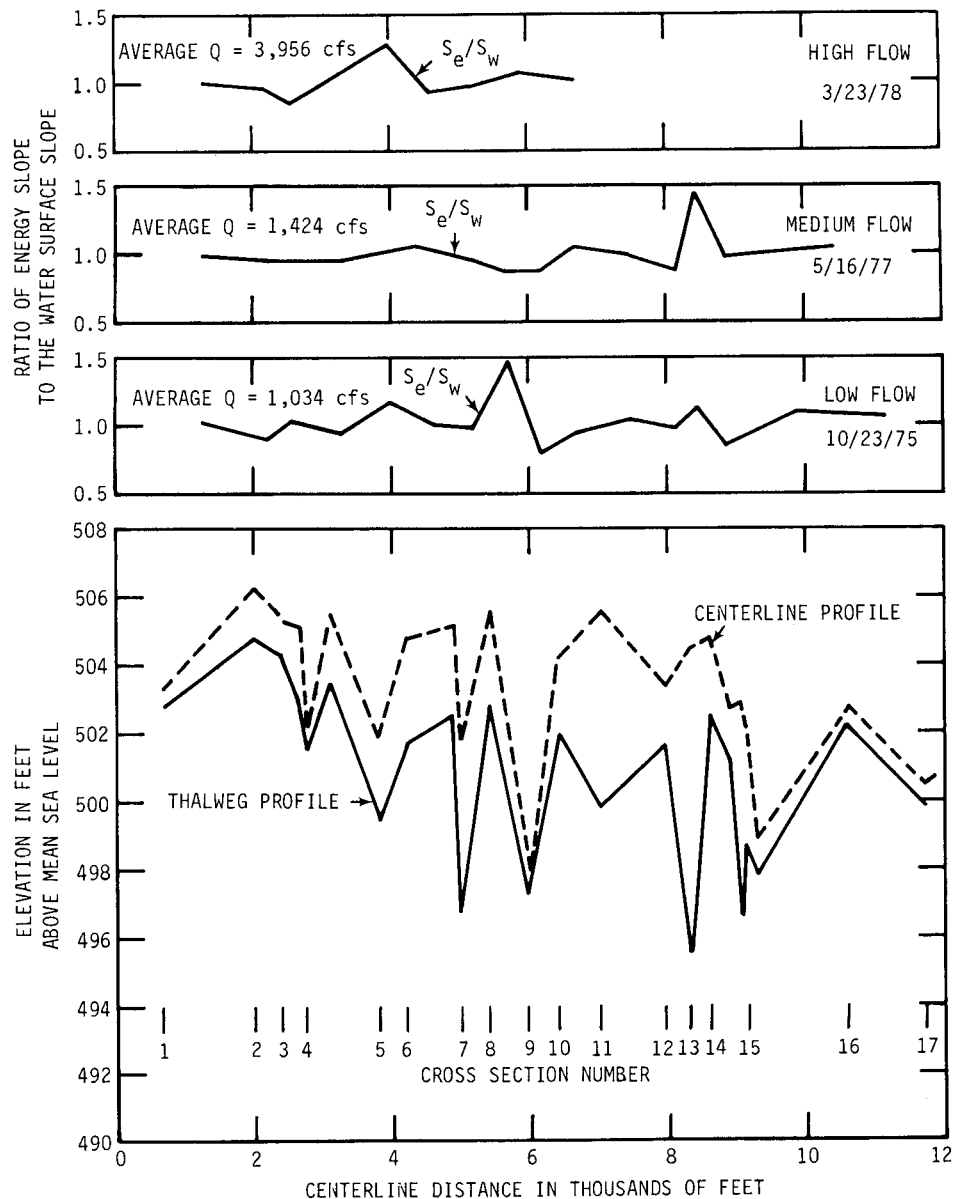
Figure 62. Ratio of S_e/S_w for Reach 1

and other obstacles in the river course changes the characteristics of flow in the open channel.

The simple and basic analyses presented thus far are extremely valuable in the study and subsequent understanding of the basic mechanics of flow in open channels.

Distribution of Unit Discharges

The detailed velocity distribution data collection for different discharges for the present investigation required a considerable amount of time and was also very expensive.

However, if a correlation can be developed between the lateral velocities in each vertical with a parameter such as the corresponding depths, then it will be very easy to measure the cross-sectional depths during low flows, and then to estimate the lateral average velocities in each vertical for varying frequencies of discharges. In this study a relationship similar to equation 43 below was found to be valid for both straight reaches and bends.

$$q/\overline{q} = K(D/\overline{D})^m \qquad (43)$$

where q is the unit discharge at depth D, $\overline{q}$ is the average unit discharge in the cross section, $\overline{D}$ is the average depth, K is a constant, and m is the coefficient of regression. A
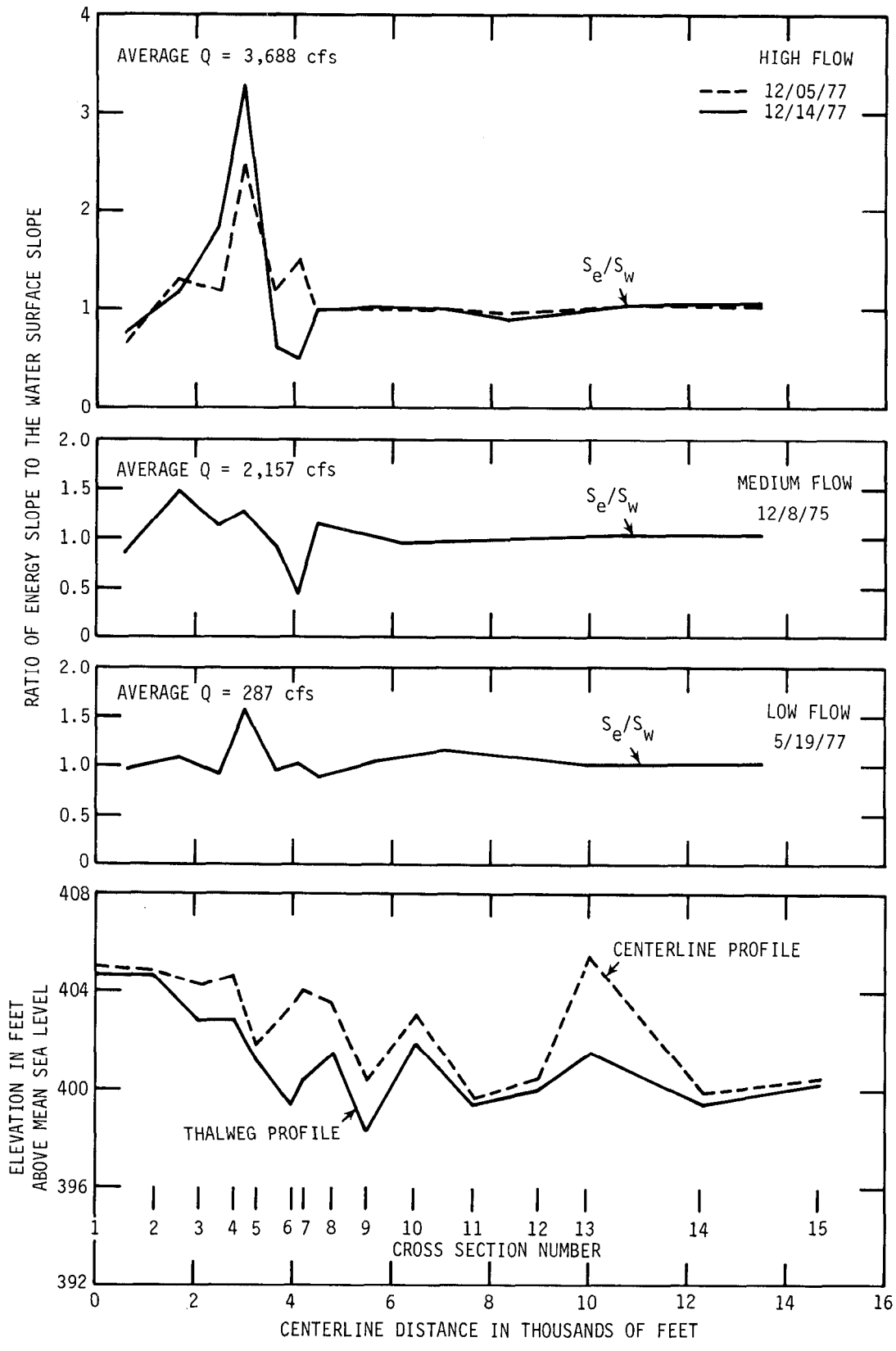
Figure 63. Ratio of S_e/S_w for Reach 2
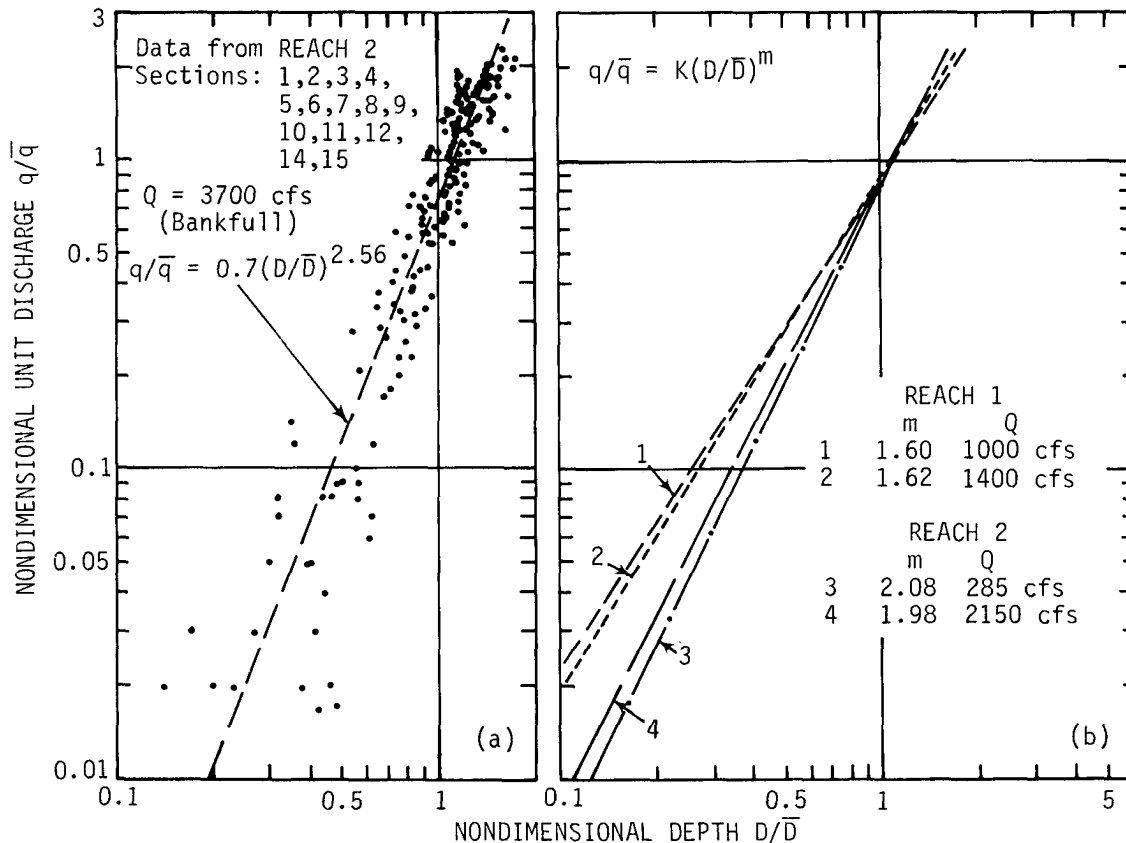
Figure 64. Nondimensional unit discharge versus nondimensional depth

similar type of relationship was also postulated by Sium (1975).

Figure 64a shows a plot of $q/\bar{q}$ versus $D/\bar{D}$ for Reach 2 for bankfull discharges where the data from the straight reaches and bends were plotted. Here K is 0.7 and m is 2.56. From other similar plots it was also observed that during bankfull stages the spread of the points from a mean line was less than that present during low flows. When the ratios of $q/\bar{q}$ and $D/\bar{D}$ were close to or more than unity, the differences between the plotted points from straight reaches and bends were negligible. However, for smaller values of $q/\bar{q}$ and $D/\bar{D}$, the difference became much more dominant, making the values of m usually greater than 2. Figure 64b shows other plots for bends relating $q/\bar{q}$ and $D/\bar{D}$ for both reaches.

These two plots indicate that a correlation between $q/\bar{q}$ and $D/\bar{D}$ can be developed for open channel flows. This type of relationship is helpful in the determination of an approximate lateral velocity distribution across the width of the channel once the individual depths are known.

Turbulence in an Open Channel

Data related to the turbulent fluctuation of the velocity component could not be collected because of the non-availability of support. Turbulent fluctuation of the velocity component is an important parameter and should be considered in the stability analysis of the bank in any open channel flow problem.

Turbulent mixing is the main mechanism for diffusion and dispersion of momentum, heat, and mass in turbulent shear flows. It is also important in reaeration and sediment transport in streams. The measurement of turbulence in streams is very difficult because of the variation of temperature of the water and the buildup of contamination on the turbulence measuring probes, such as a hot-film anemometer.

The best physical picture of turbulence is obtained by recording the velocity fluctuations with time at various points in the section of the stream. Kalinske (1942) analyzed data collected from the Mississippi River which gave an indication of the turbulent velocity fluctuations. From a

statistical analysis of the Mississippi River data collected for 10 minutes for each point, Kalinski concluded that the turbulent velocity fluctuations follow a Gaussian distribution. Defining the standard deviation s or root-mean square of the velocity fluctuations as the intensity of turbulence, Kalinski concluded that the maximum fluctuating component of the velocity ($V'_{max} - \overline{V}$) equal to 3s or greater occurs only for about 0.3 percent of the time. Thus, for all practical purposes, the maximum value of ($V'_{max} - \overline{V}$) can be taken as 3s.

The relative intensity of turbulence is defined by the ratio of the standard deviation s to mean velocity $\overline{V}$, i.e., $s/\overline{V}$. From a plot of relative depth y/D versus the relative intensity of turbulence for both streams and pipes, Kalinske (1942) concluded that $s/\overline{V}$ can easily be equal to l/3 near the boundaries. Thus with ($V'_{max} - \overline{V} = 3s$ and $s/\overline{V} = 1/3$, the maximum point velocity can easily be $2\overline{V}$.

McQuivey (1973) collected longitudinal turbulence data from canals and rivers with a hot-film anemometer and ordinary current meters. The current meter measurements were made by changing the digital output from the current meter to an analog signal and recording the data on magnetic tapes. These data were digitized for further analysis.

Comparison of longitudinal turbulence intensities measured by McQuivey (1973) at the Mississippi River near Vicksburg, Mississippi, when the depth and width of the river varied from 21 to 65 feet and 2000 to 2690 feet, respectively, showed that the longitudinal turbulence intensities measured by the current meter were always greater than those measured by the hot-film anemometer. The current meter measurements ranged from 0.066 at y/D of 0.88 to 0.24 at y/D of 0.12 where the depth y is taken from the bed and D is the total depth of water at the point of measurement. The hot-film anemometer measurements varied from 0.043 at y/D of 0.88 to 0.15 at y/D of 0.12. In all the measurements, the longitudinal turbulence intensity showed an increase with an increase in depth. The mean of the differences of the turbulence intensities measured by the current meter and by the hot-film anemometer was 0.053.

The hot-film anemometer measurements of the turbulence intensities at the Atrisco feeder canal and the Rio Grande conveyance channel in Mexico were greater than those measured by the current meter (McQuivey, 1973). The Atrisco feeder canal was 1.4 to 1.9 feet deep and 56 feet wide, whereas the Rio Grande conveyance channel was 3.1 to 3.2 feet deep and 68 feet wide.

The discrepancy between this set of data and those collected from the Mississippi River may have resulted from a difference in the scale of the turbulence and the loss of turbulence associated with the current meters due to inertial averaging (Bennett and McQuivey, 1970). The roughness elements and the depths are larger in deeper channels compared with those in shallower channels. Consequently, the turbulence scale which is a function of the effective roughness element (Kalinske, 1942) must be larger in the deeper channel compared with the shallow channel. Thus the loss of turbulence intensity due to "spectral averaging" by the propeller will be less in the larger channels. This fact in combination with the higher velocities in the Mississippi River may have contributed toward a smaller loss of turbulence intensity due to inertial averaging.

The above analysis indicates that the current meter can sometimes be used to measure the turbulence intensity in an open channel. However, if the direction of the current meter is not fixed, the freely rotating current meter will measure an average turbulence in the longitudinal direction. Depending upon the differences in water depths and flow velocities, the turbulence intensity measured by the current meter may predict a higher or a lower value compared with that measured by the hot-film anemometer.

The design and the analysis of open channel flow problems should include a consideration for the turbulent velocity fluctuations of the flowing water. The analysis presented so far showed a technique that can be used to estimate the magnitudes of turbulent velocity fluctuations. The reason for including this analysis in the report is to emphasize the fact that turbulence is an important parameter in the open channel flow problems.

Low Flow Characteristics: Pools and Riffles

The hydraulics of flow in a stream is usually different for low flows than for bankfull or flood stages. During low flows, the undulations in the bed and the roughness elements of the bed will usually modify the local hydraulics of flow, even though the overall gradient of the stream remains unchanged.

In a sand-gravel stream, pools and riffles will appear during low flows. For some discharges, the flow may pass through a critical stage (maximum discharge for this depth) at the riffle before returning to a placid condition in the pool. Whenever the bed materials are such that coarse grained materials are present, the fine materials from the riffles are washed away and an armour where only the larger particles remain is formed. The eroded fine grained particles are usually deposited in the pool.

Data from two pool-riffle sequences were collected during low flows from Reach 1 (figure 6). These data have been analyzed and some of the results were presented by Bhowmik and Stall (1978a) at the 1978 Spring Annual Meeting of the American Geophysical Union.

Figures 65 and 66 show the plan views of the two sequences of pool and riffles where detailed hydraulic and geometric data were collected. Out of the 51 bed material samples, 30 samples were collected from pool-riffle sequence A (figure 65) with the remaining 21 samples col-
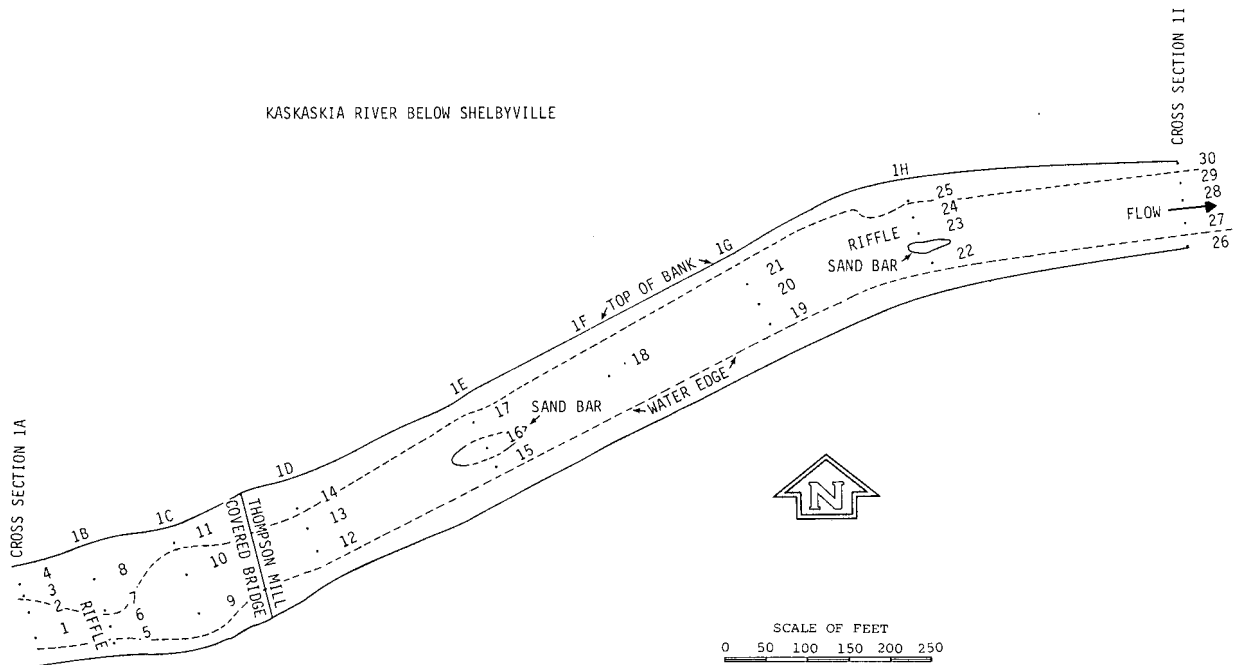
Figure 65. Plan view of pool-riffle sequence A

lected from pool-riffle sequence B (figure 66). The exact locations of the bed and bank material samples are also shown. These bed and bank material samples were analyzed to determine the particle size distributions.

Tables 12 and 13 show the d_{50} and d_{95} sizes, standard deviation σ, uniformity coefficient U, and some comments as to the general nature of the materials based on the analysis of the data from the two sequences. Normally, the bed materials at the riffle are coarser than those in the pools. The change in the sizes of the bed materials as the flow passes from the riffle to the pool is shown in figure 67 as the isolines of d_{50} sizes in millimeters. The D_{50} sizes vary from a maximum of 40 mm in the riffle for sample 6 (figure 65 and table 12) to a minimum in the pool of 0.065 mm for sample 19.

Isolines of d_{95} sizes for pool-riffle sequence A are also shown in figure 67. Here the d_{95} sizes vary from a maximum of 130 mm in the riffle, sample 2 (figure 65 and table 12) to a minimum of 0.2 mm in the pool, sample 30. The variability and the areal distribution of the d_{95} sizes are similar to those observed for the d_{50} sizes with the highest sizes occurring in the riffles and the smallest sizes in the pools.

Figure 68 shows the lines of equal d_{50} and d_{95} sizes for pool-riffle sequence B. Here the largest size of the medium diameter is in the riffle with the lowest size occurring in the pool. The largest d_{50} size of 4.6 mm is from

sample 41 (figure 66 and table 13) which is in the riffle, and the smallest value of d_{50} is 0.034 mm and is from sample 32 in the pool section of the river. For sequence B, the largest d_{95} size of 19 mm is in the riffle, samples 36, 37, and 41 (figure 66 and table 13), and the smallest d_{95} size of 0.2 mm is in the pool, sample 31. The general pattern of the variability remained the same as that observed for the d_{50} sizes.

The hydraulic and geometric data that were analyzed for the pool-riffle condition are the bed and water surface profiles, velocity and velocity head, and the head loss. Figure 69 shows the water surface and thalweg profiles for both sequences of pools and riffles. There is a sharp drop in the water surface elevation right after the riffle section. The water surface profile becomes extremely flat in the pool.

The head loss in pool-riffle sequence A was 4.44 ft/mile and for sequence B it was 2.48 ft/mile. The overall Mannings n was 0.034 in sequence A and 0.048 for sequence B.

Velocity distribution data were also used to determine various hydraulic parameters in the riffles. Figure 70 shows the variability of velocity V, Froude number F, velocity head $V^2/2g$, and depth D in the riffle section of sequence A. The depth of water and the flow velocity changed in the transverse direction. The Froude number is less than 1.0 and has a maximum value of 0.7. The flow remained subcritical throughout the riffle section. The water surface was wavey and a considerable amount of reaeration took

84
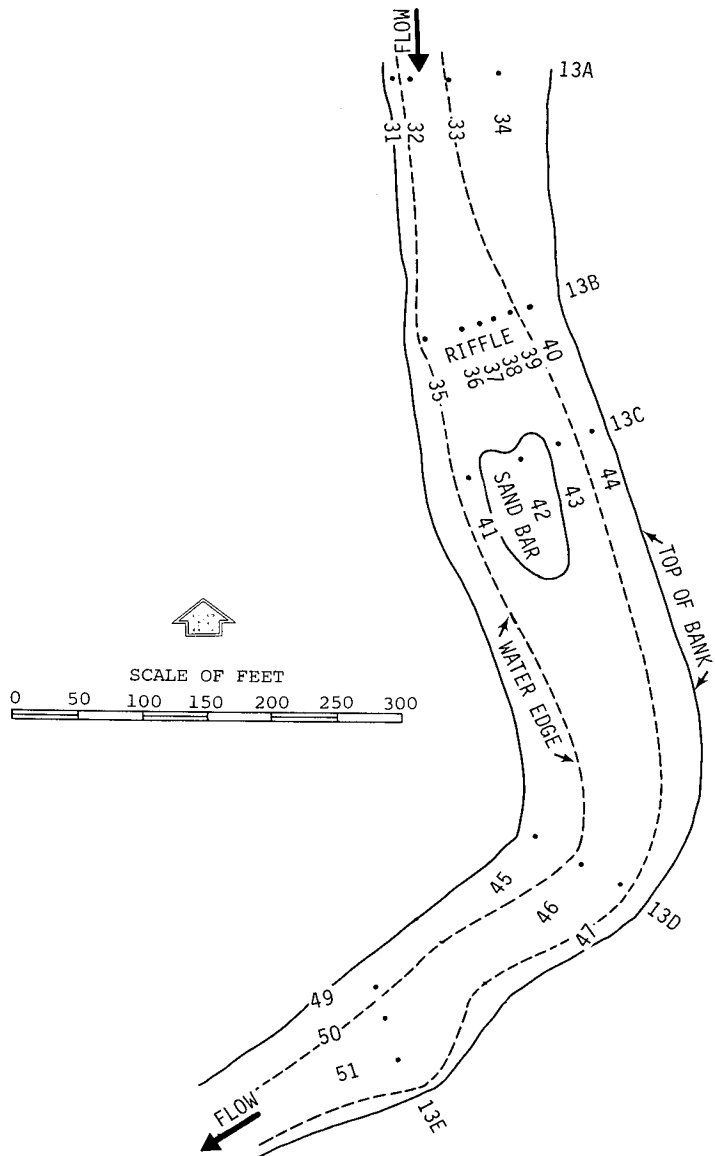
Figure 66. Plan view of pool-riffle sequence B

Table 12. Particle Size Characteristics of the Bed and Bank Materials,
Reach 1, Pool-Riffle Sequence A

Sample number	d_{50} (mm)	d_{95} (mm)	σ	U	Remarks
1	36.0	71.0	3.51	13.55	Gravelly sand
2	24.0	130.0	13.76	87.50	Gravelly sand
3	21.0	70.0	4.87	25.45	Dark brown gravelly sand
4	14.0	57.0	11.58	135.71	Dark brown gravelly sand
5	0.19	0.36	2.53	6.97	Brown loamy sand
6	40.0	62.0	1.85	3.67	Brown gravelly sand
7	15.0	55.0	8.83	55.26	Gravelly sand
8	14.0	58.0	16.91	95.24	Brown gravelly sand
9	0.40	2.3	1.89	2.05	Brown sand
10	8.5	47.0	21.44	150.00	Brown gravelly sand
11	14.0	70.0	172.37	262.50	Brown gravelly loamy sand
12	0.44	2.1	1.84	2.00	Brown sand
13	6.8	77.0	12.10	40.63	Dark brown gravelly sand
14	0.07	27.0	82.95	29.17	Dark brown sandy loam
15	0.27	0.52	1.36	1.75	Brown sand
16	0.30	0.65	1.26	1.36	Brown sand
17	0.77	8.5	4.25	2.85	Brown gravelly sand
18	0.39	1.8	1.79	1.76	Brown sand
19	0.065	0.70	4.50	13.91	Sandy loam
20	0.30	0.77	1.48	1.78	Brown sand
21	0.52	3.0	1.99	2.11	Brown sand
22	0.31	1.1	1.75	1.94	Brown sand
23	4.8	43.0	7.20	18.97	Gray brown gravelly sand
24	0.53	13.0	5.04	7.68	Dark brown gravelly sand
25	0.60	42.0	54.52	1300.0	Brown gravelly sandy loam
26	0.14	0.29	3.24	13.08	Light brown loamy sand
27	0.39	1.2	1.44	1.50	Brown sand
28	0.47	1.9	1.97	2.65	Brown sand
29	2.2	7.0	4.64	15.00	Dark brown gravelly sand
30	0.044	0.20	12.94		Light brown loam

place at the riffles. The general flow characteristics at all the riffles in both test reaches did not show much variability when compared with each other.

The change in the bed material sizes and the variability in the Froude number from riffle to pool are shown in figure 71 for sequence A. Higher values of d_{50}, d_{95}, and F are associated with the riffles with correspondingly lower values in the pools. Similar variability was also observed in the other pool-riffle sequence.

Some correlations were observed between Froude number F and the d_{50} and d_{95} sizes of the bed materials. Figure 72 shows such a relationship between F and the grain sizes. In general, higher values of Froude number are associated with higher values of the bed material sizes.

Shield's diagram (Simons and Sentürk, 1977) is normally utilized in open channel flow analysis to determine the critical shear stress on the bed of a stream. During low flows, when the flow velocity approaches a critical value near the riffle, the bed materials may be exposed to a crit-

ical shear stress and it may initiate the bed scour. In order to test whether or not the critical shear stresses on the bed approached a value that can initiate the scouring of the bed materials, the nondimensional values of the shear stress were plotted against the boundary Reynolds number in figure 73. In figure 73, τ_d is the dimensionless shear stress, τ_o is the shear stress in pounds per square foot, γ_s and γ are the unit weights of bed particles and water respectively, d_{50} is the median diameter of the bed materials, $\Re$ is the boundary Reynolds number, V_* is the shear velocity in fps, and v is the kinematic viscosity of water in square feet per second. All points except one plotted below the Shield's critical curve indicating that the shear stresses in the pool-riffle sequence were below the critical shear stress for the type and the sizes of bed material that are present in this particular reach.

During bankfull discharges, the effect of the pool and riffle on the overall flow condition is at a minimum. For pool-riffle sequence A, the thalweg was near the right bank

Table 13. Particle Size Characteristics of the Bed and Bank Materials, Reach 1, Pool-Riffle Sequence B

Sample number	d_{50}(mm)	d_{95}(mm)	σ	U	Remarks
31	0.030	0.20			Brown silt loam
32	0.034	0.24	6.34		Brown silt loam
33	0.39	1.2	1.79	1.73	Sand
34	0.17	0.36	1.39	1.64	Light brown sand
35	1.2	13.0	10.03	43.14	Dark brown gravelly loamy sand
36	4.0	19.0	6.50	20.00	Brown gravelly sand
37	3.4	19.0	5.09	14.85	Dark brown gravelly sand
38	2.4	18.0	5.85	17.62	Brown gravelly sand
39	0.027	0.21	3.94	19.55	Silt loam
40	0.21	0.48	1.38	1.53	Brown sand
41	4.6	19.0	3.86	12.77	Dark brown gravelly sand
42	0.65	6.5	2.57	2.75	Brown gravelly sand
43	0.80	14.0	6.60	13.68	Gravelly sand
44	0.12	0.25	2.33	6.84	Brown sandy loam
45	0.28	1.0	1.84	2.50	Light brown sand
46	0.50	1.6	1.79	2.39	Brown sand
47	0.10	7.0	17.58	42.86	Dark brown sandy loam
48	0.12	0.33	3.36	12.50	Light brown sandy loam
49	0.17	0.36	1.24	1.31	Light brown sand
50	0.30	0.59	1.40	1.82	Brown sand
51	0.054	0.46	7.05		Dark gray brown loam
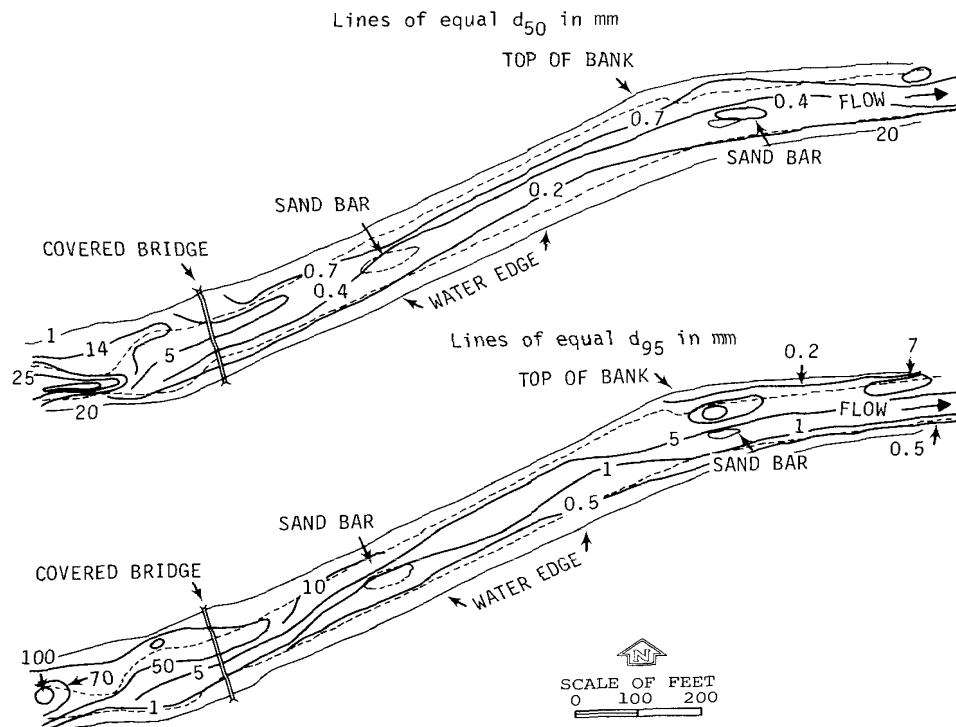
Figure 67. Isolines of d_{50} and d_{95} sizes of bed materials for pool-riffle sequence A

POOL

RIFFLE

SCALE OF FEET

0   100   200

SAND BAR

WATER EDGE

TOP OF BANK

POOL

0.1

FLOW

0.1

Lines of equal d_{50} in mm

SAND BAR

WATER EDGE

TOP OF BANK

0.5

0.5

FLOW

0.5

Lines of equal d_{95} in mm
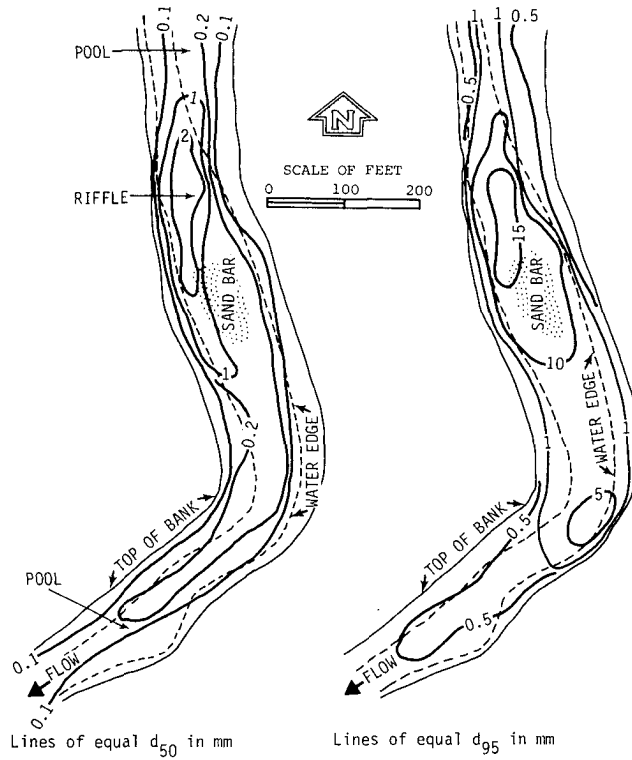
**Figure 68. Isolines of d_{50} and d_{95} sizes of bed materials
for pool-riffle sequence B**
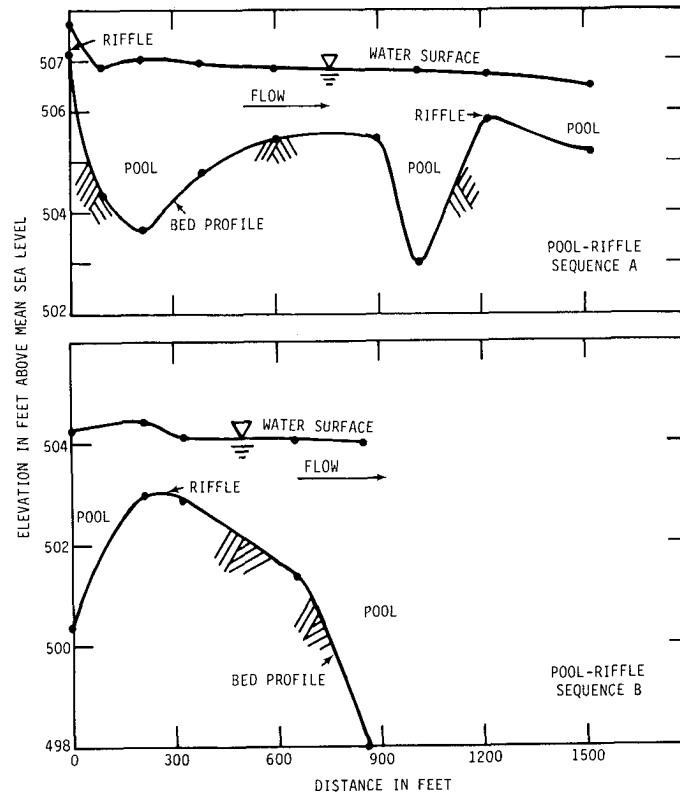
Figure 69. Thalweg and water surface profiles for pool-riffle sequences A and B

88
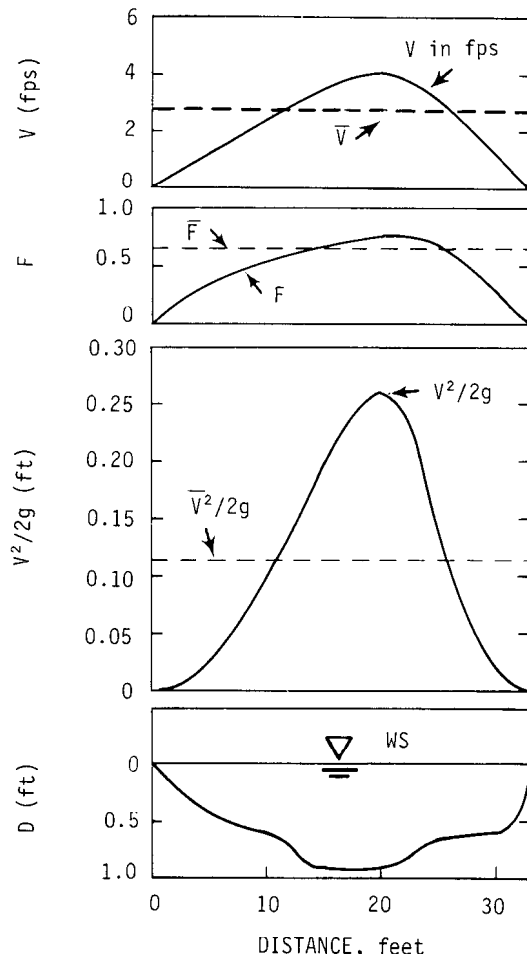
Figure 70. Hydraulic and geometric characteristics in the riffle section of sequence A
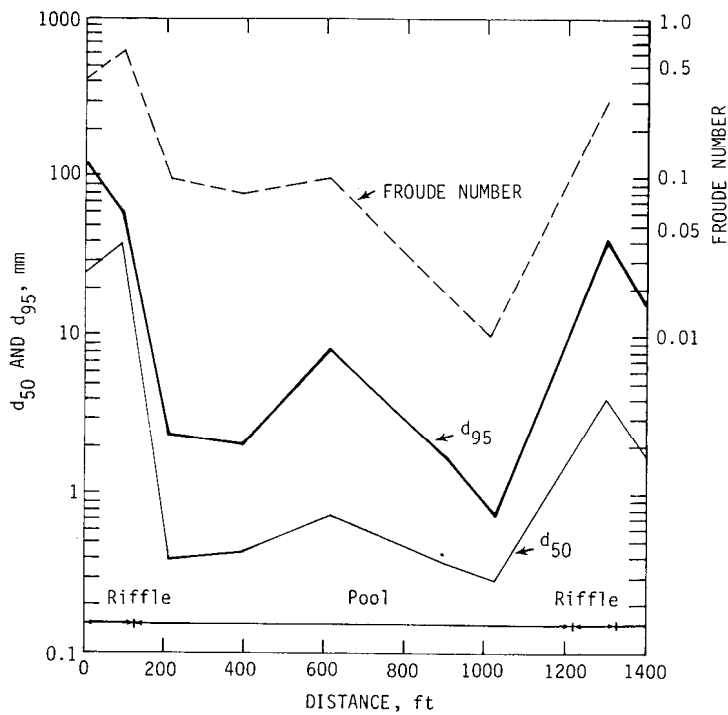
Figure 71. Distribution of bed material sizes and Froude number in pool-riffle sequence A

89
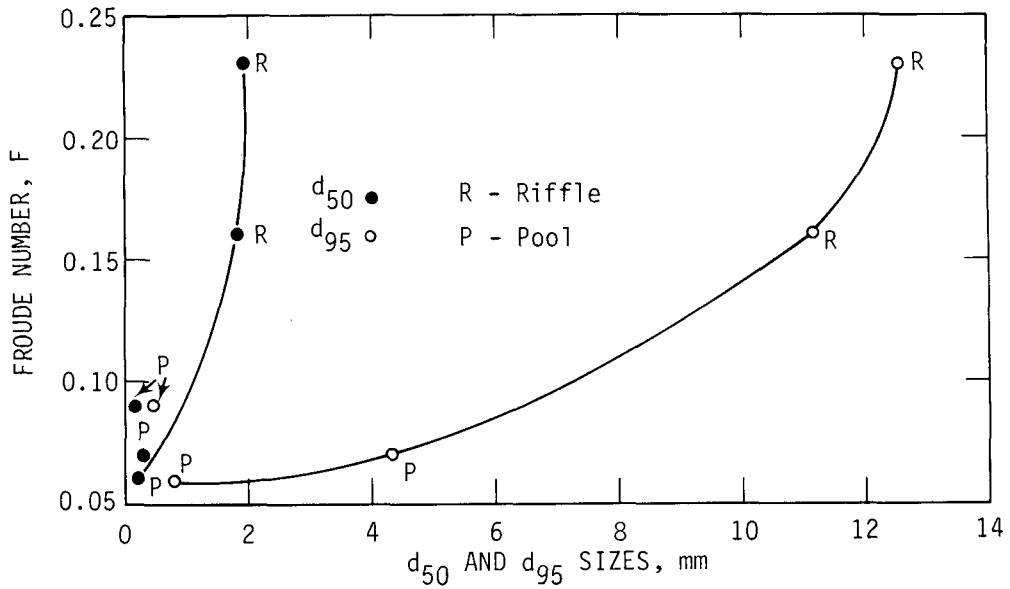
Figure 72. Average Froude number versus grain size in pool-riffle sequence A
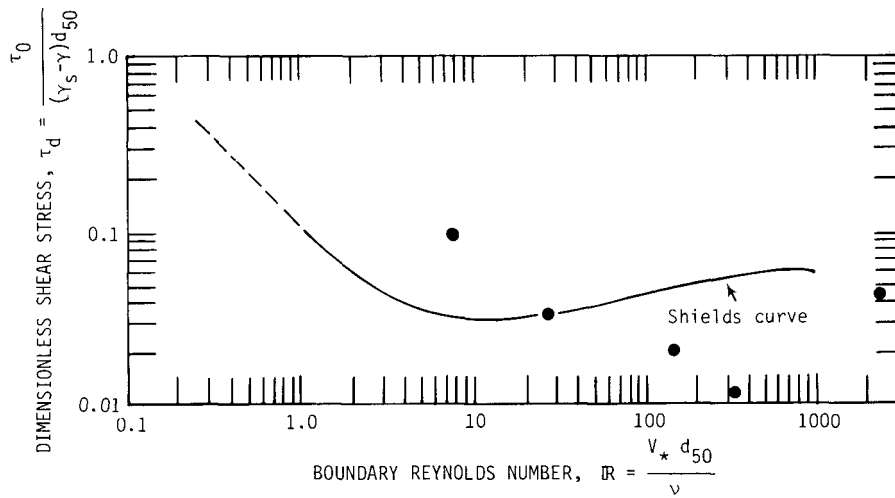
Figure 73. Shield's diagram for pool-riffle sequence A

for low flows, but for bankfull discharges the thalweg re-mained close to the left bank. However, the ratio of the lengths of the thalwegs for the entire reach for low and high flows was computed to be about 1. Because of the restraint exerted by the banks, the location of the thalweg during high flows was different from that during low flows, but the total length of the thalweg for both low and high flows remained about the same.

Data analyzed here indicate that when the river flows through a series of pools and riffles, the water surface pro-file and the invert slope are rather steep in the riffle and milder in the pools, the average velocity and Froude num-ber change from high to low from riffle to pool, the bed material sizes change from coarser to finer in the riffle-pool sequence, and considerable reaeration takes place in the rif-fles. These low flow characteristics are rather ideal for maintaining a balanced aquatic life in the stream environ-ment because they provide adequate water depths and food supply in the pools and possibly sufficient dissolved oxygen to the water near the riffles.

90

SUMMARY AND CONCLUSIONS

The hydraulics of flow was investigated at two reaches in the Kaskaskia River. One of the reaches is located about 12 miles downstream of Lake Shelbyville and the other reach is located about 7 miles downstream of Carlyle Lake.

Hydraulic data were collected for flows of 58, 1040, 1420, and 4000 cfs from the reach below Lake Shelbyville and for flows of 290, 2160, and 3700 cfs from the reach below Carlyle Lake. The flow frequencies varied from 5 to 88 percent. A total of 79 bed and bank material samples were collected and analyzed to determine the particle size distribution of these materials.

Geomorphologically the Kaskaskia River has passed the young stages of development and is presently in an equilibrium or mature stage of development. The bed materials in both reaches are sandy in nature and the average median diameter of the bed materials is about 0.39 mm. The cross-sectional shapes of the river in the straight reaches are generally trapezoidal, whereas in the bends, the cross-sectional shape is skewed with the maximum depths occurring near the outside bank of the bend where they are about 30 to 90 percent more than the average depths in the river.

Analyses of the water surface profiles and the energy grade lines indicate that, in most cases, the flow can be approximated by uniform flow equations. However, in Reach 2, the presence of a rock ledge contributed toward additional head loss. Head loss varied from 0.96 ft/mile for high flows to 1.98 ft/mile for low flows in Reach 1. Similar variability was also observed in Reach 2.

The vertical velocity distribution was found to follow a logarithmic distribution. The average depth-integrated velocities were 5 to 7 percent smaller than the average velocity determined from two point measurements in each vertical. The average velocity at 0.5 foot above the bed was approximately 95 percent of the average velocity in the cross section.

A total of 79 isovels or lines of equal velocities in the cross sections were developed from the hydraulic data collected in the field. The lateral velocity distribution in the straight portion of the river was found to be symmetrical about the centerline. However, in the bends, the velocity distribution was skewed with the high velocity cores staying close to the outside banks of the bends. Higher momentum of flow associated with increased discharge sometimes forced the cores of high velocity flow to move in a rather direct route in the stream and have thus changed the vulnerable location of the bank and bed for erosion and scour. Shifting of the high velocity cores was observed with changing discharges.

The average velocity increased as the discharge increased in the river. But the ratio of the maximum velocity to the average velocity remained almost unchanged for low, medium, and high flows. The maximum average velocity was about 145 percent more than the average velocity. In a few sections, considerable amounts of bed scour took place during high flows.

A theoretical distribution was found to predict the lateral velocity distribution in the bend satisfactorily. The magnitude of the superelevation in the bend was small. At least 3 theoretical equations predicted the superelevation within the same percent of accuracy. Direction, pattern, and the number of secondary circulation cells in the bends and also in the straight reaches can be sketched on the basis of the isovels developed for the cross sections. The number of cells was found to be the same for low, medium, and high flows.

The average value of the energy coefficient was 1.45 for straight reaches and 1.43 for bends. Similarly the average value of the momentum coefficient was 1.22 for straight reaches and 1.18 for bends. Better momentum exchange in the bends helped to reduce the numerical values of the energy and momentum coefficients in the bends.

Average Manning's roughness coefficients varied from a minimum of 0.039 to a maximum of 0.053. Roughness coefficients showed a decrease in value with an increase in discharge. In Reach 2, the presence of a bedrock ledge has changed the flow characteristics making the low and medium flow conditions similar to the flow over a low overflow type structure.

It was shown that the ratio of the energy slope S_e to the water slope S_w or to the bed slope S_o is a good indicator of the energy dissipation characteristics of the river. For $S_e/S_o > 1$, the flow is accelerating and for $S_e/S_o < 1$, the flow is decelerating and backwater effects are indicated.

Analyses of the unit discharges across the width of the river have shown that the unit discharges for various flow conditions are proportional to the respective water depths in the section. Thus a knowledge of the water depths can be utilized to estimate the distribution of the discharges across the width of the channel.

Turbulence in an open channel flow is very important toward determining the stability of bed and banks and its magnitude can sometimes be measured with the help of an ordinary current meter.

The low flow characteristics of a river are different from those present during medium and bankfull stages. The river flows through a series of pools and riffles with larger diameter bed material in the riffle and fine materials in the pool. The median diameter varied from 40 mm in the riffle to 0.04 mm in the pool. The Froude number varied from 0.7 in the riffle to 0.01 in the pool. Head loss was about 2.48 ft/mile in one pool-riffle sequence and about 4.44 ft/mile in the other. During high flows, the pool and riffles are all submerged and their effects on the overall flow condition are minimal or nonexistent.

REFERENCES

American Society of Civil Engineers. 1963. *Friction factors in open channels.* Proceedings ASCE, Journal of the Hydraulics Division v. 89(HY2):97-143.

Barnes, H. H., Jr. 1967. *Roughness characteristics of natural channels.* U.S. Geological Survey, Water-Supply Paper 1849, U.S. Government Printing Office, Washington, D.C.

Bathurst, J. C., C. R. Thorne, and R. D. Hey. 1977. *Direct measurements of secondary currents in river bends.* Nature, v. 269(5628):504-506.

Bennett, J. P., and R. S. McQuivey. 1970. *Comparison of a propeller flowmeter with a hot-film anemometer in measuring turbulence in movable-boundary open-channel flows.* U.S. Geological Survey, Professional Paper 700-B: B254-B262.

Bhowmik, N. G. 1968. *The mechanics of flow and stability of alluvial channels formed in coarse materials.* Ph.D. dissertation, Colorado State University, Fort Collins, 207 p.

Bhowmik, N. G., and John B. Stall. 1978a. *Bed material distribution in the pool-riffle sequence in a natural river.* Paper presented at the 1978 Spring Annual Meeting, American Geophysical Union, Miami, Florida, April 17-21.

Bhowmik, N. G., and John B. Stall. 1978b. *Hydraulics of flow in the Kaskaskia River.* Paper presented at the 26th Annual ASCE Hydraulics Division's Specialty Conference, University of Maryland, College Park, August 9-11, and published in Proceedings of the Conference, pp. 79-86.

Bhowmik, N. G., and R. J. Schicht. 1979. *Bank erosion of the Illinois River.* Contract Report prepared by the Illinois State Water Survey for the Division of Water Resources, Illinois Department of Transportation, 243 p.

Bhowmik, N. G., and J. B. Stall. 1979. *Hydraulic geometry and carrying capacity of floodplains.* University of Illinois Water Resources Center, Urbana, Research Report, to be published.

Blench, T. 1969. *Mobile-bed fluviology.* The University of Alberta Press, Edmonton, Alberta, Canada.

Bridge, J. S. 1976. *Bed topography and grain size in open channel bends.* Sedimentology v. 23:407-414.

Brooks, N. H. 1963. *Boundary shear stresses in curved trapezoidal channels.* Discussion, Proceedings ASCE, Journal of the Hydraulics Division v. 89(HY3):327-333.

Burkham, D. E., and D. R. Dawdy. 1976. *Resistance equations for alluvial-channel flow.* Proceedings ASCE, Journal of the Hydraulics Division v. 102(HY10):1479-1489.

Chow, V. T. 1959. *Open-channel hydraulics.* McGraw-Hill Book Company, Inc., New York.

Engelund, F. 1974. *Flow and bed topography in channel bends.* Proceedings ASCE, Journal of the Hydraulics Division v. l00(HY11):1631-1648.

Gottlieb, L. 1976. *Three-dimensional flow pattern and bed topography in meandering channels.* Technical University of Denmark, Institute of Hydrodynamics and Hydraulic Engineering, Series Paper 11.

Hulsing, H., W. Smith, and E. D. Cobb. 1966. *Velocity-head coefficients in open channels.* U.S. Geological Survey, Water-Supply Paper 1869-C, U.S. Government Printing Office, Washington, D.C.

Ippen, A. T., and P. A. Drinker. 1962. *Boundary shear stress in curved trapezoidal channels.* Proceedings ASCE, Journal of the Hydraulics Division v. 88(HY5):143.

Kalinske, A. A, 1942. *The role of turbulence in river hydraulics.* Proceedings of the Second Hydraulics Conference, University of Iowa, Iowa City, pp. 266-279.

Keller, E. A. 1978. *Pools, riffles, and channelization.* Environmental Geology v. 2(2):119-127.

Keulegan, G. H. 1938. *Laws of turbulent flow in open channels.* Journal of the National Bureau of Standards, Research Paper 1151.

Lacey, G. 1958. *Flow in alluvial channels with sandy mobile beds.* Proceedings, Institution of Civil Engineers v. 9:145-164.

Lamb, H. 1945. *Hydrodynamics.* Dover Publications, Inc., New York, N.Y., 6th Ed.

Lane, E. W. 1955. *Design of stable channels.* Transactions ASCE v. 120:1234-1279.

Leighton, M. M., G. E. Eklaw, and L. Horberg. 1948. *Physiographic divisions of Illinois.* Illinois State Geological Survey, Urbana, Report of Investigation No. 129.

Leopold, L. B., and R. Maddock. 1953. *The hydraulic geometry of stream channels and some physiographic implications,* U.S. Geological Survey, Professional Paper 252, U.S. Government Printing Office, Washington, D.C.

Leopold, L. B., et al. 1960. *Flow resistance in sinuous or irregular channels.* U.S. Geological Survey, Professional Paper 282-D, U.S. Government Printing Office, Washington, D.C.

Leopold, L. B., M. G. Wolman, and J. P. Miller. 1964. *Fluvial processes in geomorphology.* W. H. Freeman and Co., San Francisco, California.

Maddock, T., Jr. 1970. *Indeterminate hydraulics of alluvial channels.* Proceedings ASCE, Journal of the Hydraulics Division v. 96(HY11):2309-2323.

McQuivey, R. S. 1973. *Summary of turbulence data from rivers, conveyance channels, and laboratory flumes.* U.S. Geological Survey Professional Paper 802-B, p. B66.

Prus-Chacinski, T. M. 1966. Discussion of Proceedings Paper 4387. Proceedings ASCE, Journal of the Hydraulics Division v. 92(HY2):389-393.

Richardson, E. V. 1965. *Resistance to flow in sand channels.* Ph.D. dissertation, Colorado State University, Fort Collins, 82 p.

Rozovskii, I. L. 1957. *Flow of water in bends of open channels.* Academy of Sciences, Ukranian S.S.R., Kiev, U.S.S.R. Translated from Russian. Published for the National Science Foundation, Washington, D.C., and the Department of the Interior by the Israel Program for Scientific Translations, 233 p.

Sentürk, H. A. 1978. *Resistance to flow in sand-bed channels. Proceedings ASCE, Journal of the Hydraulics Division* v. 104(HY3):421-436.

Shukry, A. 1950. *Flow around bends in open flume.* Transactions ASCE v. 115:615.

Simons, D. B., and M. L. Albertson. 1963. *Uniform water conveyance channels in alluvial material.* Transactions ASCE v. 128:65-107.

Simons, D. B., and E. V. Richardson. 1961. *Forms of bed roughness in alluvial channels.* Proceedings ASCE, Journal of the Hydraulics Division v. 87(HY3):87-105.

Simons, D. B., and E. V. Richardson. 1971. *Flow in alluvial sand channels. In* River Mechanics, H. W. Shen, Ed., Fort Collins, Colorado, v. 1, Chapter 9.

Simons, D. B., and F. Senturk. 1977. *Sediment transport technology.* Water Resources Publications, Fort Collins, Colorado.

Sium, O. 1975. *Transverse flow distribution in natural streams as influenced by cross-sectional shape.* M. S. Thesis, University of Iowa, Iowa City, 99 p.

Stall, J. B., and Y. S. Fok. 1968. *Hydraulic geometry of Illinois streams.* University of Illinois Water Resources Center, Urbana, Research Report 15.

Stall, J. B., and C. T. Yang. 1970. *Hydraulic geometry of 12 selected streams of the United States.* University of Illinois Water Resources Center, Urbana, Research Report 32.

Stall, J. B., and C. T. Yang. 1972. *Hydraulic geometry and low streamflow regime.* University of Illinois Water Resources Center, Urbana, Research Report 54.

U.S. Corps of Engineers. 1968. *Missouri River channel regime studies.* MRD Sediment Series No. 13A, Omaha, Nebraska.

Woodward, S. M. 1920. *Hydraulics of Miami flood control project.* Miami Conservancy District, Dayton, Ohio, Technical Reports, Pt. VII, p. 264.

Yen, C. L. 1970. *Bed topography effect of the flow in a meander.* Proceedings ASCE, Journal of the Hydraulics Division v. 96(HY1):75-86.

NOTATIONS

A	=	Cross-sectional area in square feet
A_1	=	Constant, nondimensional
a	=	Coefficient
B_1	=	Constant, nondimensional
b	=	Coefficient
C	=	Chezy's coefficient in one-half power of feet per second
C_f	=	Centrifugal force
c	=	Coefficient
D	=	Total depth of water at any vertical in feet
D_{max}	=	Maximum depth in feet
$\bar{D}$	=	Average depth in feet
d	=	Depth of water at any point in the cross section in feet
d_f	=	Fall diameter of the bed material in feet
$d_{15.9}, d_{35}$ d_{50}, d_{60} $d_{84}, d_{84.1}$ d_{85}, d_{95}	=	Size of the bed materials where 15.9, 35, etc. percent of the particles are finer than these respective sizes in mm or feet
F	=	Froude number, nondimensional
F_i	=	Body force in the i*th* direction
f	=	Darcy-Weisbach friction factor, nondimensional
f_s	=	Silt factor
f_{ss}	=	Seepage force in pounds per square foot
g	=	Acceleration due to gravity in feet per second squared
h_L	=	Head loss in feet
I_r	=	Transverse inclination of the water surface, nondimensional
i	=	Coefficient
j	=	Coefficient
K	=	Coefficient
k, k_1	=	Coefficients
k_s	=	Equivalent roughness length in feet
l	=	Coefficient
L	=	Length between any two cross sections in feet
M_1, M_2	=	Types of backwater curves on mild slope
M	=	Momentum in pounds
m	=	Coefficient of regression
m_1	=	Coefficient
n	=	Manning's roughness coefficient
P	=	Pressure force in pounds
Q	=	Discharge in cubic feet per second
$q, \bar{q}$	=	Unit discharge and average unit discharge, respectively, in cfs per foot
$\Re$	=	Reynolds number
R	=	Hydraulic radius in feet
$r, r_c,$ r_i, r_o	=	Radius of curvature, radius of centerline, inside radius of curvature, and outside radius of curvature of bends, respectively, in feet
S_c	=	Shape factor of the cross section, nondimensional
S_e	=	Slope of energy gradeline
S_o	=	Slope of the bed
S_P	=	Shape factor of the particles, nondimensional
S_R	=	Shape factor of the reach, nondimensional
S_w	=	Water surface slope
s	=	Standard deviation of the turbulent velocity fluctuation

NOTATIONS   (Concluded)

t	=	Time in seconds
U	=	Uniformity coefficient, d_{60}/d_{10}, nondimensional
u_i	=	Mean velocity in the i*th* direction in feet per second
u_i'	=	Turbulent velocity component in the *ith* direction in feet per second
$u_i' u_j'$	=	Reynolds stress
V	=	Velocity in feet per second
$\bar{V}$	=	Average velocity in feet per second
V_{max}	=	Maximum average velocity of any vertical in feet per second
V_v	=	Average velocity in any vertical in a section in feet per second
V_{vm}	=	Maximum average velocity at a vertical in the straight portion of the stream in feet per second
V_*	=	Shear velocity in feet per second
V'	=	V_v/V_{vm}, nondimensional
V'_{max}	=	Maximum turbulent component of the velocity in feet per second
v	=	Point velocity in feet per second
W	=	Top width of the cross-section in feet
WP	=	Wetted perimeter in feet
WS	=	Water surface elevation in feet above mean sea level
w	=	Distance of a vertical from the bank
X	=	Distance in the downstream direction in feet
X'	=	Distance of any vertical from the centerline in feet
x_i	=	Distance in the i*th* direction in feet
x_j	=	Distance in the j*th* direction in feet
Y	=	Distance normal to the bed in feet
Y'	=	Distance in a vertical direction in feet
y	=	Distance of any water layer from the bed in feet
Z	=	Distance in the transverse direction in feet
α	=	Energy coefficient or Coriolis constant, nondimensional
β	=	Momentum coefficient, nondimensional
γ	=	Unit weight of water in pounds per cubic foot
γ_s	=	Unit weight of particles in pounds per cubic foot
∂	=	Partial derivative, nondimensional
ΔP	=	Pressure force
Δ	=	Deflection angle of the bend in degrees
ΔZ	=	Superelevation in feet
Δ'	=	$0.42 \Delta D_{max}(g)^{1/2}/(CW)$
k	=	Universal constant equal to 0.4
μ	=	Dynamic viscosity of water in pound-second per square foot
ν	=	Kinematic viscosity of water in square feet per second
ρ_f	=	Density of fluid
σ	=	Standard deviation of the bed or bank materials, nondimensional
τ_o	=	Shear stress in pounds per square foot
τ_d	=	Dimensionless shear stress
ϕ	=	Bed inclination, nondimensional
ψ	=	Angle of the velocity vector on the outside bank in a bend with the normal flow direction in degrees
ω	=	Fall velocity of the bed materials in feet per second

APPENDIX A. VELOCITY DISTRIBUTION DATA, KASKASKIA RIVER BELOW LAKE SHELBYVILLE

Cross Section Number 1

Date of data collection	10/20/75
Measured discharge	1106 cfs
Cross-sectional area	629 sq ft
Average velocity	1.76 fps
Water surface elevation above msl	
Left bank	512.50 ft
Right bank	512.49 ft
Distance along the centerline	
between cross sections	0

Distance from the right side looking downstream (ft)	Depth of water (ft)	Average velocity in the vertical (fps)
24	REW	
30	5.4	0.66
35	6.9	1.37
40	7.3	1.37
50	7.0	1.54
55	6.8	1.65
60	7.0	2.15
70	6.6	2.53
75	6.7	2.62
80	7.1	2.47
85	6.4	2.38
90	7.4	2.37
95	7.0	2.07
100	8.1	1.93
105	8.7	1.78
110	7.5	0.55
115	4.8	0.37
117	4.5	0.39
121	LEW	

Cross Section Number 2

Date of data collection	10/20/75
Measured discharge	1058 cfs
Cross-sectional area	649 sq ft
Average velocity	1.63 fps
Water surface elevation above msl	
Left Bank	512.23 ft
Right bank	512.21 ft
Distance along the centerline	
between cross sections 1 to 2	1300 ft

Distance from the right side looking downstream (ft)	Depth of water (ft)	Average velocity in the vertical (fps)
6	REW	
10	6.2	0.57
15	6.7	0.83
20	6.5	1.04
25	6.7	1.24
35	6.3	1.61
45	6.3	1.96
55	6.3	2.00
65	6.0	2.01
75	5.8	2.17
85	5.6	2.02
90	5.6	1.96
95	5.5	1.62
100	5.2	1.74
105	5.2	1.71
110	5.0	1.31
115	3.9	0.95
117	3.2	0.75
120	LEW	

Cross Section Number 3

Date of data collection	10/21/75
Measured discharge	1125 cfs
Cross-sectional area	623 sq ft
Average velocity	1.81 fps
Water surface elevation above msl	
Left bank	512.17 ft
Right bank	512.17 ft
Distance along the centerline	
between cross-sections 2 to 3	400 ft

Distance from the right side looking downstream (ft)	Depth of water (ft)	Average velocity in the vertical (fps)
11	REW	
15	2.8	0.79
20	6.0	0.96
25	7.3	1.00
30	6.9	1.30
35	6.7	1.55
40	6.8	1.84
50	6.5	2.12
60	6.0	2.23
70	6.1	2.30
80	6.4	2.12
90	6.5	2.09
95	6.4	2.16
100	6.4	1.87
105	6.3	1.57
110	4.8	1.18
115	2.3	0.73
120	LEW	

Cross Section Number 4

Date of data collection	10/21/75
Measured discharge	1159 cfs
Cross-sectional area	622 sq ft
Average velocity	1.86 fps
Water surface elevation above msl	
Left bank	512.12 ft
Right bank	512.12 ft
Distance along the centerline	
between cross sections 3 to 4	363 ft

Distance from the right side looking downstream (ft)	Depth of water (ft)	Average velocity in the vertical (fps)
4	REW	
10	3.1	0.36
15	4.0	0.81
20	4.9	1.55
25	5.2	1.66
30	5.2	1.77
40	5.8	2.02
50	6.1	2.02
60	8.1	1.91
70	8.8	2.02
75	9.0	2.10
80	9.1	2.05
85	9.6	1.99
90	10.0	1.75
95	8.2	1.44
100	6.5	0.73
105	4.3	0.33
112	LEW	

Note. REW = Right edge of water looking downstream
LEW = Left edge of water looking downstream

Cross Section Number 5

Date of data collection	10/21/75
Measured discharge	1177 cfs
Cross-sectional area	560 sq ft
Average velocity	2.09 fps
Water surface elevation above msl	
Left bank	511.89 ft
Right bank	511.95 ft
Distance along the centerline	
between cross sections 4 to 5	1016 ft

Distance from the right side looking downstream (ft)	Depth of water (ft)	Average velocity in the vertical (fps)
14	REW	
16	6.5	2.28
20	8.0	2.38
24	9.5	2.50
30	11.0	2.37
35	11.3	2.37
40	10.9	2.32
45	10.4	2.24
50	8.9	2.12
60	6.2	2.14
70	4.4	1.81
80	2.4	1.84
85	2.7	1.57
90	2.9	1.03
95	2.5	0.33
100	1.8	0.0
105	LEW	

Cross Section Number 6

Date of data collection	10/21/75
Measured discharge	1170 cfs
Cross-sectional area	680 sq ft
Average velocity	1.72 fps
Water surface elevation above msl	
Left Bank	511.81 ft
Right bank	511.78 ft
Distance along the centerline	
between cross sections 5 to 6	448 ft

Distance from the right side looking downstream (ft)	Depth of water (ft)	Average velocity in the vertical (fps)
12	REW	
18	5.4	0.22
24	6.7	0.96
30	6.0	.93
35	5.9	1.15
42	6.0	1.54
50	5.5	1.88
60	5.7	2.63
70	6.3	2.28
80	6.5	2.24
90	6.7	2.33
100	6.5	2.04
105	6.5	1.93
110	6.7	1.85
115	6.4	1.54
120	5.7	0.84
125	2.3	-0.36
127	1.4	-0.34
132	LEW	

Cross Section Number 7

Date of data collection	10/22/75
Measured discharge	1030 cfs
Cross-sectional area	605 sq ft
Average velocity	1.70 fps
Water surface elevation above msl	
Left bank	510.95 ft
Right bank	510.86 ft
Distance along the centerline	
between cross-sections 6 to 7	748 ft

Distance from the right side looking downstream (ft)	Depth of water (ft)	Average velocity in the vertical (fps)
10	REW	
14	1.0	1.02
18	2.2	1.22
25	4.7	1.49
30	5.8	1.49
35	6.3	1.73
45	7.0	1.77
55	8.2	1.83
65	11.0	1.63
70	12.1	1.60
75	12.1	1.67
80	11.5	1.66
85	9.4	1.78
90	6.9	1.82
93	3.8	1.46
95	LEW	

Cross Section Number 8

Date of data collection	10/22/75
Measured discharge	989 cfs
Cross-sectional area	563 sq ft
Average velocity	1.76 fps
Water surface elevation above msl	
Left bank	510.72 ft
Right bank	510.71 ft
Distance along the centerline	
between cross sections 7 to 8	452 ft

Distance from the right side looking downstream (ft)	Depth of water (ft)	Average velocity in the vertical (fps)
4	REW	
12	5.7	0.82
20	7.7	1.27
25	8.0	1.89
30	7.8	2.04
40	7.8	2.42
50	7.5	2.30
60	6.5	1.98
70	5.9	1.77
75	5.3	1.50
80	5.1	1.48
85	3.7	1.19
90	2.7	1.33
95	2.2	1.05
100	1.6	0.86
103	1.4	1.19
106	LEW	

APPENDIX A. Continued — Shelbyville

Cross Section Number 9

Date of data collection	10/22/75	
Measured discharge	1171 cfs	
Cross-sectional area	1173 sq ft	
Average velocity	1.00 fps	
Water surface elevation above msl		
Left bank	510.64 ft	
Right bank	510.64 ft	
Distance along the centerline		
between cross sections 8 & 9	552 ft	

Distance from the right side looking downstream (ft)	Depth of Water (ft)	Average velocity in the vertical (fps)
9	REW	
17	3.8	-1.31
22	7.0	0.66
27	8.0	0.69
32	10.6	0.94
37	11.9	1.25
47	12.7	1.43
57	12.7	1.76
67	13.3	1.58
77	12.8	1.25
87	12.2	1.17
97	8.5	0.91
107	6.5	0.96
112	6.9	-0.14
117	6.3	-0.30
122	6.1	-0.27
127	5.4	-0.23
132	8.5	-0.14
136	LEW	

Cross Section Number 11

Date of data collection	10/22/75	
Measured discharge	953 cfs	
Cross-sectional area	518 sq ft	
Average velocity	1.84 fps	
Water surface elevation above msl		
Left bank	510.28 ft	
Right bank	510.13 ft	
Distance along the centerline		
between cross sections 10 & 11	620 ft	

Distance from the right side looking downstream (ft)	Depth of Water (ft)	Average velocity in the vertical (fps)
16	REW	
20	3.4	1.37
25	5.3	1.99
30	5.6	1.97
35	6.2	2.01
40	6.3	1.94
50	4.7	1.91
60	3.3	1.95
70	2.4	2.04
80	2.8	1.96
90	2.7	2.37
100	3.5	2.34
105	5.4	1.90
110	7.1	0.81
115	8.2	1.77
120	8.1	1.86
125	6.7	1.49
130	3.5	0.92
134	LEW	

Cross Section Number 10

Date of data collection	10/22/75	
Measured discharge	940	
Cross-sectional area	586.0sq ft	
Average velocity	1.60 fps	
Water surface elevation above msl		
Left bank	510.50 fr	
Right bank	510.51 ft	
Distance along the centerline		
between cross sections 9 to 10	420 ft	

Distance from the right side looking downstream (ft)	Depth of Water (ft)	Average velocity in the vertical (fps)
16	REW	
20	5.9	1.00
25	8.3	1.35
30	8.9	1.23
35	8.6	0.92
40	8.4	1.56
50	7.0	1.66
60	5.5	1.95
70	4.1	2.01
80	3.2	2.02
90	3.3	1.94
100	3.9	1.91
110	4.0	1.89
115	4.0	1.91
120	3.9	1.65
125	3.3	1.43
130	2.3	1.22
135	LEW	

Cross Section Number 12

Date of data collection	10/23/75	
Measured discharge	984 cfs	
Cross-sectional area	534 sq ft	
Average velocity	1084 fps	
Water surface elevation above msl		
Left bank	509.72 ft	
Right bank	509.70 ft	
Distance along the centerline		
between cross sections 11 & 12	972 ft	

Distance from the right side looking downstream (ft)	Depth of Water (ft)	Average velocity in the vertical (fps)
33	REW	
37	2.2	1.00
42	2.9	1.19
47	3.5	1.06
52	4.3	1.21
58	5.5	1.52
65	5.9	1.86
75	5.6	1.83
85	5.6	2.05
95	5.8	2.47
105	6.4	2.04
110	6.7	2.16
115	7.0	2.11
120	7.2	1.99
125	6.5	1.62
130	5.1	1.39
132	4.5	1.22
136	LEW	

APPENDIX A. Continued — Shelbyville

Cross Section Number 13

Date of data collection	10/23/75
Measured discharge	933 cfs
Cross-sectional area	512 sq ft
Average velocity	1.82 fps
Water surface elevation above msl	
Left bank	509.57 ft
Right bank	509.65 ft
Distance along the centerline	
between cross sections 12 & 13	320 ft

Distance from the right side looking downstream (ft)	Depth of Water (ft)	Average velocity in the vertical (fps)
12	REW	
15	6.5	1.53
18	8.9	1.33
22	10.2	1.81
27	11.9	2.01
32	12.0	2.02
37	10.0	2.01
42	8.9	1.88
50	6.8	1.84
60	4.5	1.64
70	4.0	1.82
75	3.5	1.71
80	2.5	1.60
85	2.4	1.49
90	1.5	1.23
95	0.7	0.77
100	LEW	

Cross Section Number 15

Date of data collection	10/23/75
Measured discharge	954 cfs
Cross-sectional area	481 sq ft
Average velocity	1.98 fps
Water surface elevation above msl	
Left bank	509.45 ft
Right bank	509.44 ft
Distance along the centerline	
between cross sections 14 & 15	552 ft

Distance from the right side looking downstream (ft)	Depth of Water (ft)	Average velocity in the vertical (fps)
14	REW	
17	1.0	0
20	1.8	0.66
25	2.2	1.19
30	2.9	1.46
35	3.7	1.61
40	4.0	1.75
45	4.6	1.71
55	5.5	2.06
65	6.9	2.08
75	7.6	2.17
80	7.8	2.14
85	9.0	2.12
90	10.0	2.17
95	7.8	2.04
100	3.7	2.15
105	1.7	1.37
108	LEW	

Cross Section Number 14

Date of data collection	10/23/75
Measured discharge	945 cfs
Cross-sectional area	544.0 sq ft
Average velocity	1.74 fps
Water surface elevation above msl	
Left bank	509.60 fr
Right bank	509.58 ft
Distance along the centerline	
between cross sections 13 & 14	312 ft

Distance from the right side looking downstream (ft)	Depth of Water (ft)	Average velocity in the vertical (fps)
19	REW	
22	1.3	0.69
27	3.1	1.23
32	6.2	1.34
37	6.1	1.27
42	5.5	1.37
47	5.5	1.66
52	5.1	1.60
62	4.6	1.92
72	4.5	2.08
82	4.5	2.11
92	4.9	2.04
102	6.0	1.99
107	6.1	1.96
112	6.3	1.81
117	5.6	1.58
122	5.8	1.47
127	3.0	1.39
132	2.1	1.05
135	1.3	0.23
138	LEW	

Cross Section Number 16

Date of data collection	10/24/75
Measured discharge	950 cfs
Cross-sectional area	575 sq ft
Average velocity	1.65 fps
Water surface elevation above msl	
Left bank	509.27 ft
Right bank	509.21 ft
Distance along the centerline	
between cross sections 15 & 16	1448 ft

Distance from the right side looking downstream (ft)	Depth of Water (ft)	Average velocity in the vertical (fps)
24	REW	
27	1.8	0.43
32	4.7	1.23
37	5.5	1.63
42	5.5	1.95
47	5.2	2.00
52	5.0	2.21
62	5.1	2.01
72	5.1	1.93
82	5.3	2.02
92	5.6	2.06
102	5.8	1.90
107	6.1	1.70
112	6.4	1.57
117	6.3	1.30
122	6.0	0.71
127	5.5	0.72
132	4.8	0.17
134	3.0	-0.42
136	LEW	

APPENDIX A. Continued — Shelbyville

Cross Section Number 17

Date of data collection	10/24/75
Measured discharge	939 cfs
Cross-sectional area	650 sq ft
Average velocity	1.44 fps
Water surface elevation above msl	
Left bank	508.95 ft
Right bank	509.01 ft
Distance along the centerline	
between cross sections 16 & 17	1136 ft

Distance from the right side looking downstream (ft)	Depth of Water (ft)	Average velocity in the vertical (fps)
20	REW	
24	5.5	0.49
28	6.6	0.86
32	6.7	0.77
38	6.7	1.17
44	8.6	1.47
50	9.2	1.62
56	9.1	1.71
62	9.1	1.97
68	9.0	1.93
74	8.7	1.85
80	8.1	1.76
85	7.8	1.55
90	7.5	1.28
95	7.1	1.22
100	6.2	0.89
105	4.5	0.81
109	LEW	

Cross Section Number 1

Date of data collection	5/11/77
Measured discharge	1423 cfs
Cross-sectional area	817.5 sq ft
Average velocity	1.74 fps
Water surface elevation above msl	
Left bank	513.42 fr
Right bank	513.45 ft
Distance along the centerline	
between cross sections	0

Distance from the right side looking downstream (ft)	Depth of Water(ft)	Average velocity in the vertical (fps)
21	REW	0.28
26	2.3	0.58
30	6.3	1.42
35	8.1	1.74
40	8.6	1.89
50	8.4	2.09
60	9.1	2.58
70	8.8	2.29
75	8.6	2.53
80	8.7	2.38
85	8.6	2.35
90	8.8	2.12
95	9.0	1.99
100	10.0	1.46
105	9.8	0.57
110	8.6	-0.45
115	6.6	-0.27
118	5.2	
122	LEW	

Cross Section Number 2

Date of data collection	5/11/77
Measured discharge	1363 cfs
Cross-sectional area	726.3 sq ft
Average velocity	1.79 fps
Water surface elevation above msl	
Left bank	513.21 ft
Right bank	513.24 ft
Distance along the centerline	
between cross sections 1 & 2	1300 ft

Distance from the right side looking downstream (ft)	Depth of Water (ft)	Average velocity in the vertical (fps)
13	REW	
18	6.5	0.90
22	7.3	1.21
26	7.2	1.21
30	7.4	1.62
35	7.8	1.58
40	7.8	2.19
45	7.6	2.10
50	7.3	2.41
55	7.4	2.19
60	7.5	2.45
65	7.0	2.27
70	6.6	2.49
75	6.5	2.29
80	6.2	2.31
85	6.1	1.97
90	6.1	2.32
95	5.6	1.93
100	5.5	1.94
105	5.5	1.90
110	5.2	1.66
115	5.0	1.37
120	3.2	1.29
125	LEW	1.05
128		

Cross Section Number 3

Date of data collection	5/11/77
Measured discharge	1378 cfs
Cross-sectional area	725.0 sq ft
Average velocity	1.90 fps
Water surface elevation above msl	
Left bank	513.11 ft
Right bank	513.10 ft
Distance along the centerline	
between cross sections 2 & 3	400 ft

Distance from the right side looking downstream (ft)	Depth of Water(ft)	Average velocity in the vertical (fps)
9.0	REW	
13	3.1	0.76
18	6.0	1.09
25	8.5	1.47
30	8.5	1.76
35	8.4	2.09
40	8.4	2.37
45	7.9	2.48
50	7.6	2.65
55	7.5	2.38
60	7.5	2.51
65	7.5	2.23
70	7.1	2.33
75	6.4	2.22
80	6.2	2.21
85	6.2	2.02
90	5.9	2.05
95	5.7	1.75
100	5.7	1.53
105	5.4	1.39
110	5.0	1.23
115	4.2	1.09
118	1.8	0.46
121	LEW	

APPENDIX A. Continued — Shelbyville

Cross Section Number 4

Date of data collection	5/11/77
Measured discharge	1419 cfs
Cross-sectional area	773.8 sq ft
Average velocity	1.83 fps
Water surface elevation above msl	
Left bank	513.12 ft
Right bank	513.08 ft
Distance along the centerline	
between cross sections 3 & 4	363 ft

Distance from the right side looking downstream (ft)	Depth of Water (ft)	Average velocity in the vertical (fps)
3	REW	
8	3.1	0.36
12	4.1	0.93
16	4.5	1.09
22	5.2	1.63
28	5.2	1.59
36	7.0	2.07
44	7.4	2.05
50	8.0	2.26
55	8.1	2.08
60	8.5	2.34
65	8.4	2.27
70	8.7	2.35
75	9.5	2.23
80	10.0	2.16
85	10.5	2.13
90	10.6	1.91
95	9.4	1.44
100	7.3	1.32
105	5.0	1.11
108	4.2	0.42
111	REW	

Cross Section Number 7

Date of data collection	5/12/77
Measured discharge	1495 cfs
Cross-sectional area	896.3 sq ft
Average velocity	1.67 fps
Water surface elevation above msl	
Left bank	512.50 ft
Right bank	512.45 ft
Distance along the centerline	
between cross sections 5 & 7	1196 ft

Distance from the right side looking downstream (ft)	Depth of Water (ft)	Average velocity in the vertical (fps)
28	REW	
32	0.9	0.26
36	2.9	0.28
40	4.7	0.55
45	7.1	0.41
50	9.3	0.95
55	9.4	1.73
60	10.0	1.73
65	10.7	1.99
70	11.6	1.88
75	12.4	1.66
80	13.9	1.90
85	15.0	1.90
90	14.8	1.93
95	14.4	1.77
100	13.7	1.84
105	11.6	1.96
110	8.6	1.97
114	6.8	1.88
118	4.1	1.72
124	LEW	

Cross Section Number 5

Date of data collection	5/11/77
Measured discharge	1469 cfs
Cross-sectional area	746.3 sq ft
Average velocity	1.97 fps
Water surface elevation above msl	
Left bank	512.88 ft
Right bank	512.93 ft
Distance along the centerline	
between cross sections 4 & 5	1016 ft

Distance from the right side looking downstream (ft)	Depth of Water (ft)	Average velocity in the vertical (fps)
12	REW	
14	4.5	1.89
18	8.1	2.13
22	10.1	2.18
26	11.1	2.28
30	11.4	2.37
34	11.7	2.36
38	12.0	2.32
42	12.2	2.15
46	12.3	2.01
50	12.7	1.91
55	12.2	1.76
60	10.1	1.82
65	8.6	1.83
70	7.4	1.61
74	6.5	1.43
78	5.8	1.34
82	5.4	1.21
86	4.2	0.76
90	3.8	0.62
94	2.8	0.21
98	1.9	0
106	LEW	

Cross Section Number 8

Date of data collection	5/12/77
Measured discharge	1399 cfs
Cross-sectional area	712.5 sq ft
Average velocity	1.96 fps
Water surface elevation above msl	
Left bank	512.24 ft
Right bank	512.23 ft
Distance along the centerline	
between cross sections 7 & 8	452 ft

Distance from the right side looking downstream (ft)	Depth of Water (ft)	Average velocity in the vertical (fps)
7	REW	
12	2.2	0.24
15	3.2	0.94
20	4.5	1.16
25	5.7	1.92
30	5.9	2.27
35	7.5	2.41
40	7.9	2.41
50	8.2	2.62
60	8.3	2.55
65	7.1	2.34
70	6.6	2.66
75	7.4	2.46
80	7.6	2.32
85	7.5	1.96
90	7.3	1.85
95	7.0	1.56
100	7.1	1.23
105	7.1	0.90
110	5.1	0.51
114	2.3	0.15
119	LEW	

Cross Section Number 9

Date of data collection	5/13/77
Measured discharge	1530 cfs
Cross-sectional area	903.8 sq ft
Average velocity	1.69 fps
Water surface elevation above msl	
Left bank	512.24 ft
Right bank	512.27 ft
Distance along the centerline	
between cross sections 8 & 9	552 ft

Distance from the right side looking downstream (ft)	Depth of Water(ft)	Average velocity in the vertical (fps)
8	REW	
13	4.4	1.27
18	7.3	1.37
22	8.8	1.34
28	10.8	1.52
35	12.3	1.57
42	13.4	1.67
50	14..3	1.98
55	14.1	2.01
60	14.0	2.06
65	12.4	2.01
70	10.6	1.88
75	9.7	1.68
80	7.9	1.91
85	5.8	1.63
90	4.4	1.34
95	3.8	1.35
100	3.3	1.27
105	2.8	1.41
112	LEW	

Cross Section Number 10

Date of data collection	5/13/77
Measured discharge	1391 cfs
Cross-sectional area	712.5 sq ft
Average velocity	1.95 fps
Water surface elevation above msl	
Left bank	511.95 fr
Right bank	511.94 ft
Distance along the centerline	
between cross sections 9 & 10	420 ft

Distance from the right side looking downstream (ft)	Depth of Water(ft)	Average velocity in the vertical (fps)
10	REW	
15	3.7	0.68
20	6.8	1.50
24	8.4	2.00
30	10.0	1.72
35	10.0	2.18
40	10.1	2.15
45	9.0	2.21
50	8.1	2.19
55	7.3	2.01
60	6.6	2.32
65	5.8	2.19
70	5.4	2.50
75	4.9	2.35
80	4.5	2.29
85	4.4	2.11
90	4.3	2.15
95	4.3	2.13
100	4.4	2.00
105	4.4	2.06
110	4.2	1.72
115	3.9	1.76
120	3.5	1.66
125	3.0	1.57
130	2.2	0.78
135	1.3	0.54
140	LEW	

Cross Section Number 11

Date of data collection	5/13/77
Measured discharge	1436 cfs
Cross-sectional area	775 sq ft
Average velocity	1.85 fps
Water surface elevation above msl	
Left bank	511.83 ft
Right bank	511.68 ft
Distance along the centerline	
between cross sections 10 & 11	620 ft

Distance from the right side looking downstream (ft)	Depth of water(ft)	Average velocity in the vertical (fps)
12	REW	
18	1.5	0.59
22	3.4	1.68
28	5.6	2.10
35	6.3	2.17
42	6.5	2.13
50	6.1	1.82
55	5.5	1.92
60	4.4	1.98
65	4.2	1.97
70	4.4	2.14
75	5.3	2.05
80	5.8	2.25
85	6.1	1.64
90	6.8	2.08
95	8.1	1.98
100	8.9	1.99
105	9.3	1.83
110	9.5	1.90
115	9.1	1.71
120	8.0	1.71
125	8.0	1.61
130	6.6	1.37
135	5.1	1.53
137	**3.3**	1.14
142	LEW	

Cross Section Number 12

Date of data collection Number	5/13/77
Measured discharge	1406 cfs
Cross-sectional area	698.8 sq ft
Average velocity	2.01 fps
Water surface elevation above msl	
Left bank	511.35 ft
Right bank	511.31 ft
Distance along the centerline	972 ft
between cross sections 11 & 12	

Distance from the right side looking downstream (ft)	Depth of water(ft)	Average velocity in the vertical (fps)
4	REW	
8	1.9	0.31
12	3.5	0.97
16	4.1	1.06
20	6.0	1.67
25	6.2	1.80
30	7.3	2.12
35	7.2	2.26
40	7.2	2.37
45	7.3	2.53
50	7.2	2.55
55	7.1	2.43
60	7.5	2.59
65	8.1	2.42
70	8.0	2.63
75	8.0	2.27
80	8.2	2.10
85	8.5	2.25
90	6.5	2.11
95	6.9	1.62
100	6.0	1.32
105	5.0	0.86
110	2.2	0.53
113	LEW	

APPENDIX A. Continued — Shelbyville

Cross Section Number 13

Date of data collection	5/13/77
Measured discharge	1,454 cfs
Cross-sectional area	640 sq ft
Average velocity	2.27 fps
Water surface elevation above msl	
Left bank	511.21 ft
Right bank	511.23 ft
Distance along the centerline	320 ft
between cross sections 12 & 13	

Distance from the right side looking downstream (ft)	Depth of Water(ft)	Average velocity in the vertical (fps)
9	REW	
13	3.6	1.85
17	6.1	2.68
22	9.7	2.24
28	12.4	2.47
34	11.9	2.55
40	10.3	2.50
46	9.3	2.43
55	8.0	2.42
60	7.5	2.33
65	6.6	2.43
70	5.8	2.28
75	4.4	2.33
80	4.2	2.17
85	3.5	1.85
90	3.4	1.73
95	2.9	1.44
100	1.8	0.65
107	LEW	

Cross Section Number 14

Date of data collection	5/16/77
Measured discharge	1338 cfs
Cross-sectional area	687.5 sq ft
Average velocity	1.95 fps
Water surface elevation above msl	
Left bank	511.15 fr
Right bank	511.13 ft
Distance along the centerline	312 ft
between cross sections 13 & 14	

Distance from the right side looking downstream (ft)	Depth of Water(ft)	Average velocity in the vertical (fps)
15	REW	
20	1.7	0.45
24	3.0	0.84
30	5.8	1.14
35	7.5	1.74
40	7.3	1.78
45	6.7	2.25
50	6.5	2.45
55	6.3	2.56
60	6.0	2.51
65	5.7	2.36
70	5.5	2.21
75	5.3	2.35
80	5.3	2.11
85	5.2	2.25
90	5.4	2.10
95	5.7	2.37
100	6.8	2.19
105	7.0	2.10
110	7.0	2 18
115	6.5	2.07
120	7.3	1.85
125	6.1	1.71
130	3.2	1.10
135	2.0	0.41
141	LEW	

Cross Section Number 15

Date of data collection	5/16/77
Measured discharge	1453 cfs
Cross-sectional area	716.3 sq ft
Average velocity	2.03 fps
Water surface elevation above msl	
Left bank	511.00 ft
Right bank	510.98 ft
Distance along the centerline	552 ft
between cross sections 14 & 15	

Distance from the right side looking downstream (ft)	Depth of Water(ft)	Average velocity in the vertical (fps)
14	REW	
18	2.0	0
22	2.9	0.14
26	3.7	0.27
30	3.8	0.93
35	3.5	1.31
40	4.7	1.51
45	6.7	1.61
50	6.9	1.99
55	8.5	2.13
60	8.6	2.20
65	8.7	2.29
70	9.5	2.18
75	11.0	2.45
80	11.4	2.39
85	12.1	2.06
90	12.0	2.29
95	10.8	2.41
100	8.7	2.50
105	5.6	2.51
110	2.4	1.96
113	1.5	1.61
116	LEW	

Cross Section Number 17

Date of data collection	5/16/77
Measured discharge	1401 cfs
Cross-sectional area	785 sq ft
Average velocity	1.79 fps
Water surface elevation above msl	
Left bank	
Right bank	
Distance along the centerline	2584 ft
between cross sections 15 & 17	

Distance from the right side looking downstream (ft)	Depth of Water(ft)	Average velocity in the vertical (fps)
14	REW	
20	5.1	
24	6.2	
28	7.4	1.3
32	7.1	1.49
36	7.9	1.57
40	9.2	1.79
45	9.8	2.16
50	9.6	2.33
55	9.6	2.27
60	9.5	2.38
65	9.4	2.36
70	9.3	2.40
75	9.2	2.27
80	9.3	2.26
85	8.9	1.88
90	8.9	1.85
95	8.6	1.65
100	8.3	1.49
105	6.0	0.92
107	5.3	0.91
112	LEW	

APPENDIX A. Continued — Shelbyville

Cross Section Number 1

Date of data collection	3/20/78
Measured discharge	4555 cfs
Cross-sectional area	1657.9 sq ft
Average velocity	2.75 fps
Water surface elevation above msl	
Left bank	520.62 ft
Right bank	520.61 ft
Distance along the centerline between cross sections	0

Distance from the right side looking downstream (ft)	Depth of Water(ft)	Average velocity in the vertical (fps)
0	REW	
10	3.4	0.31
18	7.6	0.95
25	10.5	1.16
30	14.8	1.56
35	15.8	2.68
40	16.1	3.21
45	17.0	3.41
55	16.0	3.77
65	16.8	3.75
75	16.6	3.70
85	16.6	3.37
95	16.6	3.38
105	16.5	2.17
110	14.8	1.35
115	13.1	1.11
120	7.2	0.30
125	3.0	0.00
134	LEW	

Cross Section Number 2

Date of data collection	3/20/78
Measured discharge	4643 cfs
Cross-sectional area	1646.7 sq ft
Average velocity	2.82 fps
Water surface elevation above msl	
Left bank	520.40 ft
Right bank	520.42 ft
Distance along the centerline between cross sections 1 & 2	1300 ft

Distance from the right side looking downstream (ft)	Depth of Water(ft)	Average velocity in the vertical (fps)
0	REW	
17	5.7	0.26
22	8.8	0.81
27	13.7	1.35
32	15.3	2.01
37	15.4	2.69
47	15.7	3.23
57	15.4	3.81
67	14.5	3.92
77	14.2	3.43
87	13.6	3.53
97	12.9	3.30
107	12.2	3.17
117	12.3	2.81
122	12.0	2.50
127	10.8	2.11
132	9.4	1.61
137	6.5	1.17
138	LEW	

Cross Section Number 3

Date of data collection	3/20/78
Measured discharge	4674 cfs
Cross-sectional area	1830.6 sq ft
Average velocity	2.55 fps
Water surface elevation above msl	
Left bank	520.38 ft
Right bank	520.41 ft
Distance along the centerline between cross sections 2 & 3	400 ft

Distance from the right side looking downstream (ft)	Depth of Water(ft)	Average velocity in the vertical (fps)
0	REW	
8	8.7	0.74
13	11.9	1.03
18	13.0	1.51
28	13.2	2.40
38	13.2	2.92
48	17.3	2.64
58	17.1	3.30
68	16.0	3.45
78	15.8	3.25
88	14.7	3.30
98	13.8	3.08
108	12.9	2.84
118	11.2	2.08
128	10.5	1.36
138	5.0	0.24
143	2.3	0.00
148	2.2	0.00
168	LEW	

Cross Section Number 4

Date of data collection	3/21/78
Measured discharge	4620 cfs
Cross-sectional area	1682.8
Average velocity	2.75 fps
Water surface elevation above msl	
Left bank	520.65 ft
Right bank	520.62 ft
Distance along the centerline between cross sections 3 & 4	363 ft

Distance from the right side looking downstream (ft)	Depth of Water(ft)	Average velocity in the vertical (fps)
7	REW	
10	2.7	0.46
20	7.4	1.14
25	11.0	2.14
30	14.0	2.83
40	15.4	3.27
50	15.6	3.65
60	15.6	3.87
70	16.5	3.83
80	17.8	3.55
90	17.9	3.12
100	16.8	2.44
110	13.5	1.55
115	10.8	1.11
120	8.8	0.45
125	6.6	0.30
130	5.0	0.00
135	LEW	

APPENDIX A. Continued — Shelbyville

Cross Section Number 5

Date of data collection	3/22/78
Measured discharge	3831 cfs
Cross-sectional area	1475.9 sq ft
Average velocity	2.60 fps
Water surface elevation above msl	
Left bank	519.43 ft
Right bank	519.48 ft
Distance along the centerline between cross sections 4 & 5	1016 ft

Distance from the right side looking downstream (ft)	Depth of Water(ft)	Average velocity in the vertical (fps)
0	REW	
3	6.9	1.03
6	9.6	1.52
11	14.4	2.00
21	18.5	2.54
31	20.0	2.89
41	20.8	3.21
51	18.0	3.29
61	14.8	3.05
71	11.9	2.75
81	11.1	2.23
91	7.6	1.95
101	6.2	1.32
106	4.0	0.51
111	2.6	0.17
117	LEW	

Cross Section Number 6

Date of data collection	3/21/78
Measured discharge	3366 cfs
Cross-sectional area	1668.2 sq ft
Average velocity	2.02 fps
Water surface elevation above msl	
Left bank	520.40 ft
Right bank	520.41 ft
Distance along the centerline between cross sections 5 & 6	448 ft

Distance from the right side looking downstream (ft)	Depth of Water(ft)	Average velocity in the vertical (fps)
0	REW	
12	1.4	0.31
22	4.1	0.28
27	8.0	0.93
37	12.7	1.68
47	15.1	2.66
57	18.6	2.76
67	18.8	2.81
77	17.8	2.60
87	17.6	2.48
97	18.3	2.02
107	16.6	1.49
117	12.6	0.96
127	9.8	0.99
135	7.6	0.52
139	LEW	

Cross Section Number 7

Date of data collection	3/22/78
Measured discharge	3556 cfs
Cross-sectional area	1610.4 sq ft
Average velocity	2.21 fps
Water surface elevation above msl	
Left bank	519.29 ft
Right bank	519.24 ft
Distance along the centerline between cross sections 6 & 7	748 ft

Distance from the right side looking downstream (ft)	Depth of Water(ft)	Average velocity in the vertical (fps)
0	REW	
20	2.4	0.40
25	3.3	0.85
30	2.9	0.70
36	4.5	0.65
40	7.3	0.55
45	10.4	0.49
50	13.3	0.56
60	15.0	1.80
70	16.9	2.32
80	20.3	2.81
90	21.3	2.56
100	21.1	2.89
110	18.8	2.74
120	14.7	2.74
125	11.8	2.69
130	8.8	2.12
134	LEW	

Cross Section Number 8

Date of data collection	3/22/78
Measured discharge	3375 cfs
Cross-sectional area	1493.9 sq ft
Average velocity	2.26 fps
Water surface elevation above msl	
Left bank	519.05 ft
Right bank	519.09 ft
Distance along the centerline between cross sections 7 & 8	452 ft

Distance from the right side looking downstream (ft)	Depth of Water(ft)	Average velocity in the vertical (fps)
0	REW	
7	6.6	0.00
10	8.0	0.78
15	10.3	1.10
20	12.7	1.35
25	11.8	1.49
35	16.6	1.96
45	15.5	2.04
55	13.7	2.42
65	13.0	2.57
75	12.4	2.53
85	12.7	3.16
95	11.4	3.24
105	11.4	3.24
115	9.5	2.69
120	8.2	1.65
125	6.7	1.56
130	4.4	0.46
138	LEW	

APPENDIX A. Continued — Shelbyville

Cross Section Number 10

Date of data collection	3/23/78
Measured discharge	3,532 cfs
Cross-sectional area	1694.1 sq ft
Average velocity	2.09 fps
Water surface elevation above msl	
Left bank	517.50 ft
Right bank	517.52 ft
Distance along the centerline between cross sections 8 & 10	972 ft

Distance from the right side looking downstream (ft)	Depth of Water(ft)	Average velocity in the vertical (fps)
10	4.6	0.90
20	9.4	1.58
30	16.8	3.29
40	16.7	3.18
50	15.9	2.89
60	14.6	2.56
70	14.4	2.72
80	14.3	2.44
90	12.1	2.89
100	9.9	2.16
110	8.5	1.83
120	7.6	0.83
130	7.3	0.45
140	6.4	0.29
150	5.3	0.13
160	5.1	0.00
172	LEW	

Cross Section Number 11

Date of data collection	3/23/78
Measured discharge	3405 cfs
Cross-sectional area	1629.7 sq ft
Average velocity	2.09 fps
Water surface elevation above msl	
Left bank	517.40 ft
Right bank	517.30 ft
Distance along the centerline between cross sections 10 & 11	620 ft

Distance from the right side looking downstream (ft)	Depth of Water(ft)	Average velocity in the vertical (fps)
30	2.4	0.57
40	4.7	1.68
50	5.6	2.01
60	8.3	2.53
70	9.5	2.41
80	11.1	2.57
90	12.8	2.79
100	14.0	2.75
110	14.5	2.65
120	14.7	2.45
130	14.0	2.14
140	14.0	1.90
150	15.5	1.19
160	13.6	1.34
170	7.9	0.98
175	4.1	1.06
177	LEW	

106

APPENDIX B. VELOCITY DISTRIBUTION DATA, KASKASKIA RIVER BELOW LAKE CARLYLE

Cross Section Number 1

Date of data collection	5/17/77
Measured discharge	285 cfs
Cross-sectional area	243.8 sq ft
Average velocity	1.17 fps
Water surface elevation above msl	
Left bank	407.23 ft
Right bank	407.23 ft
Distance along the centerline between cross sections	0

Distance from the right side looking downstream (ft)	Depth of Water(ft)	Average velocity in the vertical (fps)
7	LEW	
12	1.6	0.85
18	3.0	1.02
24	2.7	1.07
30	2.1	1.02
36	1.8	1.05
42	1.4	1.05
50	1.6	1.16
55	1.8	1.37
60	1.9	1.44
65	1.8	1.63
70	2.0	1.76
80	2.0	1.81
85	1.9	1.87
90	2.0	1.72
95	1.9	1.45
100	1.9	1.52
105	1.6	1.47
110	2.3	1.19
115	2.2	0.96
120	1.9	0.59
125	2.1	0.19
128	1.8	0.34
131	REW	

Cross Section Number 2

Date of data collection	5/17/77
Measured discharge	287 cfs
Cross-sectional area	217.5 sq ft
Average velocity	1.32 fps
Water surface elevation above msl	
Left bank	
Right bank	
Distance along the centerline between cross sections 1 & 2	1200 ft

Distance from the right side looking downstream (ft)	Depth of Water(ft)	Average velocity in the vertical (fps)
6	REW	
10	2.2	0.57
14	2.2	0.84
20	1.9	1.01
25	2.0	1.01
30	1.9	1.55
35	2.0	1.62
40	2.1	1.83
45	2.1	1.90
50	2.1	1.97
55	2.1	1.82
60	2.2	1.87
65	2.1	1.83
70	2.2	1.83
75	2.1	1.51
80	2.1	1.54
85	2.2	1.58
90	1.9	1.35
95	1.9	1.22
100	1.6	0.85
105	1.5	0.37
109	1.2	0.15
112	LEW	

Cross Section Number 3

Date of data collection	5/17/77
Measured discharge	291 cfs
Cross-sectional area	253.8 sq ft
Average velocity	1.15 fps
Water surface elevation above msl	
Left bank	
Right bank	
Distance along the centerline between cross sections 2 & 3	900 ft

Distance from the right side looking downstream (ft)	Depth of Water(ft)	Average velocity in the vertical (fps)
10	REW	
20	0.5	0
25	0.8	0
30	1.2	0.25
35	1.8	0.52
40	2.1	0.76
45	2.6	0.88
50	2.9	0.94
55	3.2	1.22
60	3.3	1.28
65	3.7	1.23
70	3.9	1.21
75	3.9	1.36
80	3.8	1.46
85	4.3	1.44
90	4.2	1.44
95	4.2	1.36
100	3.0	1.35
103	2.2	1.04
106	LEW	

Cross Section Number 4

Date of data collection	5/17/77
Measured discharge	277 cfs
Cross-sectional area	188.8 sq ft
Average velocity	1.47 fps
Water surface elevation above msl	
Left bank	
Right bank	
Distance along the centerline between cross sections 3 & 4	660 ft

Distance from the right side looking downstream (ft)	Depth of Water(ft)	Average velocity in the vertical (fps)
17	REW	
30	0.6	0.44
35	0.9	0.88
40	1.4	0.86
45	1.8	0.98
50	2.2	1.18
55	2.2	1.40
60	2.2	1.56
65	2.5	1.62
70	2.9	1.60
75	3.2	1.60
80	3.4	1.57
85	3.3	1.52
90	3.5	1.54
95	3.3	1.49
100	3.4	1.55
105	3.0	1.41
108	1.4	0.79
111	LEW	

APPENDIX B. Continued — Carlyle

Cross Section Number 5

Date of data collection	5/17/77
Measured discharge	284 cfs
Cross-sectional area	333.8 sq ft
Average velocity	0.85 fps
Water surface elevation above msl	
Left bank	
Right bank	
Distance along the centerline	500 ft
between cross sections 4 & 5	

Distance from the right side looking downstream (ft)	Depth of Water(ft)	Average velocity in the vertical (fps)
14	REW	0.12
17	2.0	0.28
22	3.6	0.88
28	4.1	1.26
34	4.2	1.31
40	4.2	1.34
45	4.2	1.34
50	4.2	1.32
55	4.4	1.29
60	4.6	1.24
65	4.8	1.01
70	5,0	0.64
75	4.4	0.38
80	4.5	0.23
85	3.6	0.17
90	2.9	0.06
93	2.5	
99	LEW	

Cross Section Number 6

Date of data collection	5/18/77
Measured discharge	305 cfs
Cross-sectional area	448.8 sq ft
Average velocity	0.68 fps
Water surface elevation above msl	
Left bank	
Right bank	
Distance along the centerline	
between cross sections 5 & 6	680 ft

Distance from the right side looking downstream (ft)	Depth of Water(ft)	Average velocity in the vertical (fps)
4	REW	
7	2.3	0.15
11	3.9	0.44
15	5.3	0.39
20	6.3	0.71
25	6.9	0.72
30	7.1	0.72
35	7.1	0.78
40	7.2	0.92
45	6.9	0.95
50	6.4	0.93
55	5.9	0.85
60	5.6	0.82
65	5.6	0.74
70	4.9	0.60
75	4.1	0.37
80	2.7	0.16
90	0.9	0.16
95	LEW	

Cross Section Number 7

Date of data collection	5/17/77
Measured discharge	289 cfs
Cross-sectional area	430 sq ft
Average velocity	0.67 fps
Water surface elevation above msl	
Left bank	
Right bank	
Distance along the centerline	282 ft
between cross sections 6 & 7	

Distance from the right side looking downstream (ft)	Depth of Water(ft)	Average velocity in the vertical (fps)
5	REW	
8	2.1	0.41
12	3.7	0.63
16	4.4	0.85
20	6.2	0.93
25	7.6	0.91
30	8.0	0.87
35	8.3	0.88
40	7.9	0.74
45	7.3	0.71
50	6.9	0.58
55	6.2	0.62
60	5.4	0.65
65	4.4	0.54
70	4.0	0.33
75	2.9	0.12
83	LEW	

Cross Section Number 8

Date of data collection	5/18/77
Measured discharge	277 cfs
Cross-sectional area	268.75 sq ft
Average velocity	1.03 fps
Water surface elevation above msl	
Left bank	
Right bank	
Distance along the centerline	568 ft
between cross sections 7 & 8	

Distance from the right side looking downstream (ft)	Depth of Water(ft)	Average velocity in the vertical (fps)
4	REW	
7	1.6	0.42
11	2.9	0.74
15	3.3	0.91
20	4.7	0.56
25	4.8	0.98
30	3.9	1.27
35	4.4	1.00
40	4.4	1.34
45	3.9	1.18
50	3.5	1.19
55	2.7	1.42
60	2.7	1.42
65	2.5	1.28
70	3.2	1.03
75	2.3	0.93
80	1.7	0.81
85	1.4	0.61
90	1.1	0.35
95	0.6	0.25
98	LEW	

APPENDIX B. Continued — Carlyle

Cross Section Number 10

Date of data collection		5/18/77
Measured discharge		296 cfs
Cross-sectional area		353.8 sq ft
Average velocity		0.84 fps
Water surface elevation above msl		
Left bank		
Right bank		
Distance along the centerline etween cross sections 8 & 10		1660 ft

Distance from the right side looking downstream (ft)	Depth of Water(ft)	Average velocity in the vertical (fps)
10	REW	
14	2.1	0.52
18	2.2	0.79
22	2.3	1.07
26	2.7	1.35
30	2.9	1.36
35	3.3	1.44
40	3.6	1.53
45	3.8	1.47
50	3.9	1.43
55	4.0	1.43
60	4.1	1.38
65	4.2	0.67
70	4.4	0.55
75	4.5	0.23
80	4.9	0.36
85	5.0	0.79
90	4.8	0.30
95	4.3	0.20
100	3.5	0.22
105	2.3	0.27
108	1.0	0
113	LEW	

Cross Section Number 11

Date of data collection		5/19/77
Measured discharge		286 cfs
Cross-sectional area		407.5 sq ft
Average velocity		0.70 fps
Water surface elevation above msl		
Left bank		
Right bank		
Distance along the centerline between cross sections 10 & 11		1200 ft

Distance from the right side looking downstream (ft)	Depth of Water(ft)	Average velocity in the vertical (fps)
6	REW	
10	2.1	0
15	3.3	0.11
20	4.1	0.22
25	4.1	0.32
30	4.7	0.62
35	5.1	0.63
40	5.3	0.85
45	5.2	0.95
50	5.1	1.01
55	5.1	1.04
60	5.1	1.09
65	4.8	0.92
70	4.2	0.81
75	5.2	0.85
80	5.4	0.63
85	5.1	0.63
90	4.4	0.59
95	3.0	0.39
99	1.6	0.28
102	LEW	

Cross Section Number 14

Date of data collection		5/19/77
Measured discharge		286 cfs
Cross-sectional area		387.5 sq ft
Average velocity		0.74 fps
Water surface elevation above msl		
Left bank		
Right bank		
Distance along the centerline between cross sections 11 & 14		4624 ft

Distance from the right side looking downstream (ft)	Depth of Water(ft)	Average velocity in the vertical (fps)
7	REW	
11	1.5	0.0
15	2.5	0.14
20	3.3	0.37
25	3.7	0.56
30	4.3	0.60
35	4.6	0.85
40	4.8	0.83
45	4.4	0.98
50	4.5	0.99
55	4.4	1.16
60	4.3	1.13
65	4.2	1.09
70	4.3	1.20
75	4.3	1.17
80	4.4	0.99
85	4.6	0.63
90	4.6	0.32
95	4.2	0.10
100	3.2	0.10
105	2.1	0.20
108	LEW	

Cross Section Number 15

Date of data collection		5/19/77
Measured discharge		283 cfs
Cross-sectional area		400 sq ft
Average velocity		0.71 fps
Water surface elevation above msl		
Left bank		
Right bank		
Distance along the centerline between cross sections 14 & 15		2370 ft

Distance from the right side looking downstream (ft)	Depth of Water(ft)	Average velocity in the vertical (fps)
3	REW	
7	2.9	0.14
12	3.9	0.22
18	3.6	0.47
26	3.8	0.67
32	3.6	0.86
40	3.7	0.79
48	3.7	0.83
55	3.5	0.91
60	3.6	0.89
65	3.7	0.96
70	3.6	0.97
75	3.6	0.89
80	3.7	1.02
85	3.6	0.93
90	3.3	0.69
95	3.0	0.85
100	2.9	0.73
105	2.7	0.56
110	3.1	0.39
115	2.6	0.59
120	2.1	0.42
124	LEW	

APPENDIX B. Continued — Carlyle

Cross Section Number 1

Date of data collection	12/8/75
Measured discharge	2143 cfs
Cross-sectional area	1136.2 sq ft
Average velocity	1.89 fps
Water surface elevation above msl	
Left bank	414.08 ft
Right bank	404.05 ft
Distance along the centerline between cross sections	0

Distance from the right side looking downstream (ft)	Depth of Water(ft)	Average velocity in the vertical (fps)
14	REW	
20	3.85	0,95
25	7.25	0.98
30	8.25	0.95
35	9.40	1.18
40	9.55	1.33
50	8.70	2.03
60	8.00	2.14
70	8.30	2.51
80	8.50	2.37
90	8.70	2.68
100	8.70	2.49
110	8.55	2.32
120	9.40	1.95
130	9.70	1.80
135	9.90	1.68
140	9.90	1.35
145	8.70	1.23
150	6.30	0.77
153	2.70	0.43
157	LEW	

Cross Section Number 2

Date of data collection	12/11/75
Measured discharge	2210 cfs
Cross-sectional area	971.3 sq ft
Average velocity	2.28 fps
Water surface elevation above msl	
Left bank	413.88 ft
Right bank	413.88 ft
Distance along the centerline between cross sections 1 & 2	1200 ft

Distance from the right side looking downstream (ft)	Depth of Water(ft)	Average velocity in the vertical (fps)
14	REW	
21	4.1	0.51
26	7.7	1.26
34	9.0	2.08
42	8.9	2.29
50	8.9	2.49
60	8.9	3.08
65	8.9	3.20
70	8.9	3.18
80	8.9	3.25
90	8.9	2.87
100	8.9	2.18
107	8.2	1.60
115	7.4	1.63
122	7.5	1.35
127	7.7	1.25
152	5.5	0.82
136	LEW	

Cross Section Number 3

Date of data collection	12/11/75
Measured discharge	2200 cfs
Cross-sectional area	1047.8 sq ft
Average velocity	2.10 fps
Water surface elevation above msl	
Left bank	413.85 ft
Right bank	413.86 ft
Distance along the centerline between cross sections 2 & 3	900 ft

Distance from the right side looking downstream (ft)	Depth of Water(ft)	Average velocity in the vertical (fps)
34	REW	
41	4.1	0.95
48	6.9	1.31
55	8.3	1.71
62.5	8.4	1.71
70	9.3	2.12
80	9.7	2.24
90	9.5	2.30
100	10.1	2.30
110	10.5	2.62
120	10.8	2.72
130	11.1	2.32
137.5	10.6	2.01
145	7.6	1.56
150	5.4	1.48
153	3.9	1.09
158	LEW	

Cross Section Number 4

Date of data collection	12/11/75
Measured discharge	2228 cfs
Cross-sectional area	1127.3 sq ft
Average velocity	1.98 fps
Water surface elevation above msl	
Left bank	413.81 ft
Right bank	413.80 ft
Distance along the centerline between cross sections 3 & 4	660 ft

Distance from the right side looking downstream (ft)	Depth of Water(ft)	Average velocity in the vertical (fps)
26	REW	
34	2.7	0.56
40	4.4	1.14
48	6.4	1.21
55	7.5	1,75
65	7.9	2.26
75	8.7	2.21
85	8.8	2.46
95	10.0	2.41
105	10.0	2.45
115	10.5	2.56
125	9.8	2.35
132.5	10.3	2.14
140	10.4	1.37
147.5	10.3	1.17
155	8.9	1.31
160	5.6	1.56
166	LEW	

APPENDIX B. Continued — Carlyle

Cross Section Number 5

Date of data collection	12/9/75
Measured discharge	2169 cfs
Cross-sectional area	1141.7 sq ft
Average velocity	1.90 fps
Water surface elevation above msl	
Left bank	413.78 ft
Right bank	413.81 ft
Distance along the centerline between cross sections 4 & 5	500 ft

Distance from the right side looking downstream (ft)	Depth of Water(ft)	Average velocity in the vertical (fps)
8	REW	
14	2.9	0.43
20	4.85	0.75
30	7.1	1.18
40	8.4	1.29
50	9.7	2.00
60	11.4	2.63
70	11.9	2.81
80	12.0	2.71
90	11.9	2.29
100	11.5	1.70
110	10.8	1.19
120	8.8	0.81
130	8.8	0.97
136	8.0	1.19
150	LEW	

Cross Section Number 6

Date of data collection	12/9/75
Measured discharge	2112 cfs
Cross-sectional area	1185.7 sq ft
Average velocity	1.78 fps
Water surface elevation above msl	
Left bank	413.76 ft
Right bank	413.80
Distance along the centerline between cross sections 5 & 6	680 ft

Distance from the right side looking downstream (ft)	Depth of Water(ft)	Average velocity in the vertical (fps)
10	REW	
16	8.5	0.96
22	11.4	1.10
30	13.5	1.42
40	14.3	1.88
50	14.5	2.14
60	11.7	1.92
70	11.1	2.03
80	9.7	2.35
90	8.9	2.26
100	7.6	2.11
110	6.6	1.67
120	5.9	1.25
125	4.7	1.01
130	3.6	0.76
137	LEW	

Cross Section Number 7

Date of data collection	12/9/75
Measured discharge	2161 cfs
Cross-sectional area	1052.3 sq ft
Average velocity	2.05 fps
Water surface elevation above msl	
Left bank	413.75 ft
Right bank	413.76 ft
Distance along the centerline between cross sections 6 & 7	282 ft

Distance from the right side looking downstream (ft)	Depth of Water(ft)	Average velocity in the vertical (fps)
20	REW	
27	4.7	1.28
32	8.3	1.42
40	12.3	1.87
48	14.1	2.28
55	14.4	2.26
65	12.0	1.94
75	11.3	2.08
85	10.2	2.32
95	8.9	2.37
105	7.8	2.05
115	6.5	2.04
122	5.4	1.50
128	4.4	1.14
133	4.0	0.94
142	LEW	

Cross Section Number 8

Date of data collection	12/9/75
Measured discharge	1583 cfs
Cross-sectional area	934.1 sq ft
Average velocity	1.69 fps
Water surface elevation above msl	
Left bank	413.66 ft
Right bank	413.67 ft
Distance along the centerline between cross sections 7 & 8	568 ft

Distance from the right side looking downstream (ft)	Depth of Water(ft)	Average velocity in the vertical (fps)
8	REW	
16	5.7	0.90
22	9.5	1.32
30	11.1	1.46
40	11.5	1.83
50	10.7	2.15
65	10.0	2.01
80	10.2	2.21
95	9.2	2.13
105	8.8	1.95
115	7.6	1.41
125	5.6	1.27
132	4.5	0.75
137	3.2	0.86
146	LEW	

Cross Section Number 11

Date of data collection	12/10/75
Measured discharge	2288 cfs
Cross-sectional area	1083.2 sq ft
Average velocity	2.11 fps
Water surface elevation above msl	
Left bank	413.28 ft
Right bank	413.29 ft
Distance along the centerline between cross sections 8 & 11	2860 ft

Distance from the right side looking downstream (ft)	Depth of Water(ft)	Average velocity in the vertical (fps)
12	REW	
22	2.2	0.51
30	5.8	0.62
38	8.2	1.40
48	10.9	1.77
55	10.8	1.97
65	10.0	2.36
75	10.0	2.60
85	10.4	2.52
95	9.9	2.56
105	10.7	2.37
115	10.5	2.15
122	10.1	2.05
130	7.4	1.55
136	4.9	1.17
143	LEW	

Cross Section Number 12

Date of data collection	12/10/75
Measured discharge	2025 cfs
Cross-sectional area	993.9 sq ft
Average velocity	2.04 fps
Water surface elevation above msl	
Left bank	413.04 ft
Right bank	413.07 ft
Distance along the centerline between cross sections 11 & 12	1328 ft

Distance from the right side looking downstream (ft)	Depth of Water(ft)	Average velocity in the vertical (fps)
14	REW	
18	3.2	1.48
22	4.7	1.86
28	5.9	1.72
36	7.2	2.41
44	8.8	2.73
52	10.1	2.69
60	10.7	2.61
70	11.6	2.48
80	12.0	2.06
90	12.0	2.08
100	12.2	1.70
107	11.1	1.18
110	12.1	1.51
115	7.1	0.62
120	2.7	0.51
124	LEW	

Cross Section Number 14

Date of data collection	12/10/75
Measured discharge	2183 cfs
Cross-sectional area	1254.9 sq ft
Average velocity	1.74 fps
Water surface elevation above msl	
Left bank	412.26 ft
Right bank	412.26 ft
Distance along the centerline between cross sections 12 & 14	3296 ft

Distance from the right side looking downstream (ft)	Depth of Water(ft)	Average velocity in the vertical (fps)
17	REW	
21	3.6	0.35
26	6.5	0.81
30	7.4	1.08
38	9.8	1.41
46	11.1	1.51
55	11.6	1.76
65	12.1	2.10
75	11.8	2.12
85	11.5	2.37
95	11.6	2.23
105	11.5	2.00
115	12.2	1.66
122	11.0	1.26
130	9~3	1.33
136	5.3	1.03
141	3.0	0.50
147	LEW	

Cross Section Number 15

Date of data collection	12/10/75
Measured discharge	2165 cfs
Cross-sectional area	1409.9 sq ft
Average velocity	1.54 fps
Water surface elevation above msl	
Left bank	411.93 ft
Right bank	411.91 ft
Distance along the centerline between cross sections 14 & 15	2370 ft

Distance from the right side looking downstream (ft)	Depth of Water(ft)	Average velocity in the vertical (fps)
17	REW	
21	3.3	0.38
28	9.4	0.93
36	12.0	1.14
44	11.3	1.63
50	11.3	1.66
60	11.3	1.85
70	11.4	1.83
80	11.6	2.09
90	11.4	1.97
100	11.2	1.86
110	11.0	1.70
120	10.7	1.46
130	10.6	1.30
137	10.5	1.01
145	9.0	0.97
150	6.4	0.66
158	LEW	

APPENDIX B. Continued — Carlyle

Cross Section Number 1

Date of data collection	12/13/77
Measured discharge	3999 cfs
Cross-sectional area	1738.9 sq ft
Average velocity	2.30 fps
Water surface elevation above msl	
Left bank	417.62 ft
Right bank	417.65 ft
Distance along the centerline	0
between cross sections	

Distance from the right side looking downstream (ft)	Depth of water (ft)	Average velocity in the vertical (fps)
0	REW	
5	4.5	0.44
10	7.9	1.48
15	9.6	1.37
20	11.8	1.52
25	13.3	1.95
35	13.2	2.85
45	12.4	2.92
55	11.9	3.01
65	12.3	3.10
75	12.3	2.80
85	12.5	2.66
95	12.5	2.68
105	13.0	2.64
115	12.8	2.41
125	13.2	2.01
130	13.4	1.59
135	13.0	1.26
140	11.8	0.93
145	6.5	0.36
150	3.4	0.00
156	LEW	

Cross Section Number 2

Date of data collection	12/13/77
Measured discharge	4013 cfs
Cross-sectional area	1491.3 sq ft
Average velocity	2.69 fps
Water surface elevation above msl	
Left bank	417.63 ft
Right bank	417,57 ft
Distance along the centerline	
between cross sections 1 & 2	1200 ft

Distance from the right side looking downstream (ft)	Depth of water (ft)	Average velocity in the vertical (fps)
0	REW	
11	4.0	0.17
16	5.3	0.27
21	6.4	0.60
26	8.2	0.77
31	10.6	1.18
36	12.7	1.75
41	12.3	1.97
51	12.4	2.51
61	12.6	3.01
71	12.7	3.36
81	12.7	3.69
91	12.7	3.66
101	12.7	3.75
111	12.7	3.33
121	12.0	3.06
126	11.4	2.71
131	10.7	2.54
136	8.6	1.58
140	6.7	1.35
144	LEW	

Cross Section Number 3

Date of data collection	12/13/77
Measured discharge	4027 cfs
Cross-sectional area	1594 sq ft
Average velocity	2.52 fps
Water surface elevation above msl	
Left bank	417.55 ft
Right bank	417.51 ft
Distance along the centerline	
between cross sections 2 & 3	900 ft

Distance from the right side looking downstream (ft)	Depth of water (ft)	Average velocity in the vertical (fps)
0	REW	
33	5.4	0.40
36	7.2	0.75
41	9.3	1.14
46	10.8	1.63
51	11.0	1.71
56	11.4	2.04
61	11.7	2.12
71	13.6	2.39
81	13.8	2.81
91	13.9	3.01
101	15.0	3.31
111	14.9	3.30
121	15.1	3.09
131	15.3	3.13
141	13.4	2.41
145	10.4	2.21
149	8.7	1.55
153	6.7	1.11
156	LEW	

Cross Section Number 4

Date of data collection	
Measured discharge	12/13/77
Cross-sectional area	3810 cfs
Average velocity	1618.3 sq ft
Water surface elevation above msl	2.35 fps
Left bank	
Right bank	417.55 ft
Distance along the centerline	417.48 ft
between cross sections 3 & 4	660 ft

Distance from the right side looking downstream (ft)	Depth of water (ft)	Average velocity in the vertical (fps)
0	REW	
21	3.8	0.00
26	5.3	0.12
31	7.1	0.44
36	8.1	0.83
41	8.7	1.29
51	9.8	9.92
61	11.1	2.25
71	10.8	2.42
81	11.4	2.51
91	13.1	2.66
101	14.1	2.83
111	14.4	2.97
121	14.4	3.14
131	14.3	3.09
141	14.3	2.53
149	14.1	2.39
153	10.8	2.40
158	8.4	1.90
161	LEW	

Cross Section Number 5

Date of data collection	12/14/77
Measured discharge	4013 cfs
Cross-sectional area	2001.3 sq ft
Average velocity	2.01 fps
Water surface elevation above msl	
Left bank	418.47 ft
Right bank	418.44
Distance along the centerline	
between cross sections 4 & 5	500 ft

Distance from the right side looking downstream (ft)	Depth of water (ft)	Average velocity in the vertical (fps)
0	REW	
32	7.0	0.67
38	8.9	0.79
43	8.8	0.98
48	10.1	1.16
53	10.7	1.45
58	13.2	1.14
63	14.7	1.53
68	16.0	2.43
73	16.3	2.44
78	16.0	2.49
83	16.1	2.55
93	16.5	2.76
103	16.8	2.79
113	17.4	2.70
123	17.3	2.57
133	15.6	2.43
138	13.8	2.07
143	14.0	1.86
148	12.8	1.77
153	11.6	1.52
158	10.0	0.97
163	8.0	0.25
168	5.4	0.29
171	LEW	

Cross Section Number 6

Date of data collection	12/14/77
Measured discharge	3799 cfs
Cross-sectional area	1832.4 sq ft
Average velocity	2.07 fps
Water surface elevation above msl	
Left bank	418.39 ft
Right bank	418.49 ft
Distance along the centerline	
between cross sections 5 & 6	680 ft

Distance from the right side looking downstream (ft)	Depth of water (ft)	Average velocity in the vertical (fps)
4	REW	
11	11.4	1.49
15	14.2	1.82
20	15.9	2.14
25	17.6	2.34
35	18.5	2.51
45	18.6	2.53
55	18.8	2.55
65	15.7	2.35
75	14.1	2.17
85	13.1	2.24
95	11.7	2.19
105	10.3	2.29
115	9.8	1.81
120	9.0	1.45
125	8.5	1.01
130	8.2	0.59
135	6.9	0.19
140	4.0	0.00
145	3.1	0.00
150	1.9	0.00
160	LEW	

Cross Section Number 7

Date of data collection	12/14/77
Measured discharge	3680 cfs
Cross-sectional area	1849.5 sq ft
Average velocity	1.99 fps
Water surface elevation above msl	
Left bank	418.22 ft
Right bank	418.27 ft
Distance along the centerline	
between cross sections 6 & 7	282 ft

Distance from the right side looking downstream (ft)	Depth of water (ft)	Average velocity in the vertical (fps)
4	REW	
6	7.0	0.38
10	9.6	0.60
15	14.0	0.94
20	14.8	1.32
25	15.1	1.86
30	15.8	2.18
40	17.9	2.43
50	18.9	2.35
60	19.8	2.35
70	18.4	2.40
80	16.3	2.38
90	13.1	2.21
100	12.2	2.31
110	10.5	2.02
115	9.5	1.79
120	8.4	1.39
125	7.5	0.87
130	6.1	0.35
135	3.7	0.19
140	2.6	0.00
145	1.8	0.00
155	LEW	

Cross Section Number 8

Date of data collection	12/14/77
Measured discharge	3573 cfs
Cross-sectional area	1783.3 sq ft
Average velocity	2.00 fps
Water surface elevation above msl	
Left bank	418.18 ft
Right bank	418.25 ft
Distance along the centerline	
between cross sections 7 & 8	568 ft

Distance from the right side looking downstream (ft)	Depth of water (ft)	Average velocity in the vertical (fps)
10	REW	
14	9.2	0.69
20	12.6	1.51
25	13.8	1.79
35	16.4	1.93
45	16.1	2.52
55	14.9	2.51
65	13.8	2.49
75	14.0	2.40
85	13.5	2.38
95	13.2	2.41
105	12.7	2.24
115	11.6	2.03
125	10.2	1.88
135	8.4	1.34
140	7.4	0.95
145	6.5	0.53
150	5.2	0.20
155	2.8	0.00
180	LEW	

APPENDIX B. Continued — Carlyle

Cross Section Number 10

Date of data collection	12/15/77
Measured discharge	3460 cfs
Cross-sectional area	1785.9 sq ft
Average velocity	1.94 fps
Water surface elevation above msl	
Left bank	417.45 ft
Right bank	417.44 ft
Distance along the centerline between cross sections 8 & 10	1660 ft

Distance from the right side looking downstream (ft)	Depth of water (ft)	Average velocity in the vertical (fps)
0	REW	
65	2.7	0.00
75	5.9	0.68
80	7.3	0.77
85	8.7	1.08
90	10.3	1.38
95	12.2	1.66
100	12.8	1.85
105	13.1	1.94
110	13.5	2.22
120	13.8	2.43
130	14.3	2.55
140	14.5	2.49
150	15.0	2.28
160	15.4	2.28
170	15.7	2.25
180	14.8	1.95
185	13.8	1.69
190	12.4	1.77
195	11.2	1.30
199	9.8	1.35
203	8.0	0.98
208	6.8	0.44
213	LEW	

Cross Section Number 11

Date of data collection	12/15/77
Measured discharge	3297 cfs
Cross-sectional area	1790.1 sq ft
Average velocity	1.84 fps
Water surface elevation above msl	
Left bank	417.38 ft
Right bank	417.37 ft
Distance along the centerline between cross sections 10 & 11	1200 ft

Distance from the right side looking downstream (ft)	Depth of water (ft)	Average velocity in the vertical (fps)
0	REW	
14	4.6	0.00
19	6.6	0.00
24	9.1	0.34
29	11.4	0.84
34	12.8	1.23
39	14.6	1.49
49	16.2	2.09
59	17.5	2.36
69	17.2	2.19
79	17.2	2.19
89	16.7	2.42
99	16.7	2.18
109	14.9	2.06
119	14.6	1.84
123	13.2	1.63
127	10.8	1.72
131	9.9	1.50
136	6.8	0.36
140	LEW	

Cross Section Number 12

Date of data collection	12/15/77
Measured discharge	3461 cfs
Cross-sectional area	1731.7 sq ft
Average velocity	2.00 fps
Water surface elevation above msl	
Left bank	417.14 ft
Right bank	417.19 ft
Distance along the centerline between cross sections 11 & 12	1328 ft

Distance from the right side looking downstream (ft)	Depth of water (ft)	Average velocity in the vertical (fps)
0	REW	
6	2.8	0.63
11	5.8	0.73
16	11.2	1.04
21	13.6	1.53
31	13.9	2.11
41	14.3	2.20
51	14.9	2.22
61	16.0	2.14
71	16.6	1.96
81	16.2	2.01
91	13.2	2.46
101	12.6	2.53
111	12.5	2.32
121	11.5	1.96
125	12.1	1.61
129	10.5	1.53
133	9.1	1.28
137	4.0	0.77
143	LEW	

Cross Section Number 14

Date of data collection	12/15/77
Measured discharge	3388 cfs
Cross-sectional area	1937.9 sq ft
Average velocity	1.75 fps
Water surface elevation above msl	
Left bank	416.72 ft
Right bank	416.78 ft
Distance along the centerline between cross sections 12 & 14	3296 ft

Distance from the right side looking downstream (ft)	Depth of water (ft)	Average velocity in the vertical (fps)
0	REW	
7	5.2	0.24
12	7.9	0.69
17	10.0	0.99
22	11.6	1.16
32	14.6	1.43
42	15.7	1.92
52	16.4	2.19
62	16.4	2.36
72	16.2	2.38
82	16.0	2.29
92	15.6	2.05
102	16.0	1.99
112	16.5	1.59
122	14.3	1.38
127	12.6	1.39
132	9.7	1.11
137	7.0	0.40
142	4.4	0.18
148	2.7	0.00
155.5	LEW	

APPENDIX B. Concluded — Carlyle

Cross Section Number 15

Date of data collection   12/16/77
Measured discharge   3442 cfs
Cross-sectional area   2149.6 sq ft
Average velocity   1.60 fps
Water surface elevation above msl
       Left bank   416.82 ft
       Right bank   416.80 ft
Distance along the centerline
     between cross sections 14 & 15   2370 ft

Distance from the right side looking downstream (ft)	Depth of water (ft)	Average velocity in the vertical (fps)
0	REW	
6	2.8	0.00
11	5.2	0.08
16	8.8	0.67
21	14.6	1.09
26	15.7	1.43
31	16.1	1.47
36	16.0	1.58
41	16.0	1.70
51	16.1	2.11
61	16.2	2.00
71	16.1	2.12
81	16.3	2.07
91	16.1	1.96
101	16.5	1.79
111	15.9	1.74
121	15.4	1.35
131	15.1	1.29
136	14.5	1.17
141	12.8	0.93
145	10.7	0.90
149	8.5	0.49
153	5.2	0.11
159	LEW	